Leibniz-Institut
für Festkörper- und
Werkstoffforschung
Dresden

Angle-resolved photoemission spectroscopy (ARPES)

Daniil Evtushinsky

Kourovka, 1st of March 2012

Angle-resolved photoemission

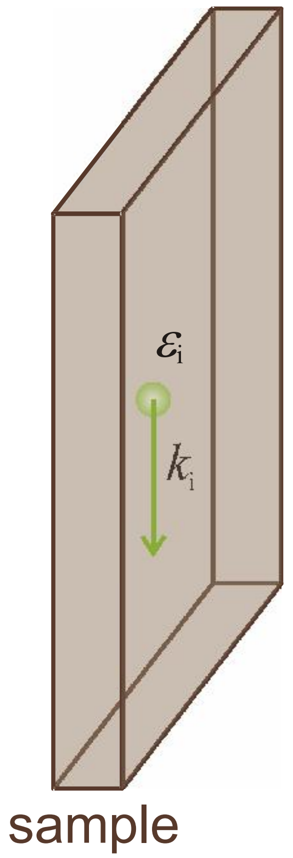

Angle-resolved photoemission

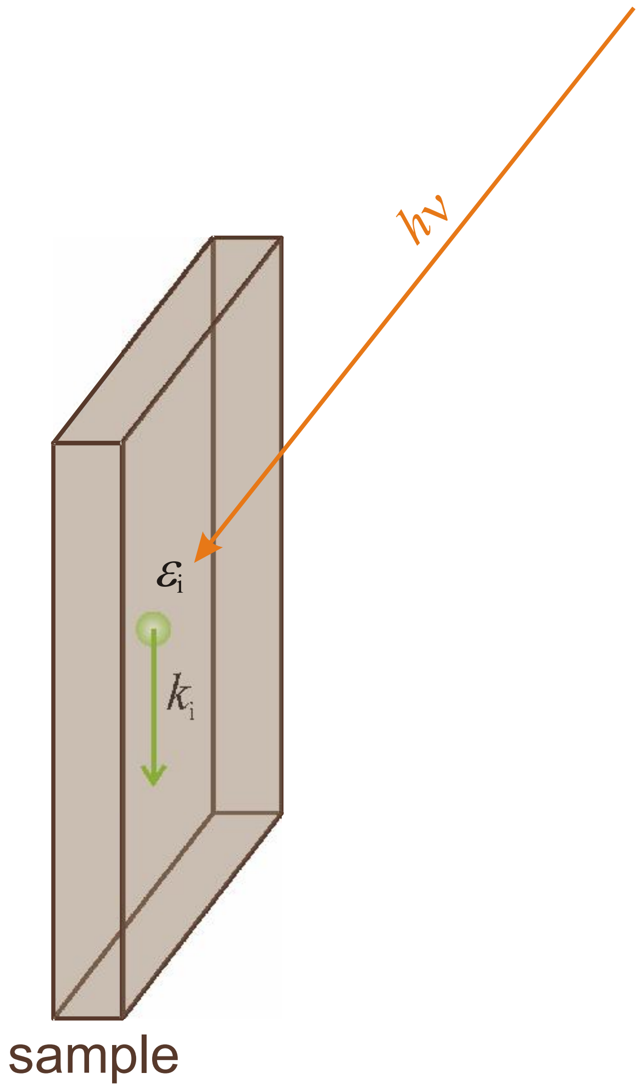

Angle-resolved photoemission

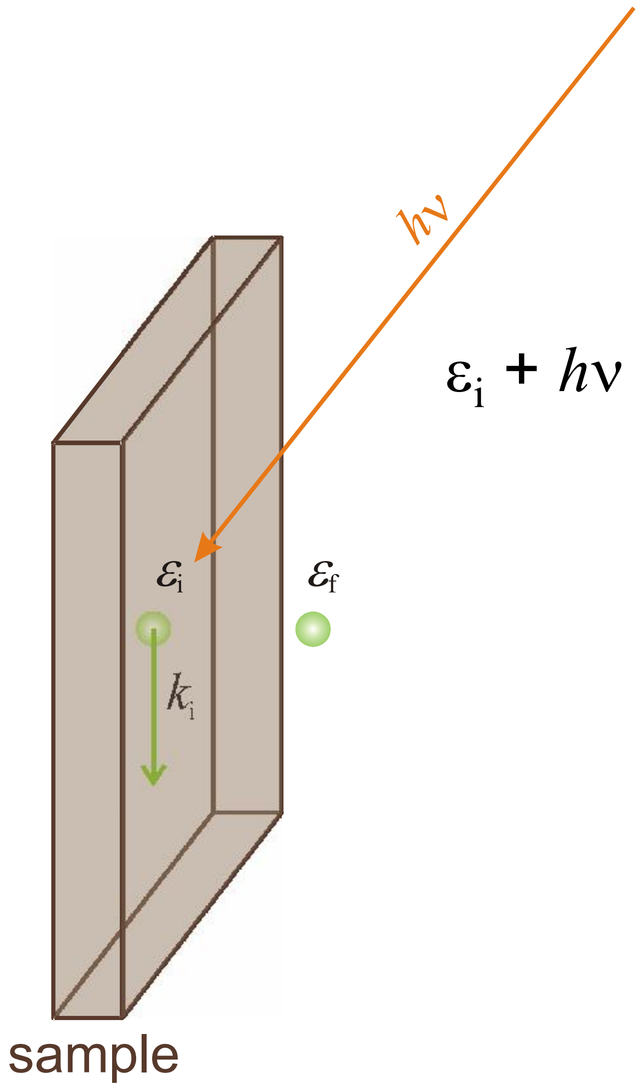

$$\varepsilon_i + h\nu - A = \varepsilon_f$$

Angle-resolved photoemission

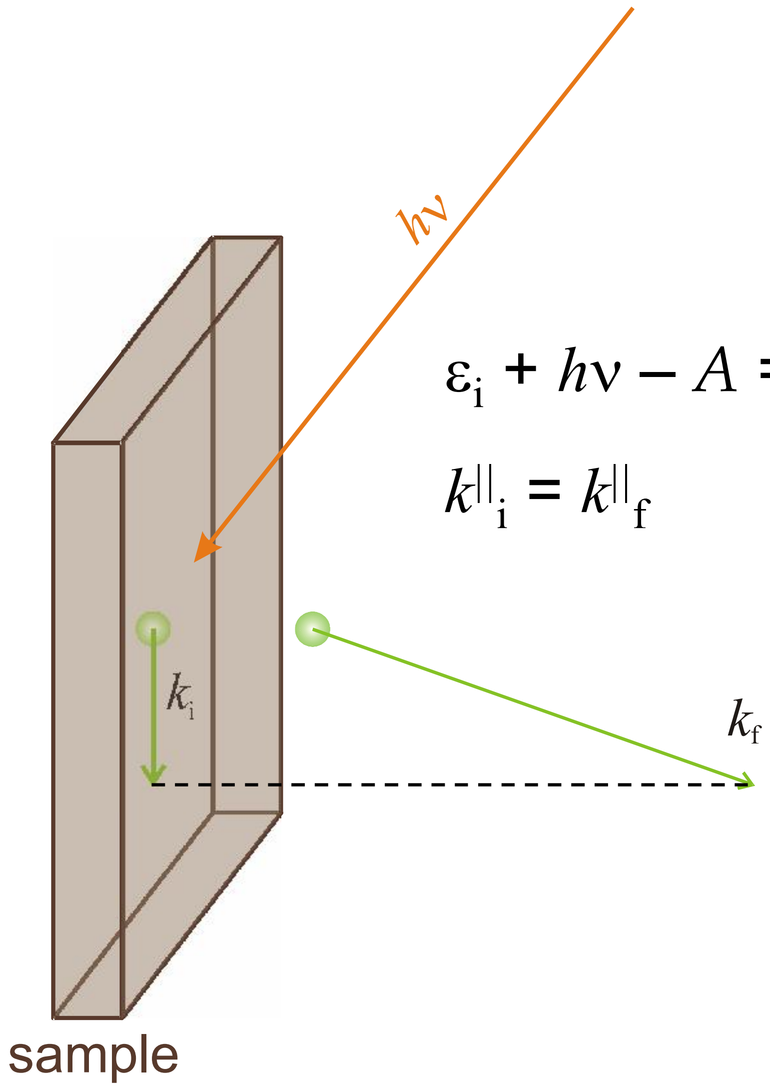

$$\varepsilon_i + h\nu - A = \varepsilon_f$$

$$k^{||}_i = k^{||}_f$$

Momentum conservation

$$H = \sum_i \frac{\mathbf{p}_i^2}{2m} + \sum_i V(\mathbf{r}_i)$$

$$u_i e^{-i\mathbf{k}_i\mathbf{r}} \qquad u_f e^{-i\mathbf{k}_f\mathbf{r}}$$

$$\Delta = \frac{e}{mc}\mathbf{A}\mathbf{p}$$

$$w \propto |\langle\psi_f|\Delta|\psi_i\rangle|^2 \delta(\varepsilon_f - \varepsilon_i - h\nu) \propto \left[\int \psi_f^* \mathbf{A}\cdot\nabla\psi_i d^3\mathbf{r}\right]^2 \delta(\varepsilon_f - \varepsilon_i - h\nu)$$

$$\int \psi_f^* \mathbf{A}\cdot\nabla\psi_i d^3\mathbf{r}\ \delta(\varepsilon_f - \varepsilon_i - h\nu) = \mathbf{A}\cdot\int u_f^* e^{-i\mathbf{k}_f\mathbf{r}}\nabla(u_i e^{i\mathbf{k}_i\mathbf{r}})d^3\mathbf{r}\ \delta(\varepsilon_f - \varepsilon_i - h\nu) =$$

$$= \mathbf{A}\cdot\int u_f^* e^{-i\mathbf{k}_f\mathbf{r}}(e^{i\mathbf{k}_i\mathbf{r}}\nabla u_i + u_i i\mathbf{k}_i e^{i\mathbf{k}_i\mathbf{r}})d^3\mathbf{r}\ \delta(\varepsilon_f - \varepsilon_i - h\nu) =$$

$$= \mathbf{A}\cdot\int u_f^*(\nabla u_i + u_i i\mathbf{k}_i)e^{i(\mathbf{k}_i - \mathbf{k}_f)\mathbf{r}}d^3\mathbf{r}\ \delta(\varepsilon_f - \varepsilon_i - h\nu)$$

$$\mathbf{k}_i - \mathbf{k}_f = \mathbf{G}$$

Momentum conservation for semi-infinite case

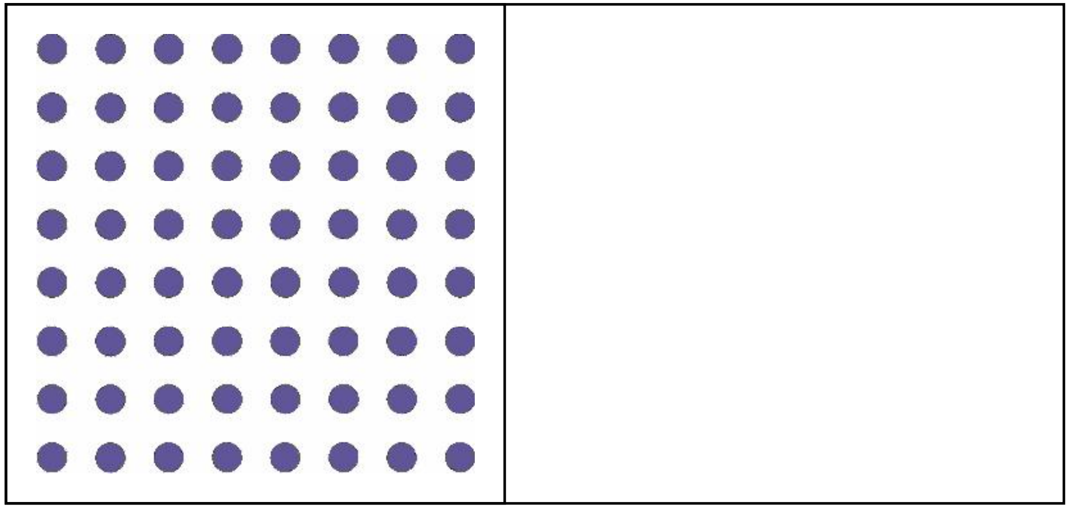

$$\varepsilon_i = \varepsilon_f - h\nu, \qquad \mathbf{k}_i^{\|} = \mathbf{k}_f^{\|} + \mathbf{G}$$

Angle-resolved photoemission

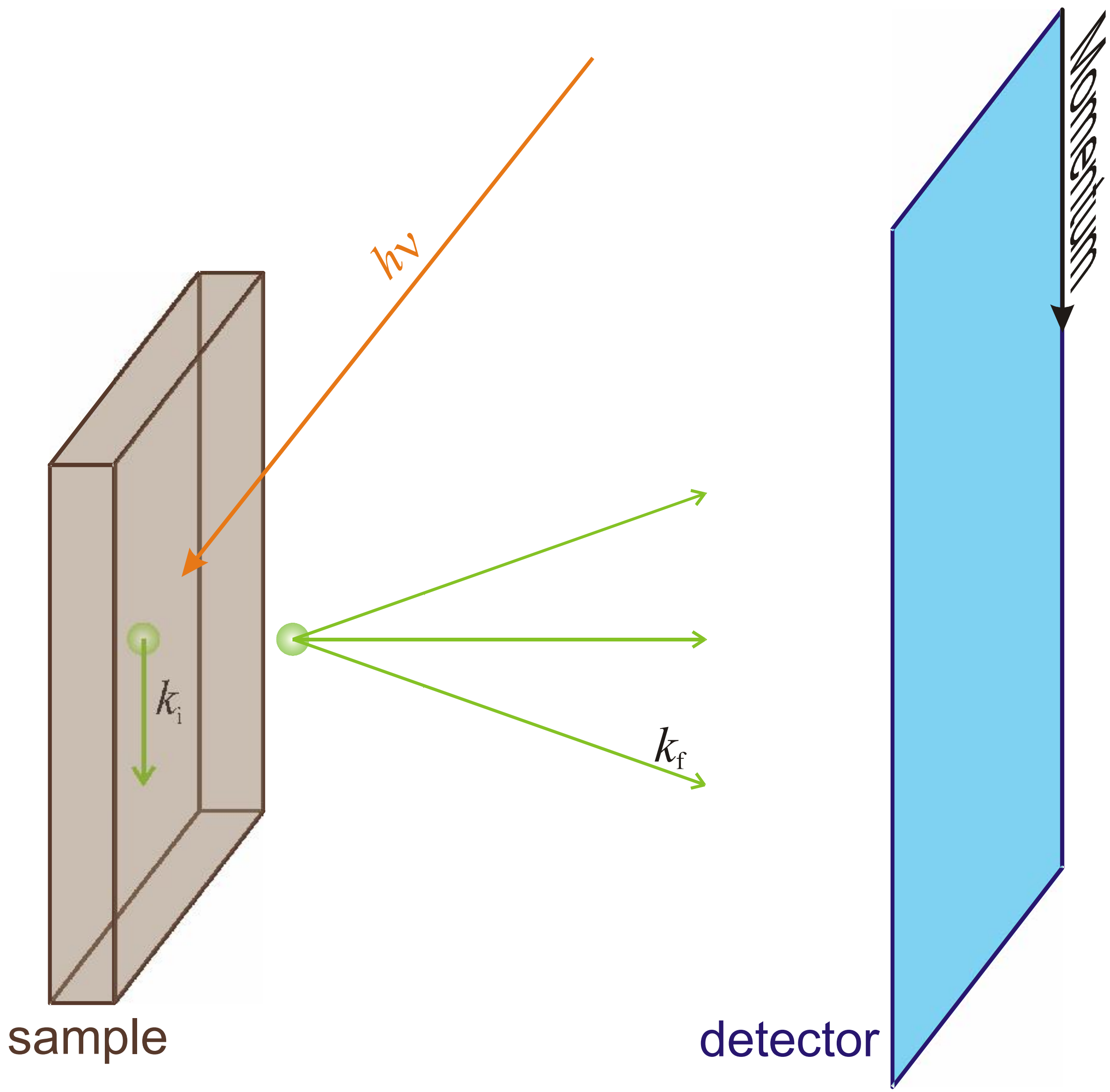

Angle-resolved photoemission

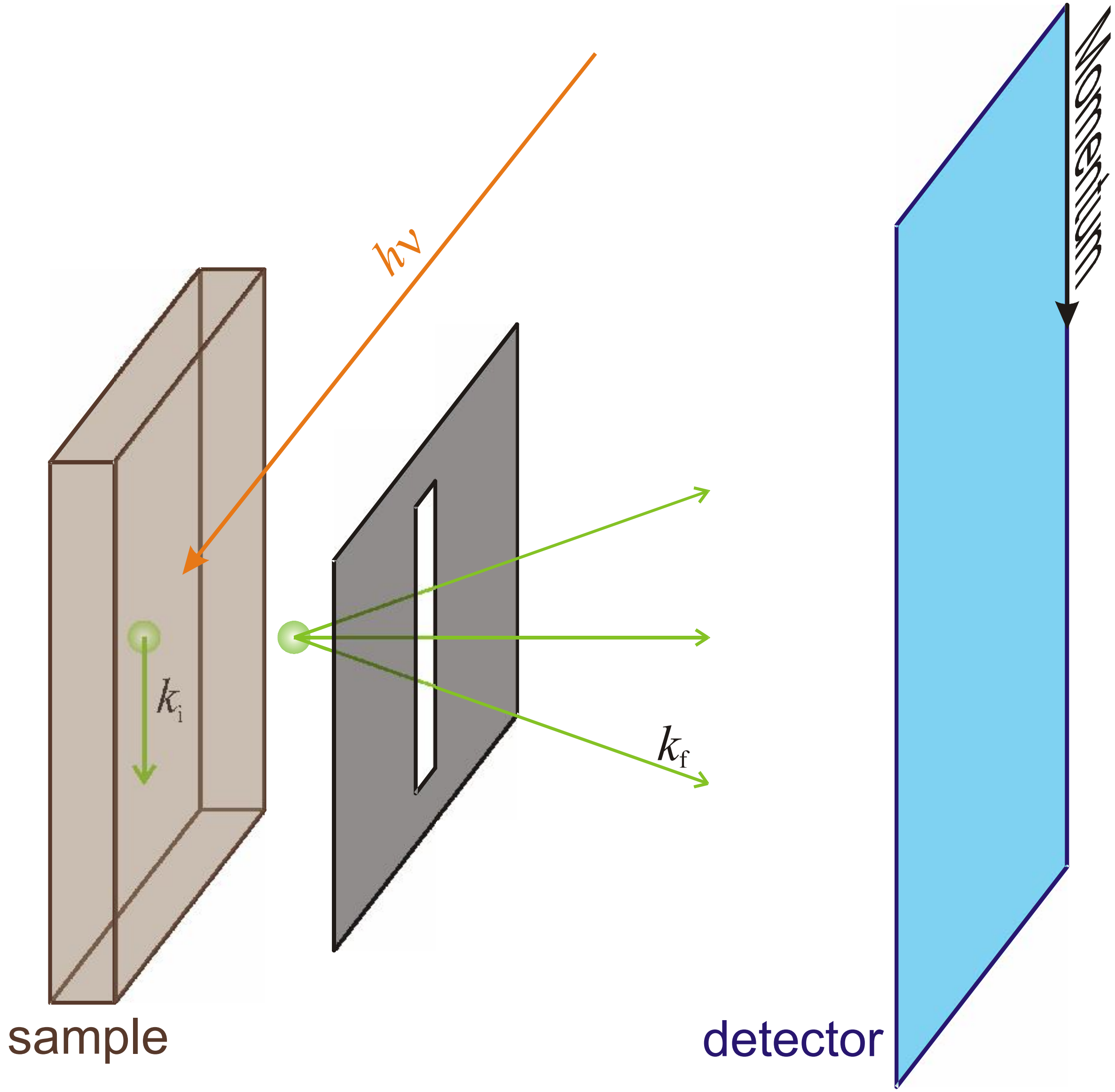

Angle-resolved photoemission

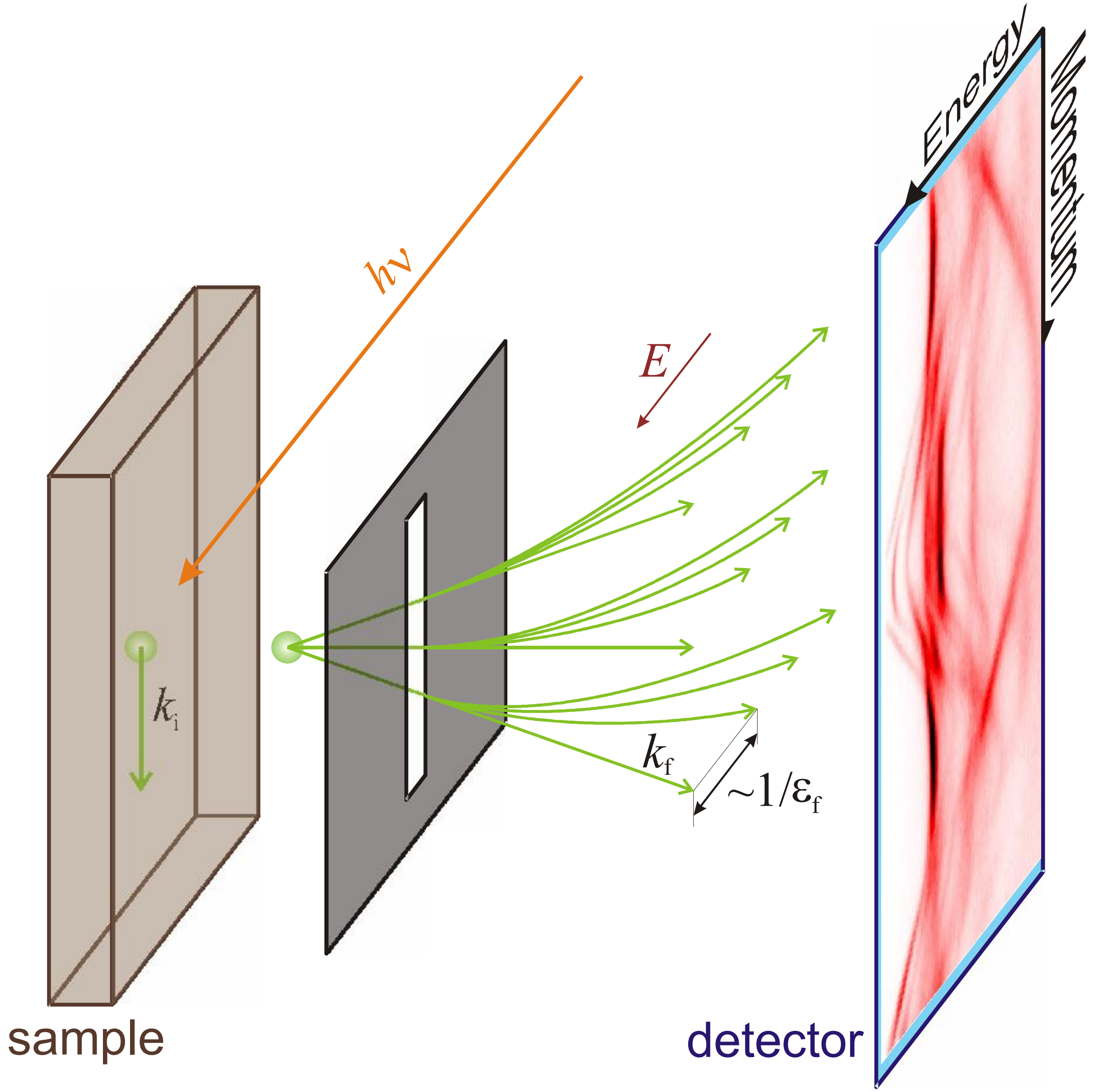

Angle-resolved photoemission spectroscopy (ARPES)

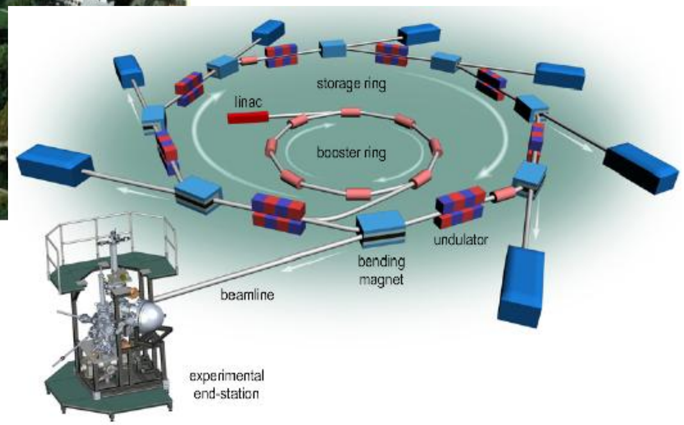

BESSY 1^3 station

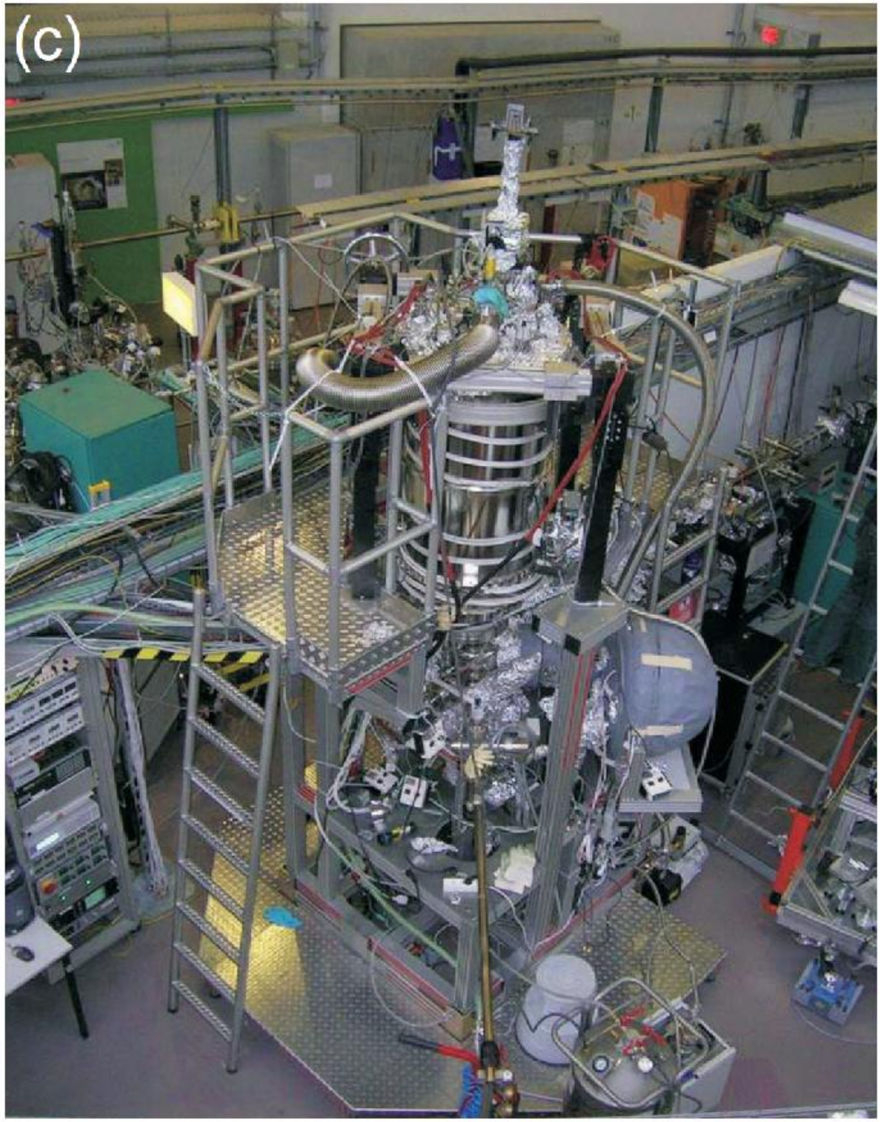

Scienta electron analyzer

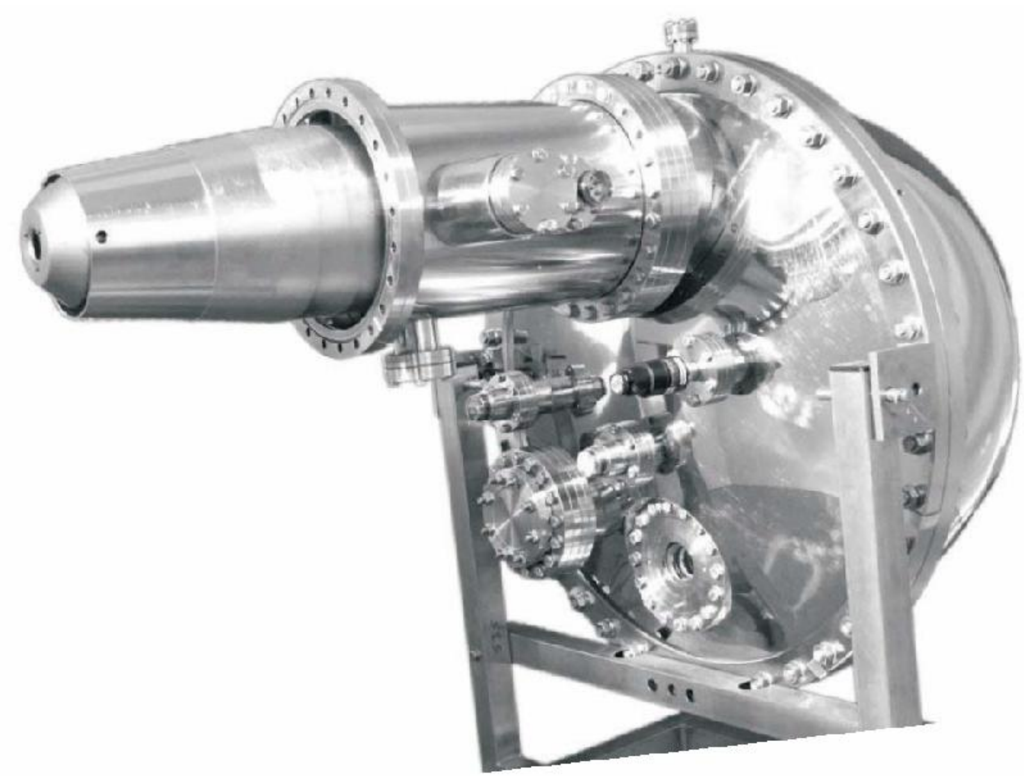

Sample preparation

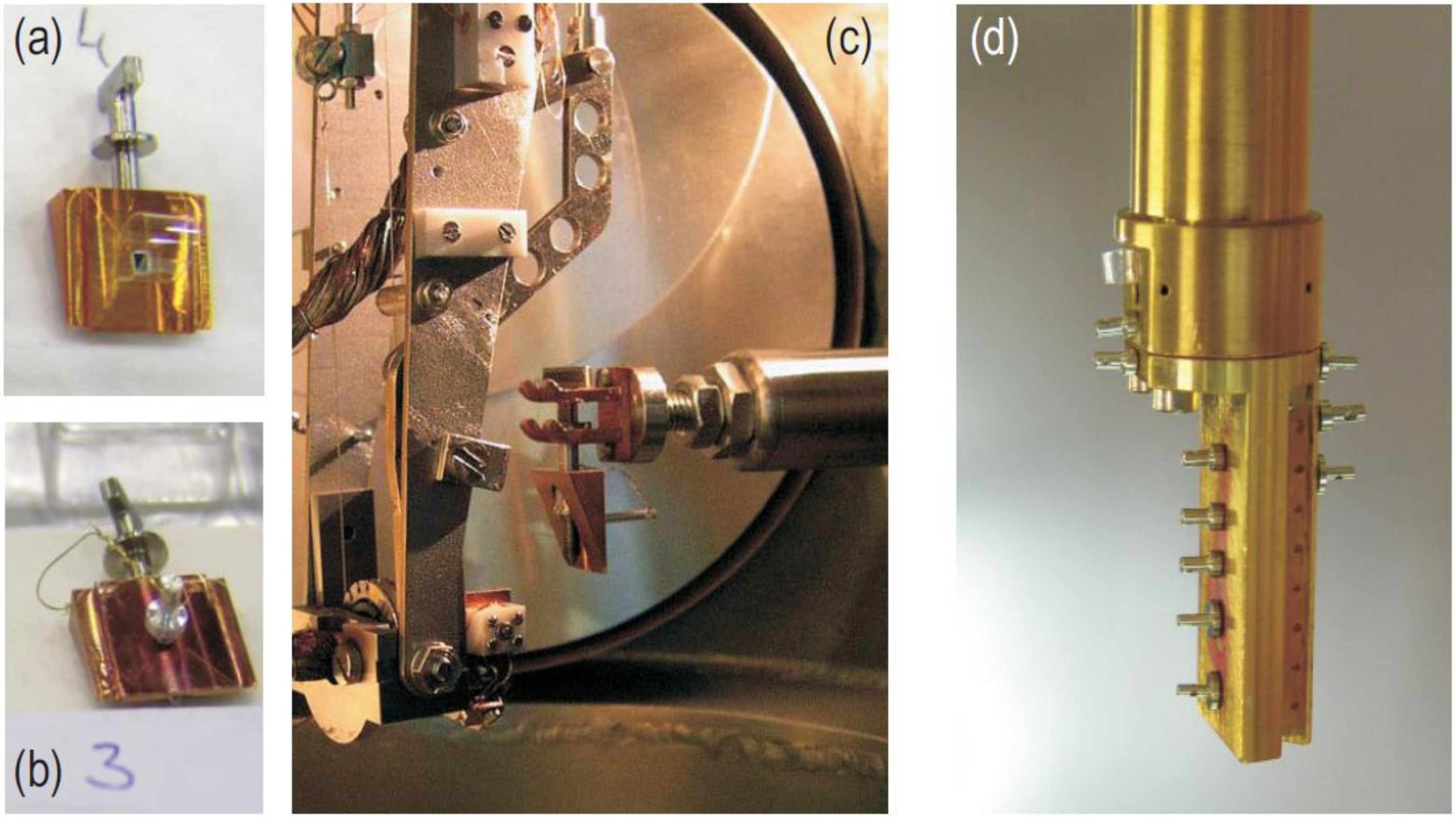

Sample preparation

BESSY 1^3 station

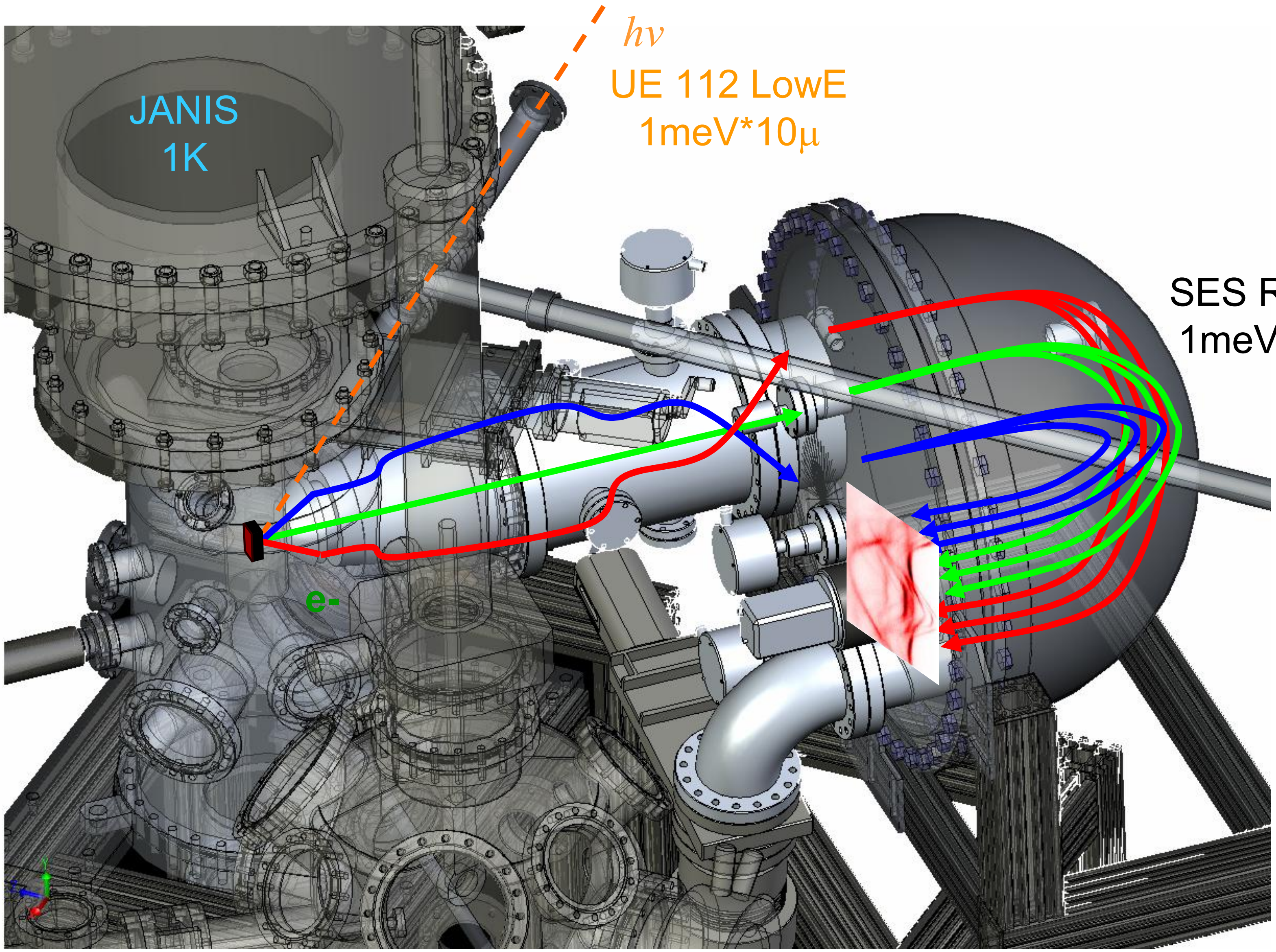

Unitary ARPES image

Electronic band dispersion

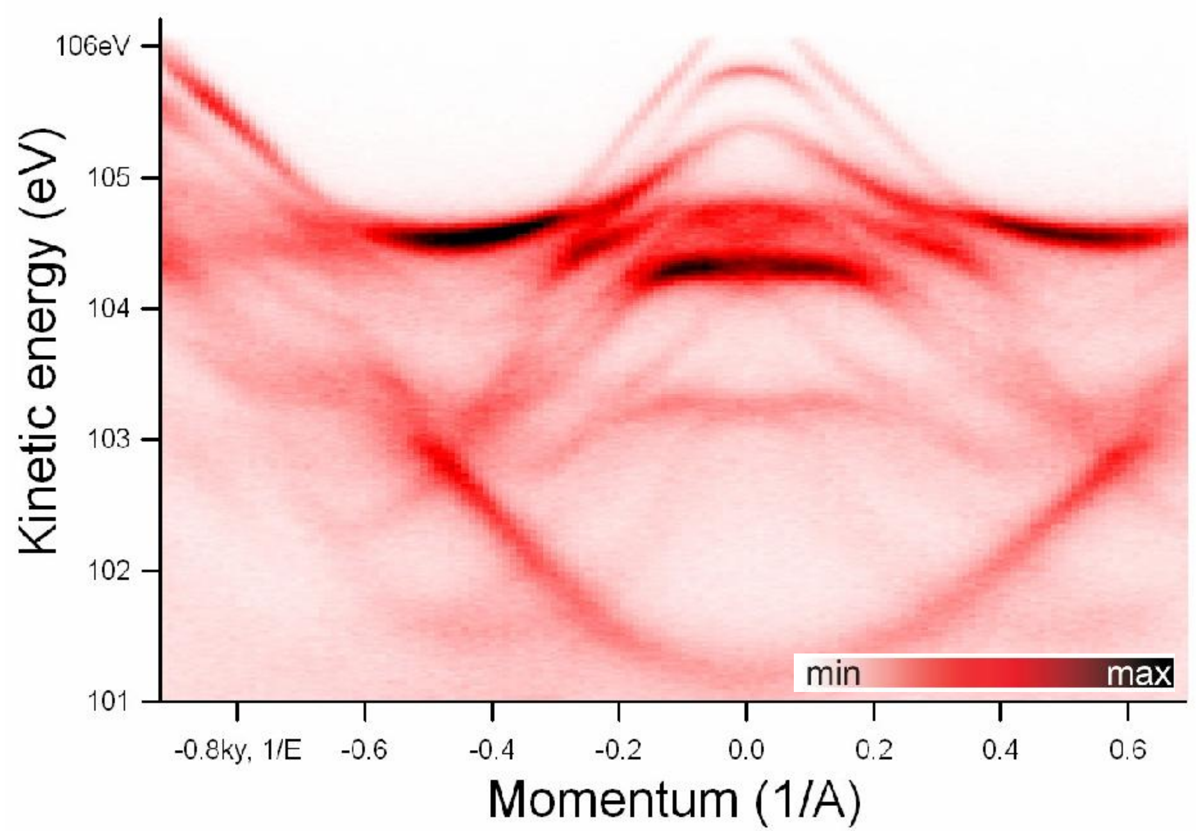

Unitary ARPES image

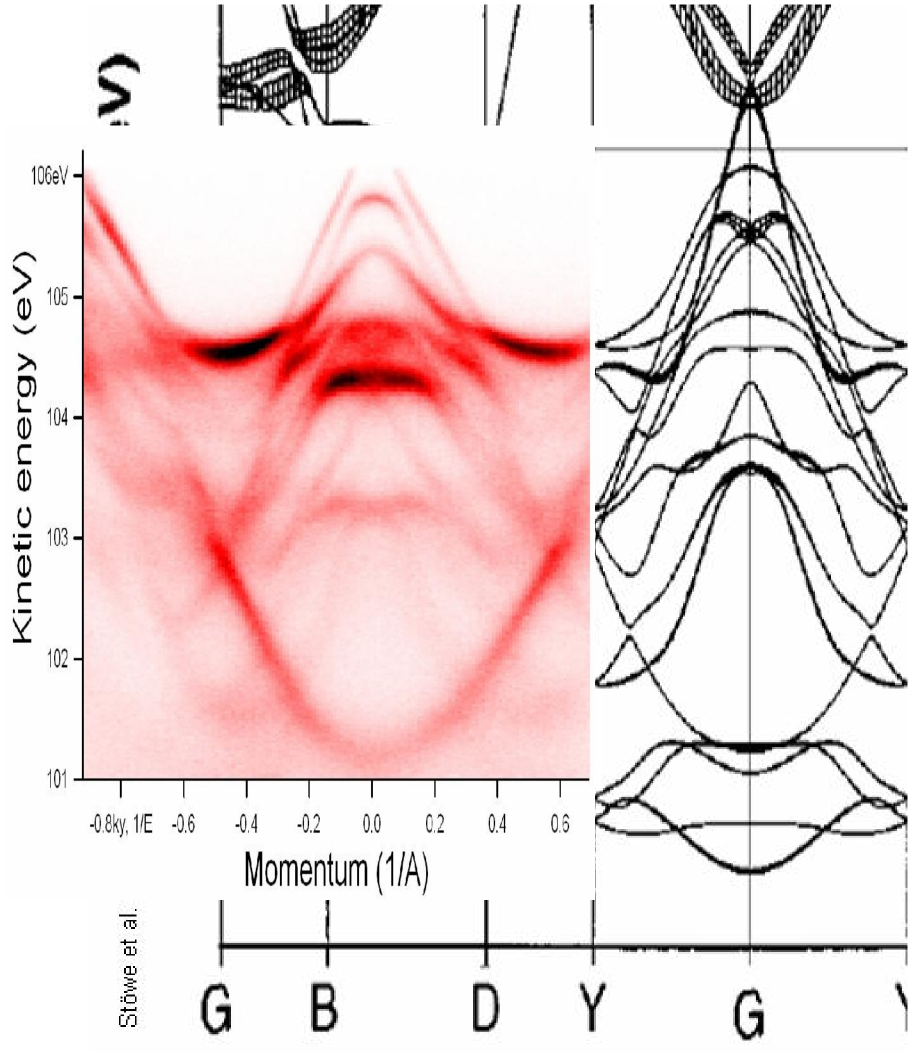

Band dispersion from ARPES

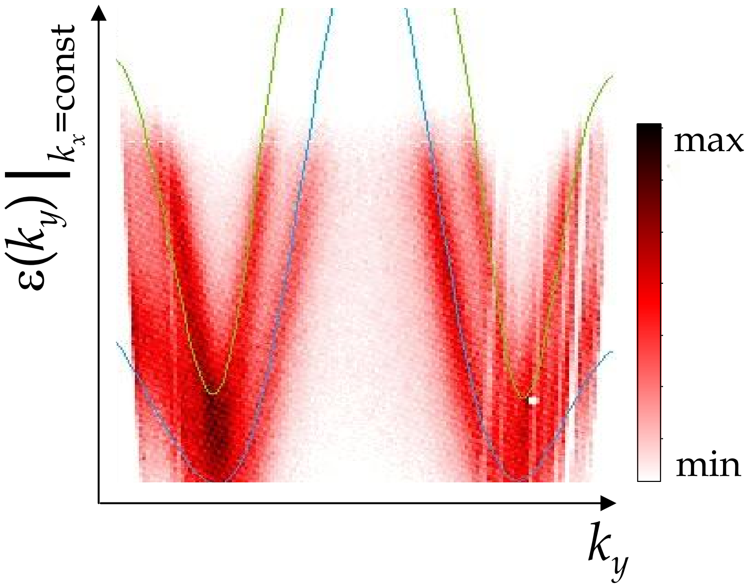

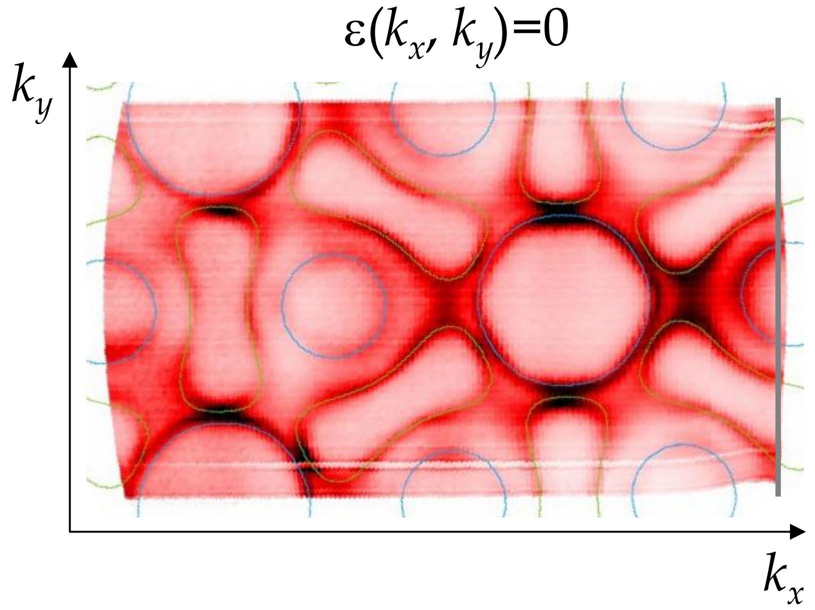

2H-$TaSe_2$

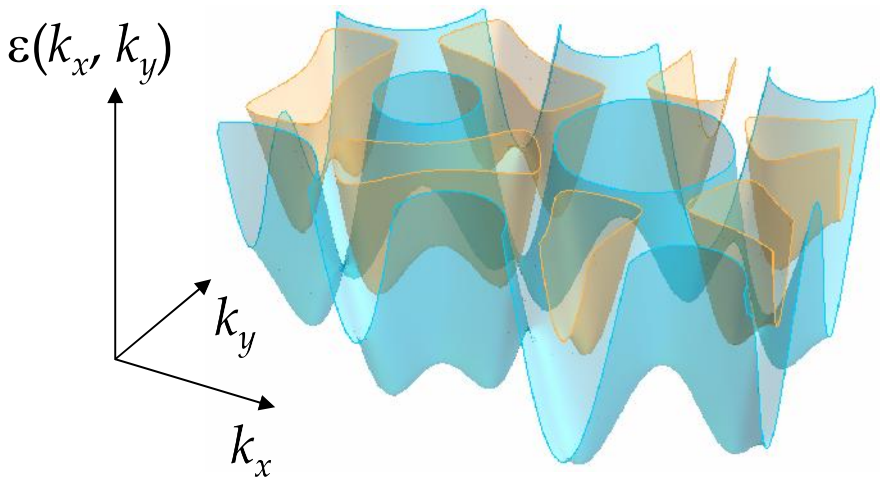

Another typical experimental data set: 1T-$TiSe_2$

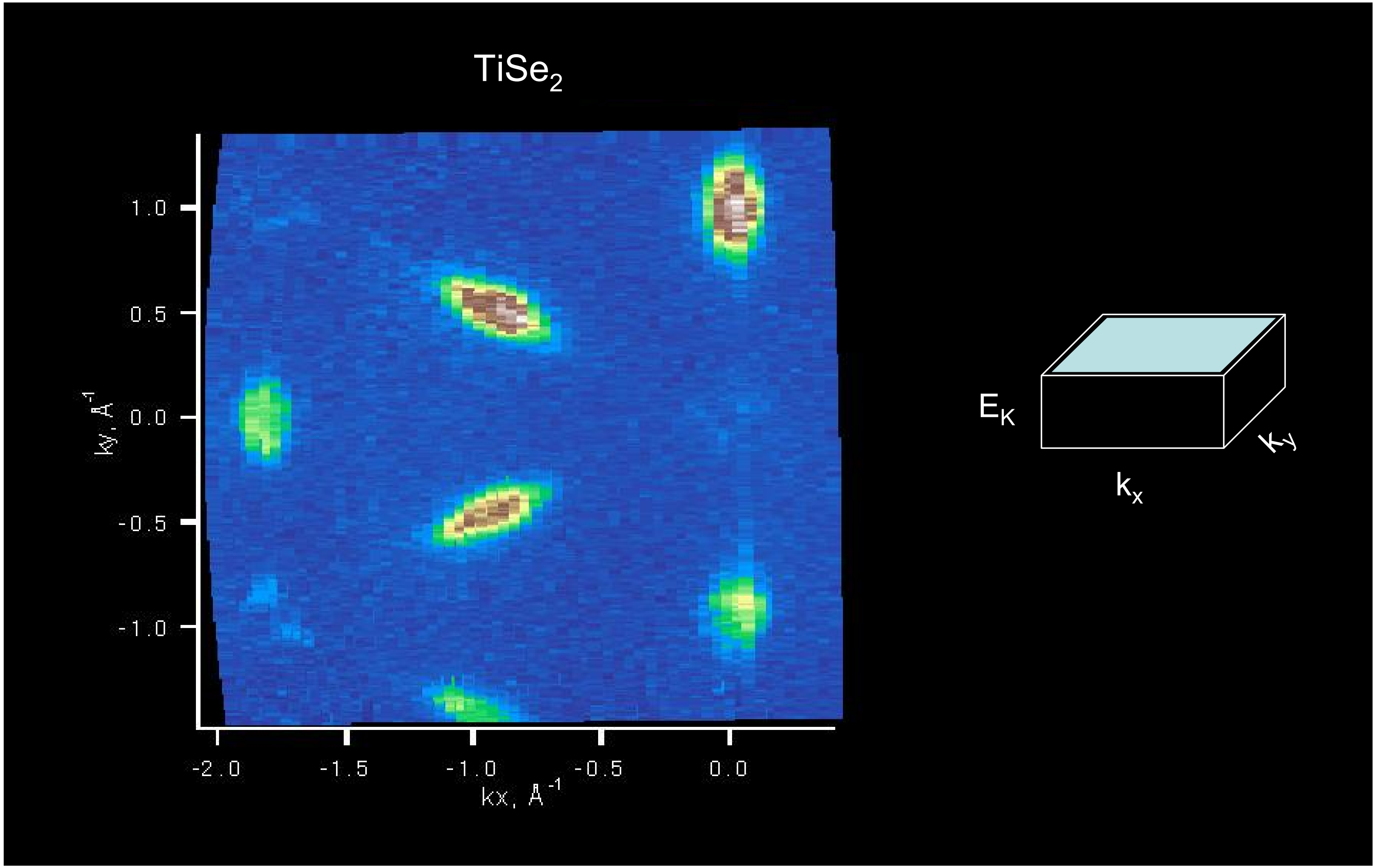

Another typical experimental data set: 1T-$TiSe_2$

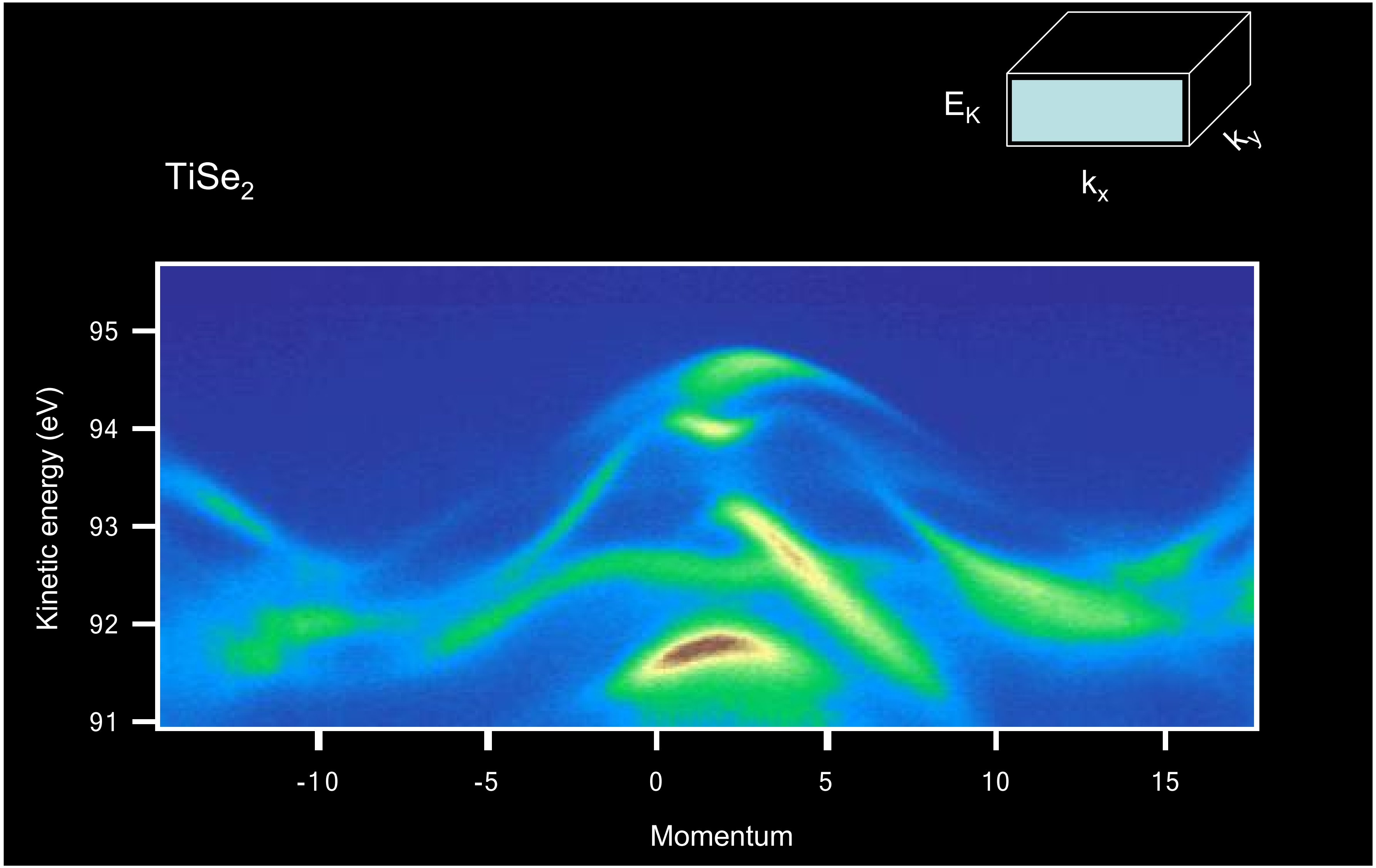

Beamline

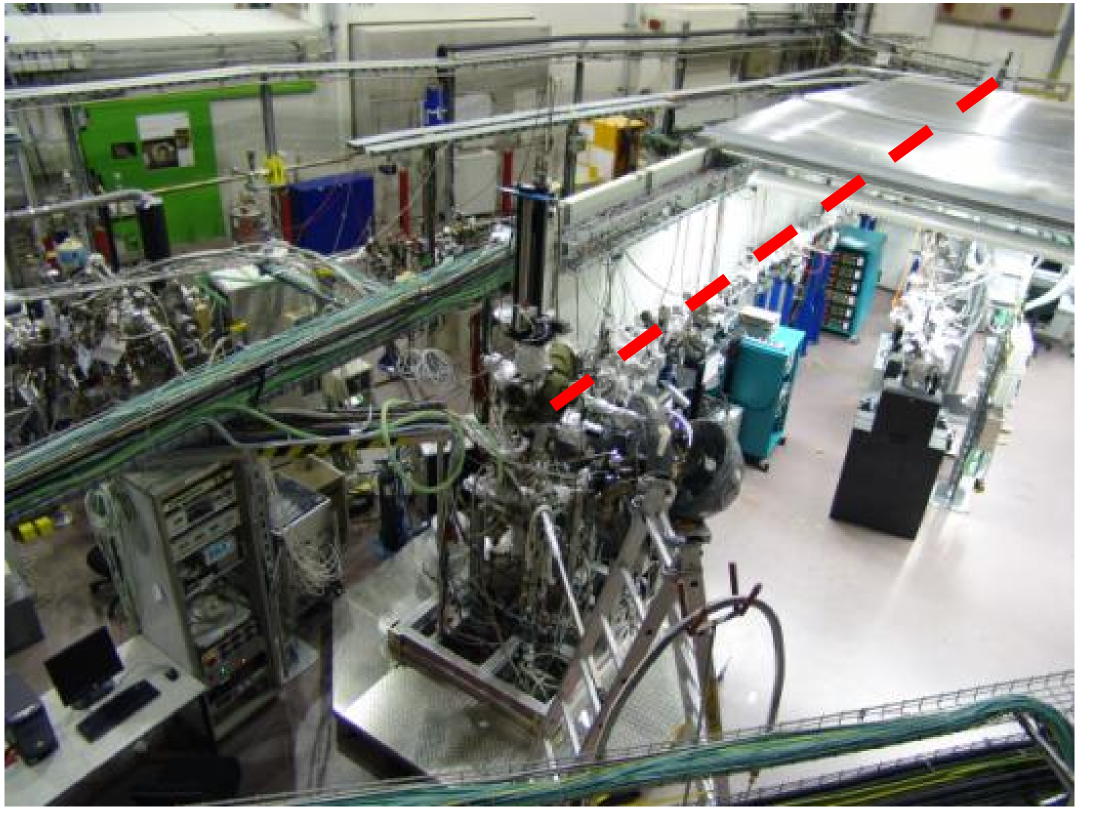

Excitation energy range

hν=9 eV

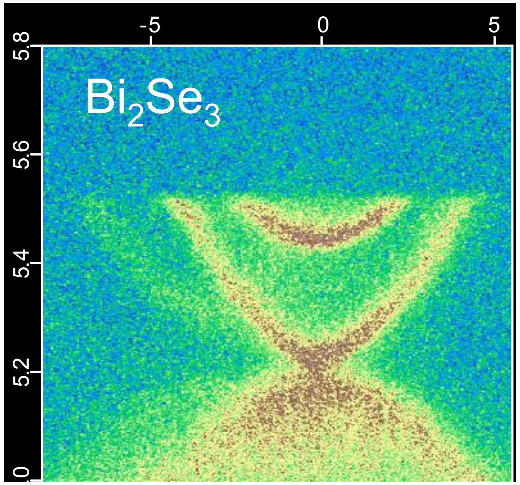

hν=200

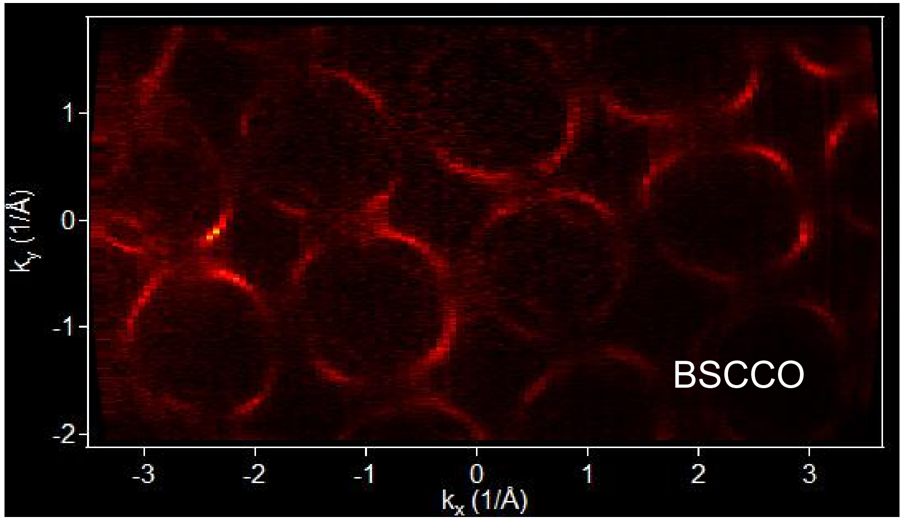

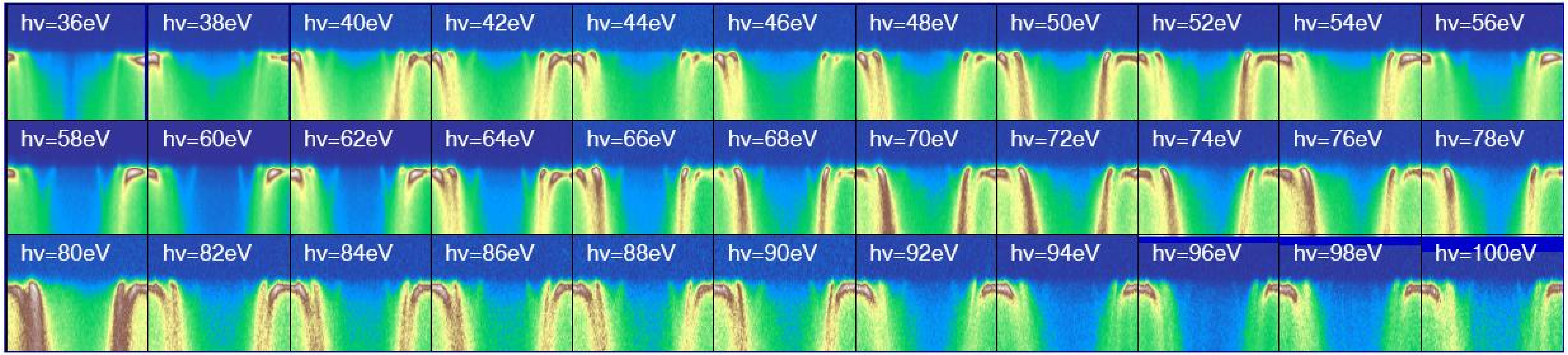

Cuprates

Fermi surface

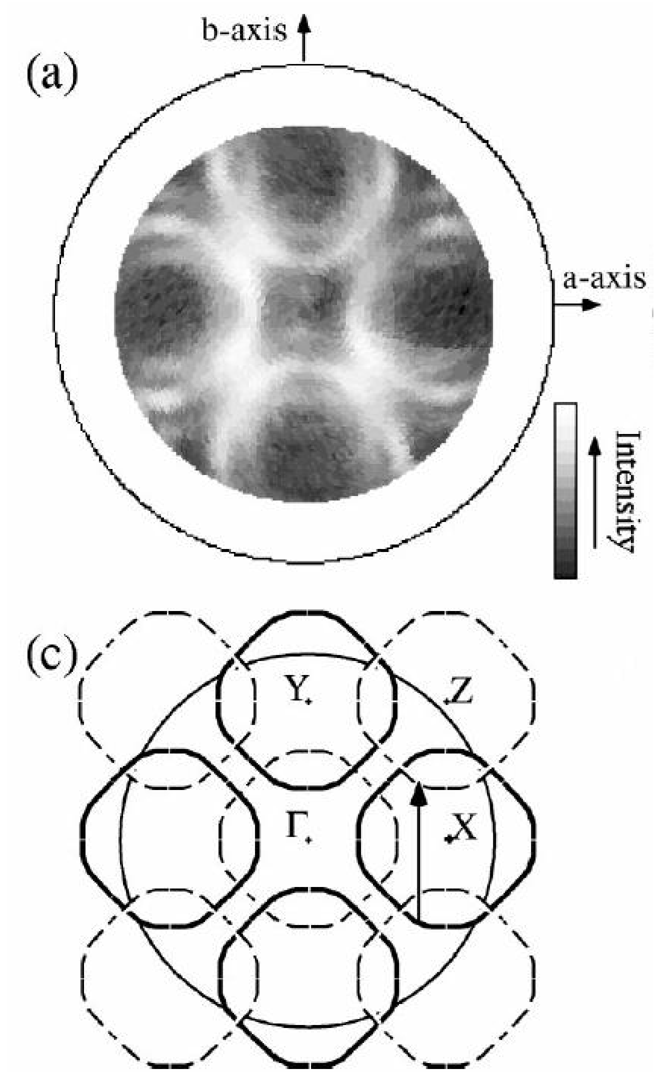

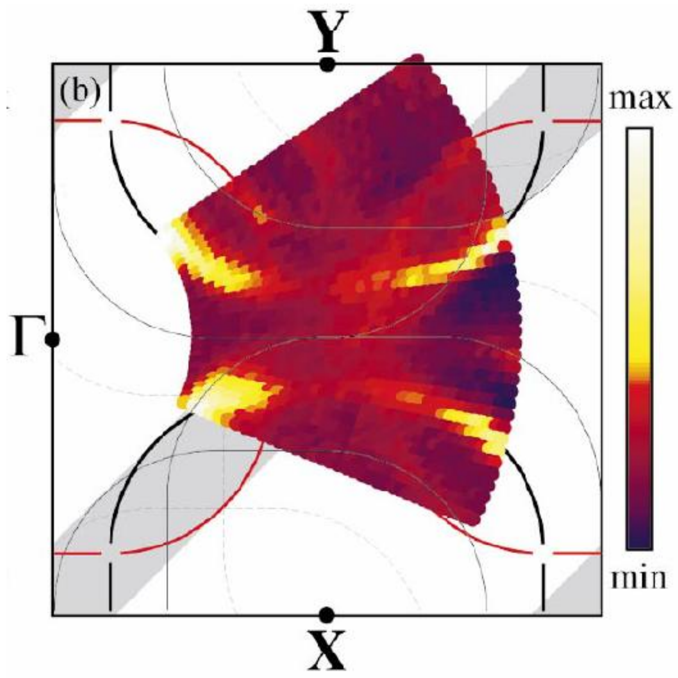

Aebi *et al*. (1996)

Borisenko *et al*. (1999)

d-wave

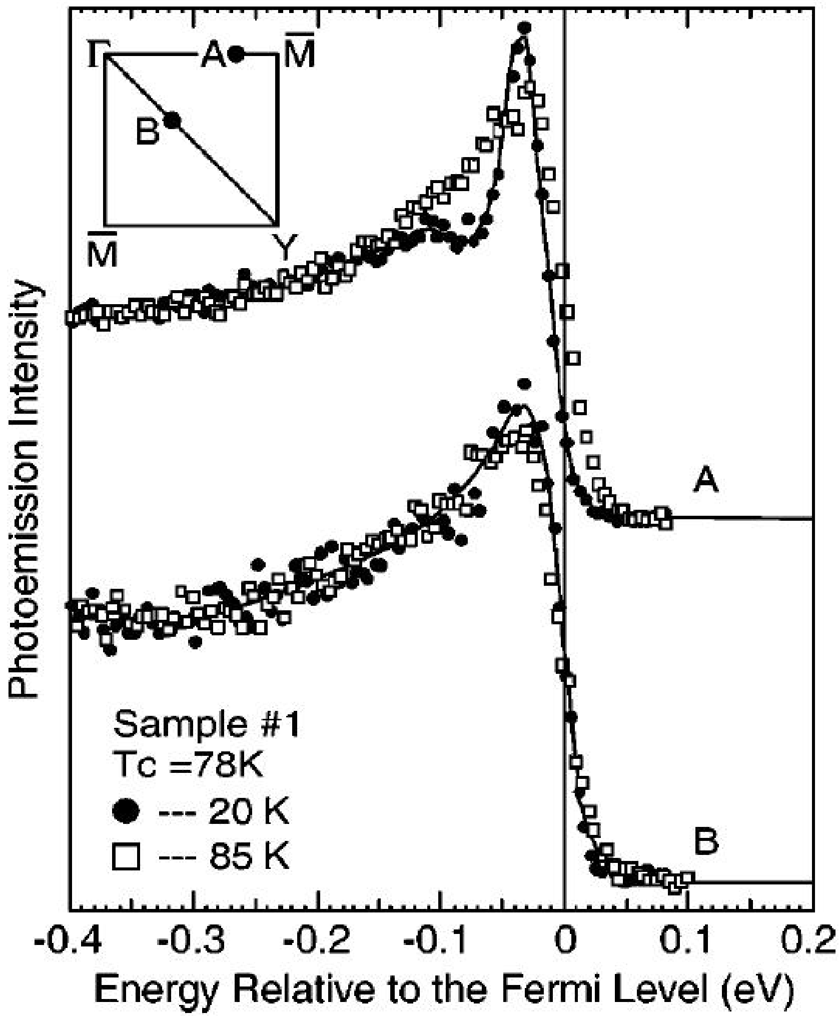

Shen *et al*. (1993)

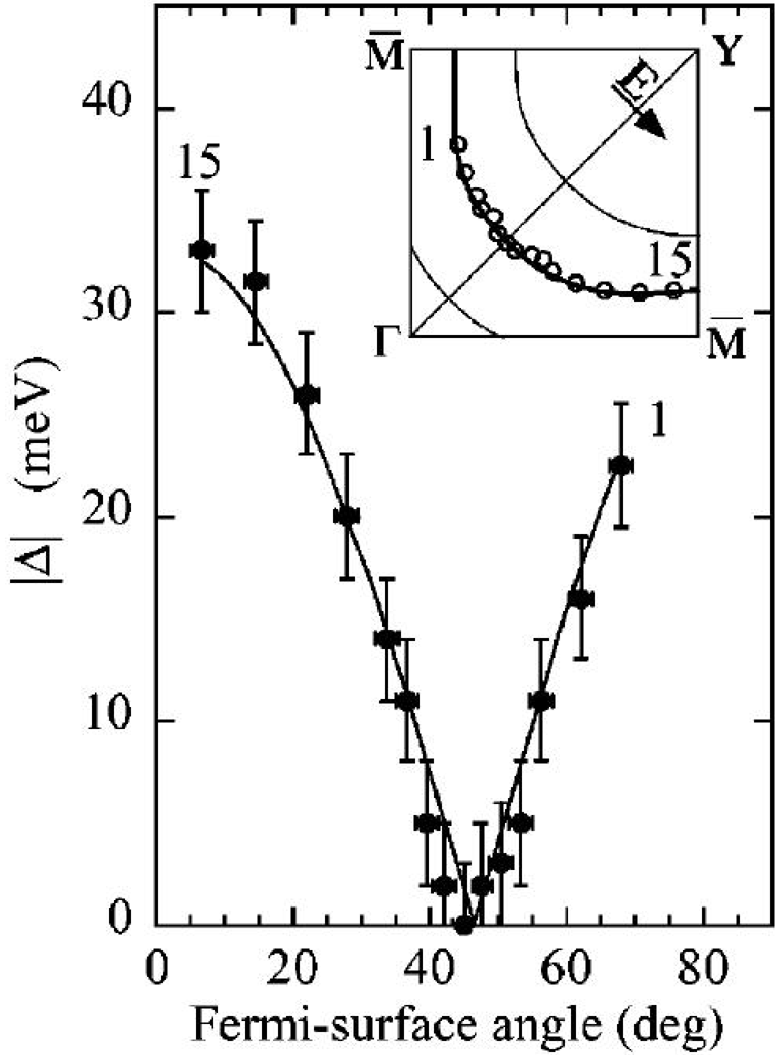

Ding *et al*. (1996)

Effects of interaction with bosonic mode

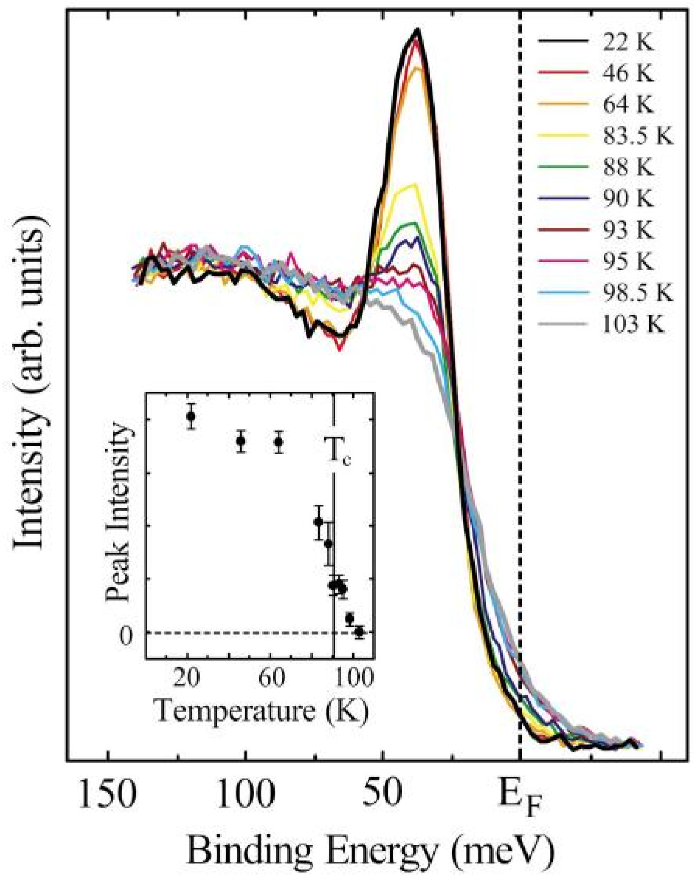

Fedorov *et al.* (1999)

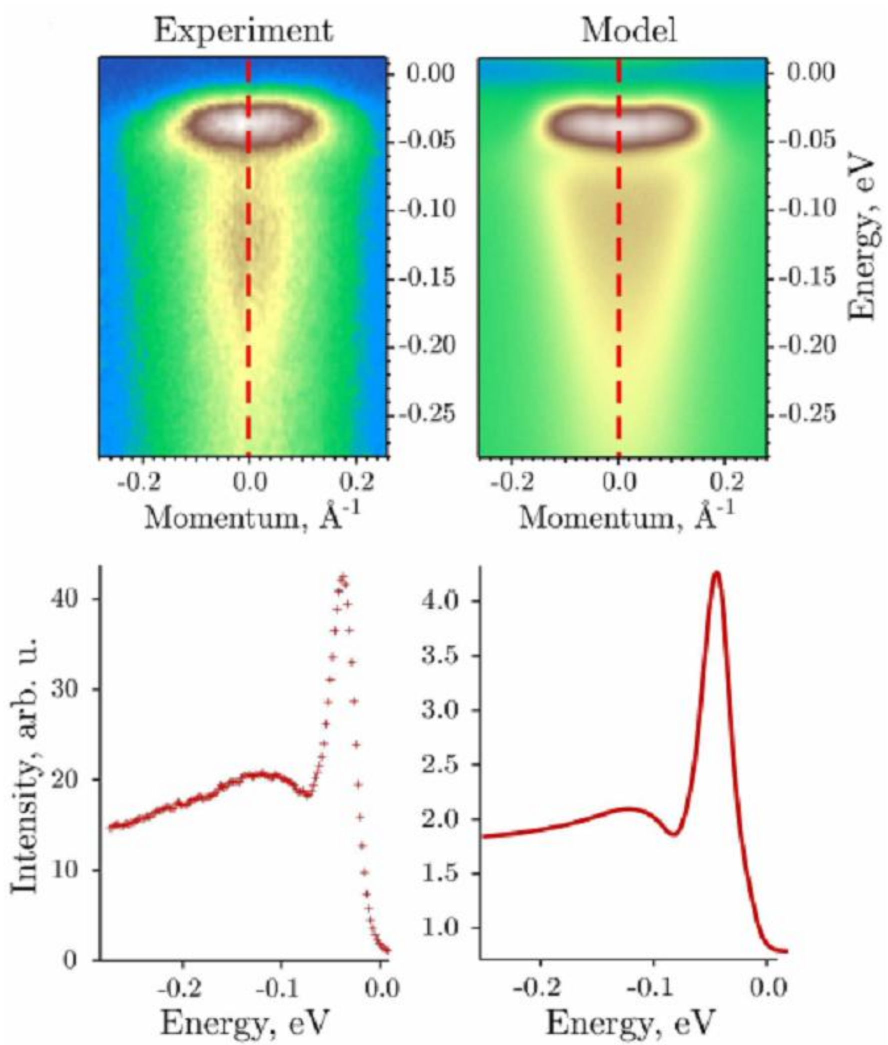

Inosov *et al.*, *PRB* (2006)

Pseudogap

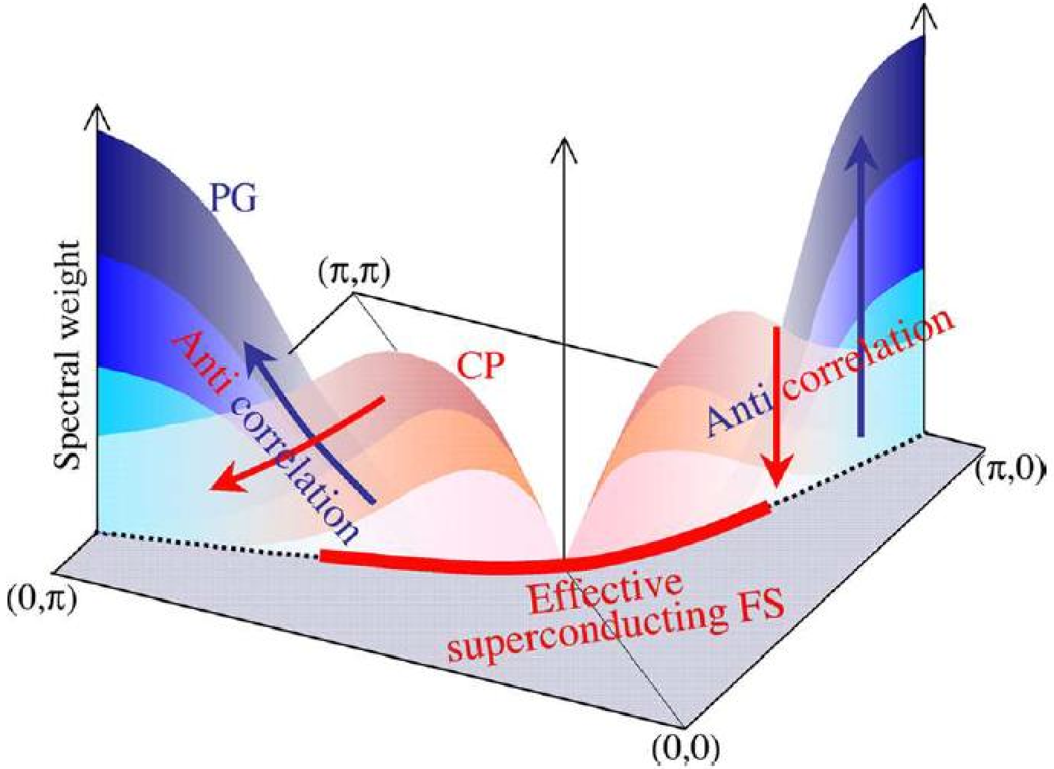

Kondo *et al.*, *Nature* (2009)

ARPES data analysis

Ideal and measured signal

$$g(x) = [f \otimes R](x)$$

$$f = g \otimes^{-1} R$$

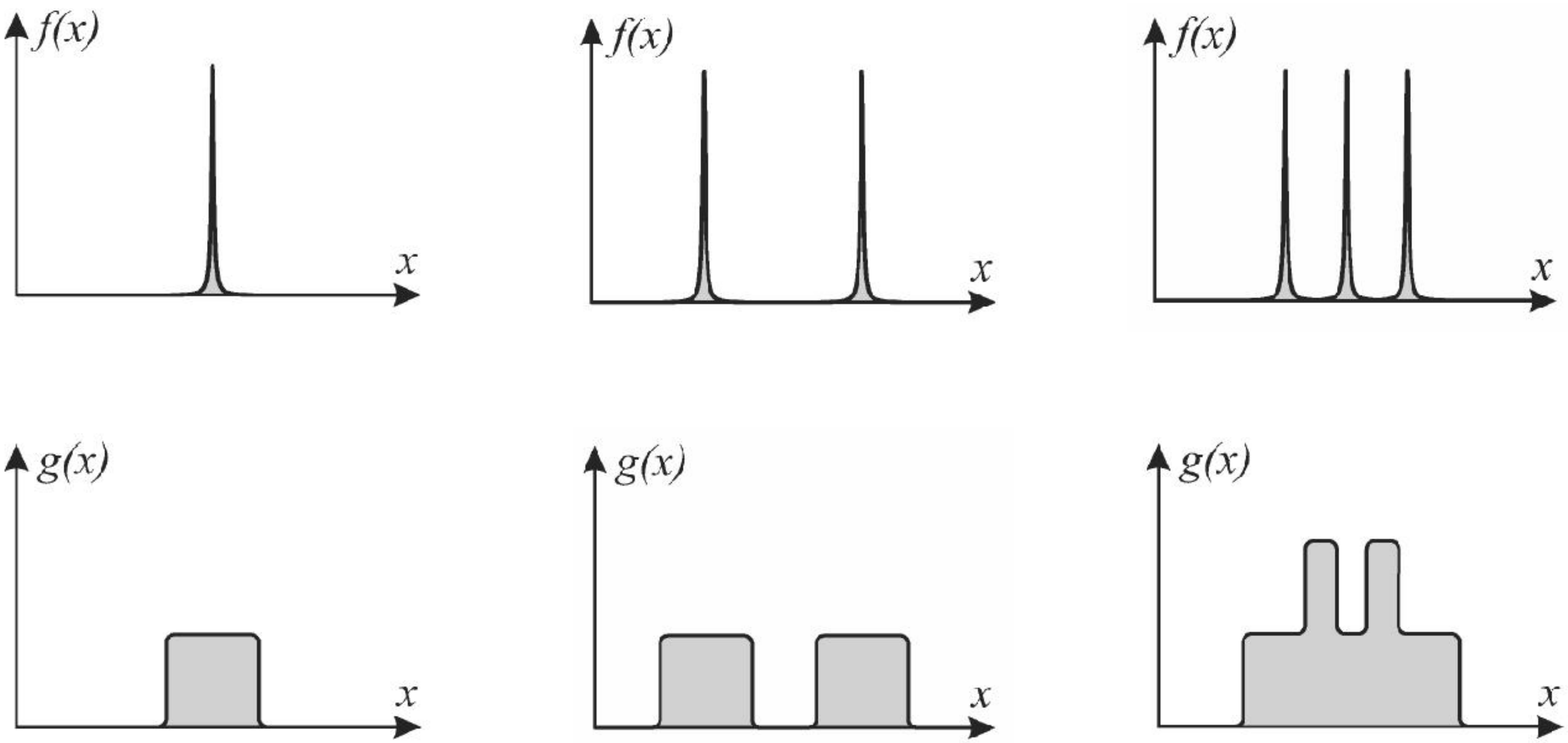

Nodal Direction of cuprates

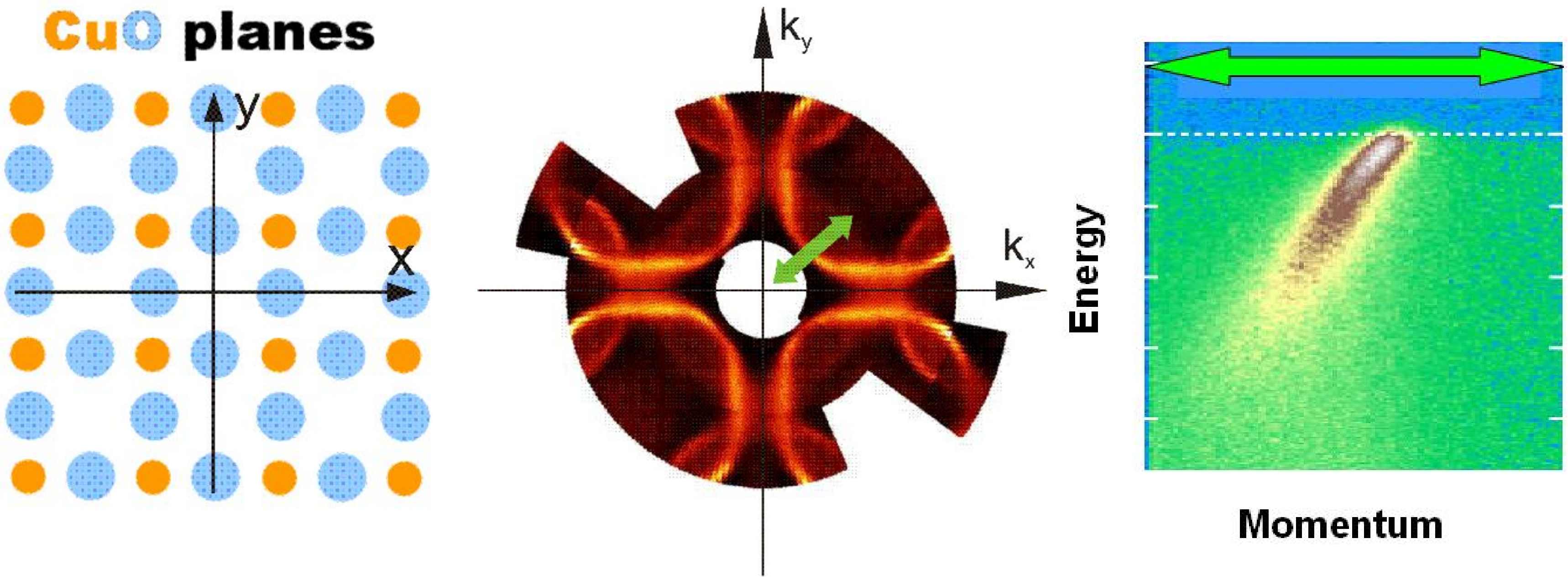

No gap

Voigt fit of energy-momentum cut

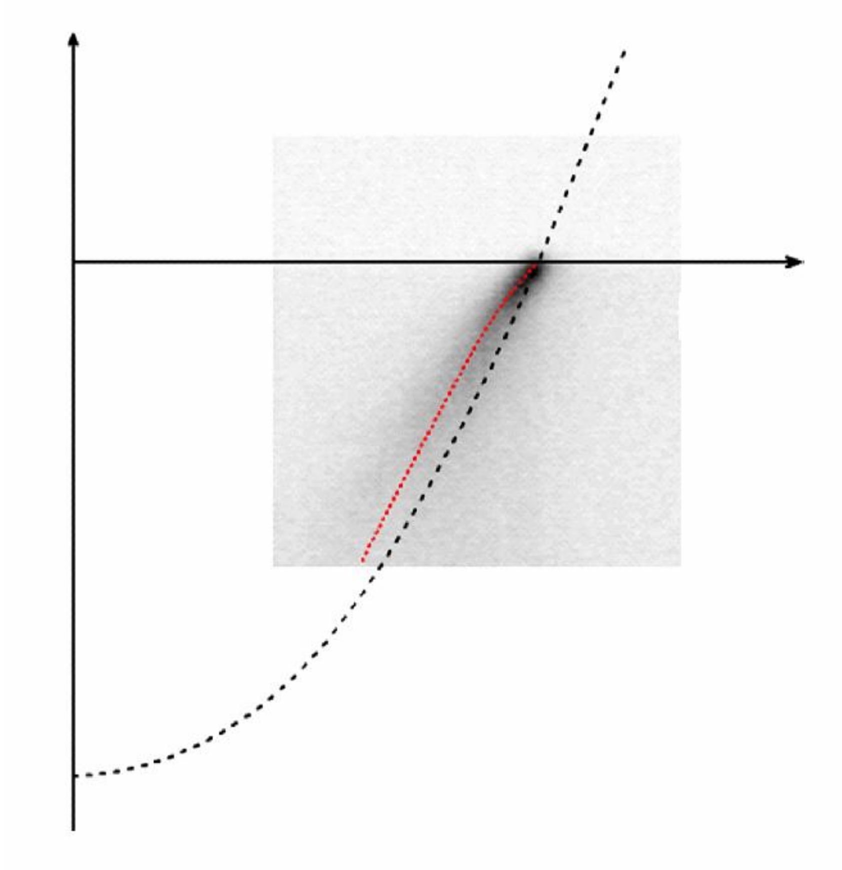

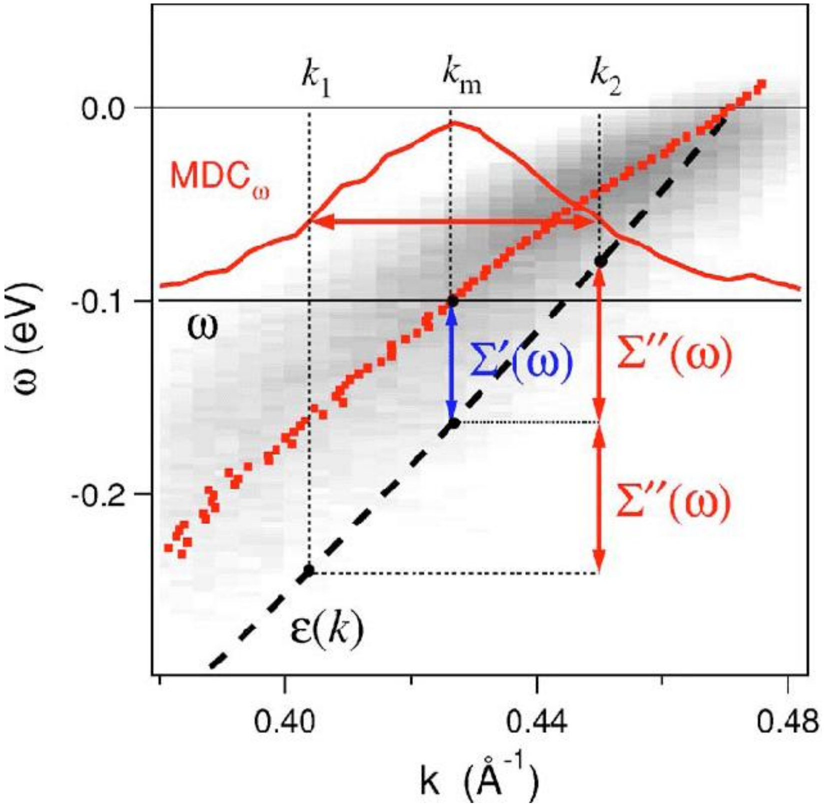

Evtushinsky *et al.*, *PRB* (2006)

Spectral Function Extraction from ARPES Data

$$I(k, \omega) \propto A(k, \omega) \otimes R(k, \omega)$$

We measure $I(k, \omega)$

We are interested in $A(k, \omega)$

We need to remove $R(k, \omega)$

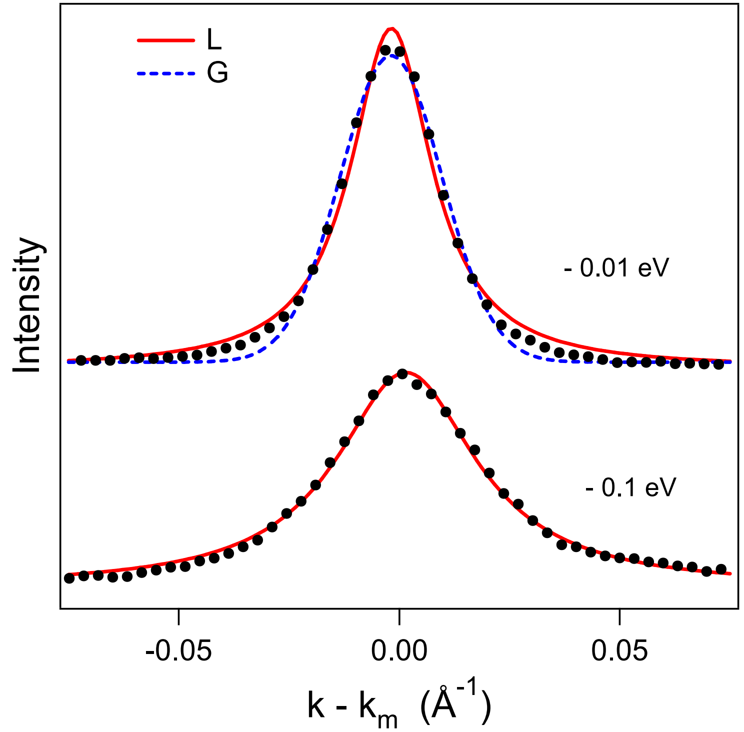

Spectral line shape

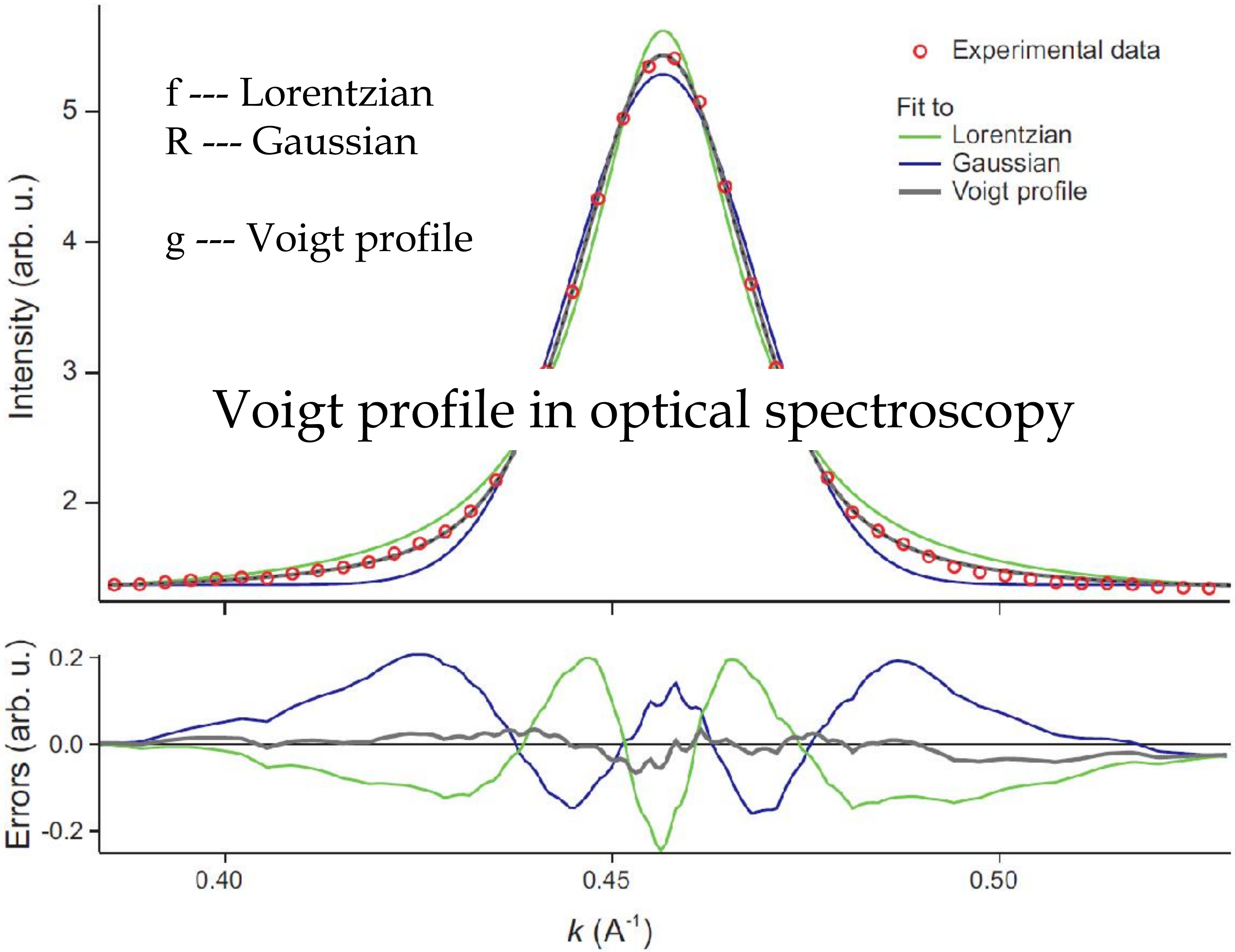

f --- Lorentzian
R --- Gaussian

g --- Voigt profile

Voigt profile in optical spectroscopy

Linewidth from Voigt Fit

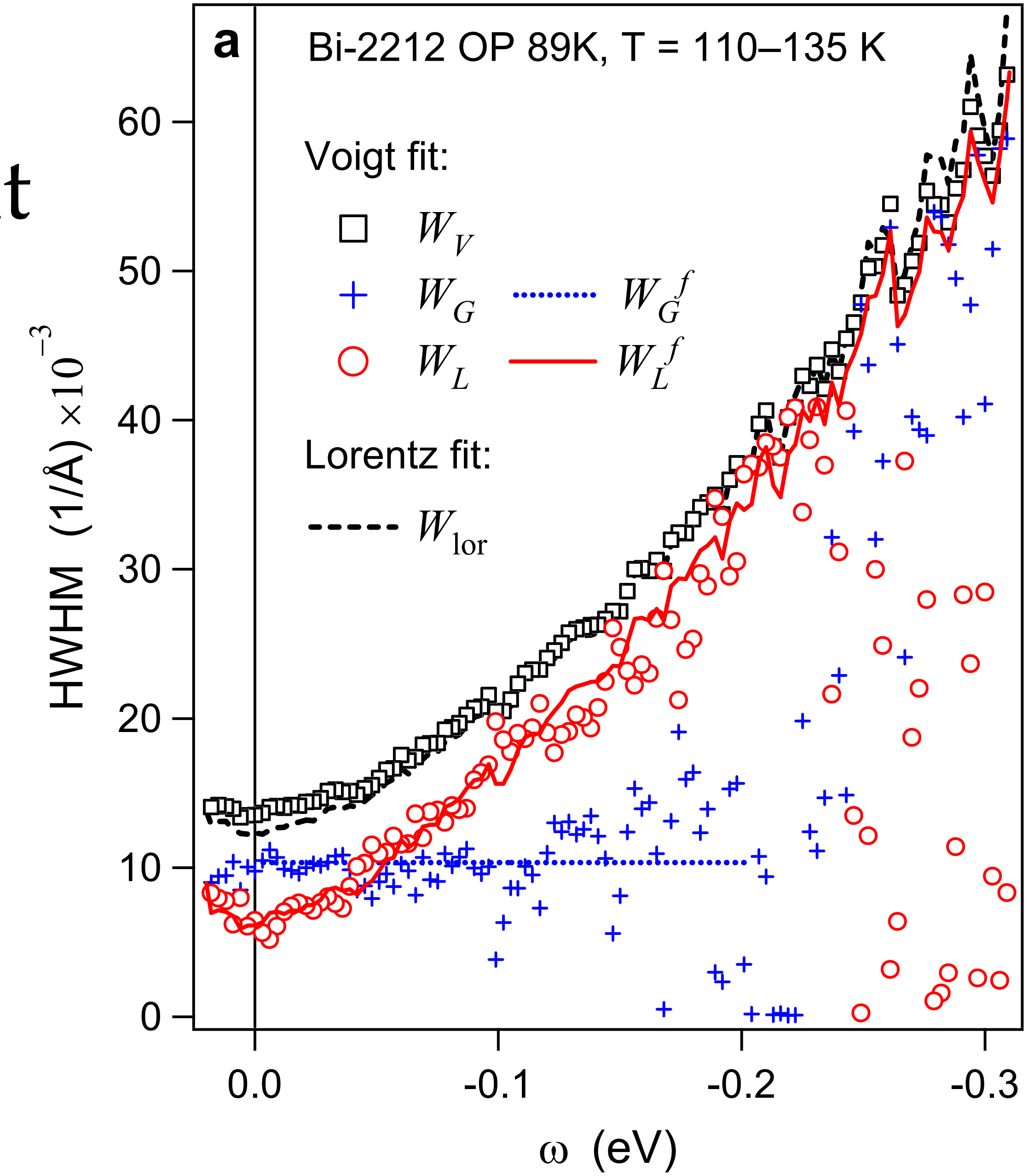

Evtushinsky *et al.*, *PRB* (2006)

Linewidth from Voigt Fit

Intrinsic width, W_L

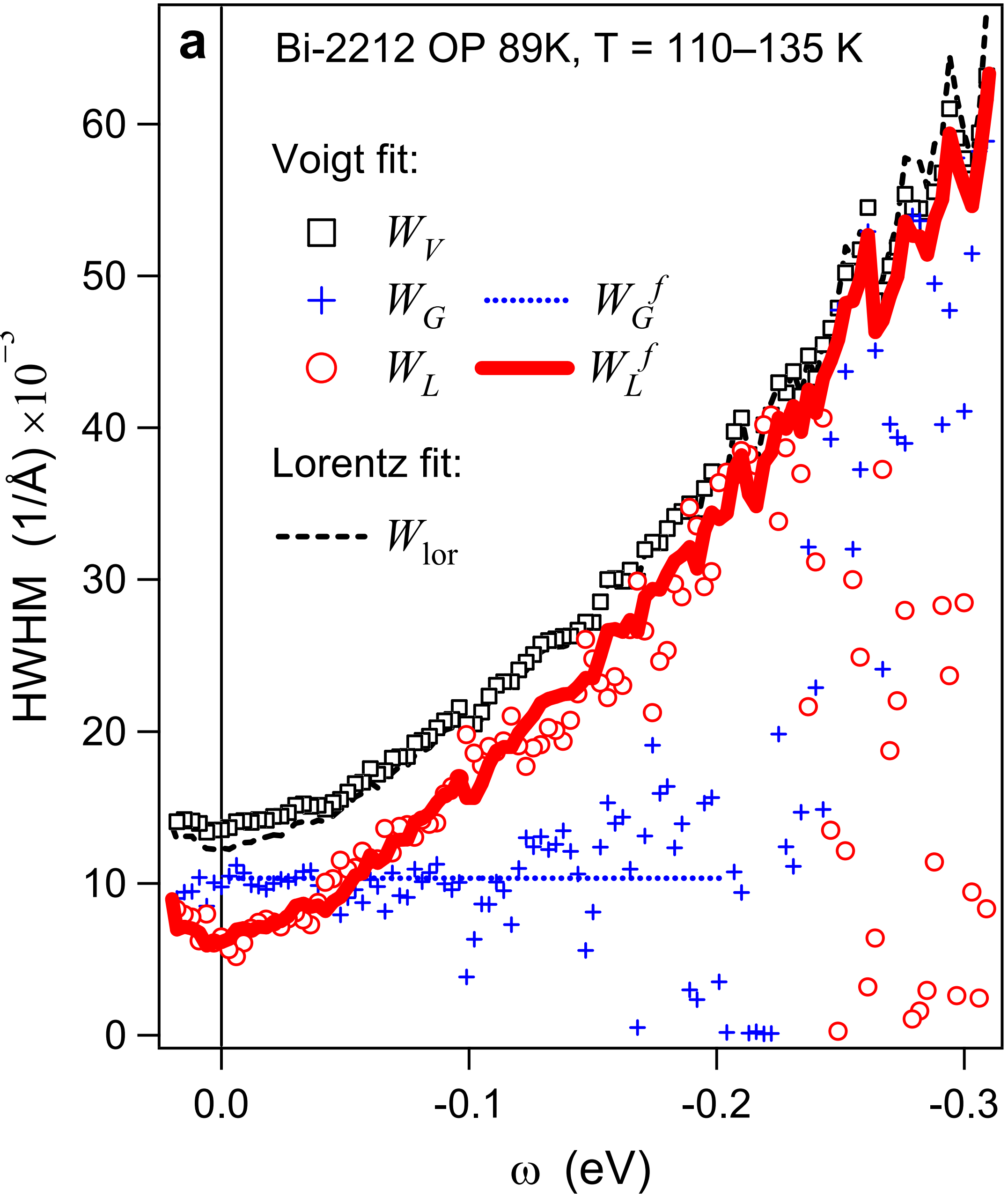

Evtushinsky *et al.*, *PRB* (2006)

Linewidth from Voigt Fit

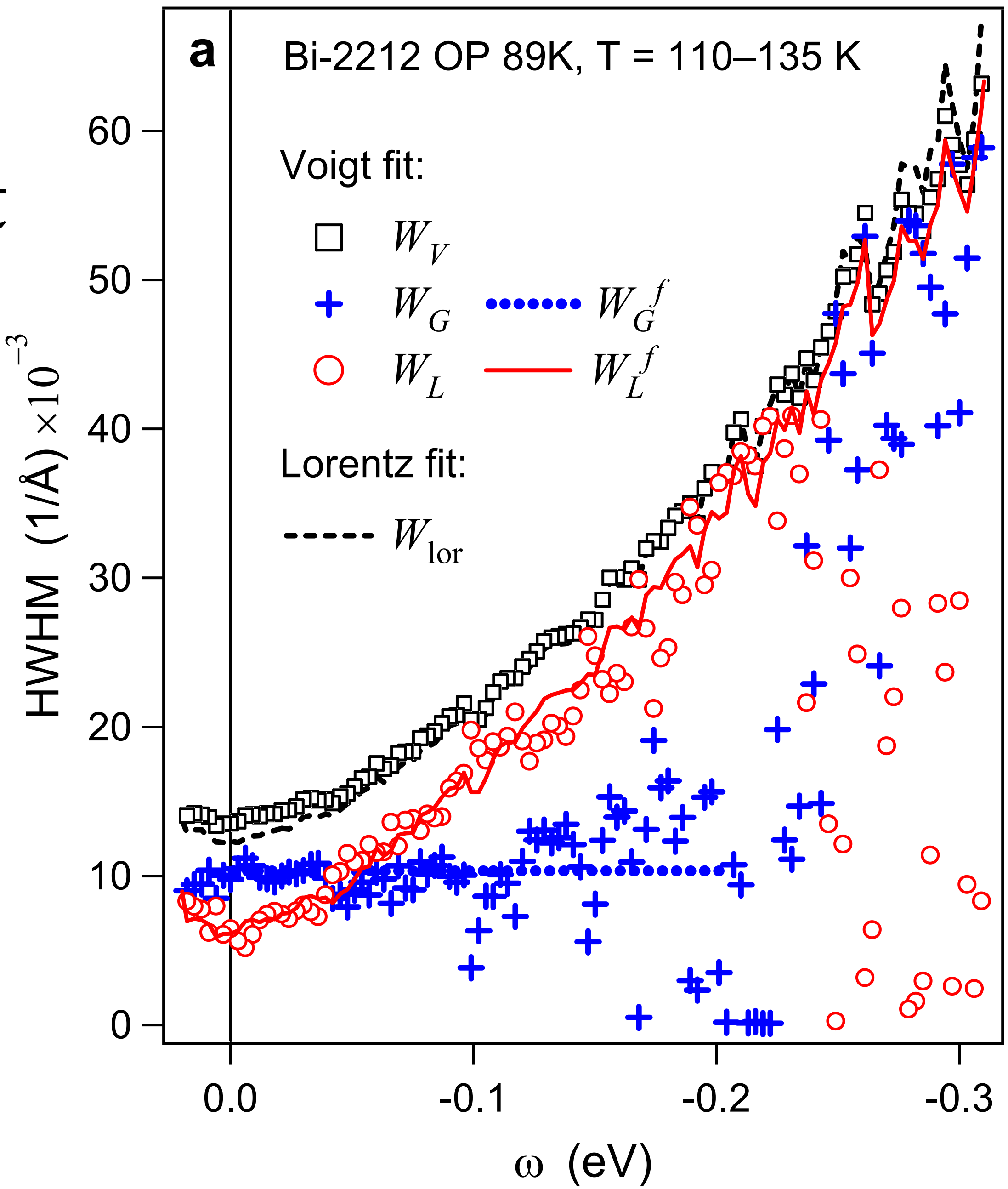

Resolution:

W_G=*const*

Evtushinsky *et al.*, *PRB* (2006)

Comparison to the low-energy high-resolution data

$R \sim (h\nu - \phi)^{-1/2}$

$R_{6eV\ LASER}/R_{27eV\ synchrotron} = 0.25$

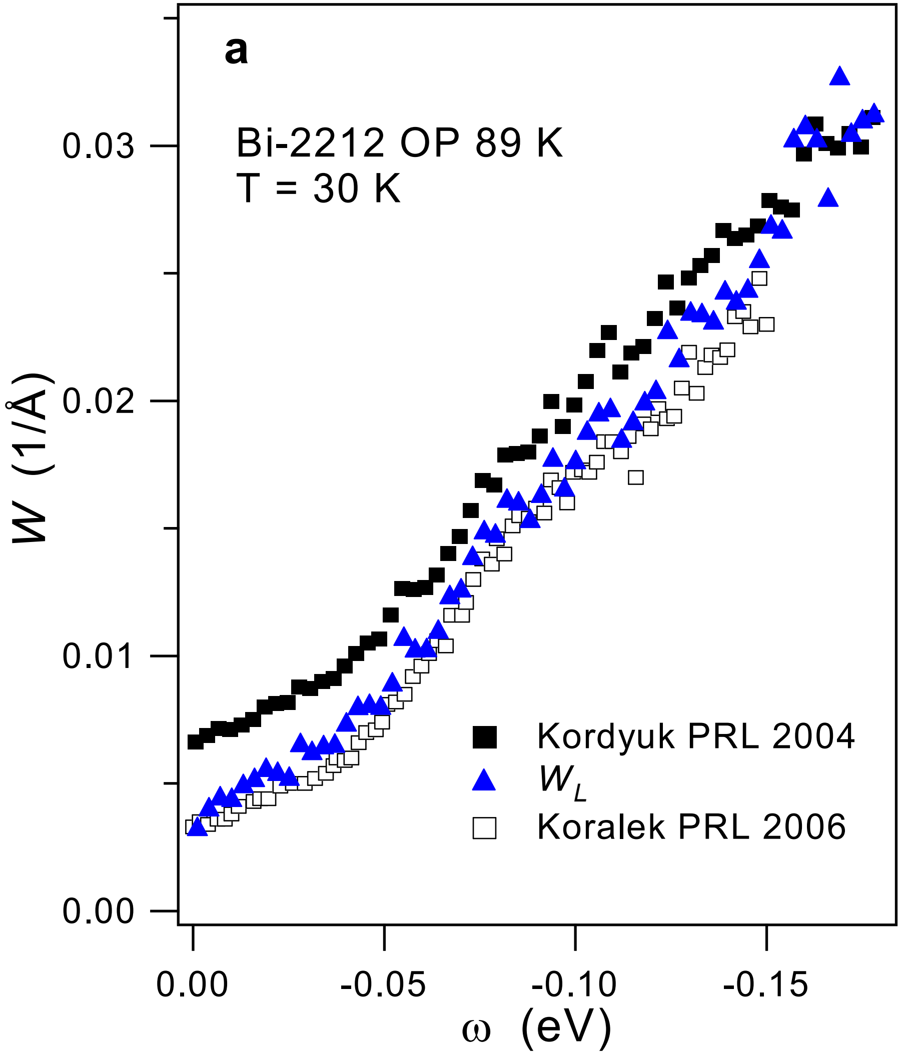

J. D. Koralek *et al.*, PRL 2006

Temperature dependence of scattering rate

$\Sigma''(\omega=0,T)$

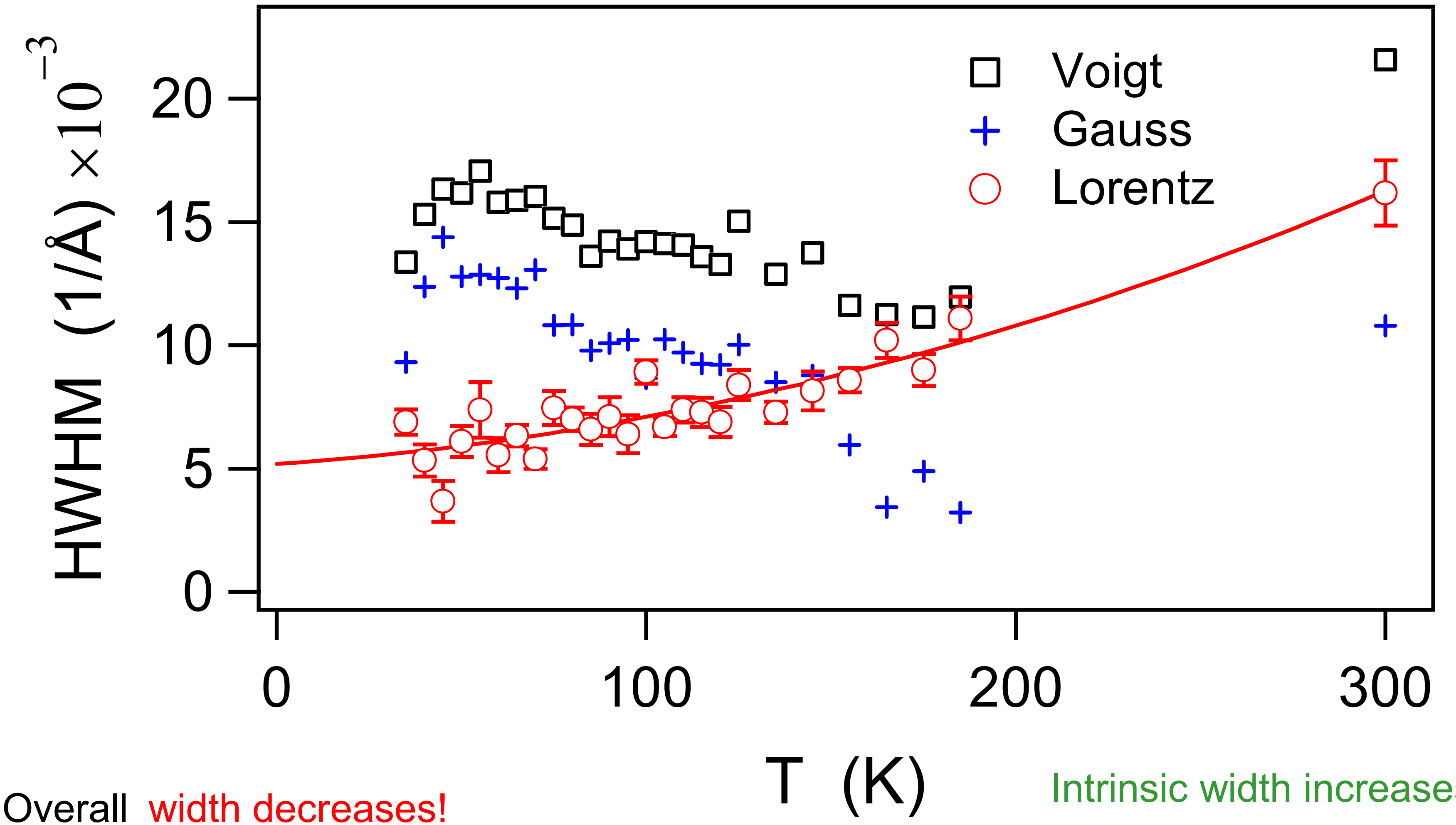

Overall width decreases!

Intrinsic width increases

Temperature dependence of scattering rate

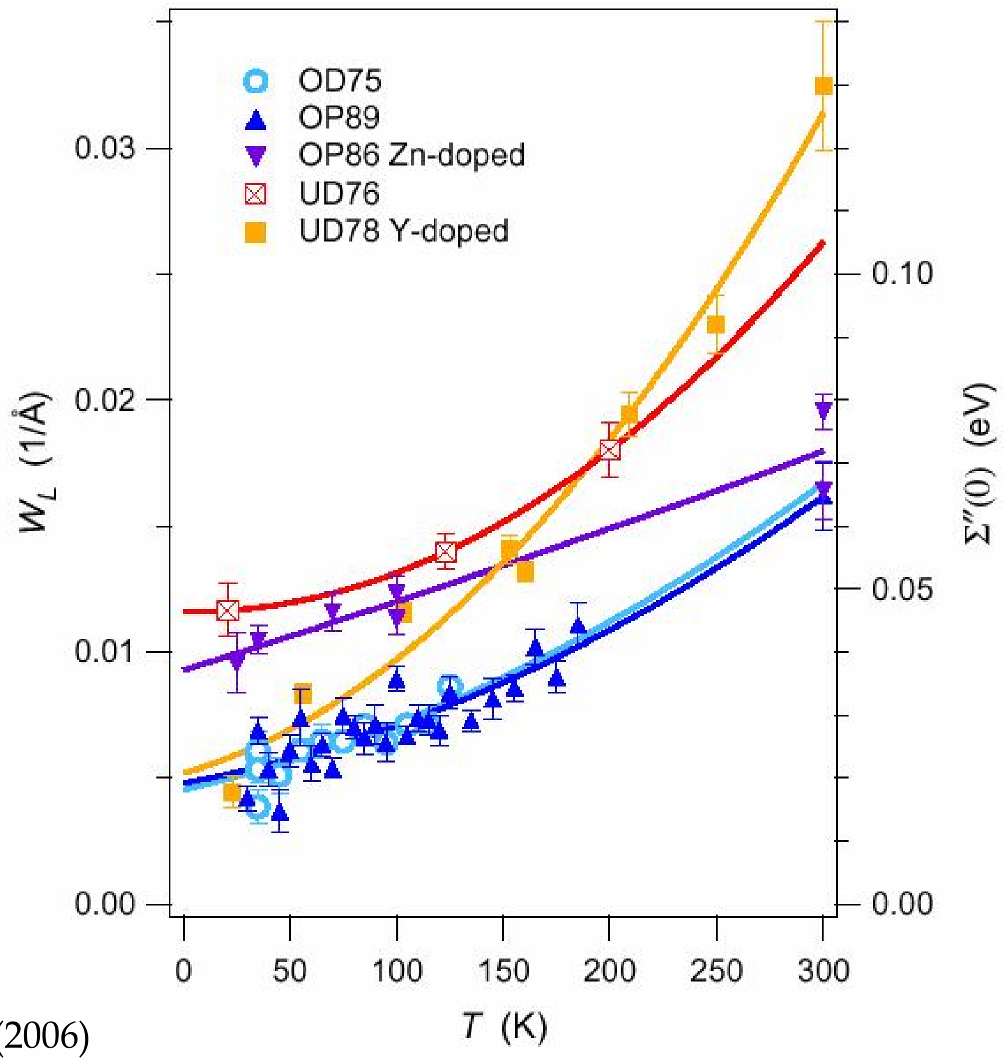

Evtushinsky *et al.*, *PRB* (2006)

ARPES on charge-density-wave compounds

Phase diagram

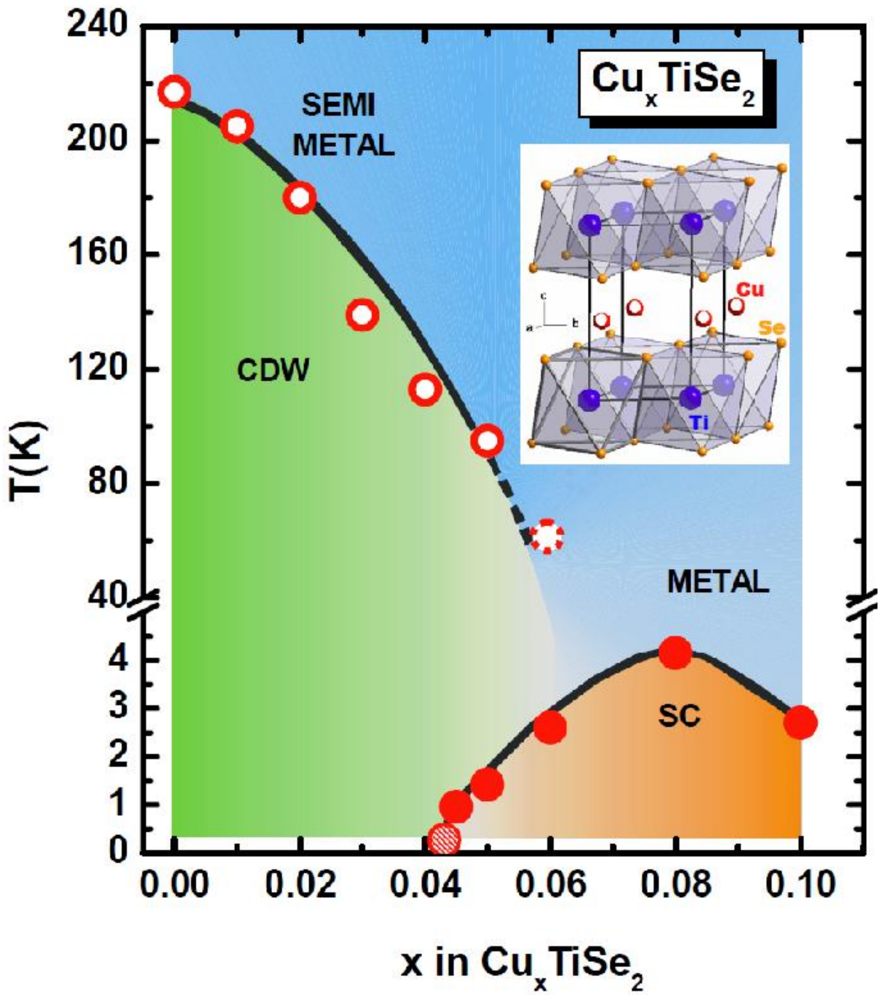

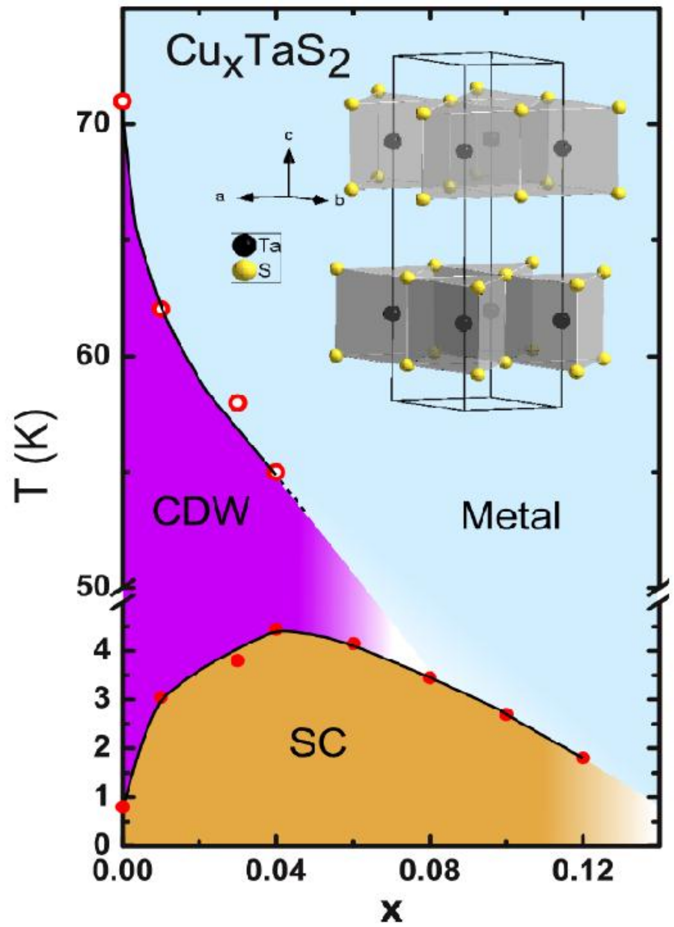

Morosan *et al.*, *Nat. Phys.* (2006); *PRB* (2008)

Electronic structure modification by modulating potential

$$H \quad \sum_{k}\{\epsilon(k)c_k^{+}c_k + \sum_{q}[V(q)c_{k+q}^{+}c_k + H.c]\} \quad \mathrm{V(x)} \quad \mathrm{V\cos}(\tfrac{\pi}{a}\mathrm{x})$$

$$\hat{H} = \sum_{\substack{\mathbf{q}\in \mathrm{RBZ} \\ m,n}} (\delta_{m,n}\varepsilon_{\mathbf{q}+\mathbf{g}_m} + V_{m,n})\hat{c}^{\dagger}_{\mathbf{q}+\mathbf{g}_m}\hat{c}_{\mathbf{q}+\mathbf{g}_n}; \quad V_{n,m}(\mathbf{q}) = \begin{pmatrix} 0 & V_c \\ V_c & 0 \end{pmatrix}$$

$$A^{<}_{\mathbf{k}}(\omega) = \sum_{\substack{\mathbf{q}\in \mathrm{RBZ}, \\ i,m}} \left| D^{*}_{m,i}(\mathbf{k}-\mathbf{g}_m) \right|^2 \delta(E_i(\mathbf{k}-\mathbf{g_m}) - \omega).$$

$$\hat{H} = \sum_{\substack{\mathbf{q}\in \mathrm{RBZ} \\ i,m,n}} D^{*}_{m,i}(\mathbf{q})E_i(\mathbf{q})D_{i,n}(\mathbf{q})\hat{c}^{\dagger}_{\mathbf{q}+\mathbf{g}_m}\hat{c}_{\mathbf{q}+\mathbf{g}_n} = \sum_{\substack{\mathbf{q}\subset \mathrm{RBZ} \\ i}} E_i(\mathbf{q})\hat{a}^{\dagger}_{\mathbf{q},i}\hat{a}_{\mathbf{q},i}$$

normal state, V=0

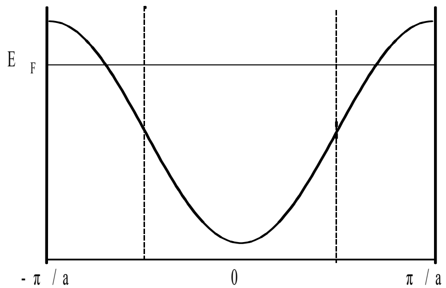

modulated state, V ≠ 0

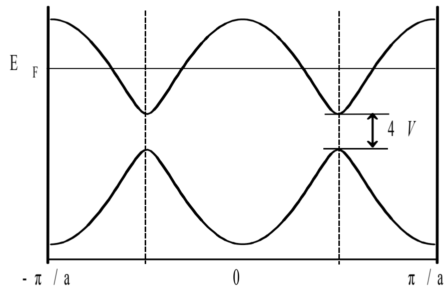

$A(k, \omega)$

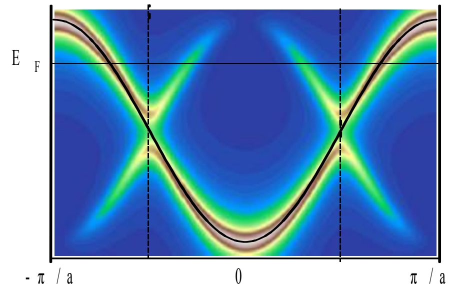

Band dispersion of 2H-TMDs

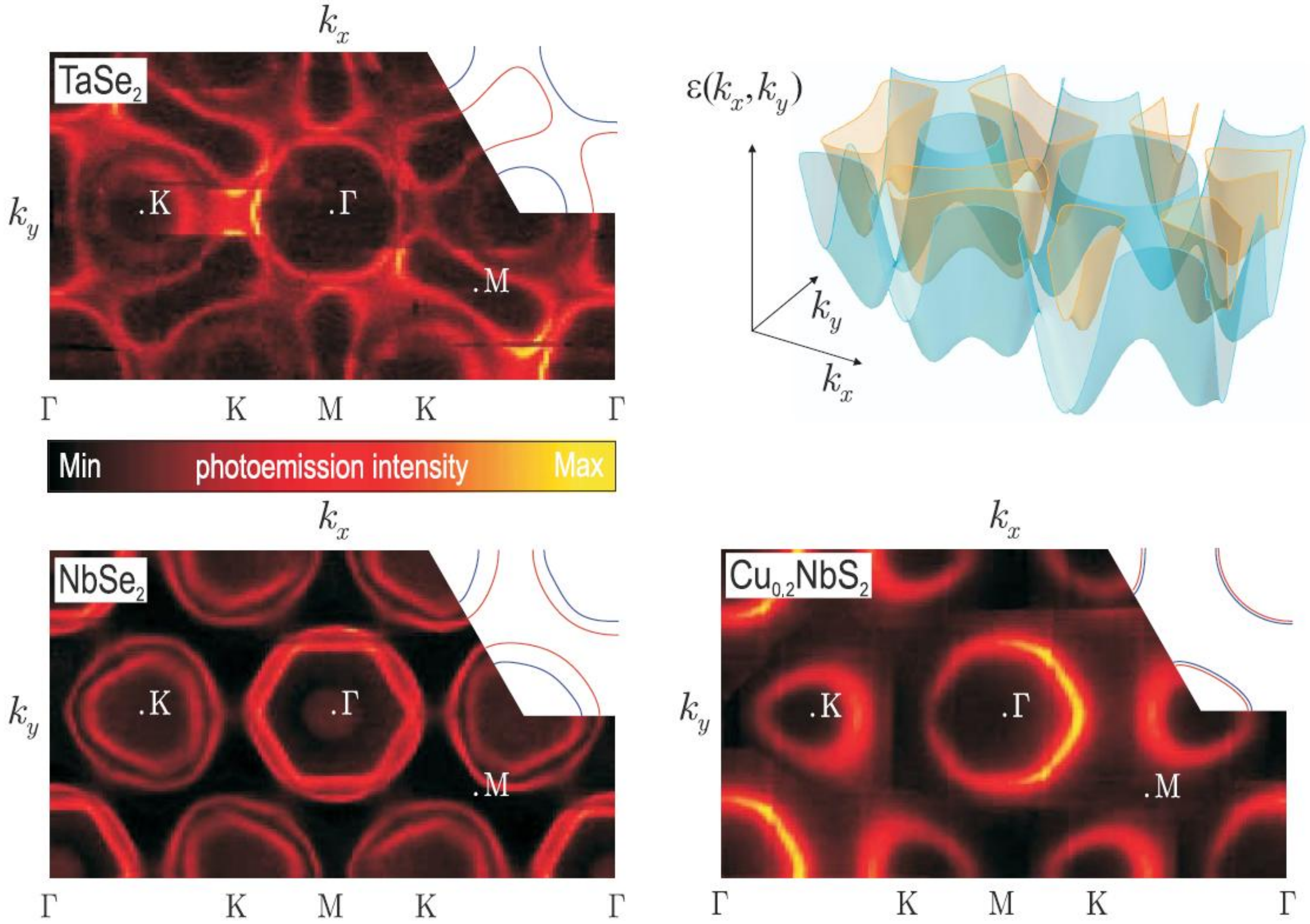

2H-$TaSe_2$

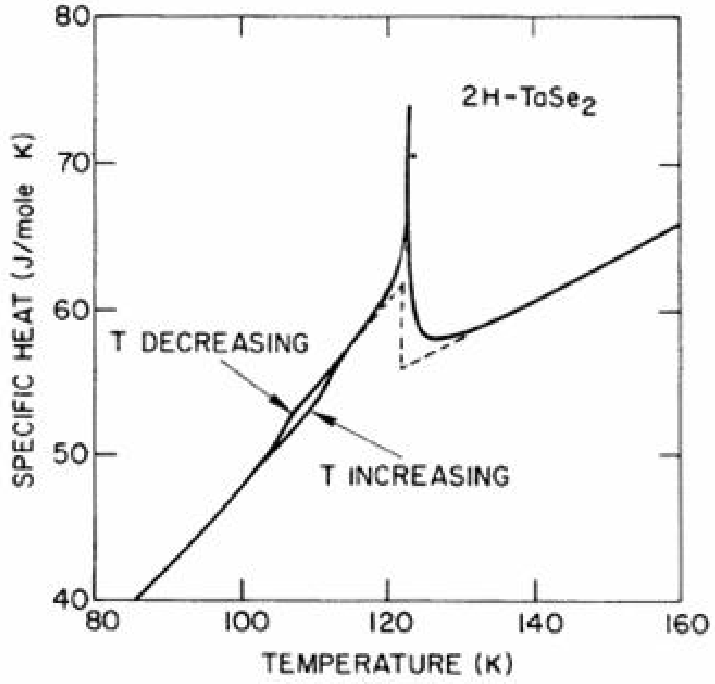
2H-TaSe2
SPECIFIC HEAT (J/mole K)
TEMPERATURE (K)
T DECREASING
T INCREASING
80
70
60
50
40
80
100
120
140
160

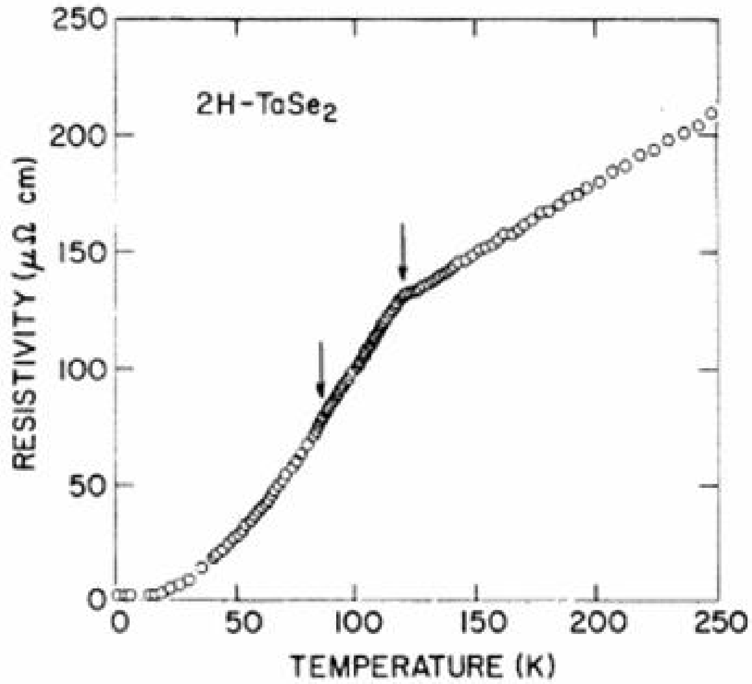
2H-TaSe2
RESISTIVITY (μΩ cm)
TEMPERATURE (K)
250
200
150
100
50
0
0
50
100
150
200
250

CDW-induced Change in Electronic Structure

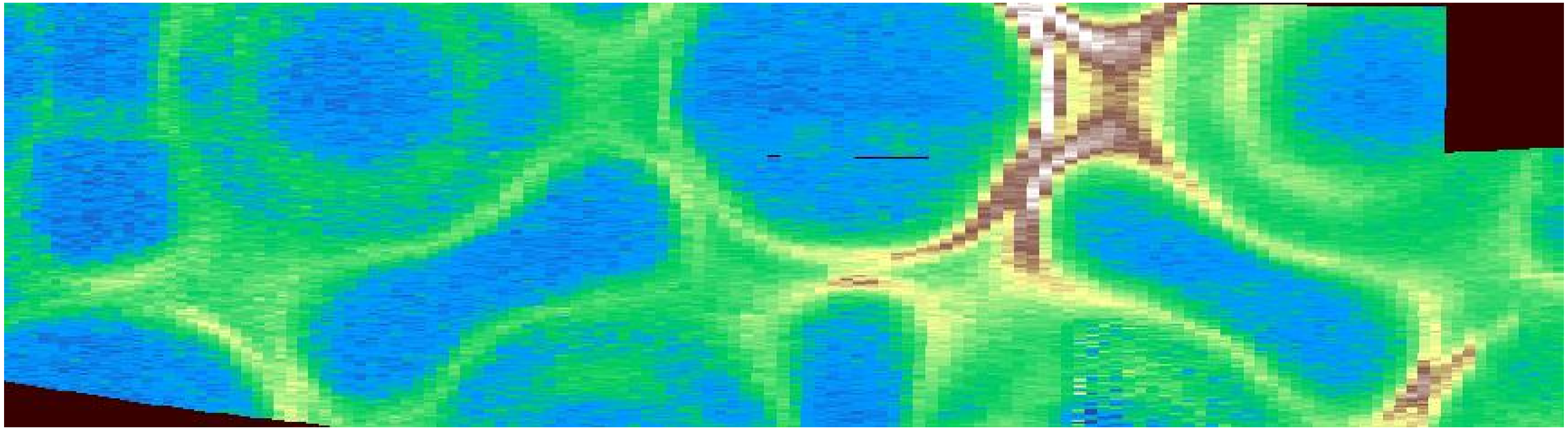

180K

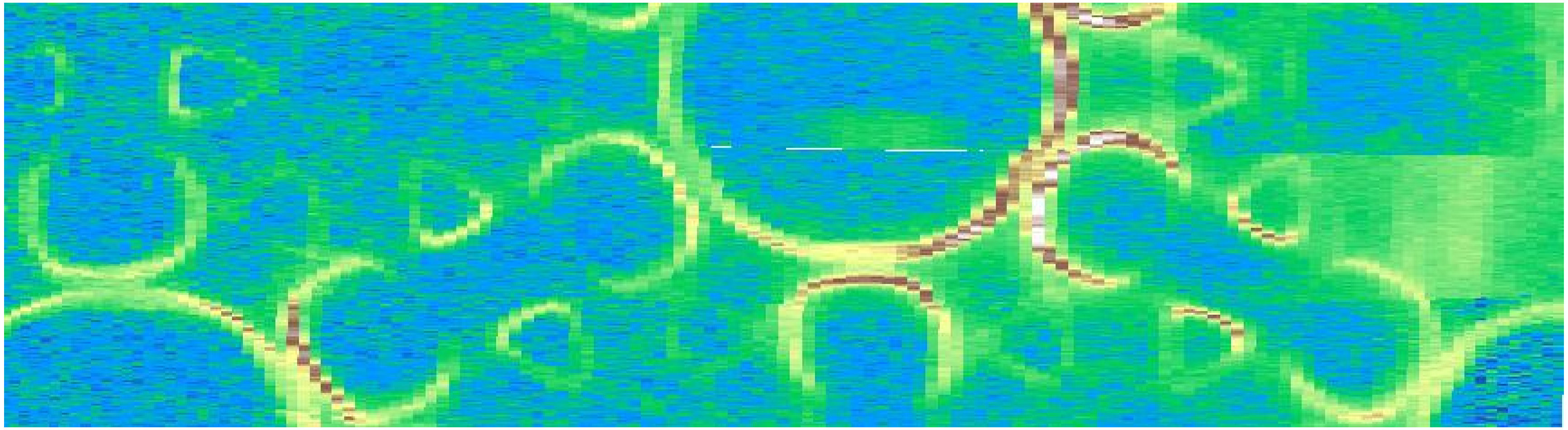

30K

New Parts of Fermi surface

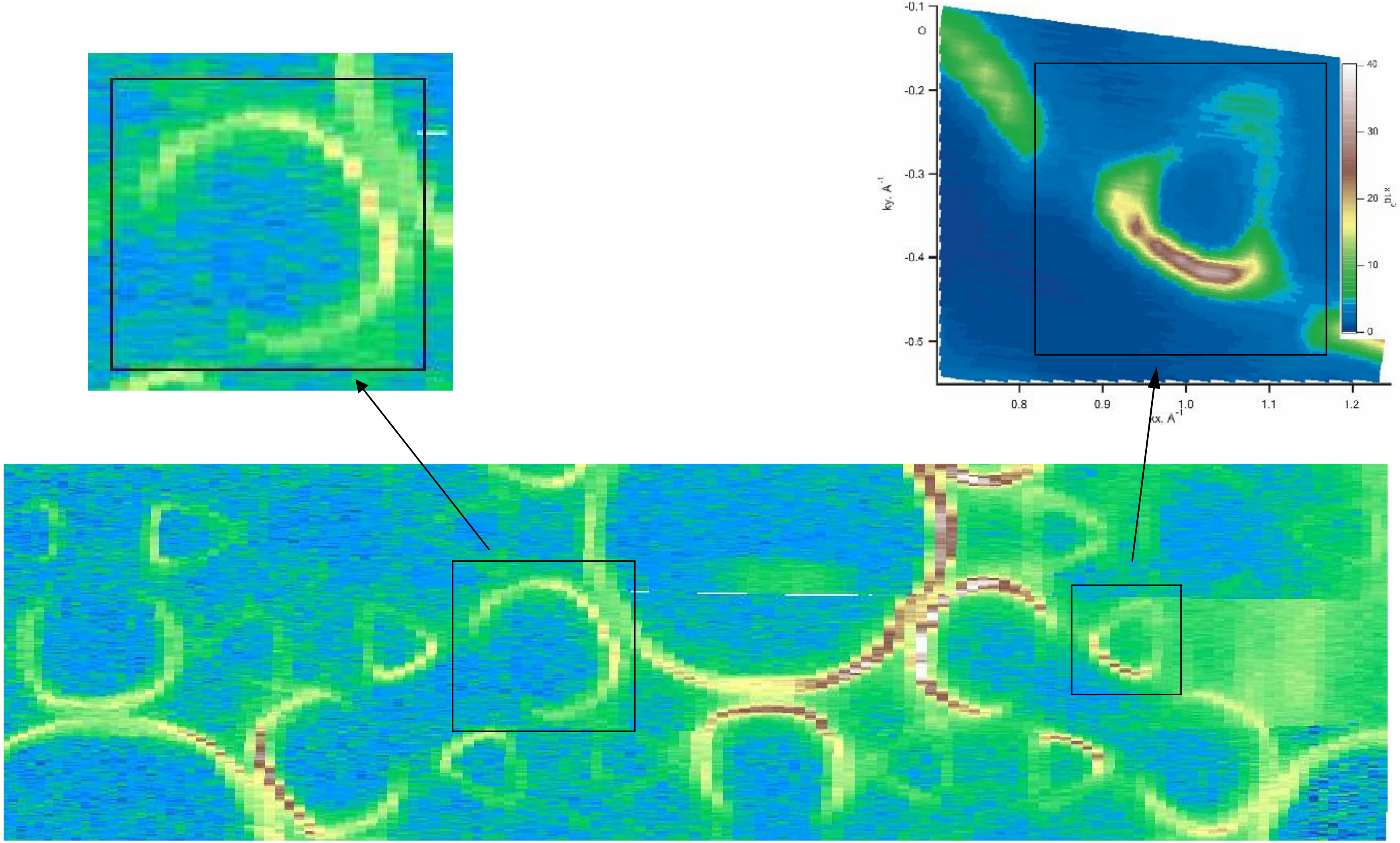

Fermi surface nesting and superstructure formation

$$\varepsilon(\mathbf{k}) \to \chi(\mathbf{q})$$

nesting vector
in the momentum space

$$\Updownarrow$$

periodicity of the superstructure
in the coordinate space

Charge ordering in 2H-$TaSe_2$ and $NbSe_2$

2H-$TaSe_2$

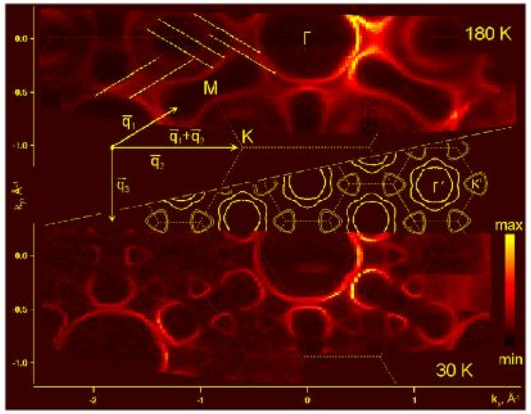

S. V. Borisenko *et al., PRL* (2008)

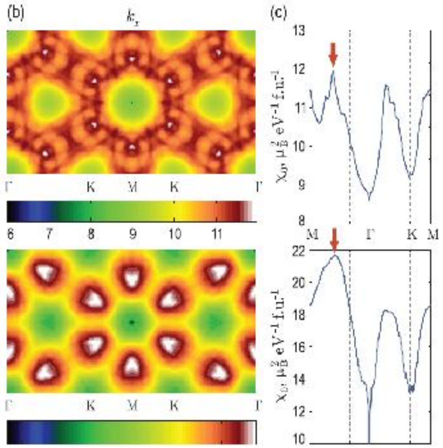

D. S. Inosov *et al., NJP* (2008)

2H-$NbSe_2$

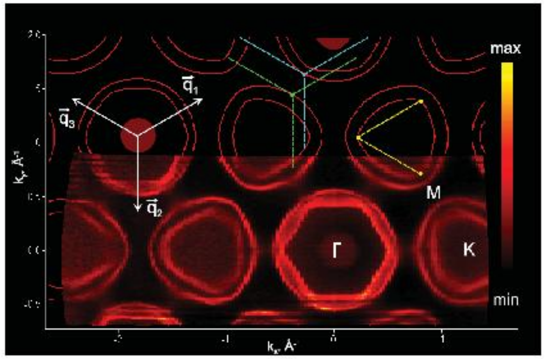

S. V. Borisenko *et al., PRL* (2009)

2H-$NbSe_2$

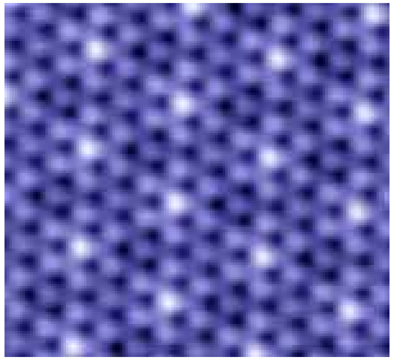

Davis *et al.*

Magnetic ordering in Gd_2PdSi_3 and Tb_2PdSi_3

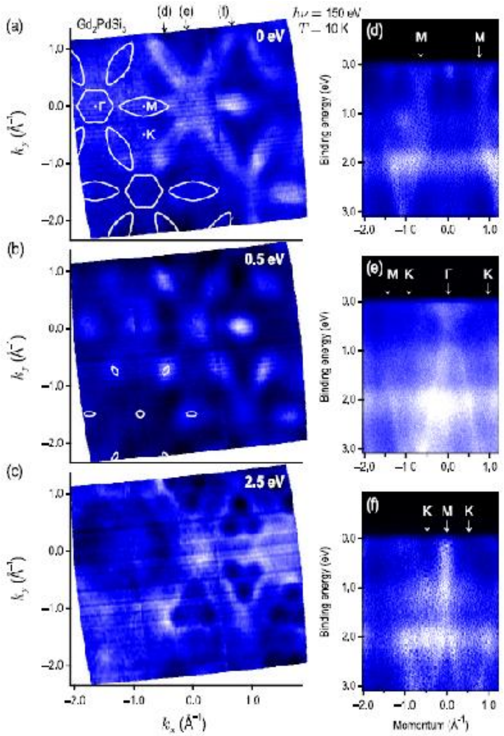

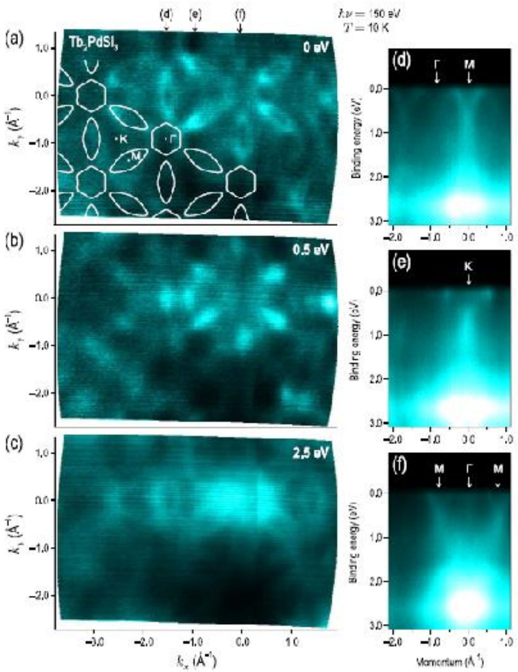

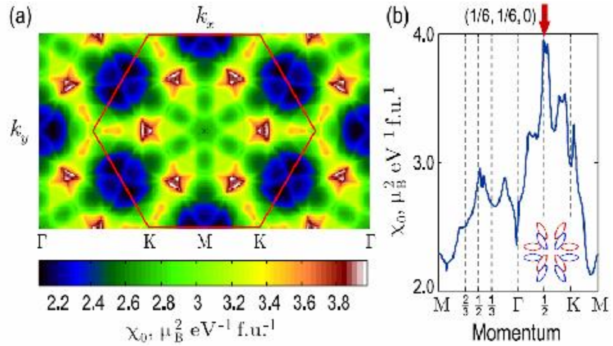

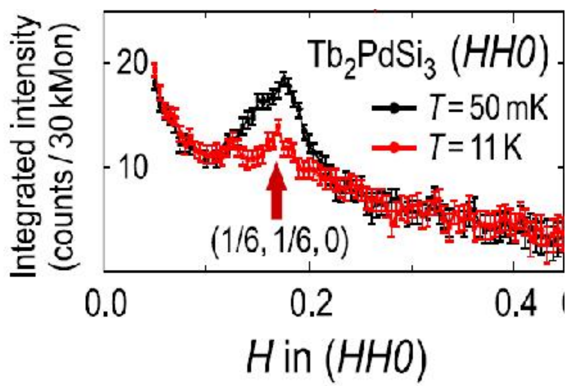

D. S. Inosov *et al., PRL* (2009)

Charge-orbital ordering in $La_{0.5}Sr_{1.5}MnO_4$

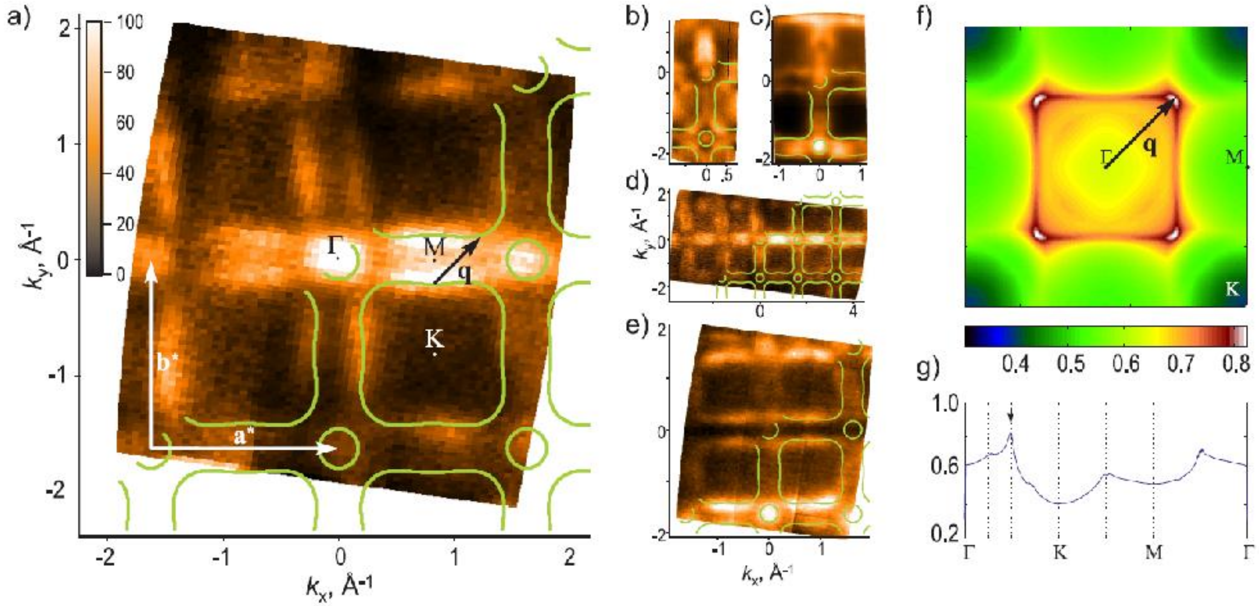

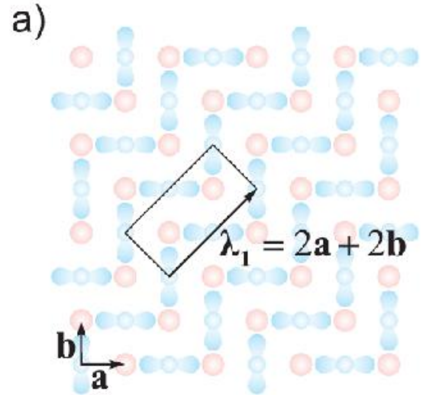

D. V. Evtushinsky *et al., PRL* (2010)

Comparison to complementary measurements of electronic structure

ARPES	Electron transport, thermodynamics, etc.
$\varepsilon(\mathbf{k})$	$\int \Phi[\varepsilon(\mathbf{k})]d\mathbf{k}$

Bloch wave packet
~~Electron~~ dynamics in applied field

$$\hbar \frac{d\mathbf{k}}{dt} = -e\mathbf{E} - e\mathbf{v} \times \mathbf{B}$$

$$\frac{\partial f(\mathbf{k})}{\partial \mathbf{k}} \cdot \frac{d\mathbf{k}}{dt} = -\frac{f(\mathbf{k}) - f_0(\mathbf{k})}{\tau(\mathbf{k})}$$

$$\sigma_{ij} = \frac{e^2}{4\pi^3} \int_{\text{all } \mathbf{k}} \left[-\frac{df_0}{d\varepsilon} \right] \tau(\mathbf{k}) v_i(\mathbf{k}) v_j(\mathbf{k}) d^3\mathbf{k}$$

$$\sigma_{ij} = \frac{e^2}{4\pi^3} \int_{\{\mathbf{k} | \, \varepsilon(\mathbf{k}) = \varepsilon_F\}} \tau(\mathbf{k}) v_i(\mathbf{k}) v_j(\mathbf{k}) \frac{1}{|\mathbf{v}(\mathbf{k})|} d^2\mathbf{k}$$

Electronic response to the weak external field

Resistivity ρ, Hall coefficient R_H, and magnetoresistance $\delta\rho/\rho$

$$\sigma_{xx} = \frac{\tau e^2}{2\pi L_c h} \int v_F(\mathbf{k}) \mathrm{d}k \qquad \sigma_{xy} = \frac{\tau^2 B e^3}{L_c h^2} \int \frac{v_F^2(\mathbf{k})}{\rho_F(\mathbf{k})} \mathrm{d}k$$

$$\delta\sigma_{xx} = -\frac{4\pi\tau^3 B^2 e^4}{L_c h^3} \int \left\{ v_F(\mathbf{k}) \left[\frac{\mathrm{d}v_F(\mathbf{k})}{\mathrm{d}k} \right]^2 + \frac{v_F^3(\mathbf{k})}{2\rho^2(\mathbf{k})} \right\} \mathrm{d}k$$

$$\rho = \frac{1}{\sigma_{xx}}, \ R_H = \frac{\sigma_{xy}}{B \cdot \sigma_{xx}^2}, \ \text{and} \ \frac{\delta\rho}{\rho} = -\frac{\delta\sigma_{xx}}{\sigma_{xx}} - \frac{\sigma_{xy}^2}{\sigma_{xx}^2}$$

where

$$v_F(\mathbf{k}) \equiv \frac{1}{\hbar} |\nabla\varepsilon(\mathbf{k})| \qquad \frac{1}{\rho_F(\mathbf{k})} \equiv \frac{\nabla\varepsilon(\mathbf{k})}{\hbar v_F(\mathbf{k})} - \frac{(\nabla v_F(\mathbf{k}), \nabla\varepsilon(\mathbf{k}))}{\hbar v_F^2(\mathbf{k})} \qquad \int \equiv \int_{\{\varepsilon(\mathbf{k})=0\}}$$

Seebeck coefficient (thermopower)
Nernst effect
Electronic specific heat
Electronic heat conductivity

} Can be expressed in a similar way

Calculated and measured R_H for simple metals

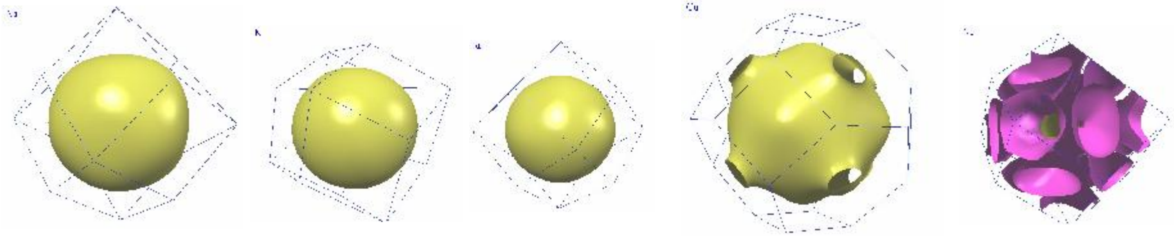

	Na	K	Rb	Cu	Nb
Calculation	-2.38	-4.49	-5.4	-0.530	+0.752
Experiment	-2.50	-4.20	-5.0	-0.517	+0.875

R_H (10^{-10} m^3/C)

T. P. Beaulac, *PRB* (1981)
http://www.phys.ufl.edu/fermisurface/

Hall effect in 2H-$TaSe_2$ and NbS_2

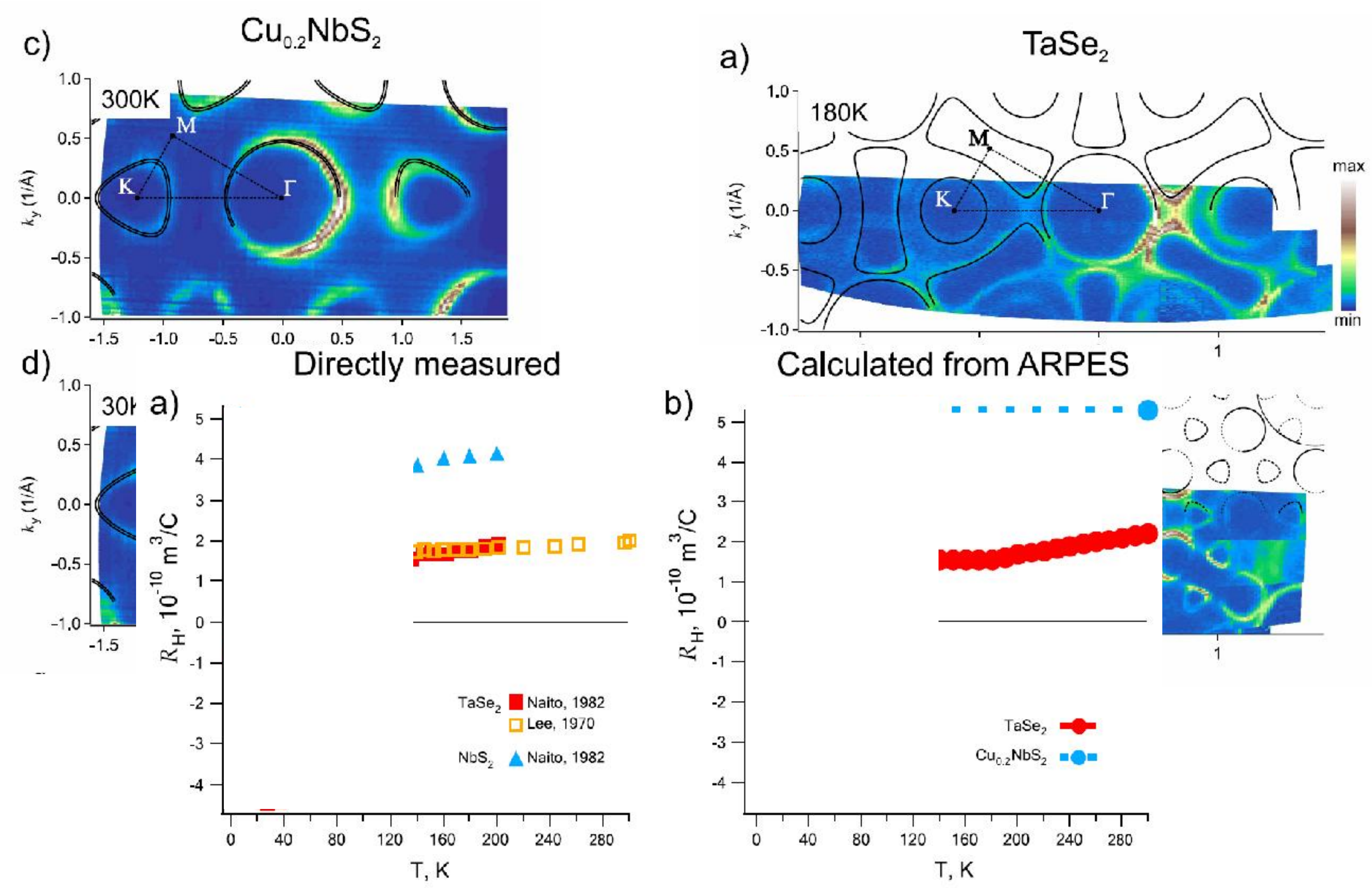

Evtushinsky *et al., PRL* (2008)

Hall effect in 2H-$TaSe_2$ and NbS_2

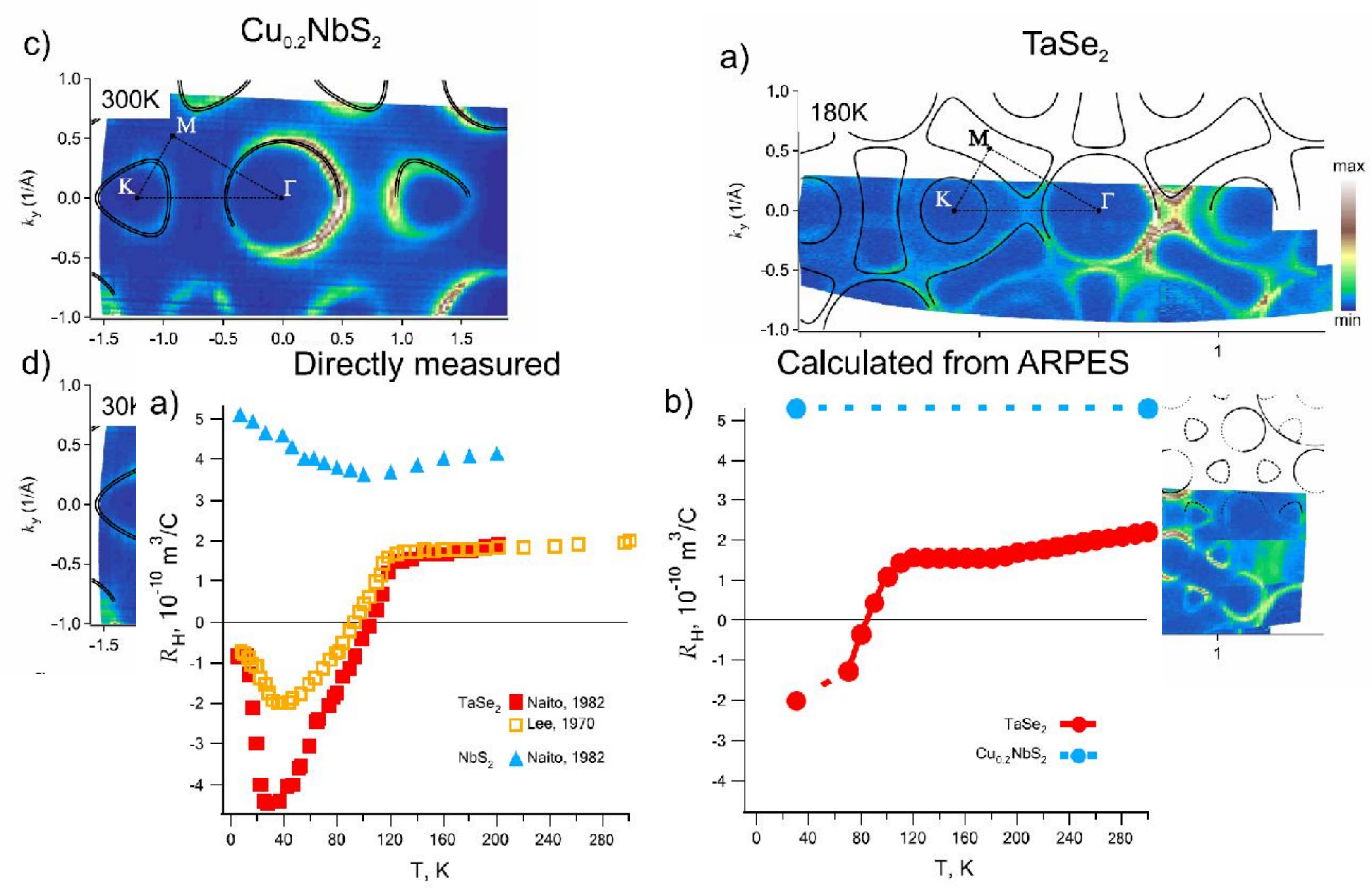

Evtushinsky *et al., PRL* (2008)

Band dispersion of 2H-TMDs

2H-TaSe$_2$, 2H-NbSe$_2$, 2H-NbS$_2$

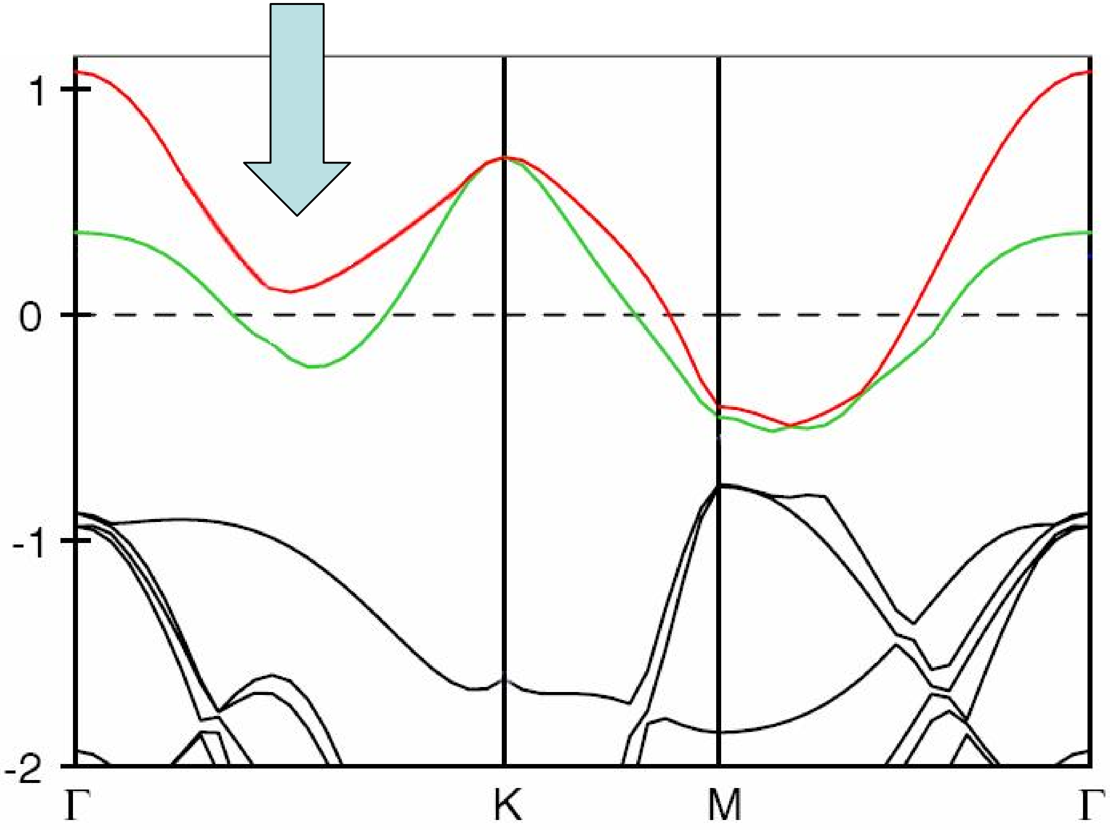

ARPES on iron-based superconductors

Iron-based superconductors

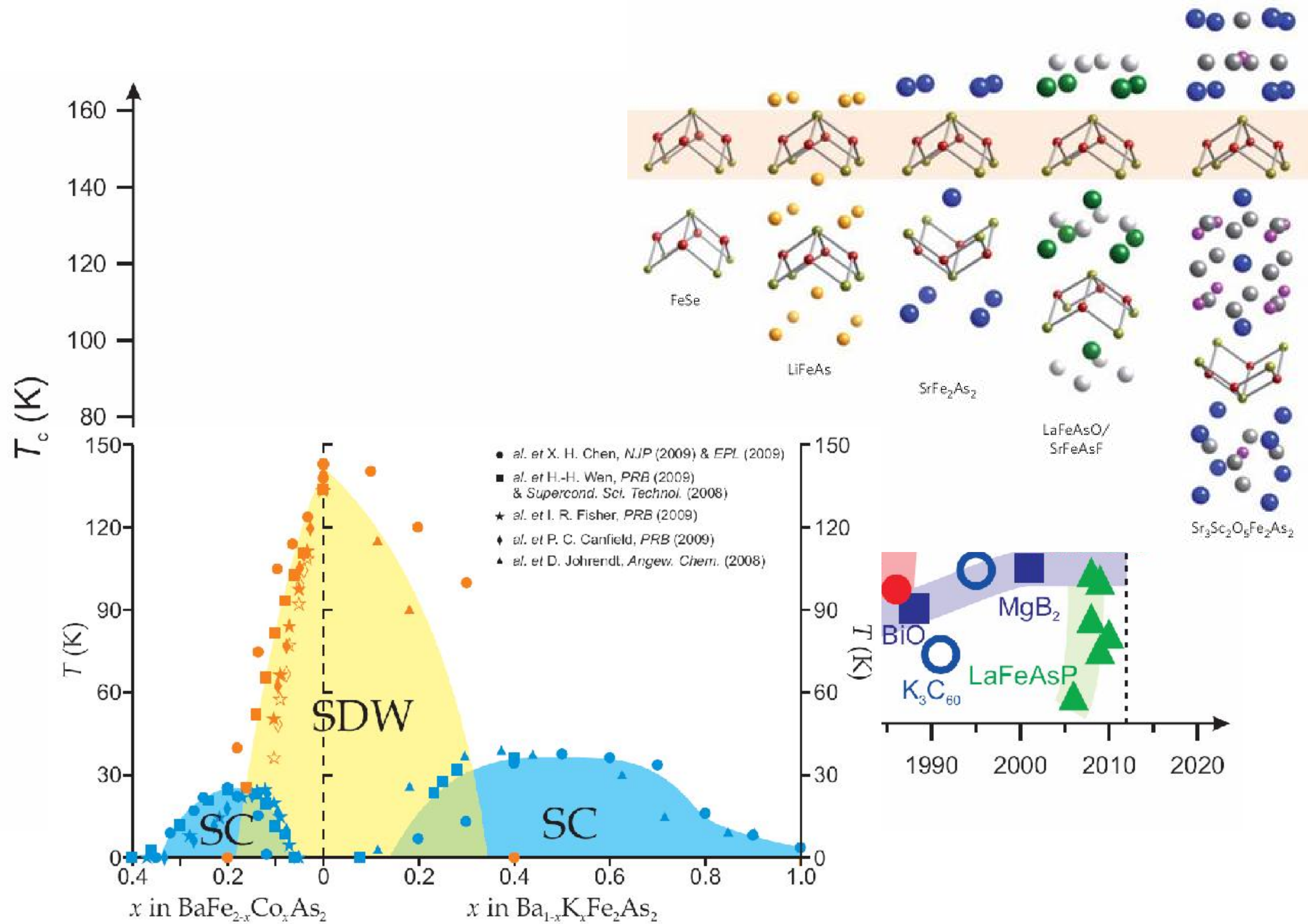

Fermi surfaces of iron-based superconductors

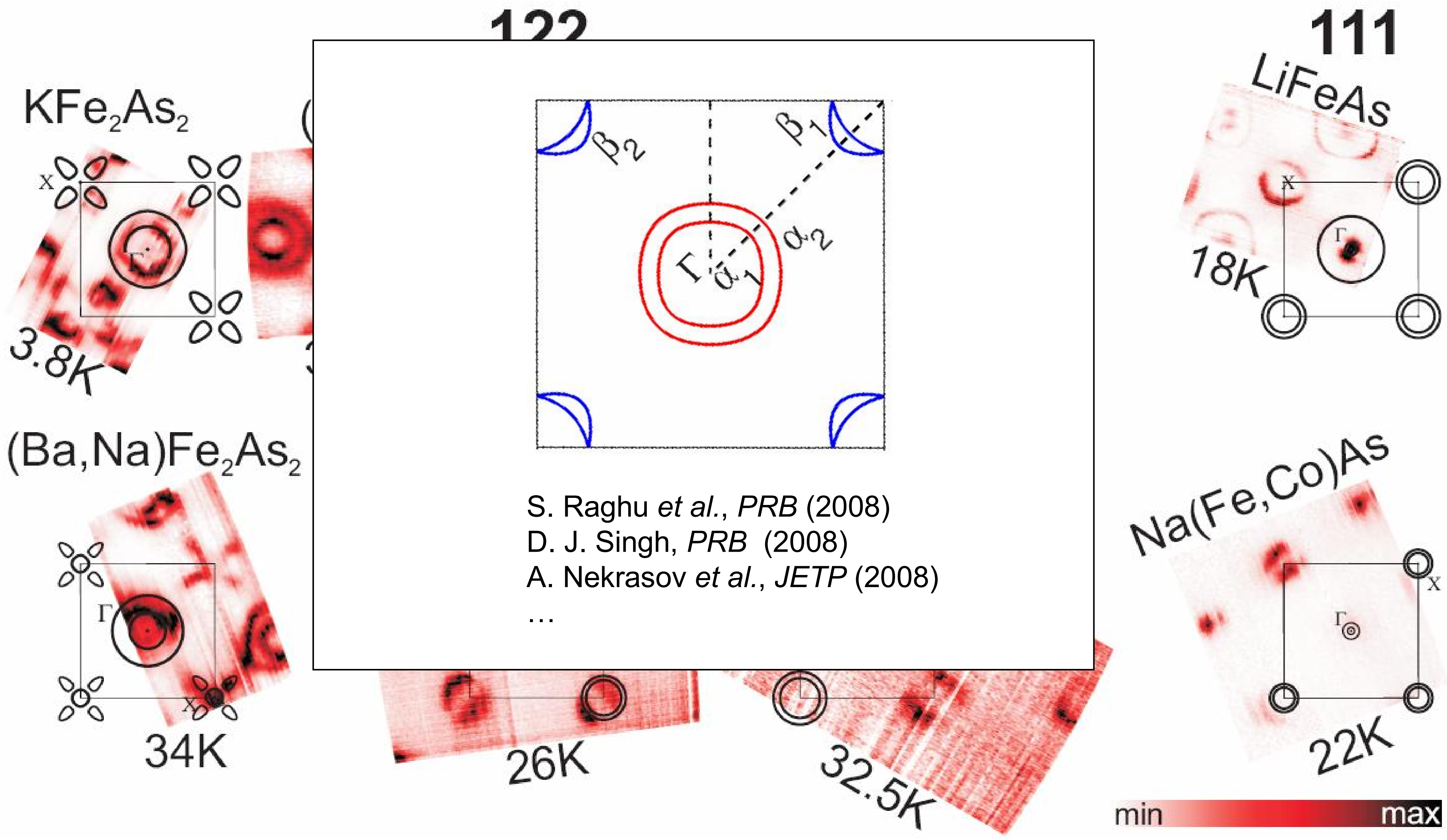

S. Raghu *et al.*, *PRB* (2008)
D. J. Singh, *PRB* (2008)
A. Nekrasov *et al.*, *JETP* (2008)
…

Fermi surfaces of iron-based superconductors

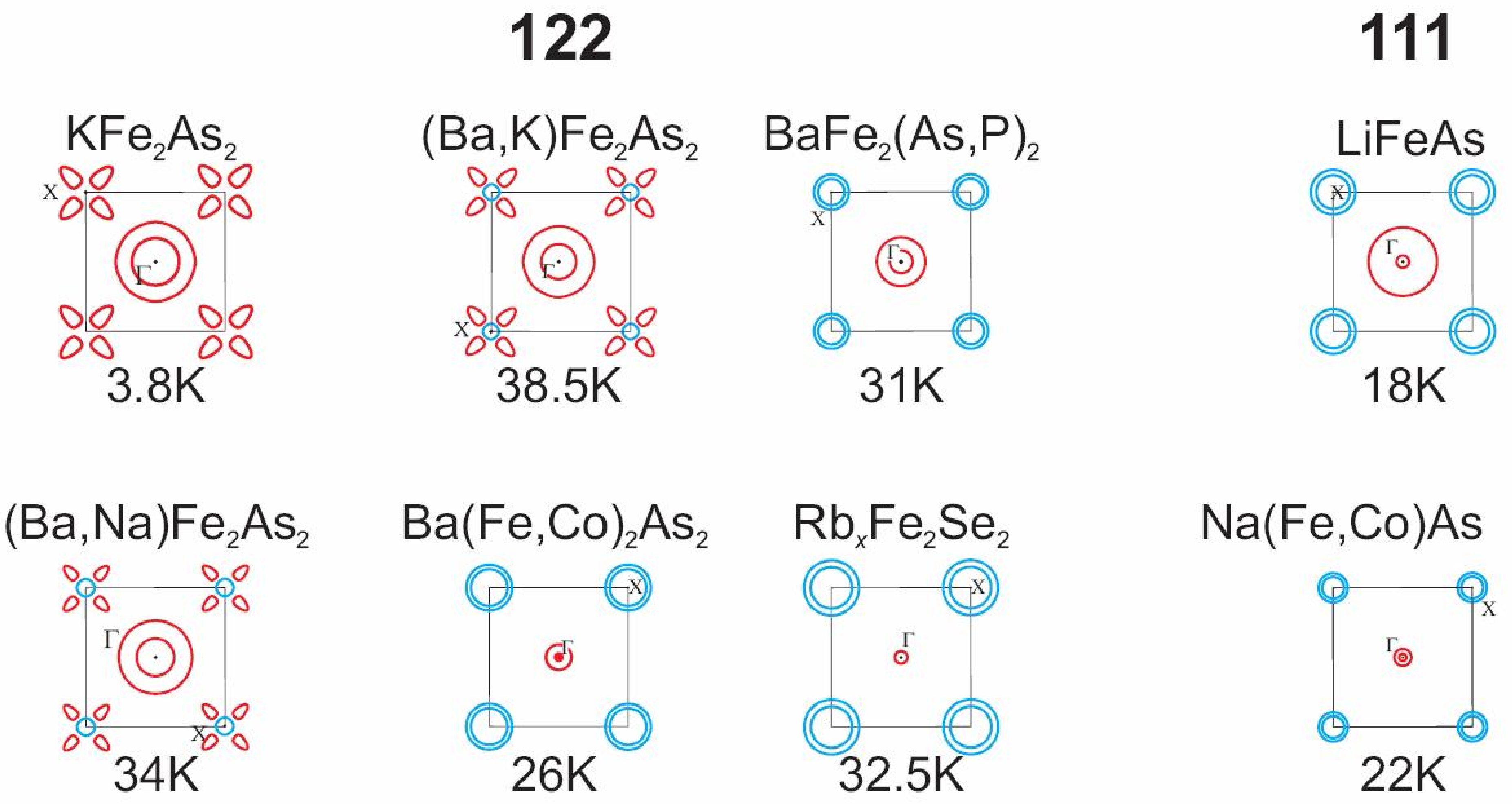

Electronic bands at Fermi level

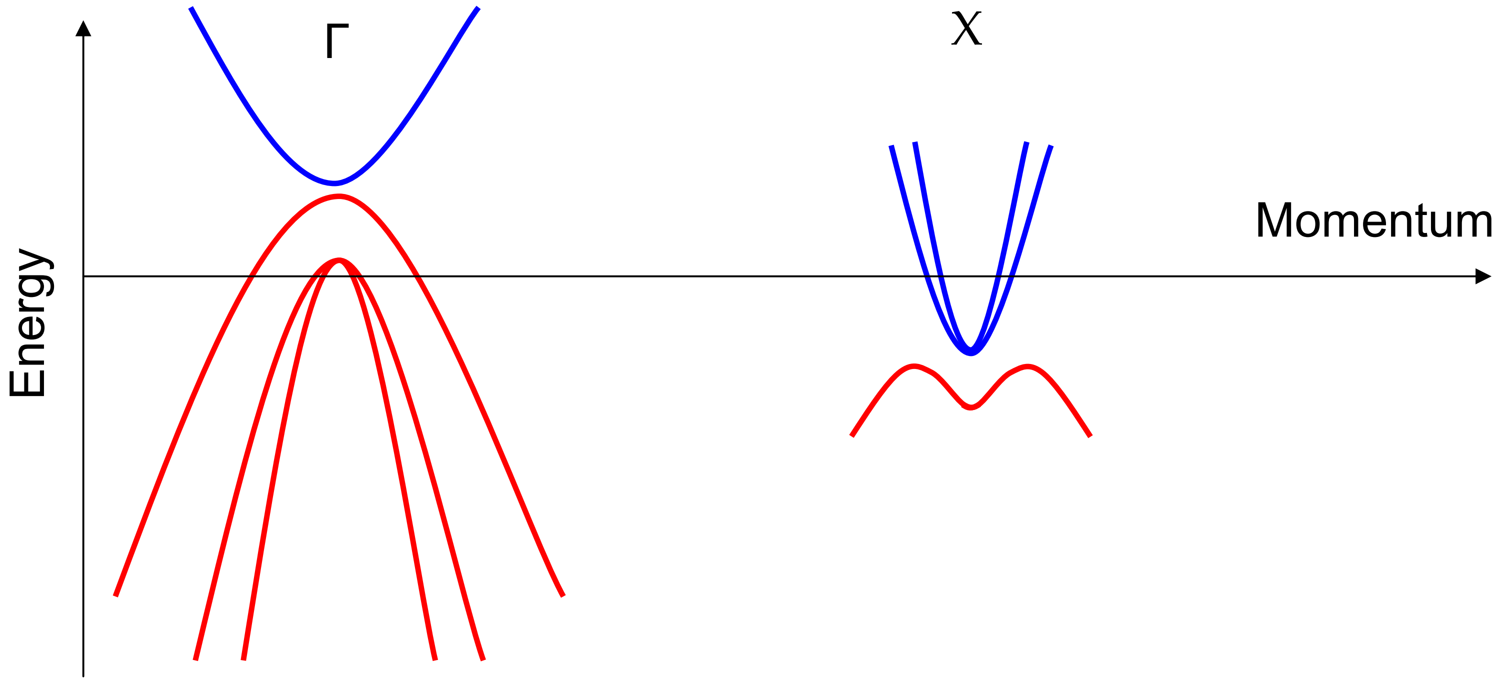

Fermi surface of $Ba_{1-x}K_xFe_2As_2$

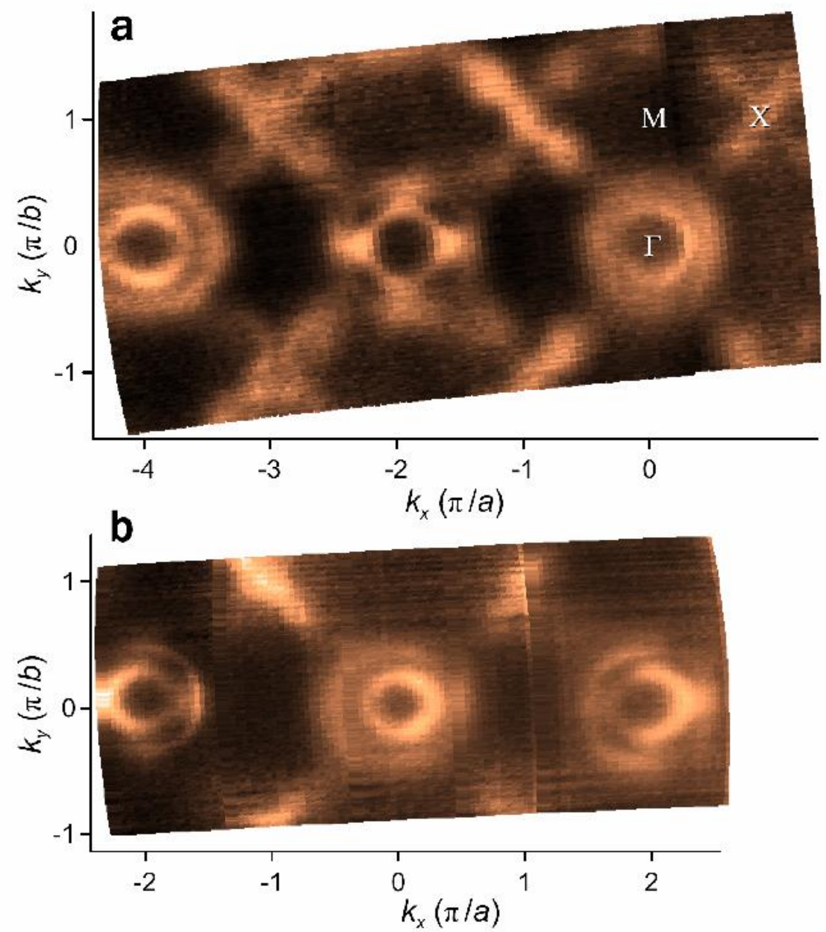

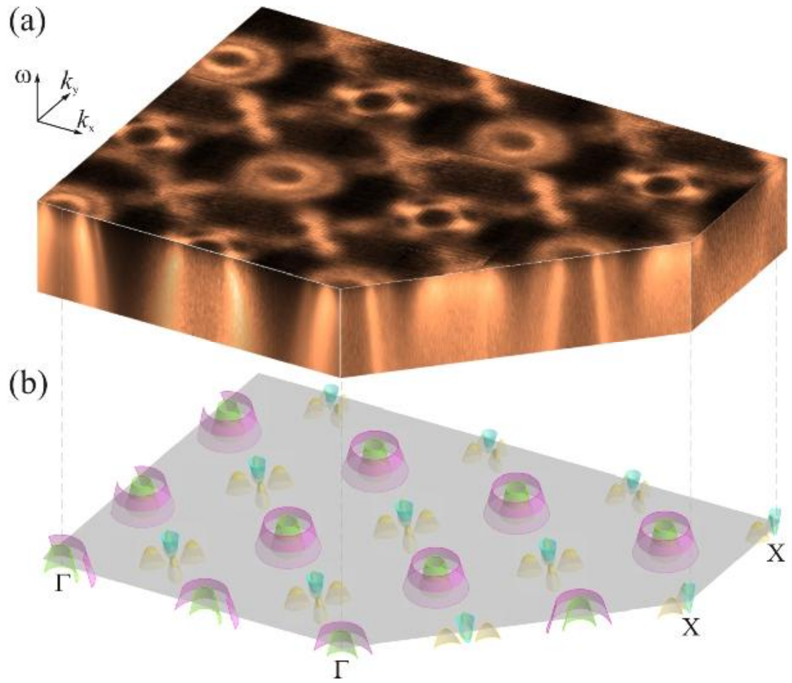

$\varepsilon(k_x, k_y)$

Evtushinsky *et al.*, *JPSJ* (2011)

Zabolotnyy *et al.*, Nature (2009)

Band dispersion near Fermi level in $Ba_{1-x}K_xFe_2As_2$ from ARPES

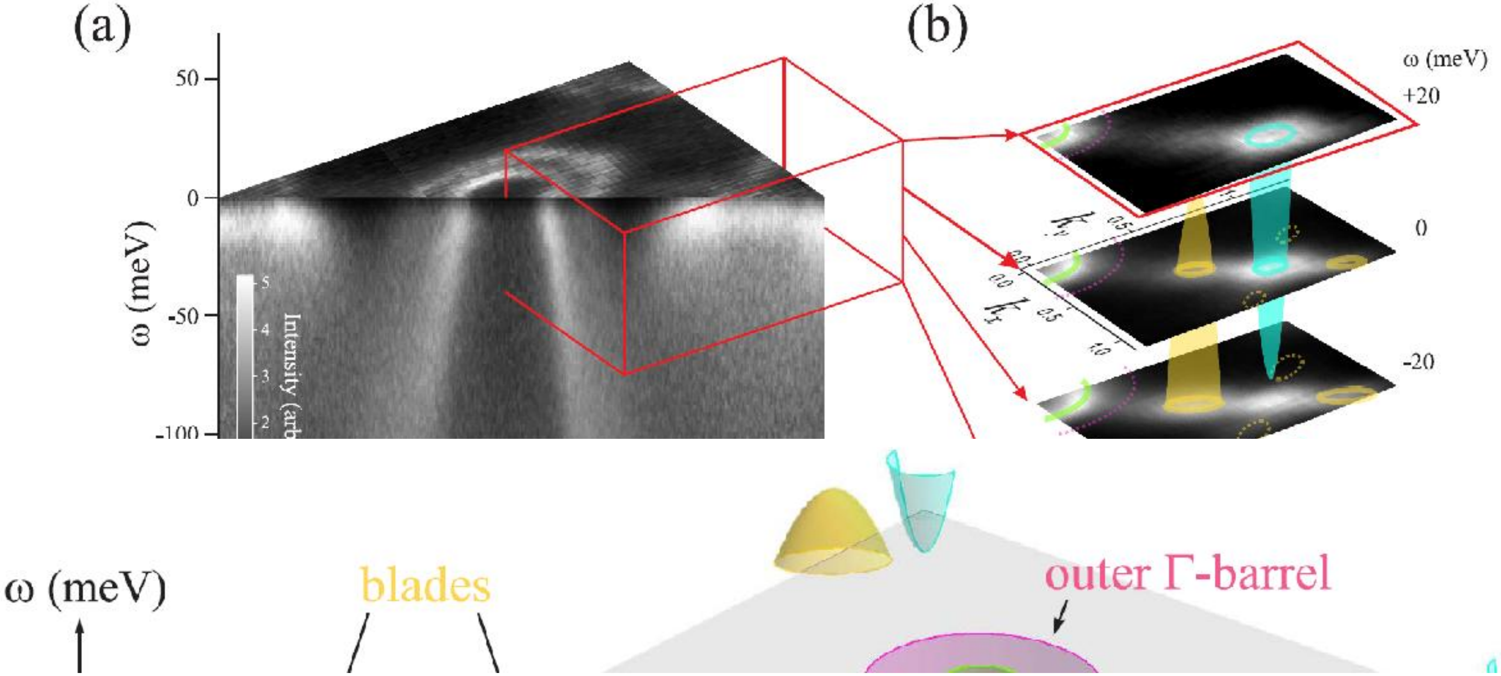

Zabolotnyy *et al.*, *Nature* (2009);*Physica C* (2009)
Evtushinsky *et al.*, *NJP* (2009);*JPSJ* (2011)

Propellers again

17th of October

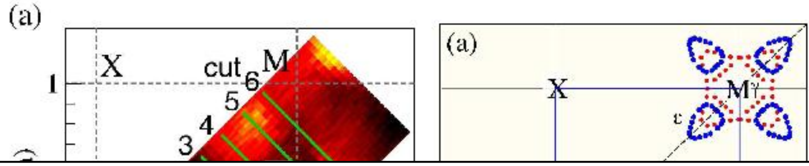

15th of August

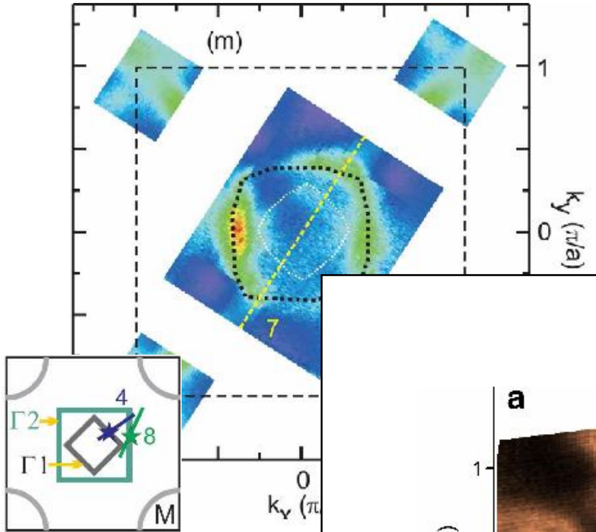

L. Wray *et al.*,ar

11th of December

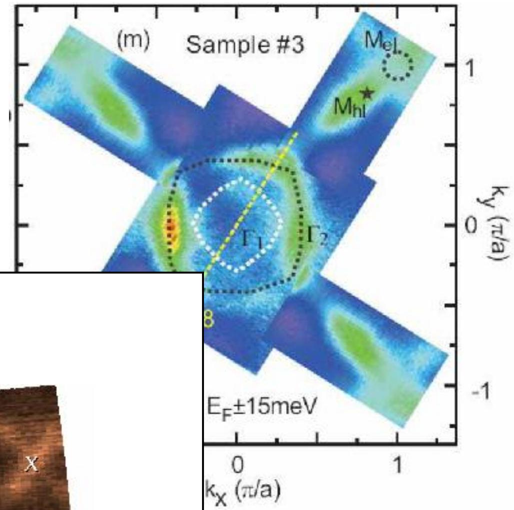

.,arXiv:0812.2061

18th of August

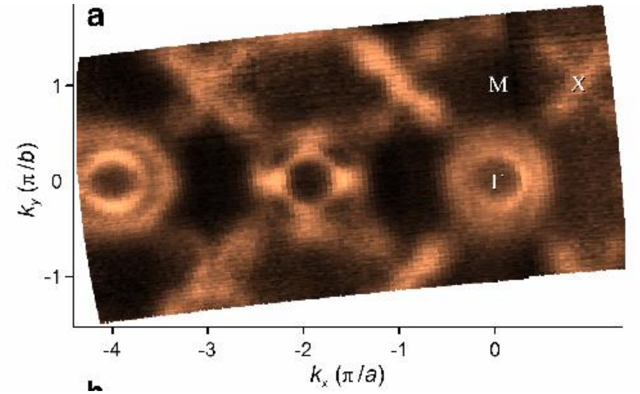

V. B. Zabolotnyy *et al.*,arXiv:0808.2454

Hall and FS in parent

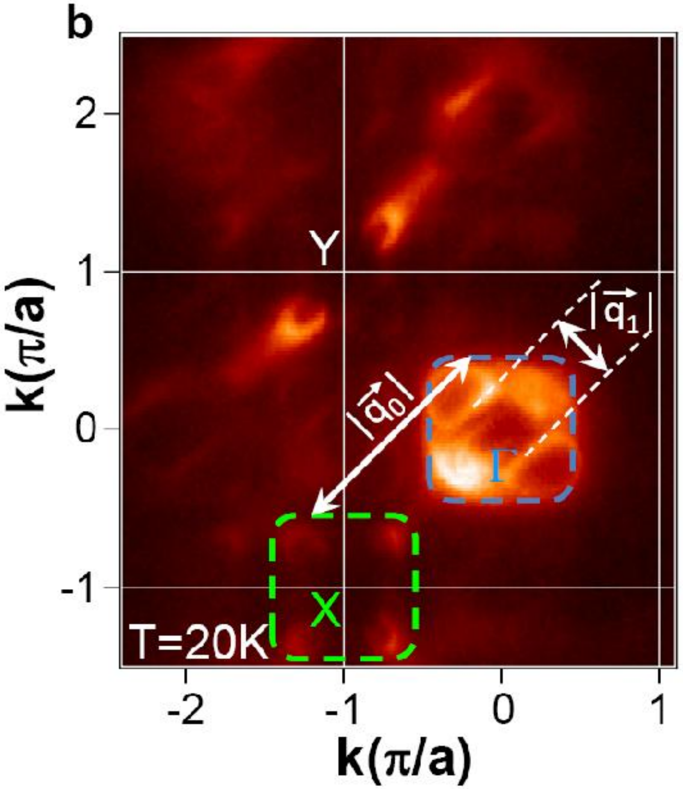

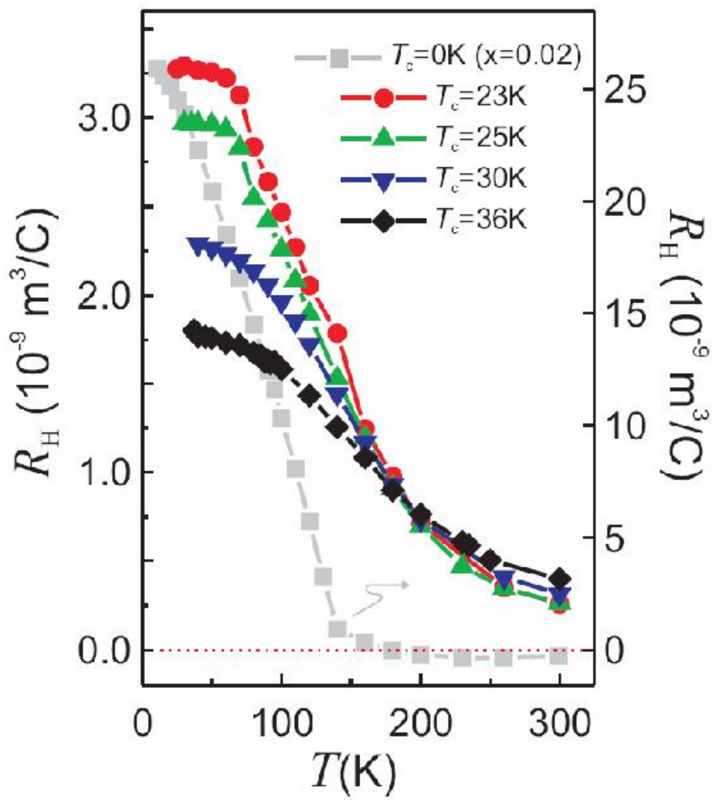

LiFeAs: no nesting, no magnetism, superconductivity

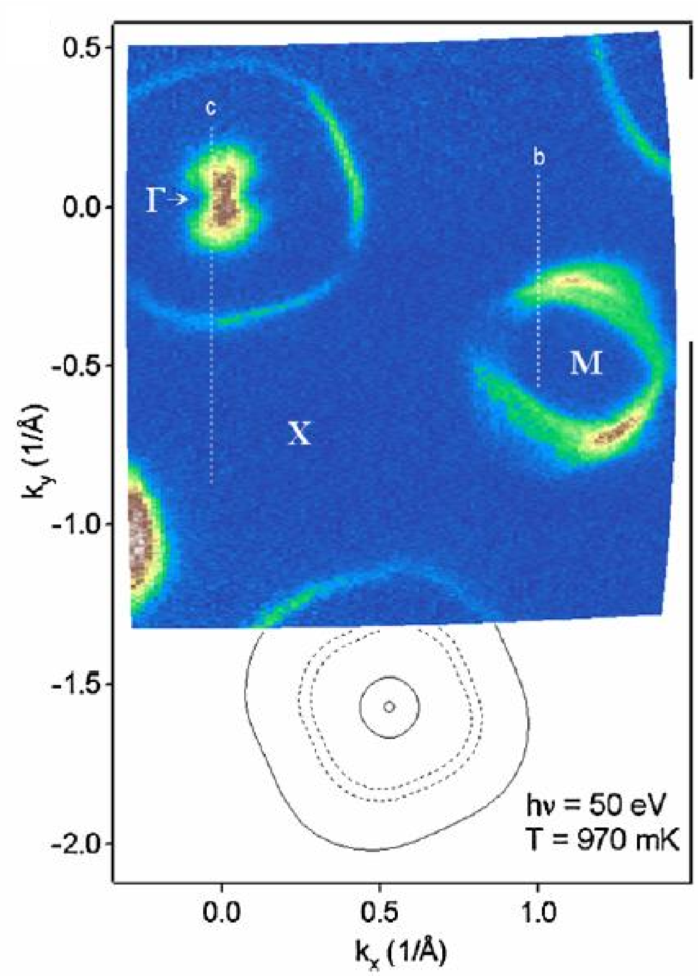

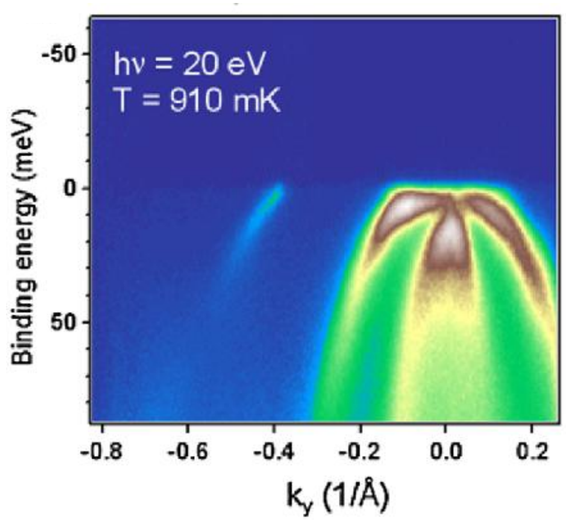

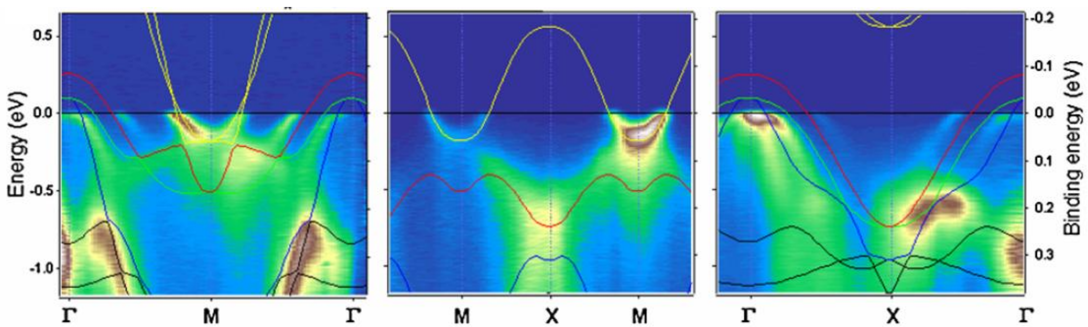

Borisenko *et al.*, *PRL* (2009)

LiFeAs map

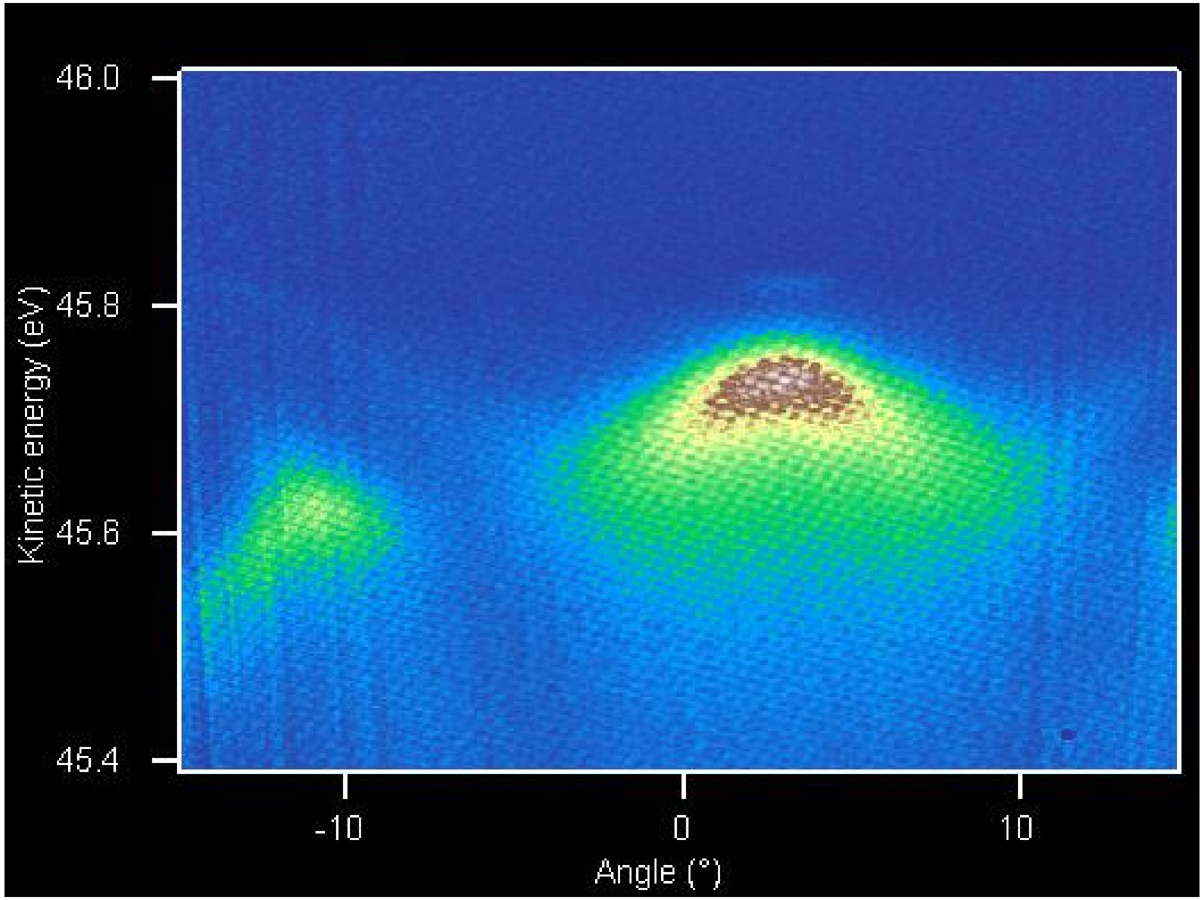

Band renormalization in LiFeAs

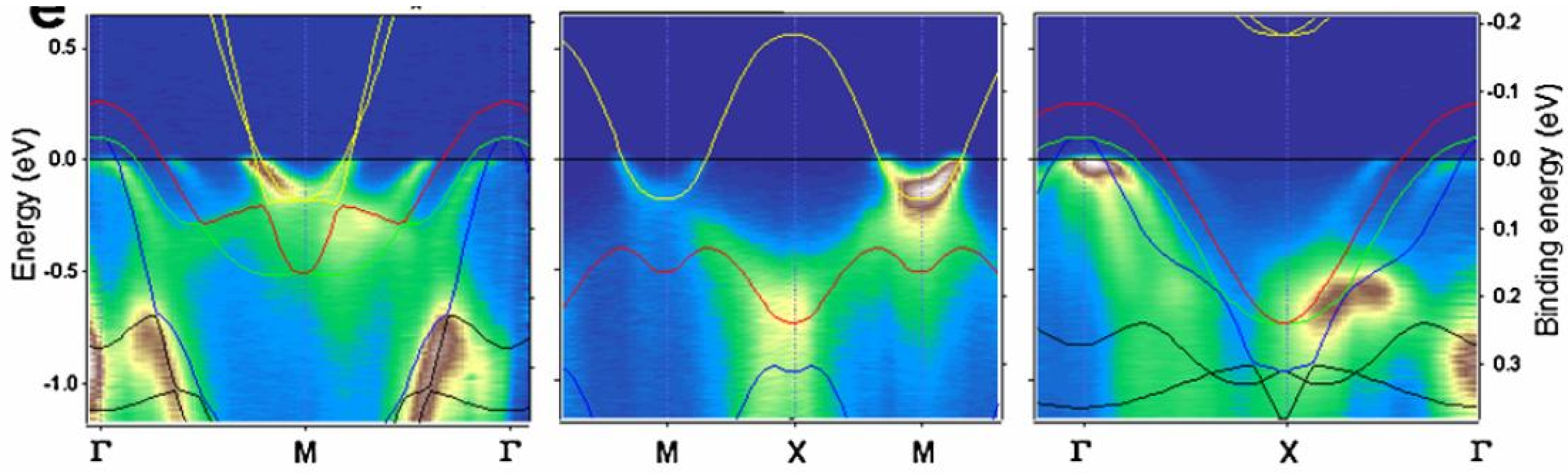

~3

Superconducting gap extraction from ARPES spectra

Opening of the superconducting gap in electronic dispersion

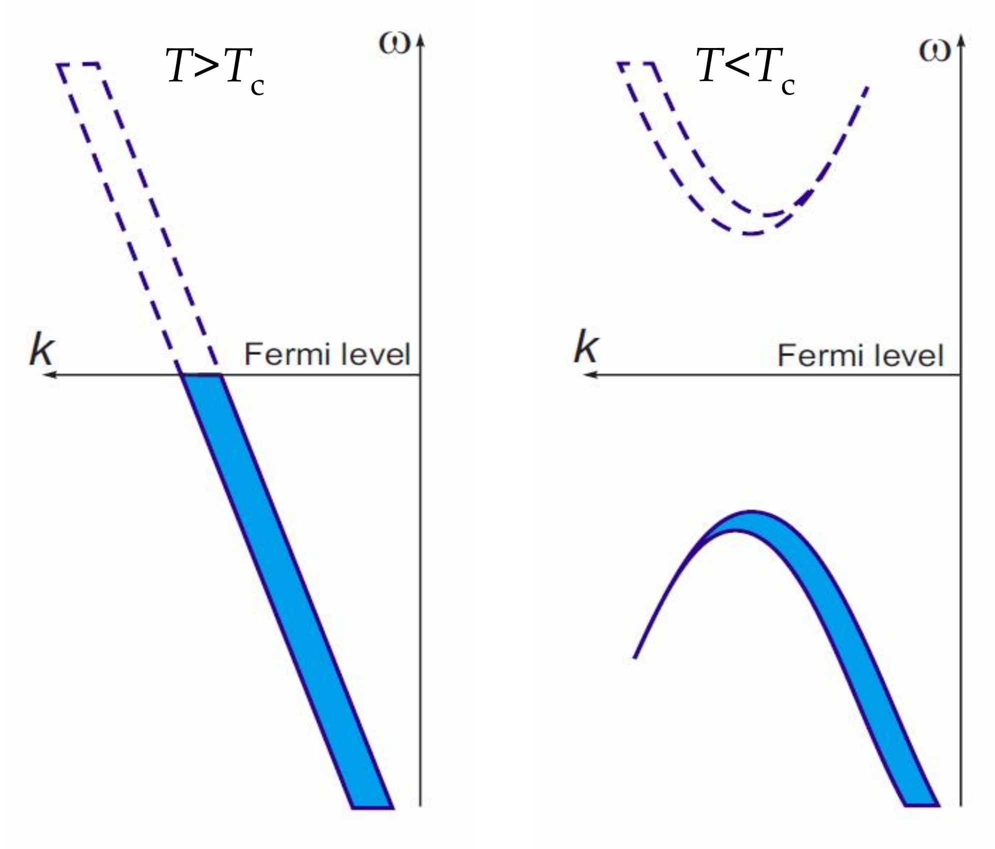

Superconducting gap in ARPES spectra

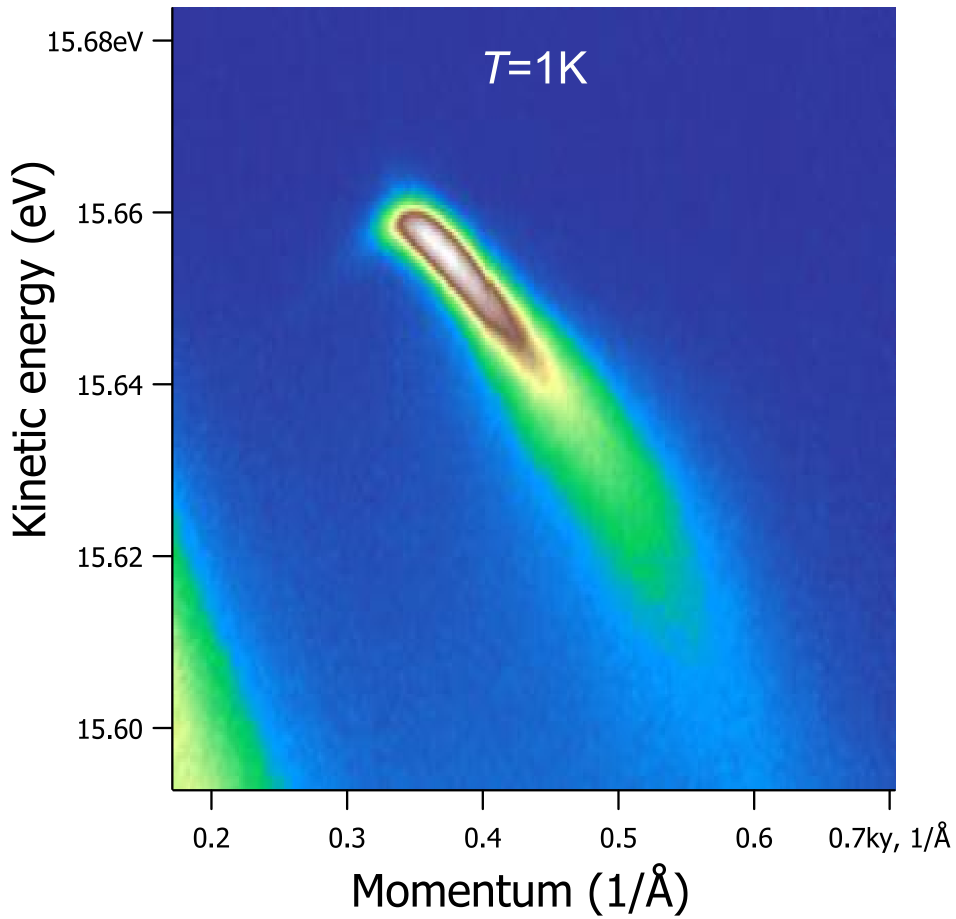

Superconducting gap in ARPES spectra

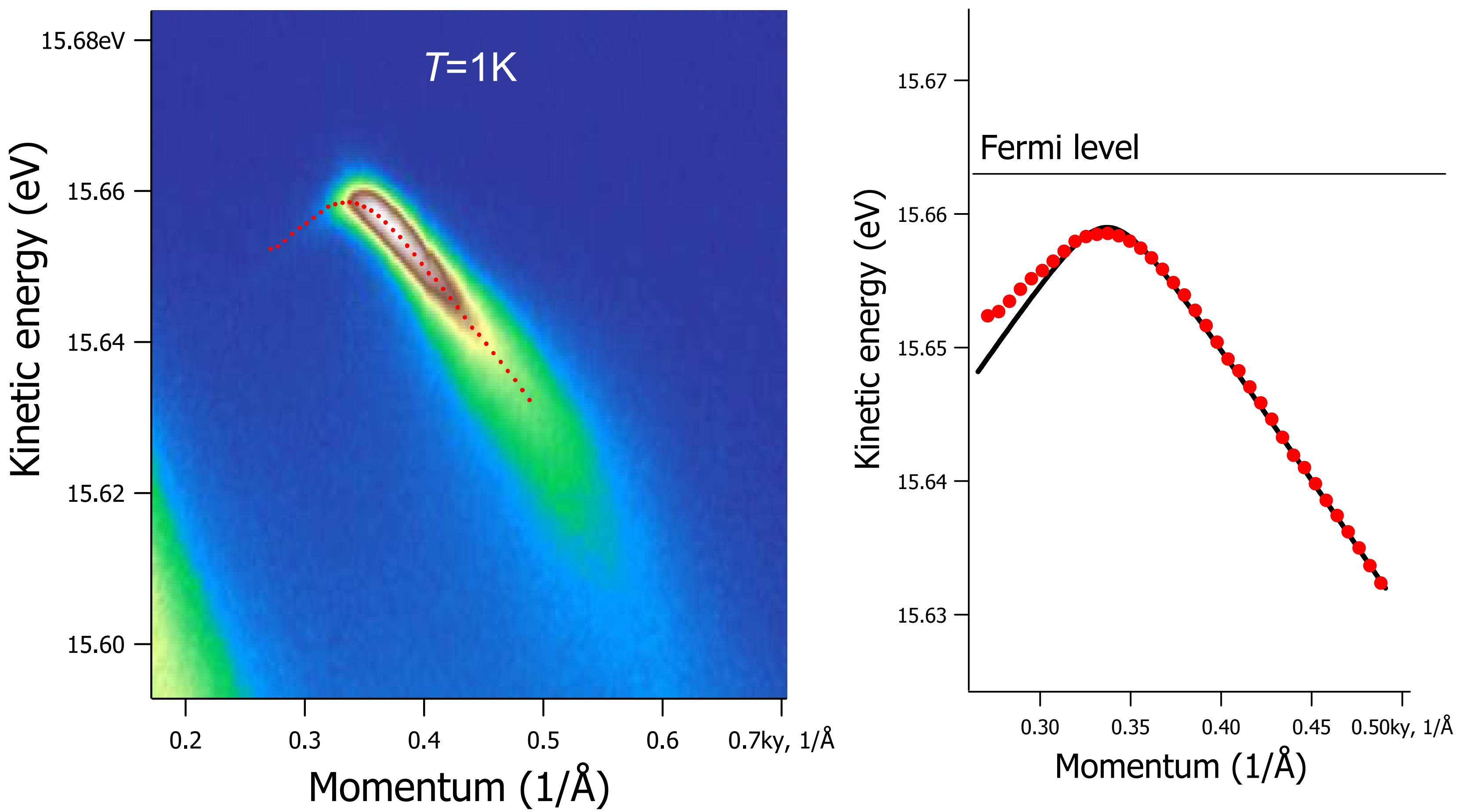

Superconducting gap opening in ARPES spectra

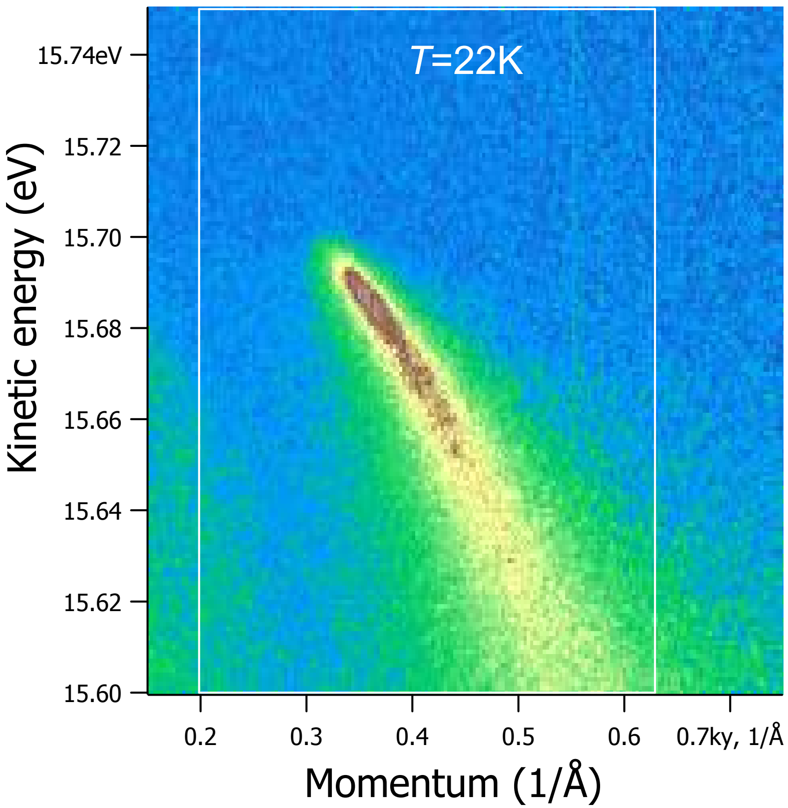

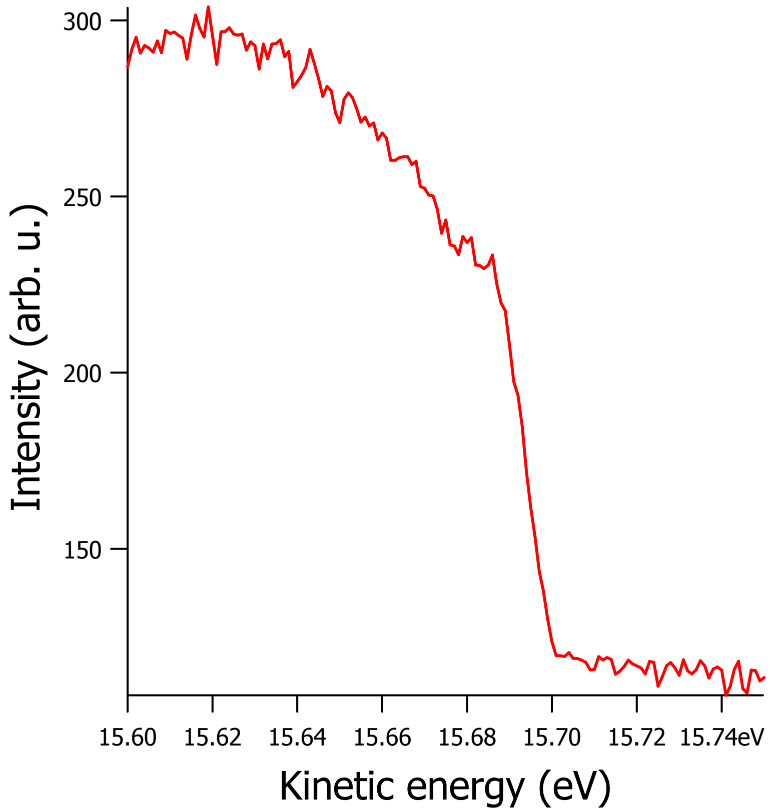

Superconducting gap opening in ARPES spectra

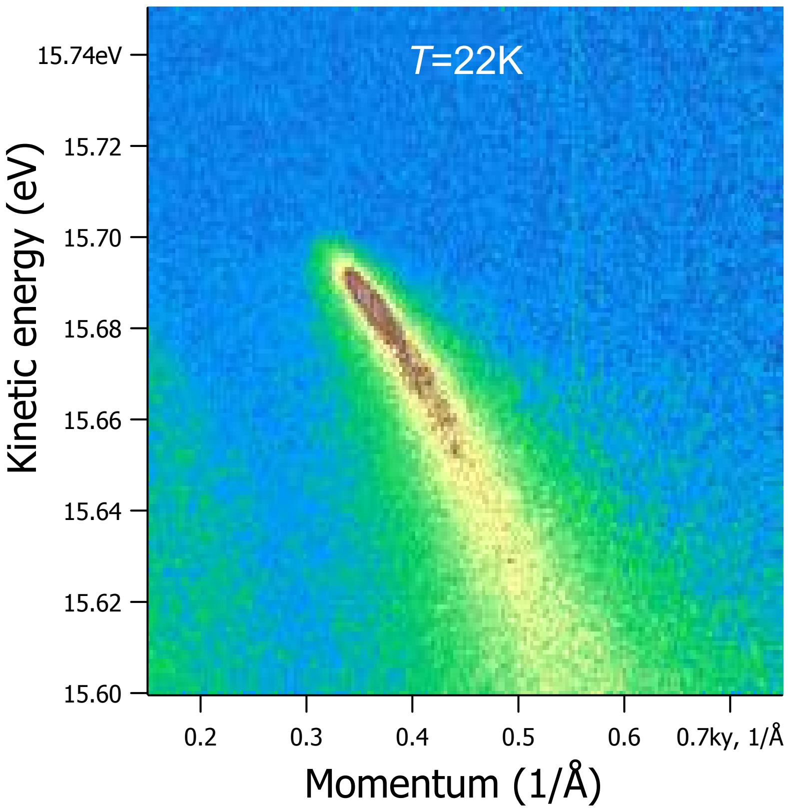

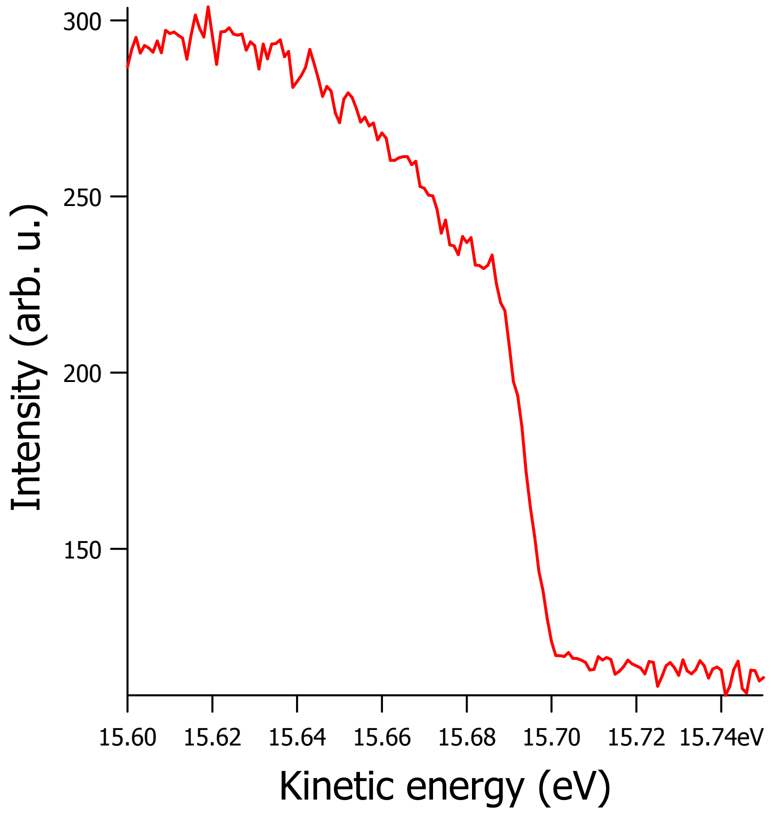

Superconducting gap opening in ARPES spectra

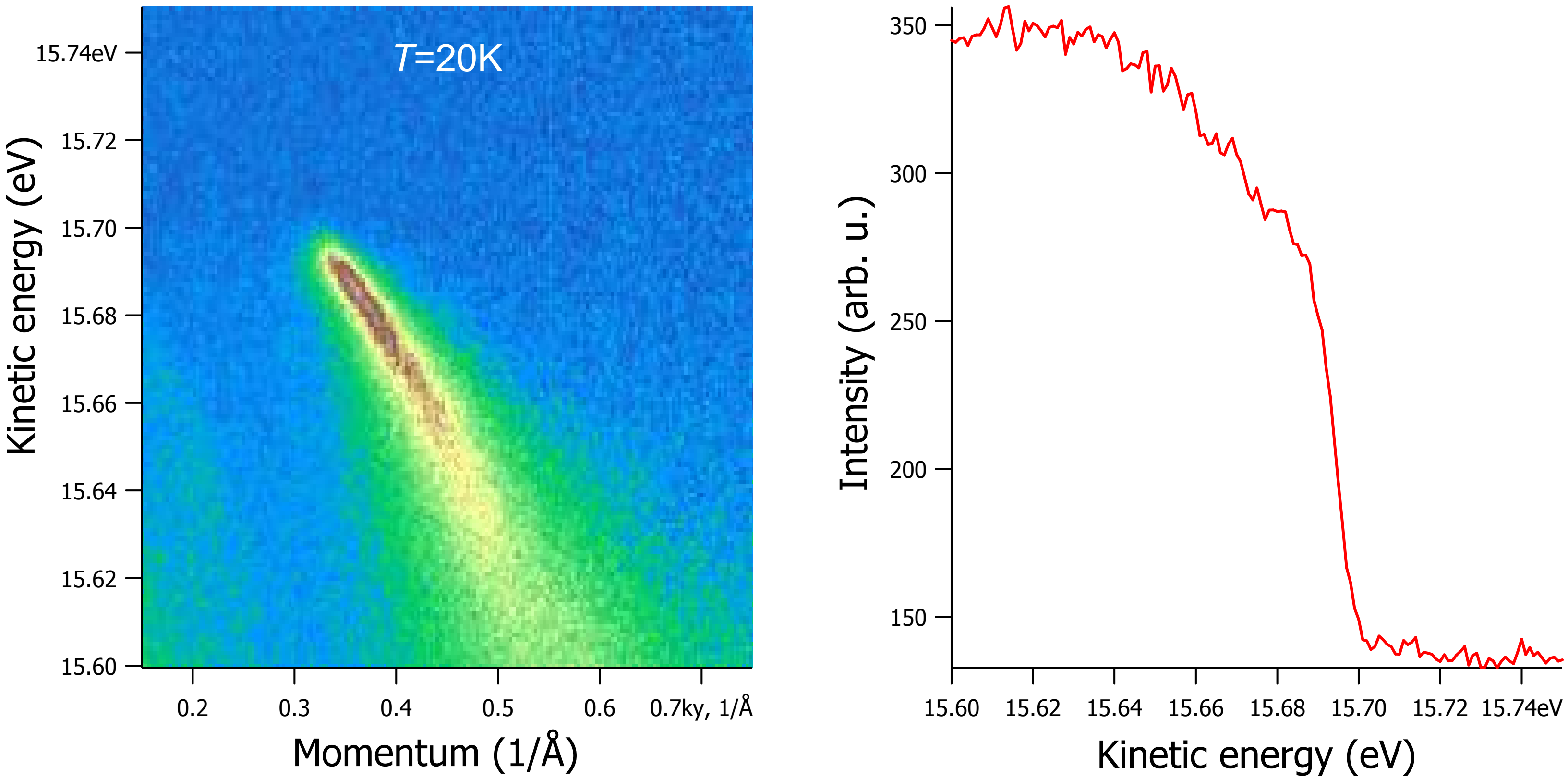

Superconducting gap opening in ARPES spectra

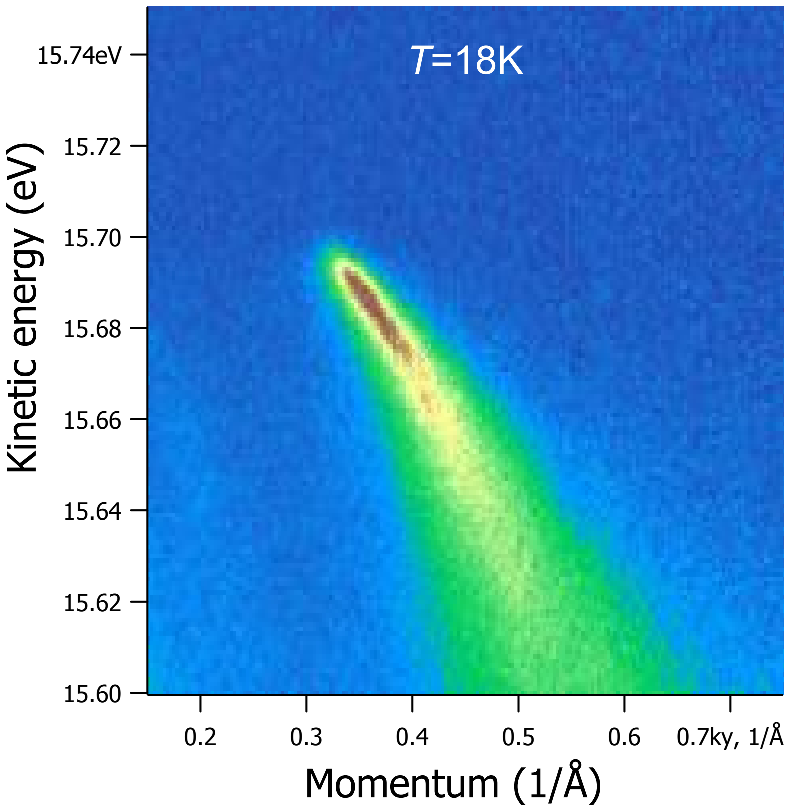

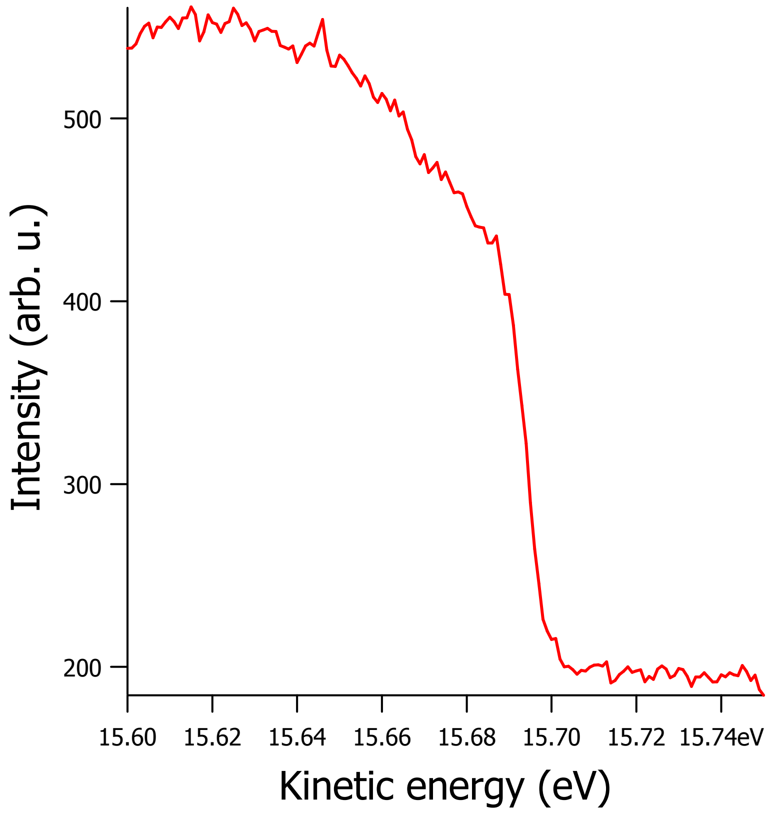

Superconducting gap opening in ARPES spectra

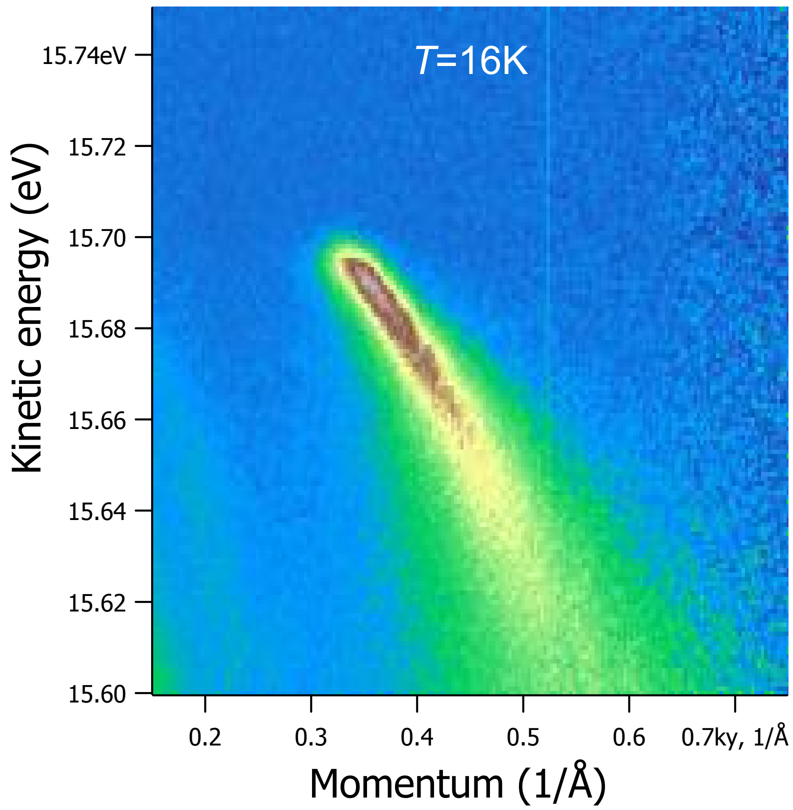

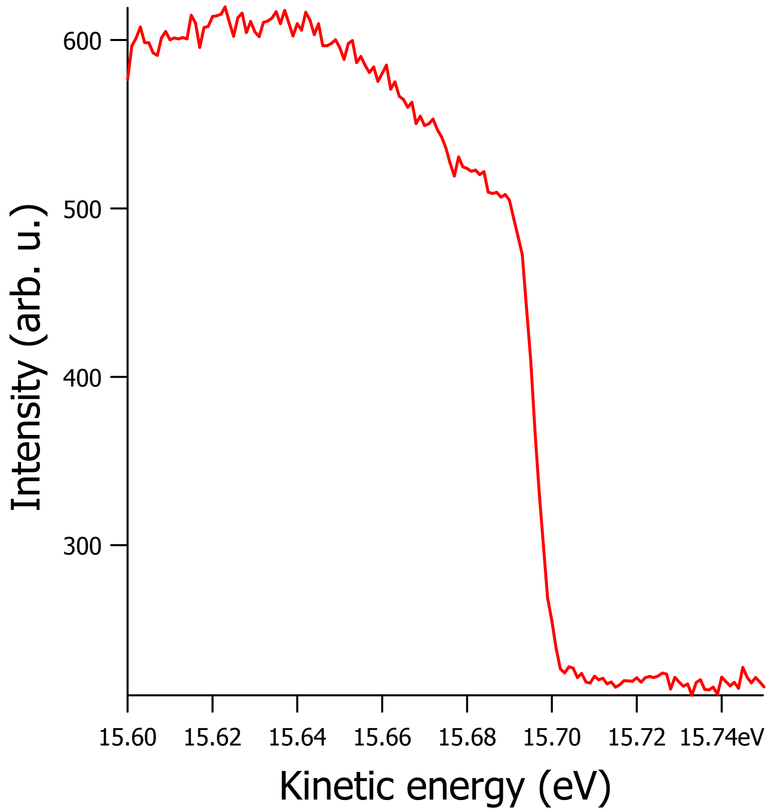

Superconducting gap opening in ARPES spectra

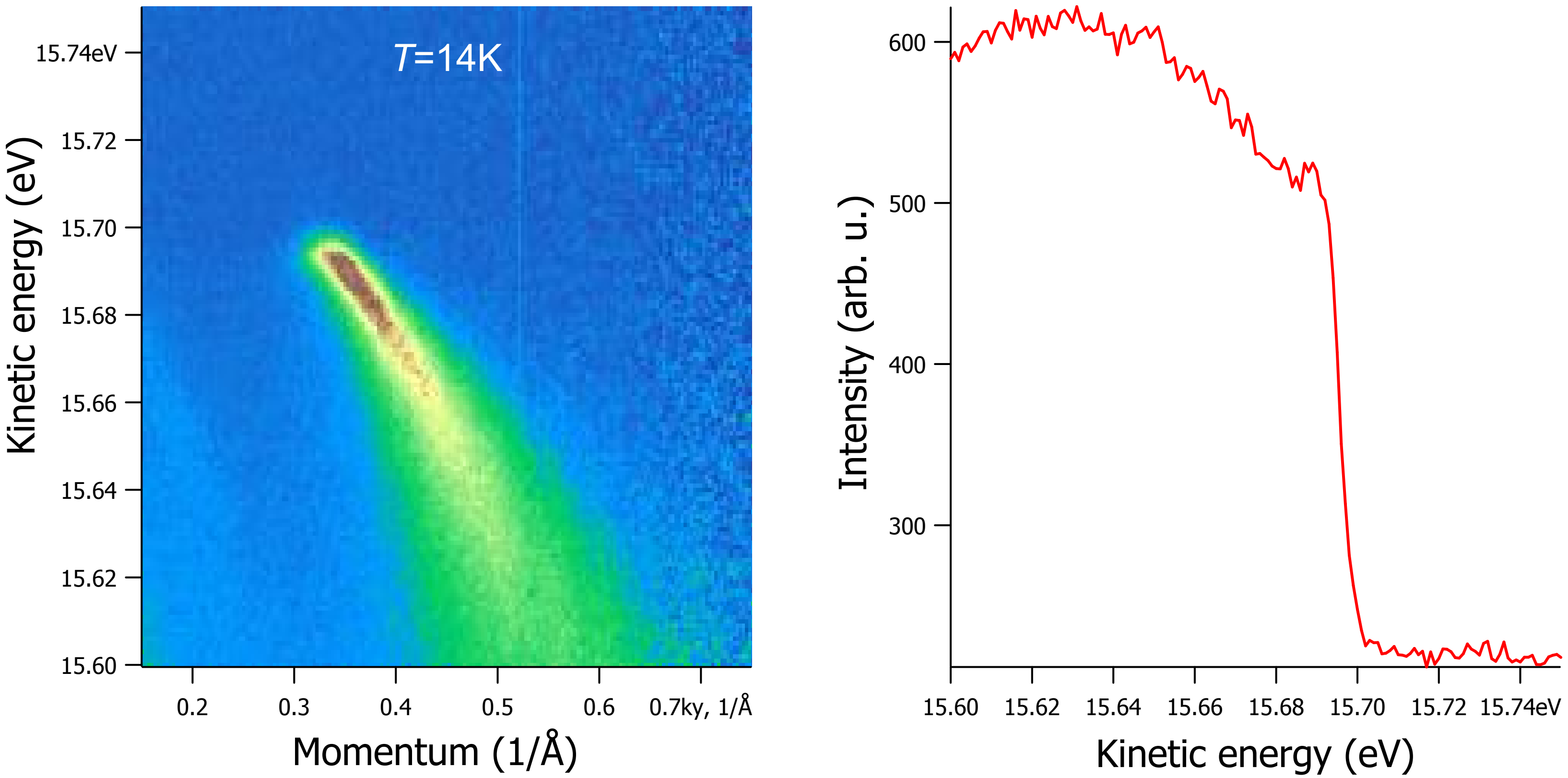

Superconducting gap opening in ARPES spectra

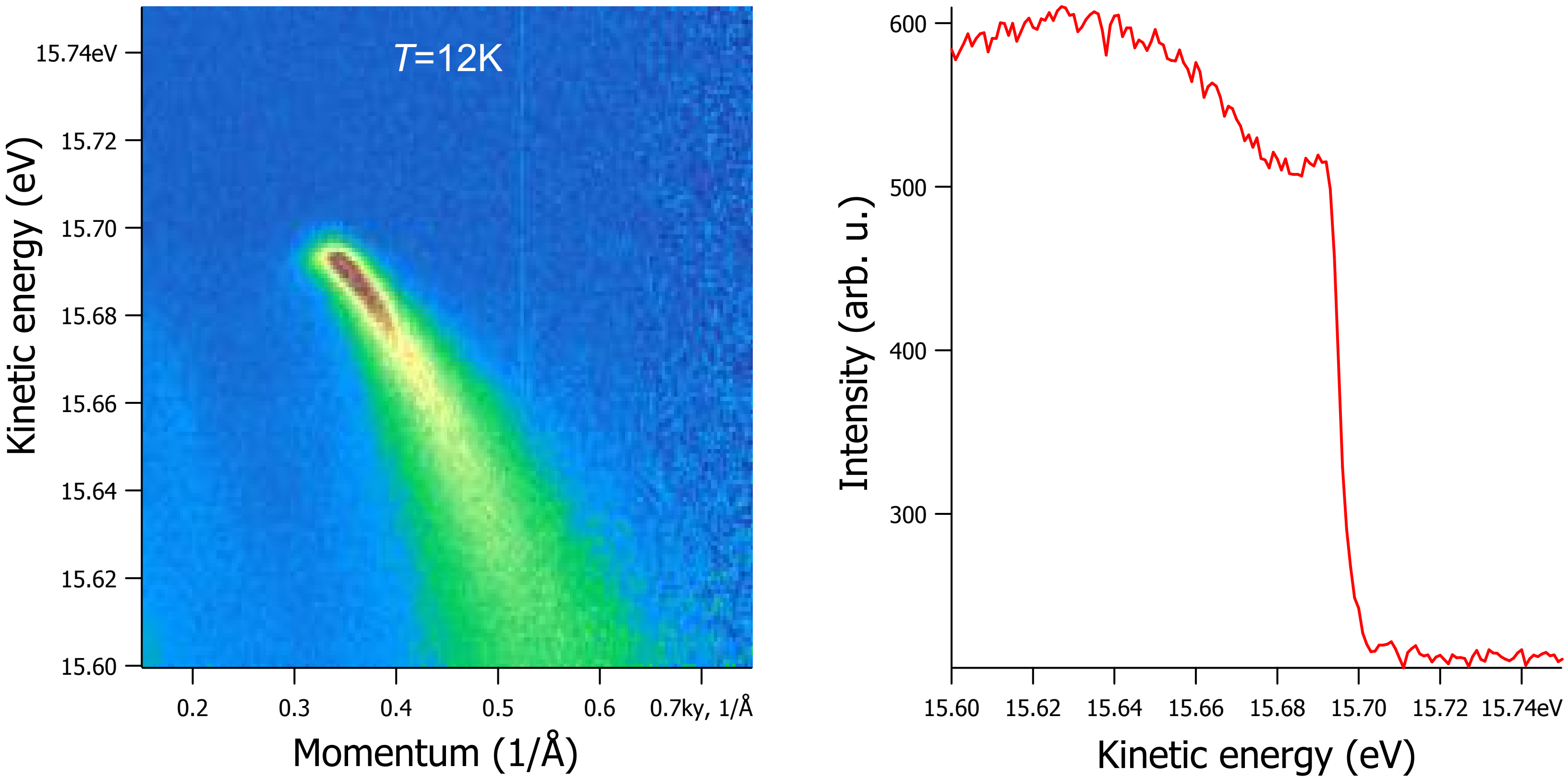

Superconducting gap opening in ARPES spectra

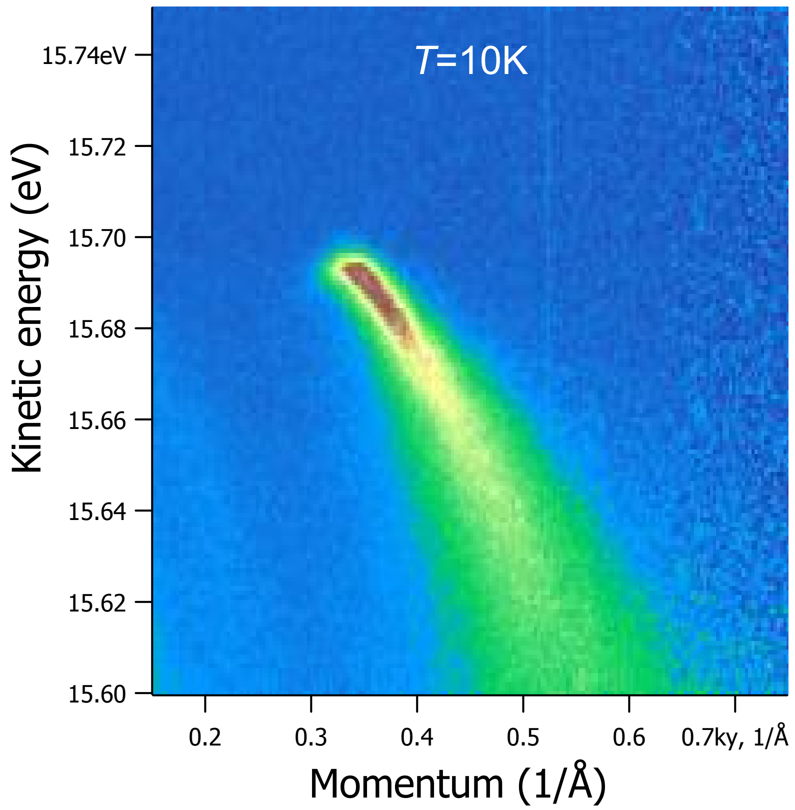

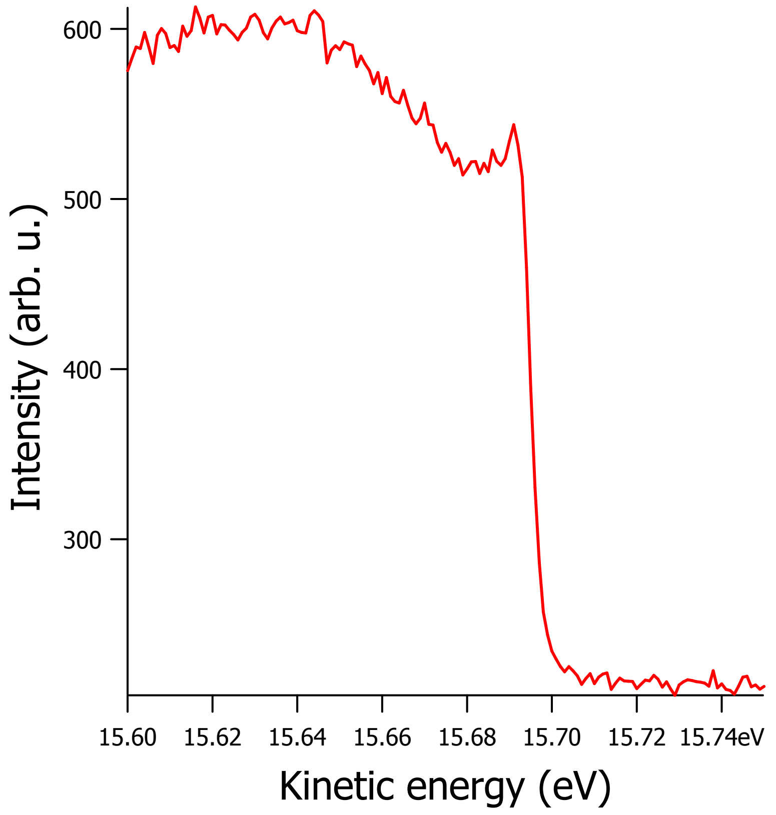

Superconducting gap opening in ARPES spectra

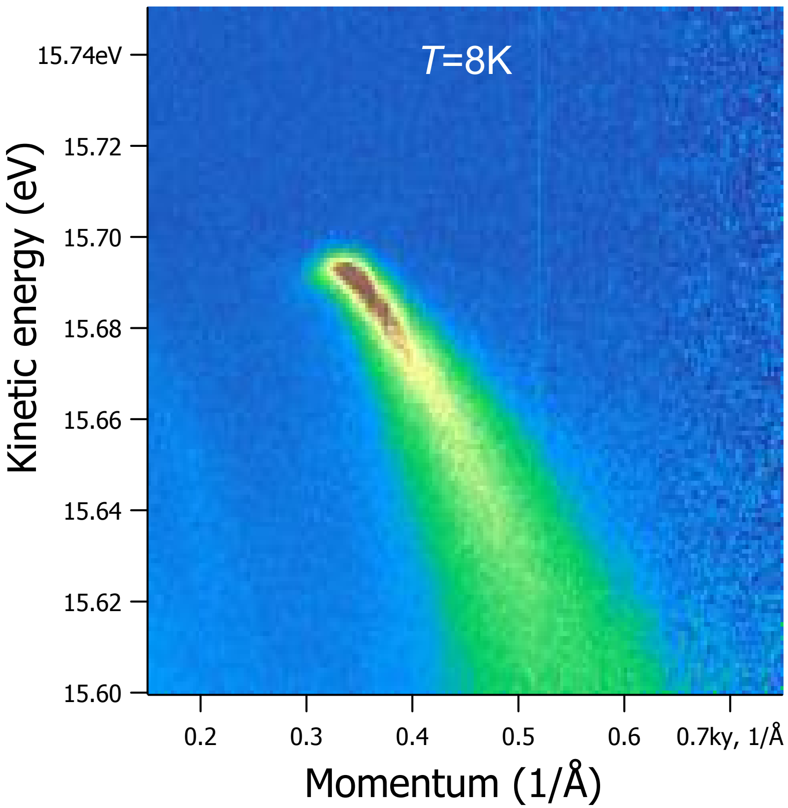

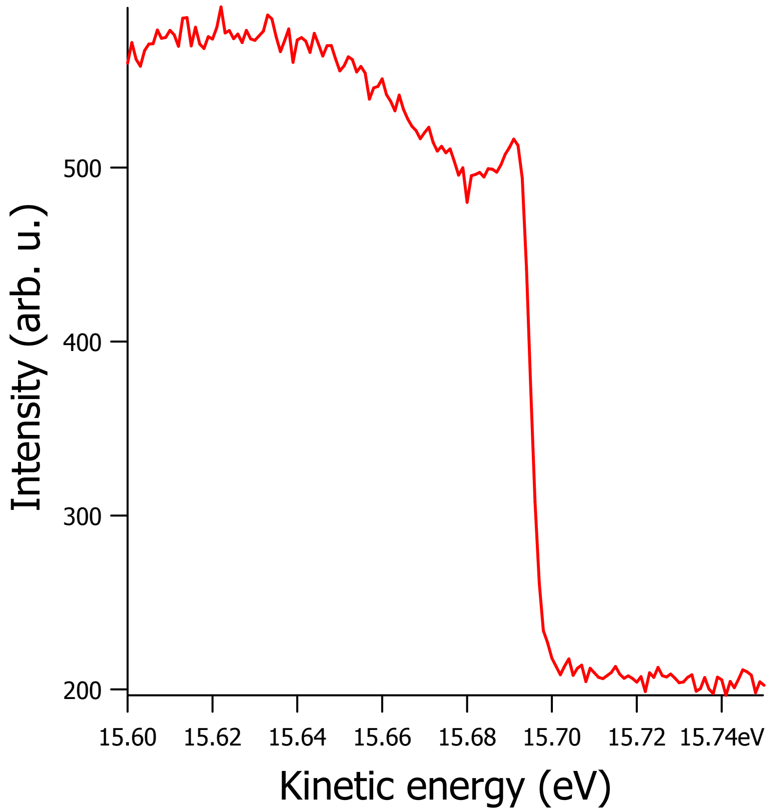

Superconducting gap opening in ARPES spectra

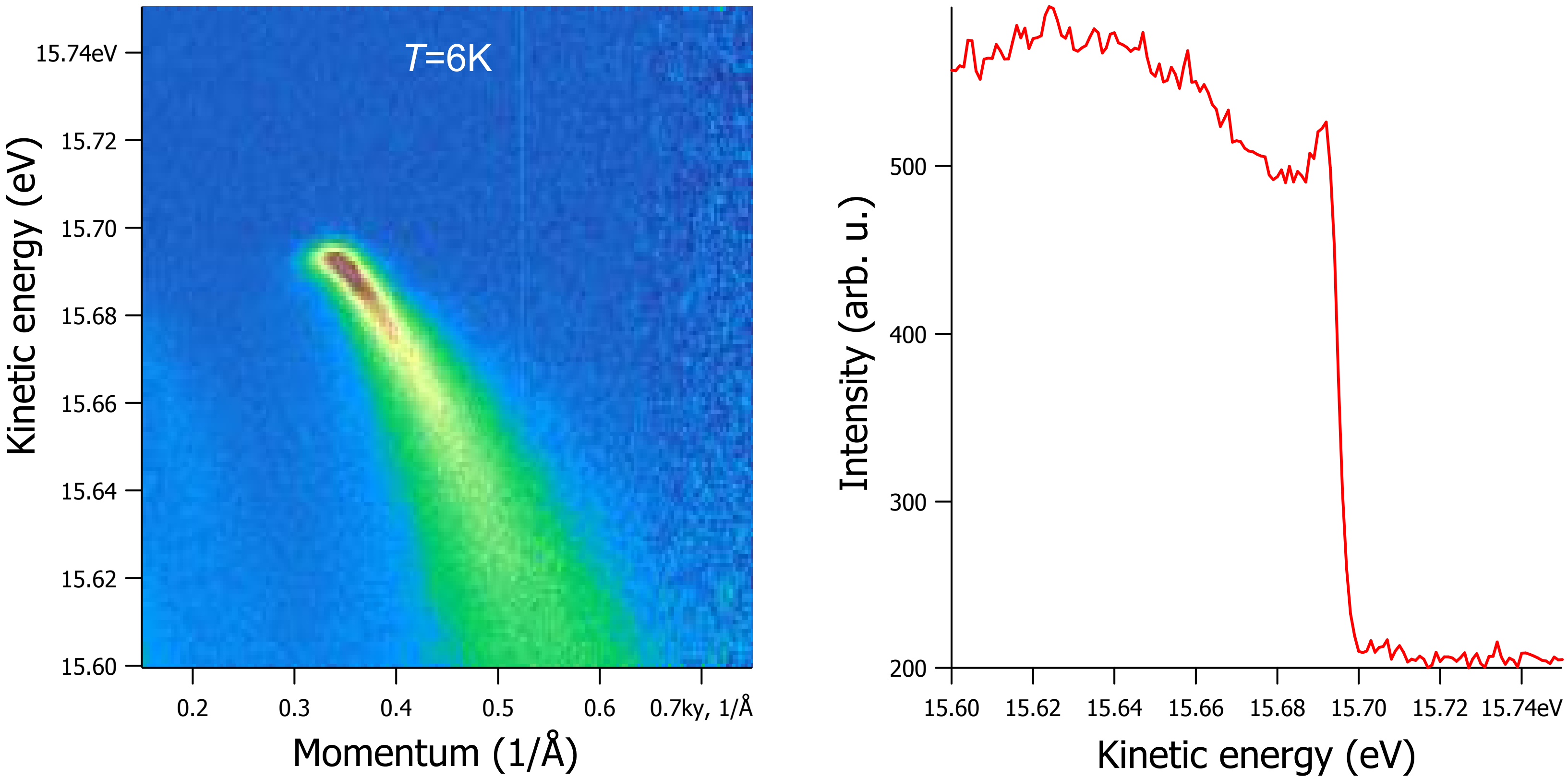

Superconducting gap opening in ARPES spectra

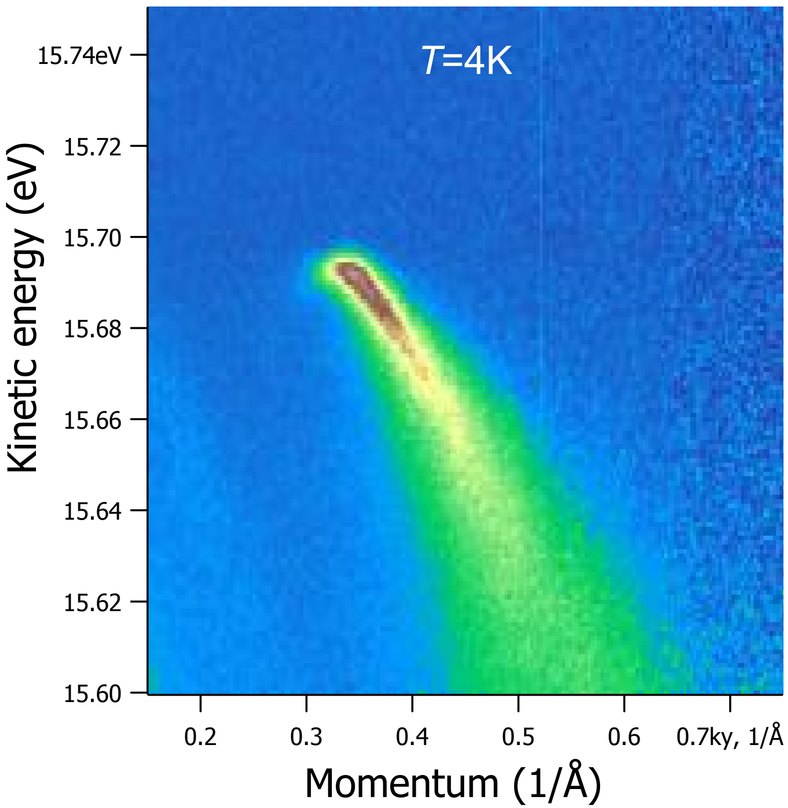

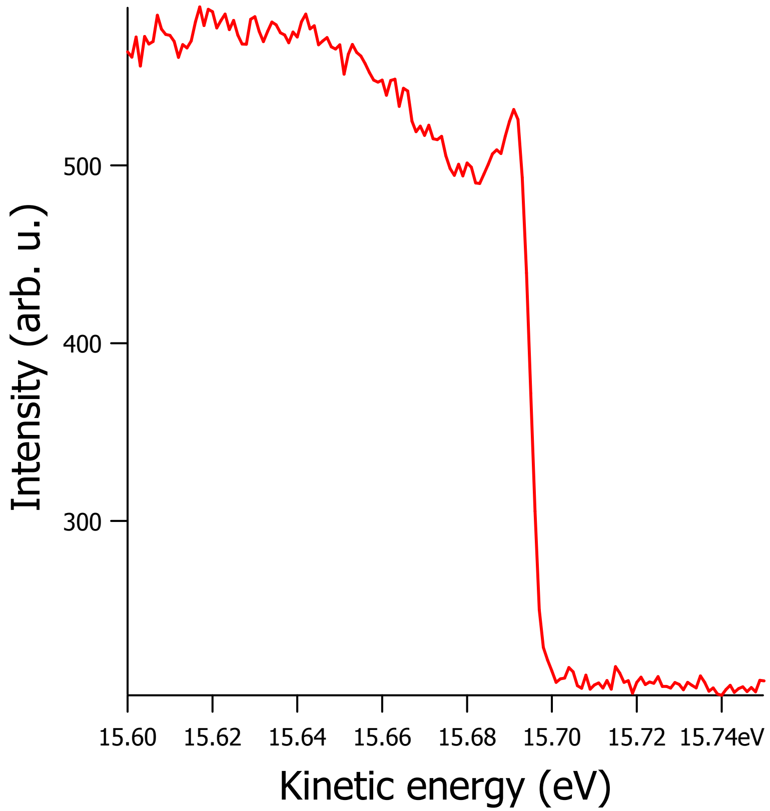

Superconducting gap opening in ARPES spectra

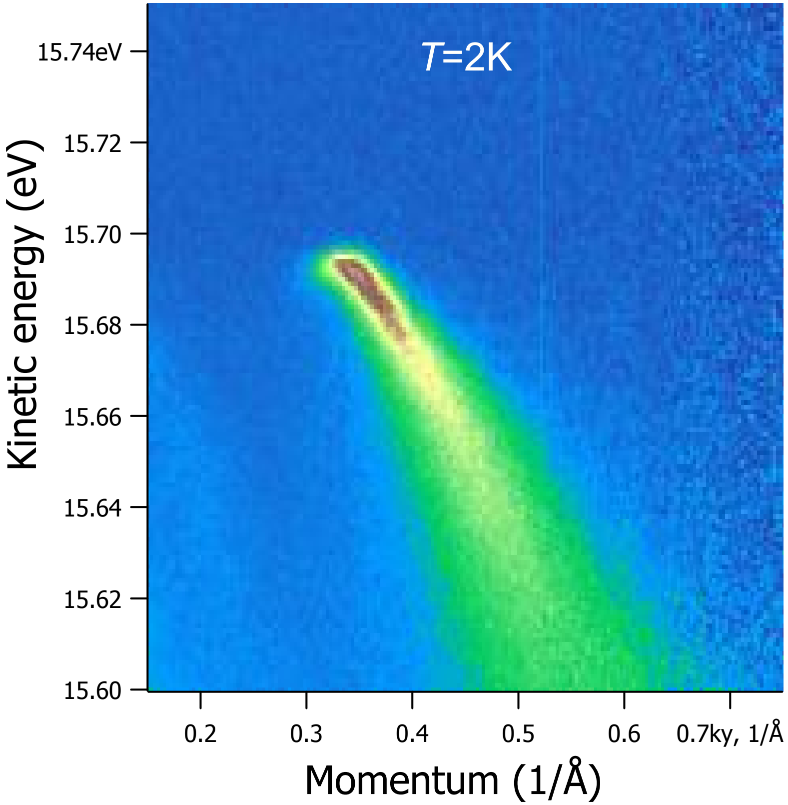

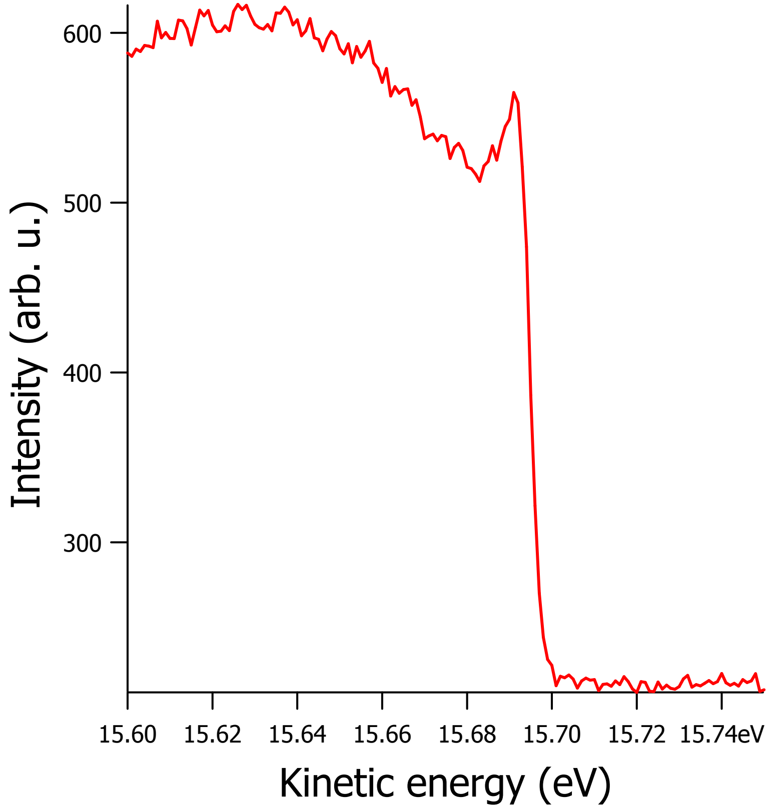

Gap extraction from ARPES data

Fit of IEDC

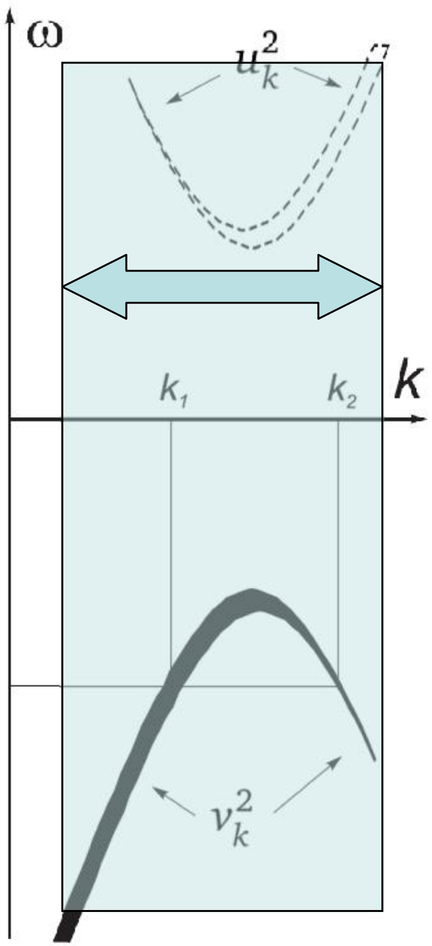

$$A(k,\omega) = 2\pi[u_k^2\delta(\omega - E_k) + v_k^2\delta(\omega + E_k)],$$

where

$$u_k^2 = \frac{1}{2}\left(1 + \frac{\xi_k}{E_k}\right), \quad v_k^2 = \frac{1}{2}\left(1 - \frac{\xi_k}{E_k}\right),$$

$$E_k = \sqrt{\xi_k^2 + \Delta^2}$$

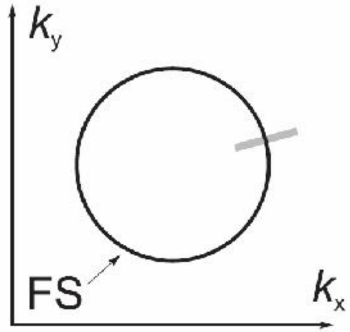

$$\mathrm{IEDC}(\omega) = \left[f(\omega, T) \cdot \left| \mathrm{Re} \frac{\omega + i\Sigma''}{E} \right| \right] \otimes R_\omega(\delta E)$$

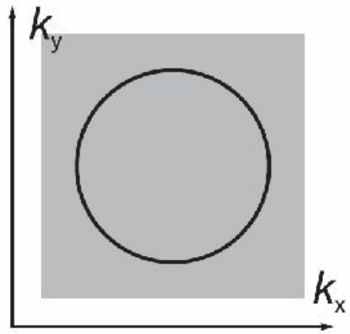

Dynes *et al.*, *PRL* (1978)

Evtushinsky *et al.*, *PRB* (2009)

Gap extraction from ARPES data

Fit vs. Symmetrization

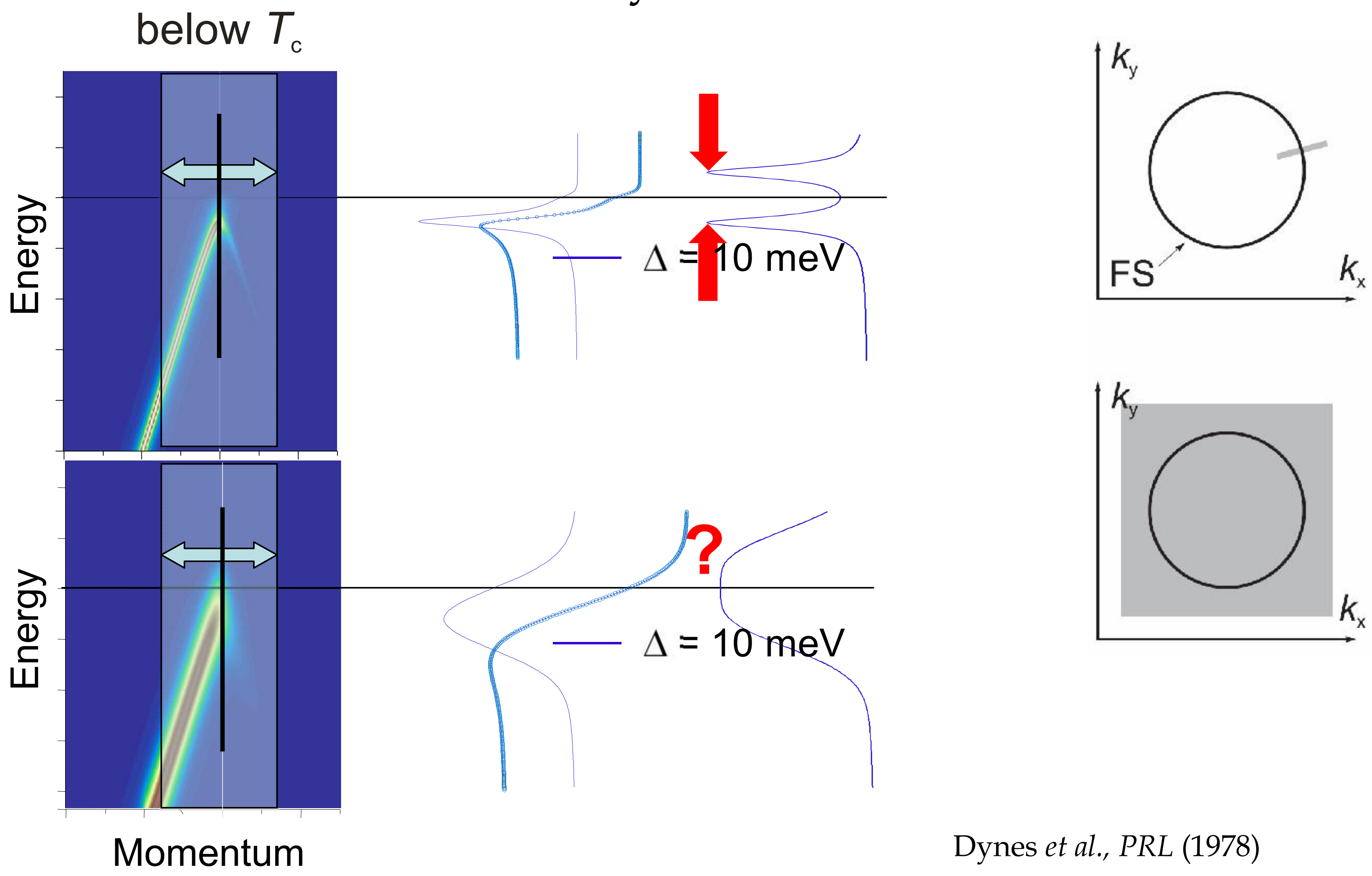

Dynes *et al.*, *PRL* (1978)

Evtushinsky *et al.*, *PRB* (2009)

Superconducting gap in $Ba_{1-x}K_xFe_2As_2$

Fermi surfaces of iron-based superconductors

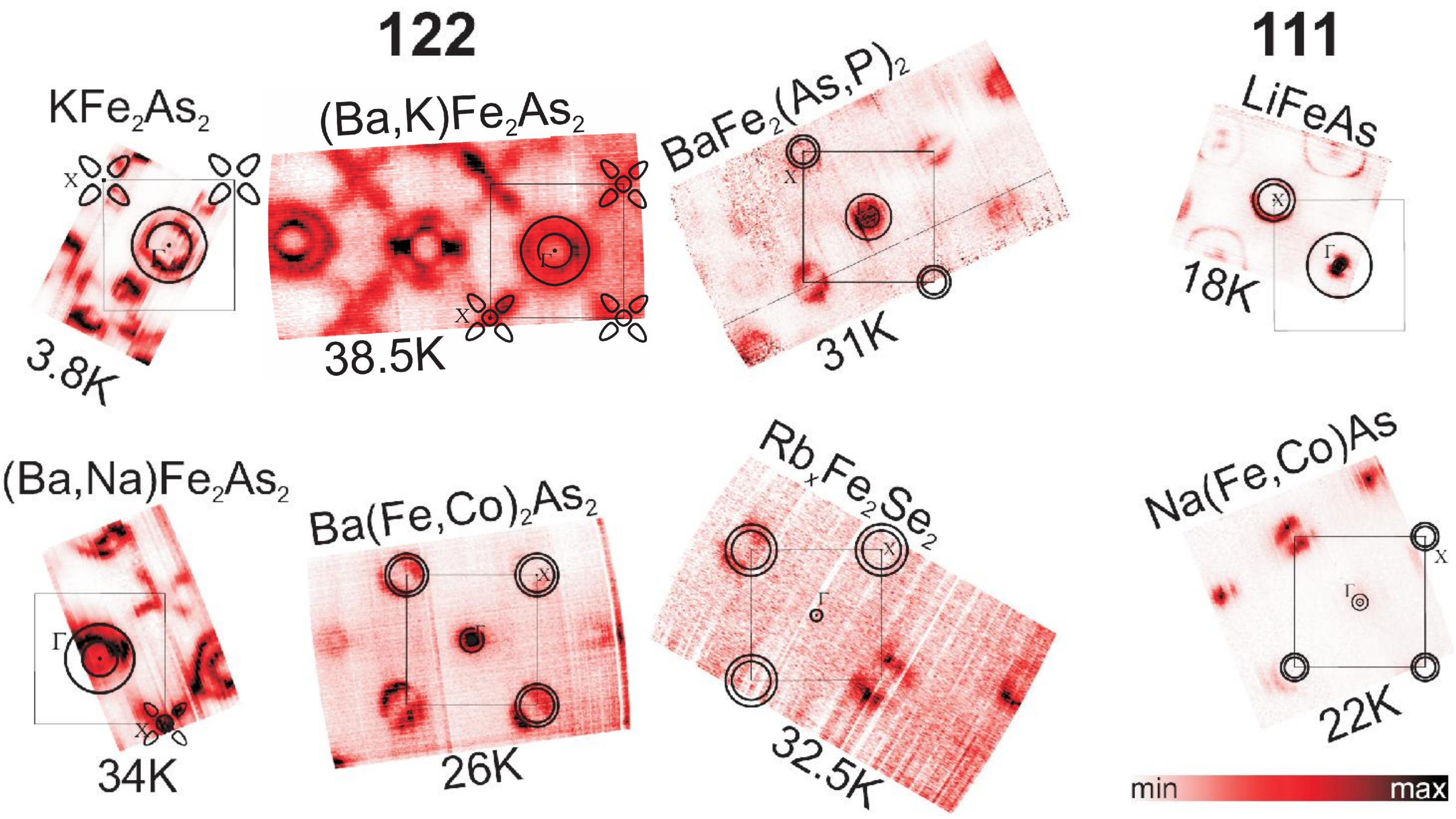

Hole-doped $BaFe_2As_2$

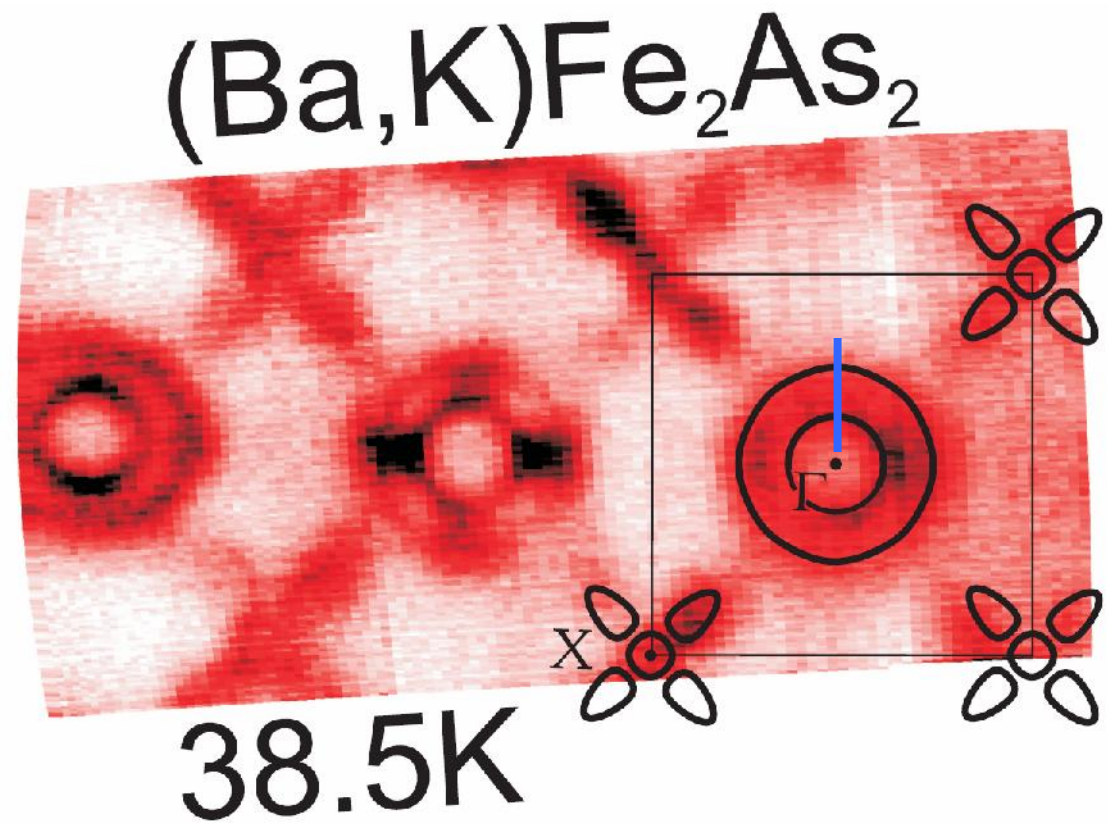

Superconducting gap distribution for $Ba_{1-x}K_xFe_2As_2$ (Γ FS sheets)

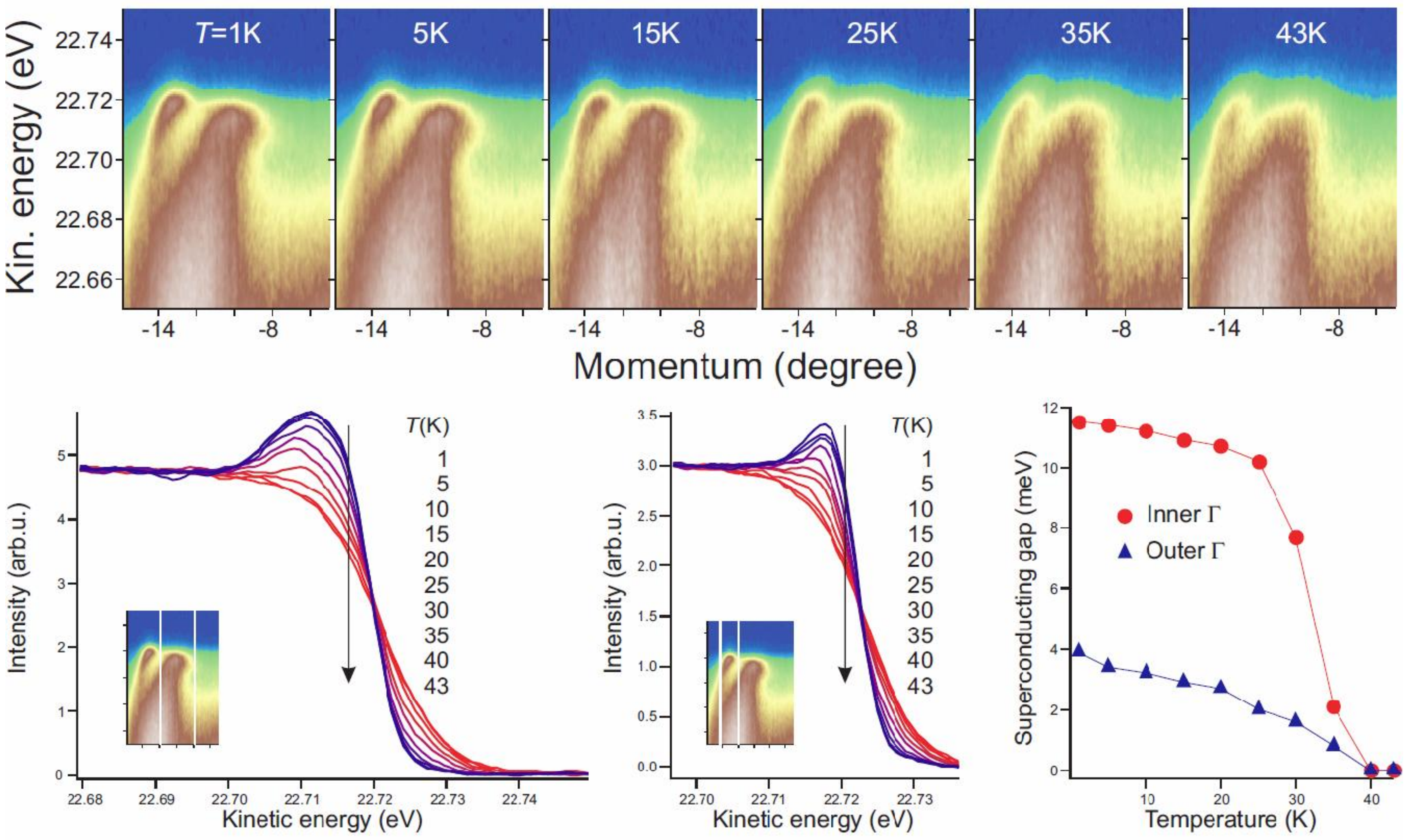

Hole-doped $BaFe_2As_2$

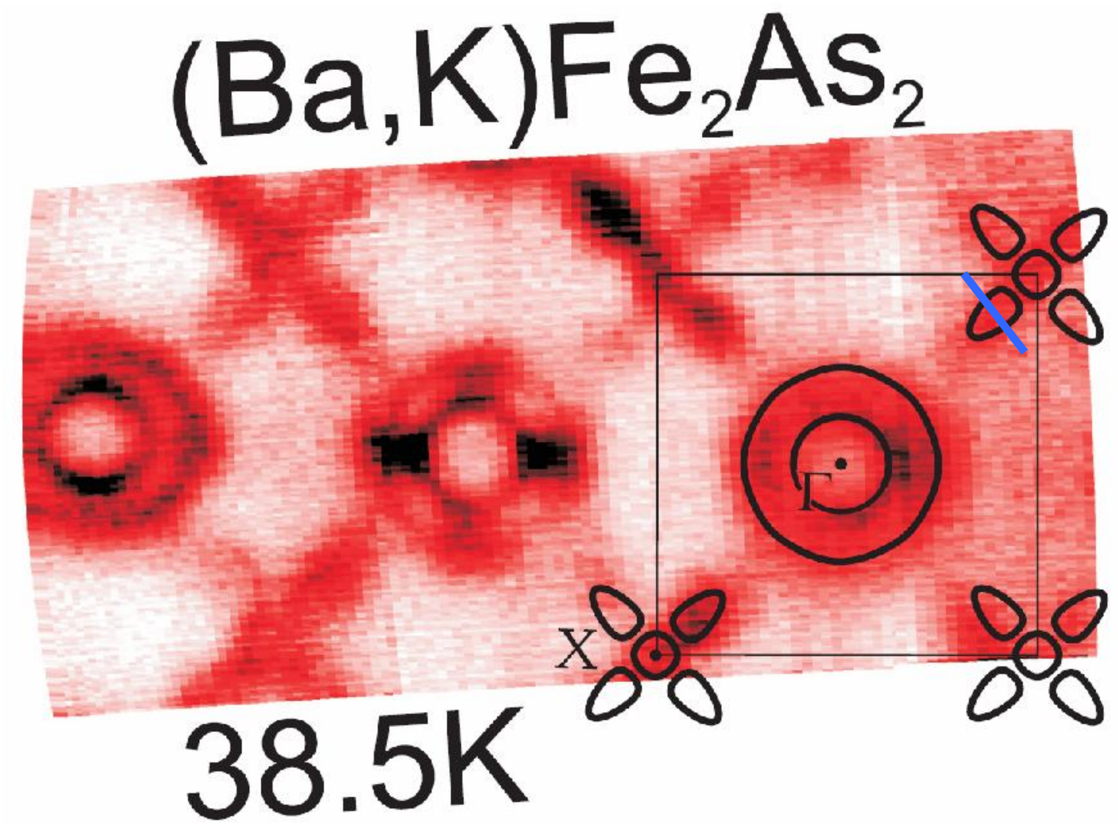

Gap on propeller-like structure

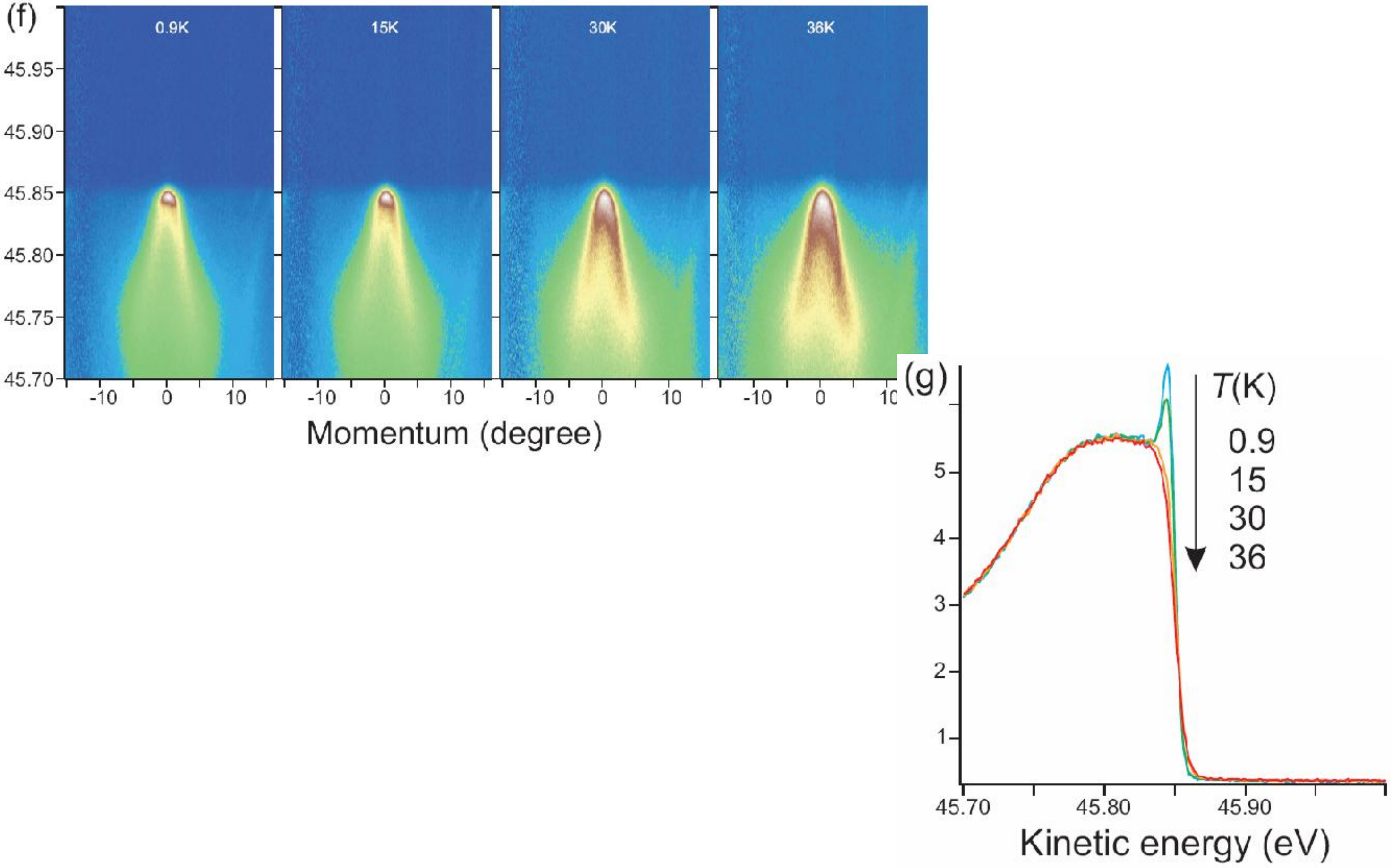

Hole-doped $BaFe_2As_2$

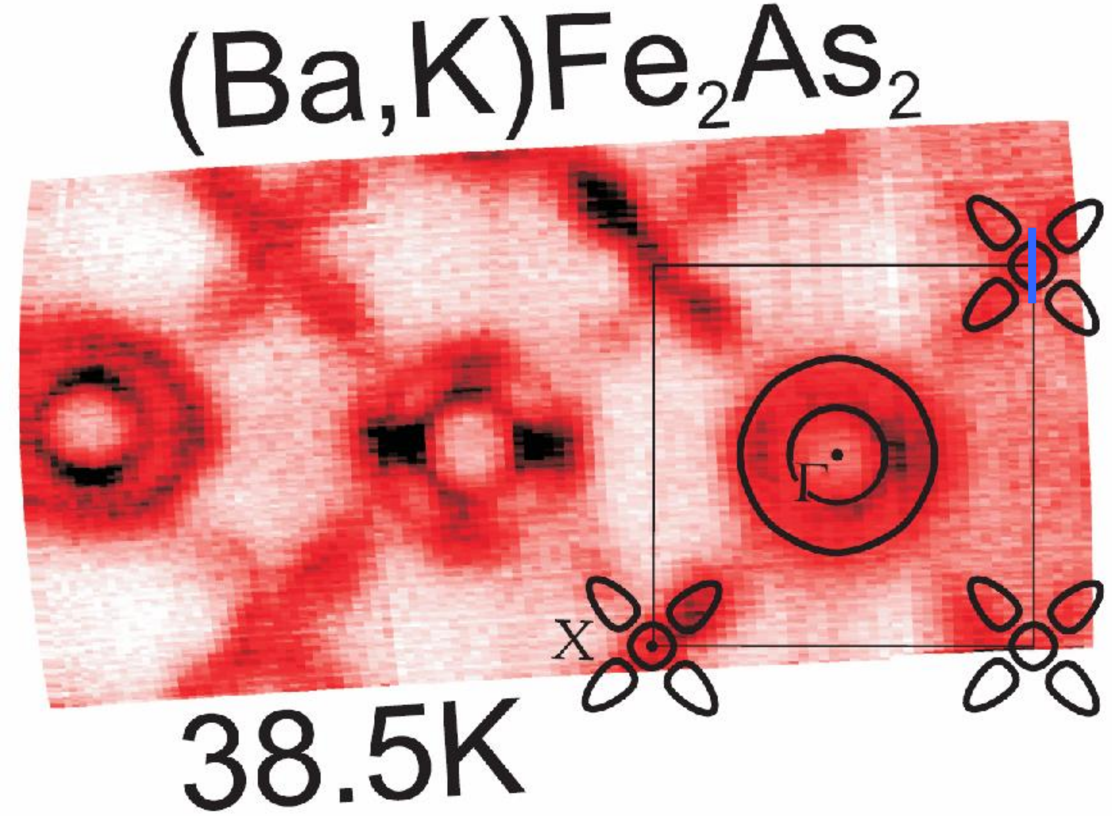

Gap on propeller-like structure

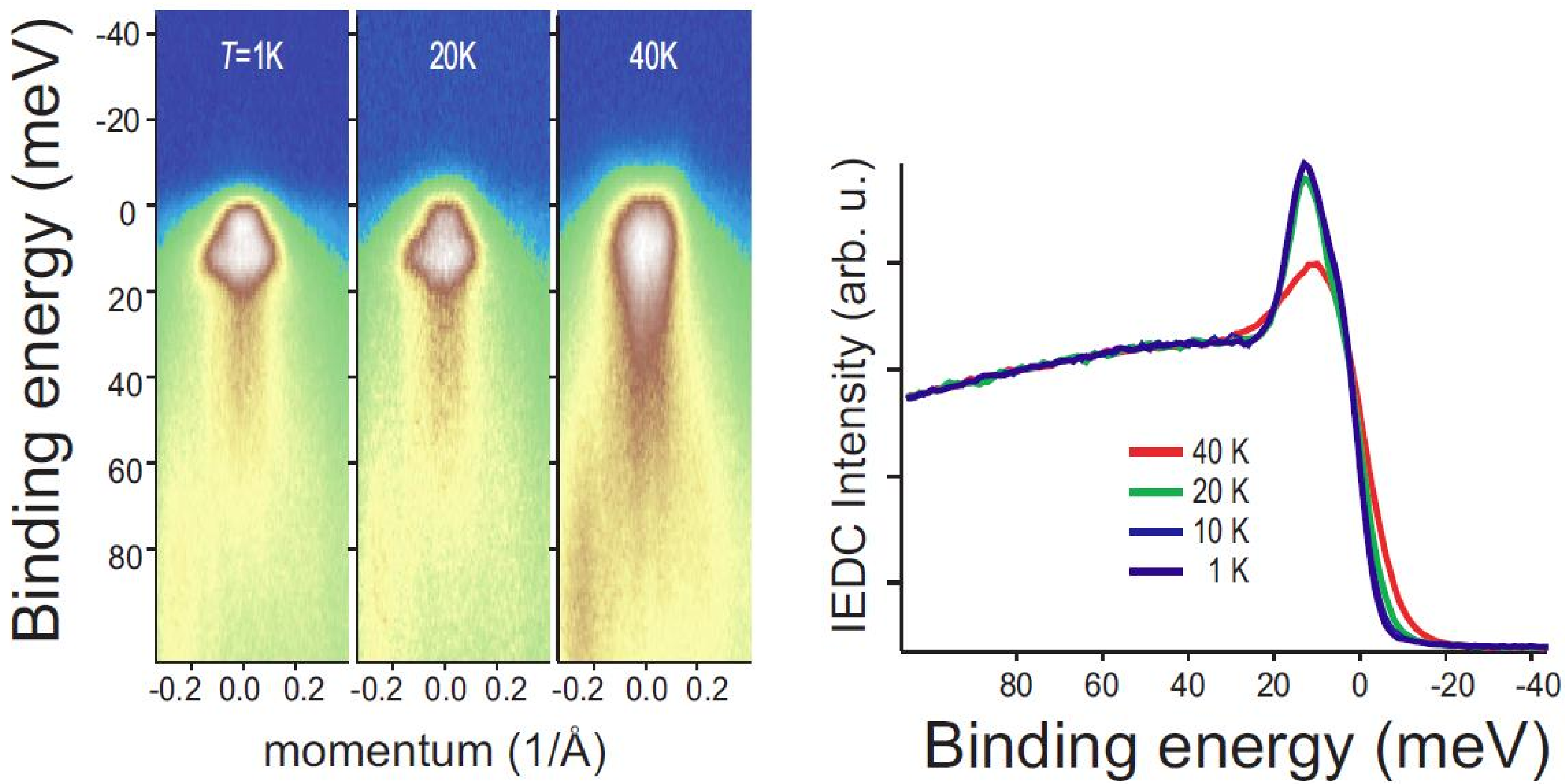

Gap anisotropy

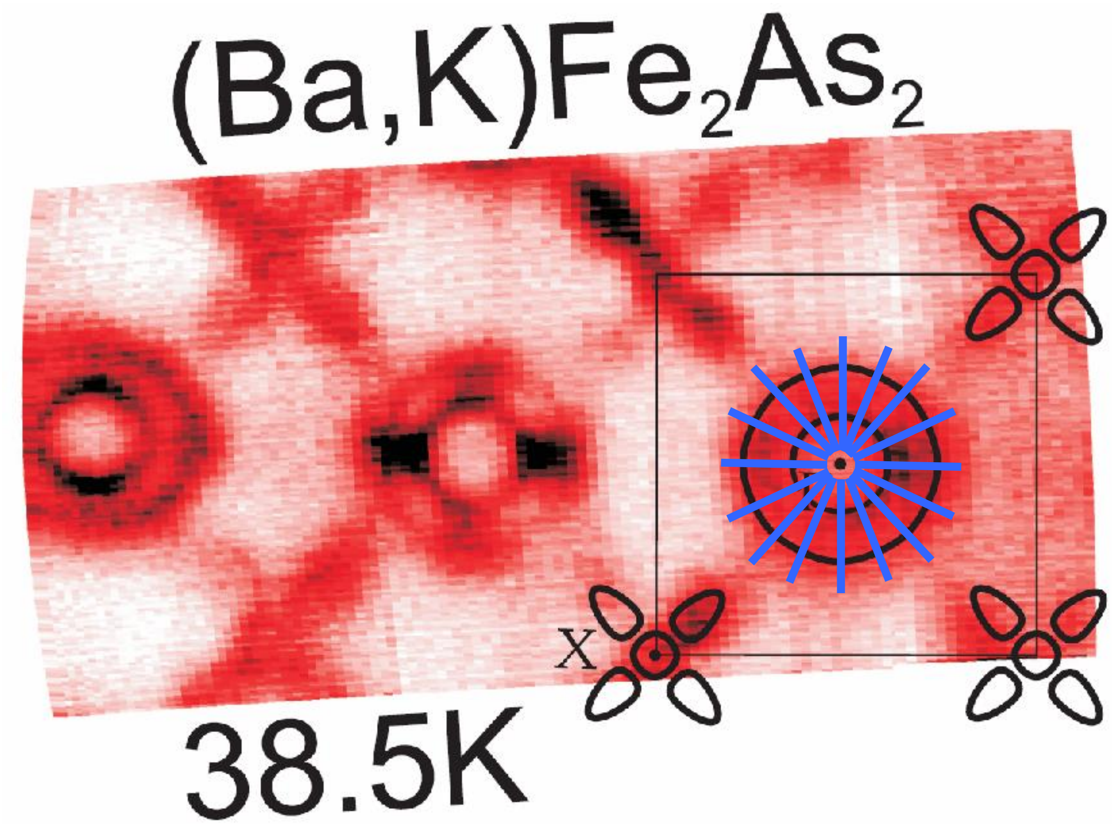

Anisotropy of gap for Γ-barrels

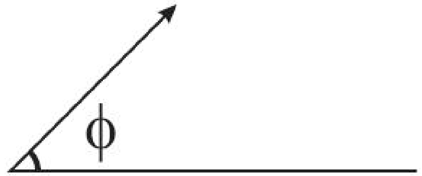

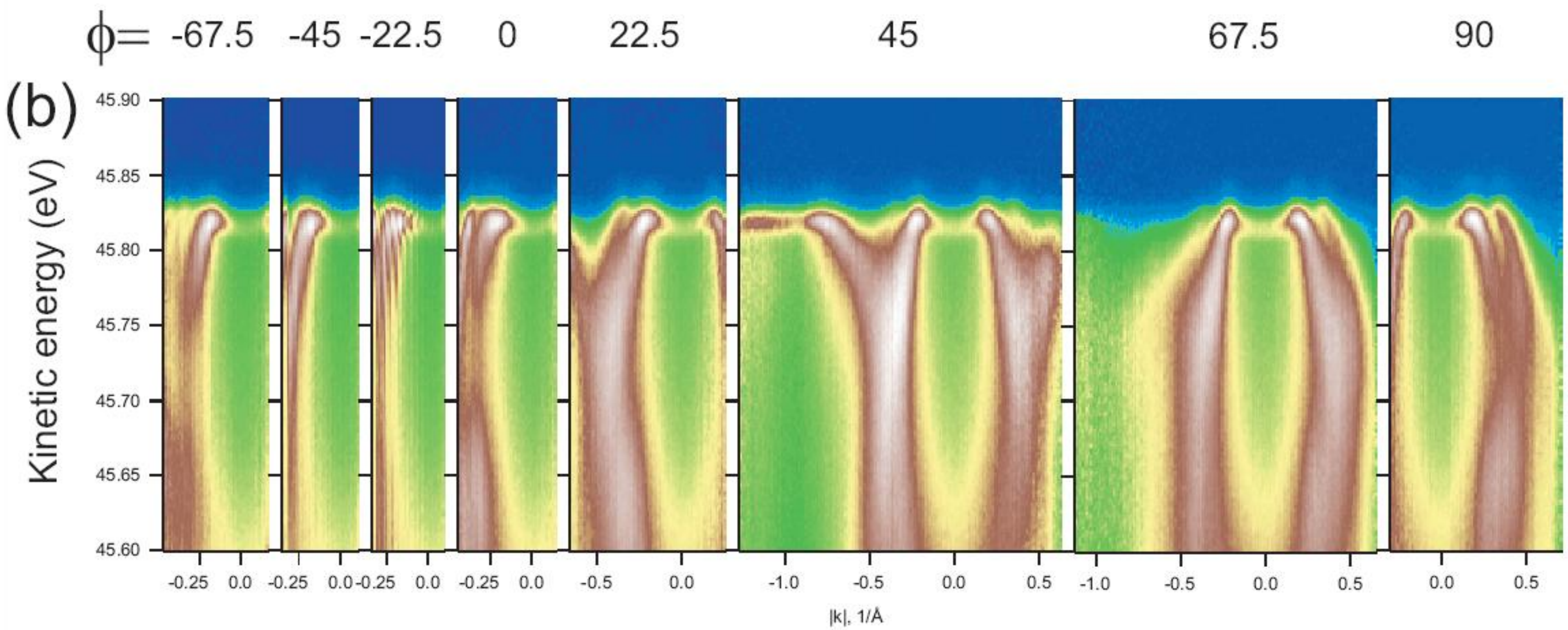

Momentum dependence of the superconducting gap in $Ba_{1-x}K_xFe_2As_2$

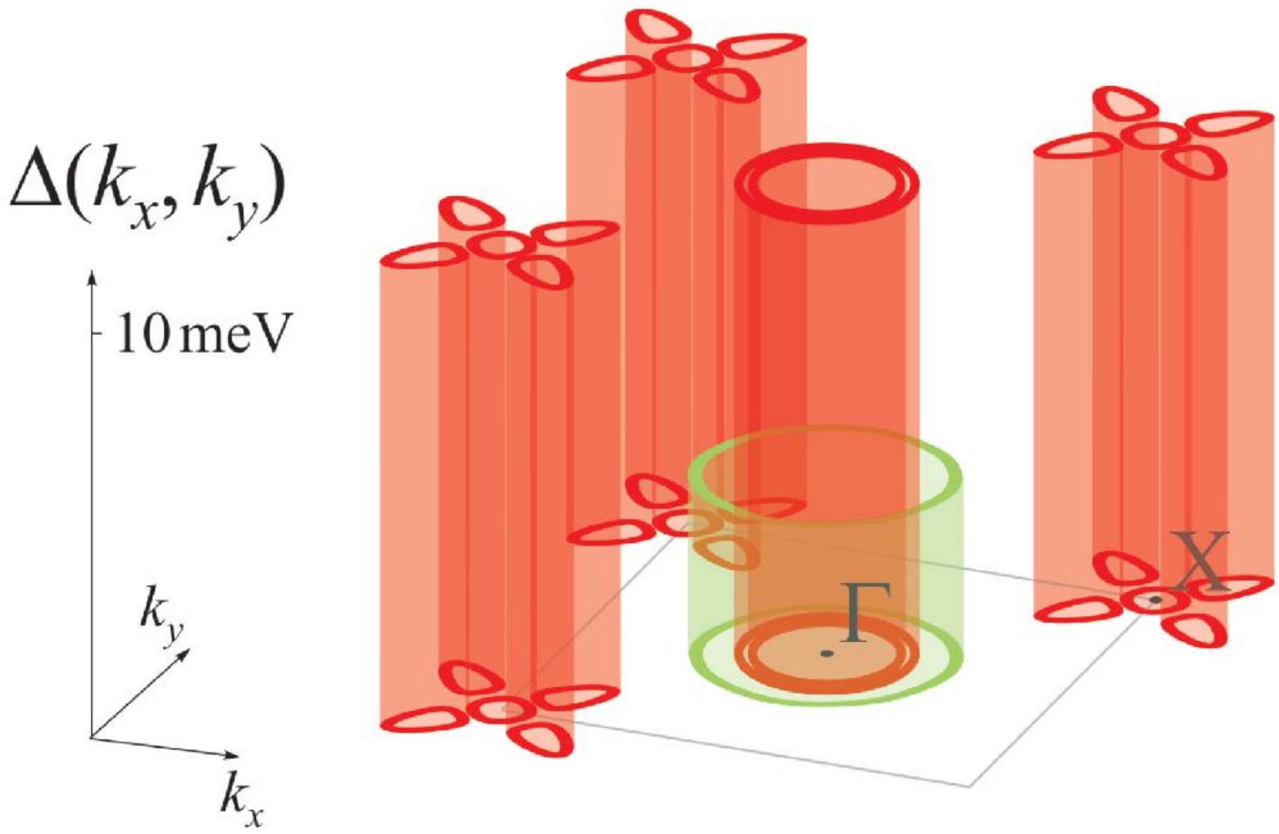

Fermi surface and gap distribution in cuprate superconductors

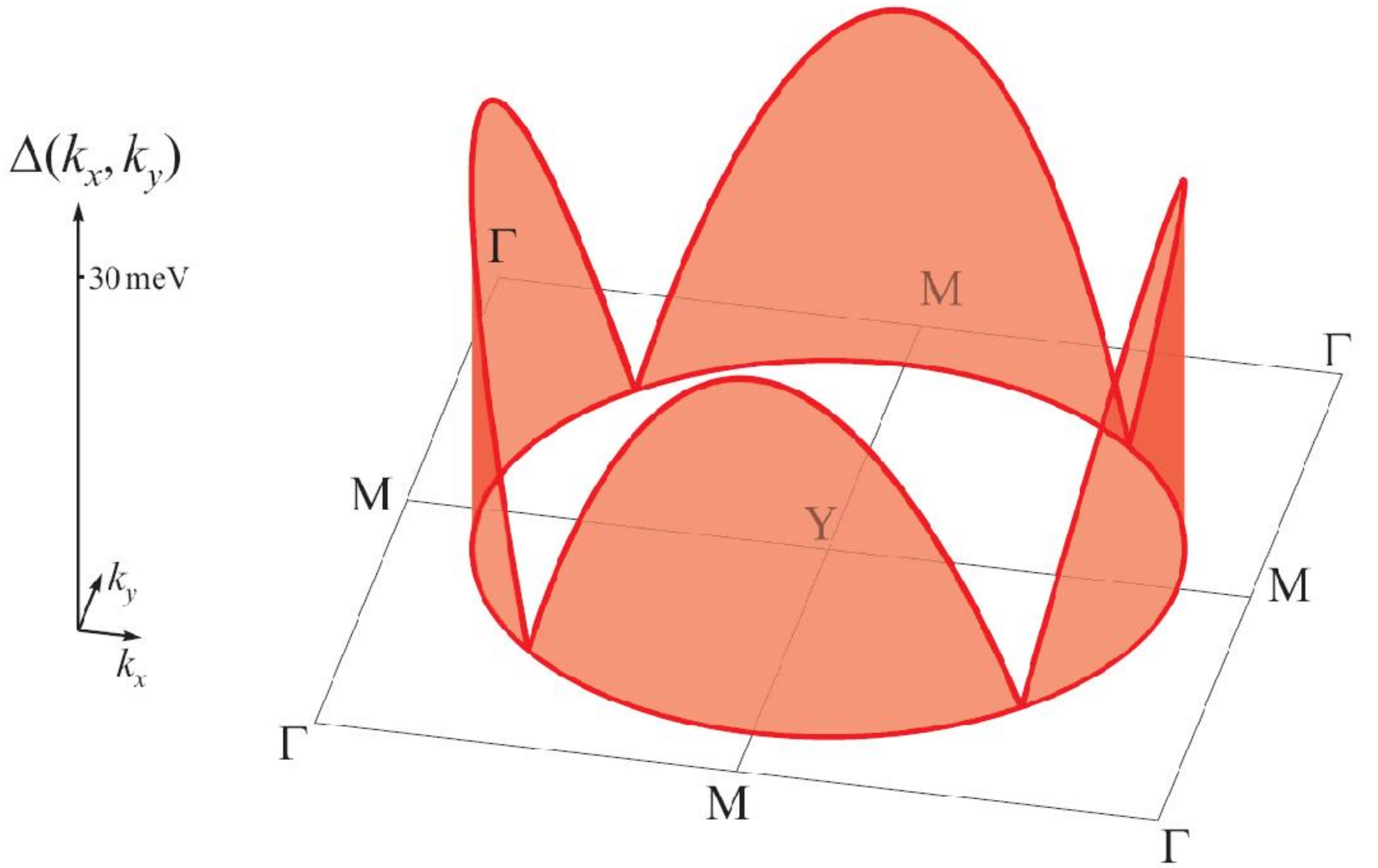

Superconducting gap in LiFeAs from fit of ARPES spectra

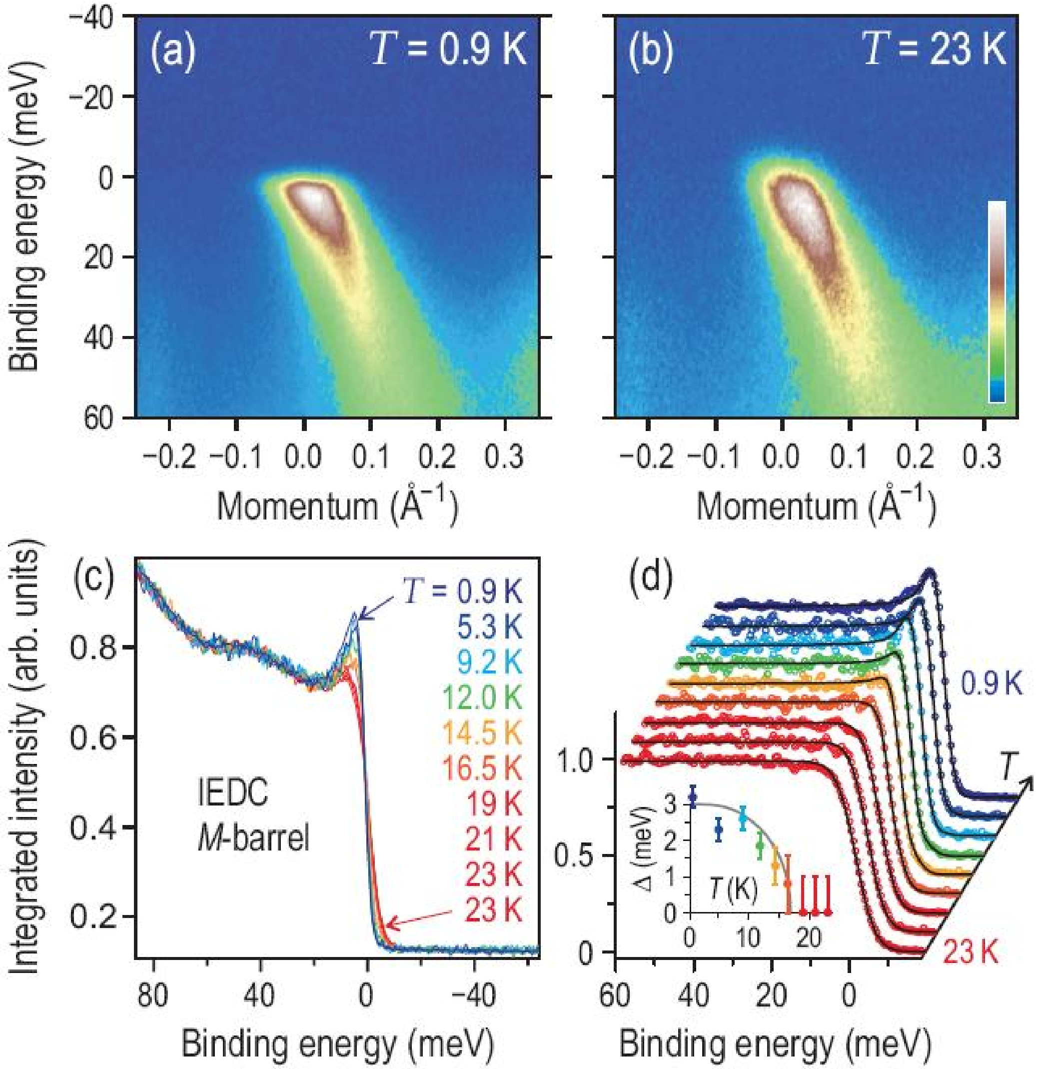

Superconducting gap of 1.7meV in underdoped $Ba_{1-x}Na_xFe_2As_2$ with T_c=10K

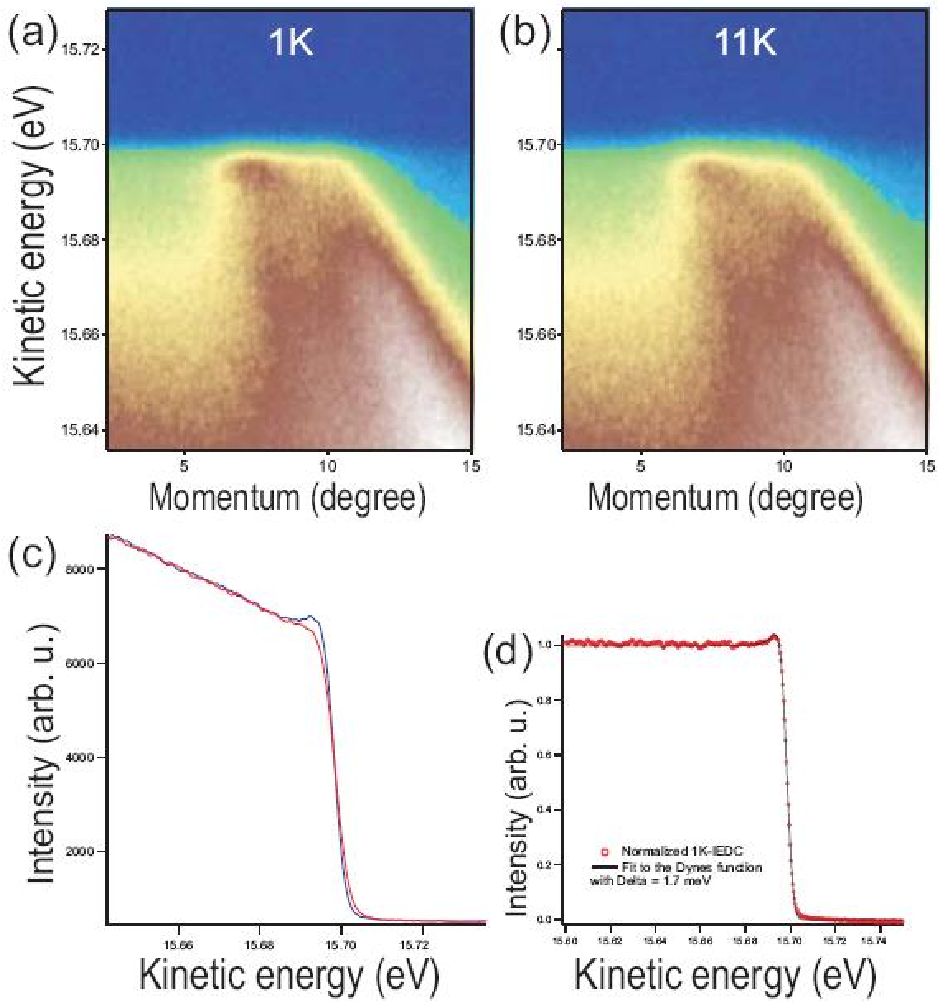

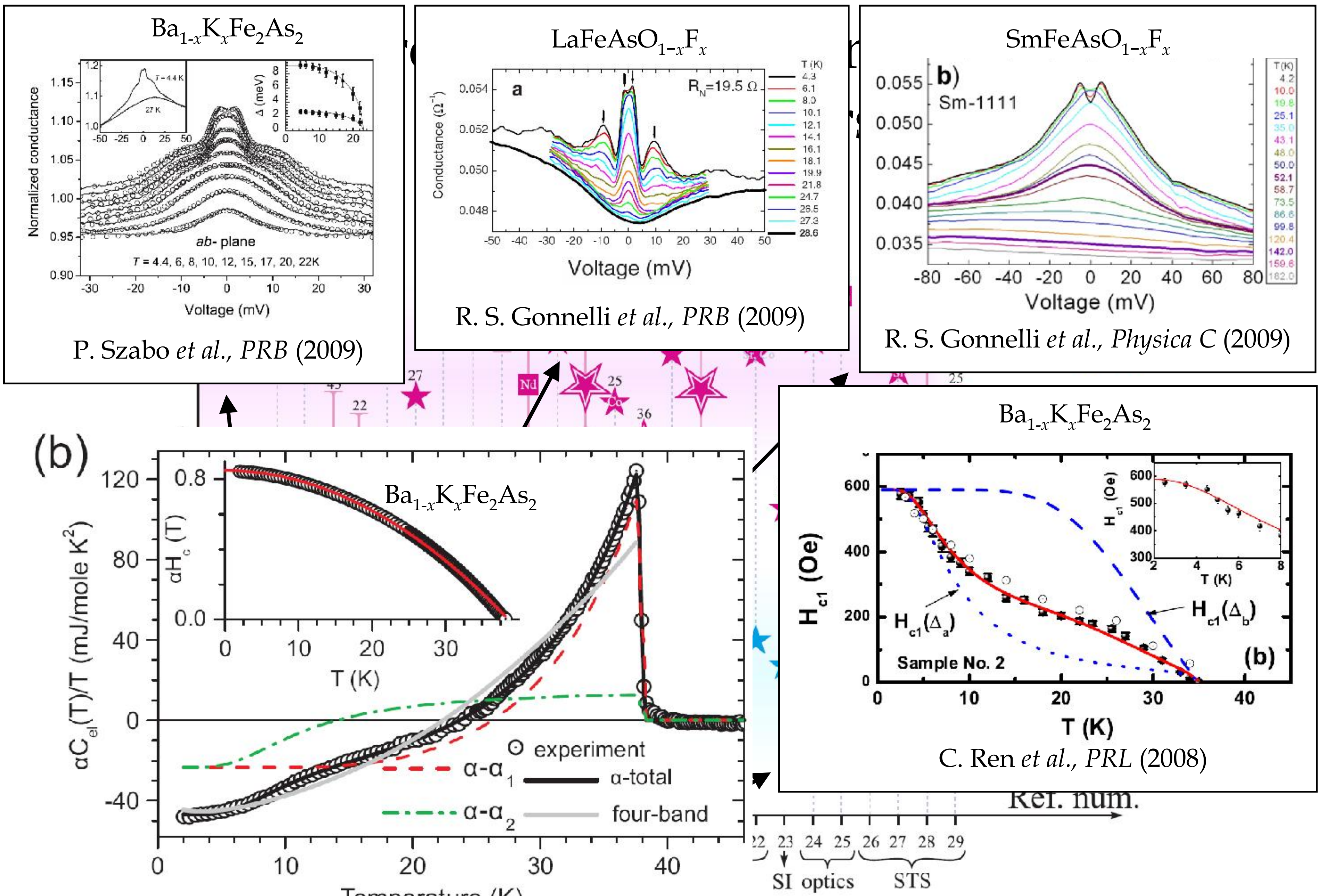

Evtushinsky *et al.*, *NJP* (2009)

Comparison to complementary measurements of electronic structure in superconducting state

ARPES

$\varepsilon(\mathbf{k}),\ \Delta(\mathbf{k})$

μSR, H_{c1},
specific heat, etc.

$$\int \Phi[\varepsilon(\mathbf{k}),\ \Delta(\mathbf{k})]\,d\mathbf{k}$$

Superfluid density in $Ba_{1-x}K_xFe_2As_2$ from ARPES

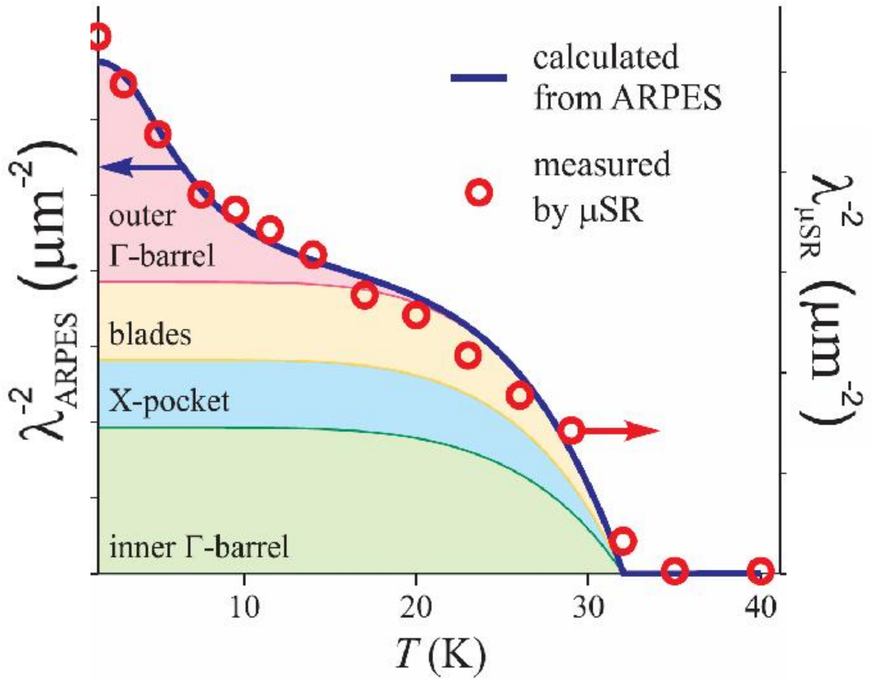

Khasanov *et al.*, *PRL* (2009)
Evtushinsky *et al.*, *NJP* (2009)

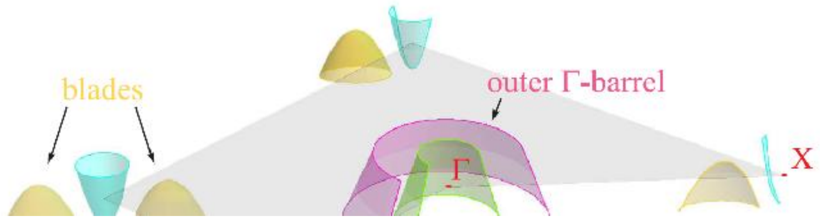

Superfluid density in LiFeAs

Inosov et al., *PRL* (2010)

$$\frac{1}{\lambda^2(T)} = \frac{e^2}{2\pi\varepsilon_0 c^2 h L_c} \cdot \int_{\mathrm{FS}} v_{\mathrm{F}}(\mathbf{k}) \left[1 - \int_{-\infty}^{+\infty} \left(-\frac{\partial f_T(\omega)}{\partial \omega}\right) \left|\mathrm{Re}\frac{\omega}{\sqrt{\omega^2 - \Delta_{\mathbf{k}}^2(T)}}\right| \mathrm{d}\omega\right] \mathrm{d}k$$

Chandrasekhar and Einzel, *Ann. Physik* (1993)

3D

Sensitivity to 3D electronic structure via scanning $h\nu$

$$E_{\mathrm{kin}} = (p_\perp^2 + p_\parallel^2)/2m = h\nu - E_{\mathrm{bind}} - \Phi$$

$$k_\perp + n_\perp G_\perp = \sqrt{\frac{2m}{\hbar^2}(E_{\mathrm{kin}} + V_0) - (k_\parallel + n_\parallel G_\parallel)^2}$$

$$= \sqrt{0.262\,\frac{\mathring{\mathrm{A}}^{-2}}{\mathrm{eV}}(h\nu - E_{\mathrm{bind}} + V_0 - \Phi) - (k_\parallel + n_\parallel G_\parallel)^2}$$

Inosov et al., PRB (2008)

k_z-dispersion in iron arsenides

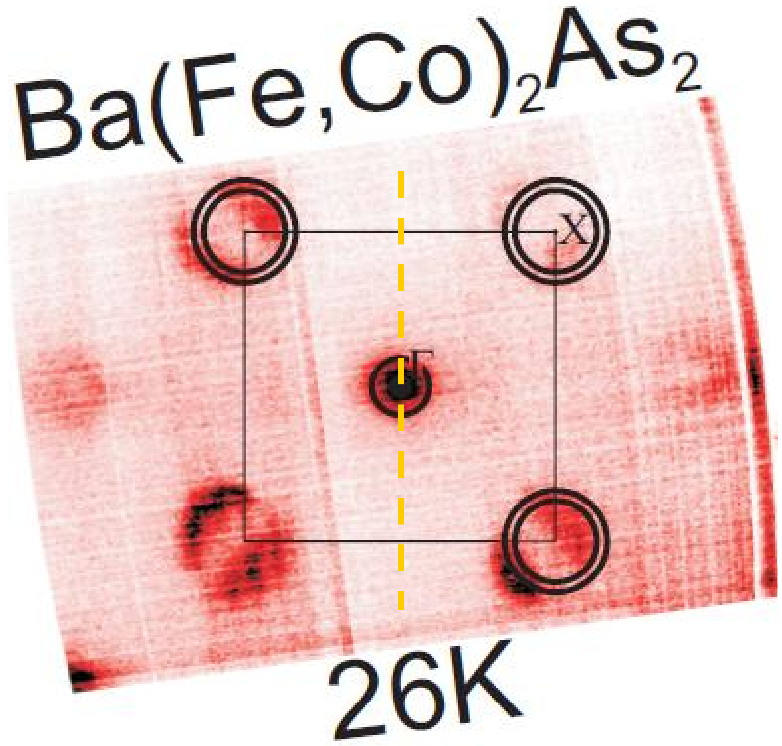

k_z-dispersion in iron arsenides

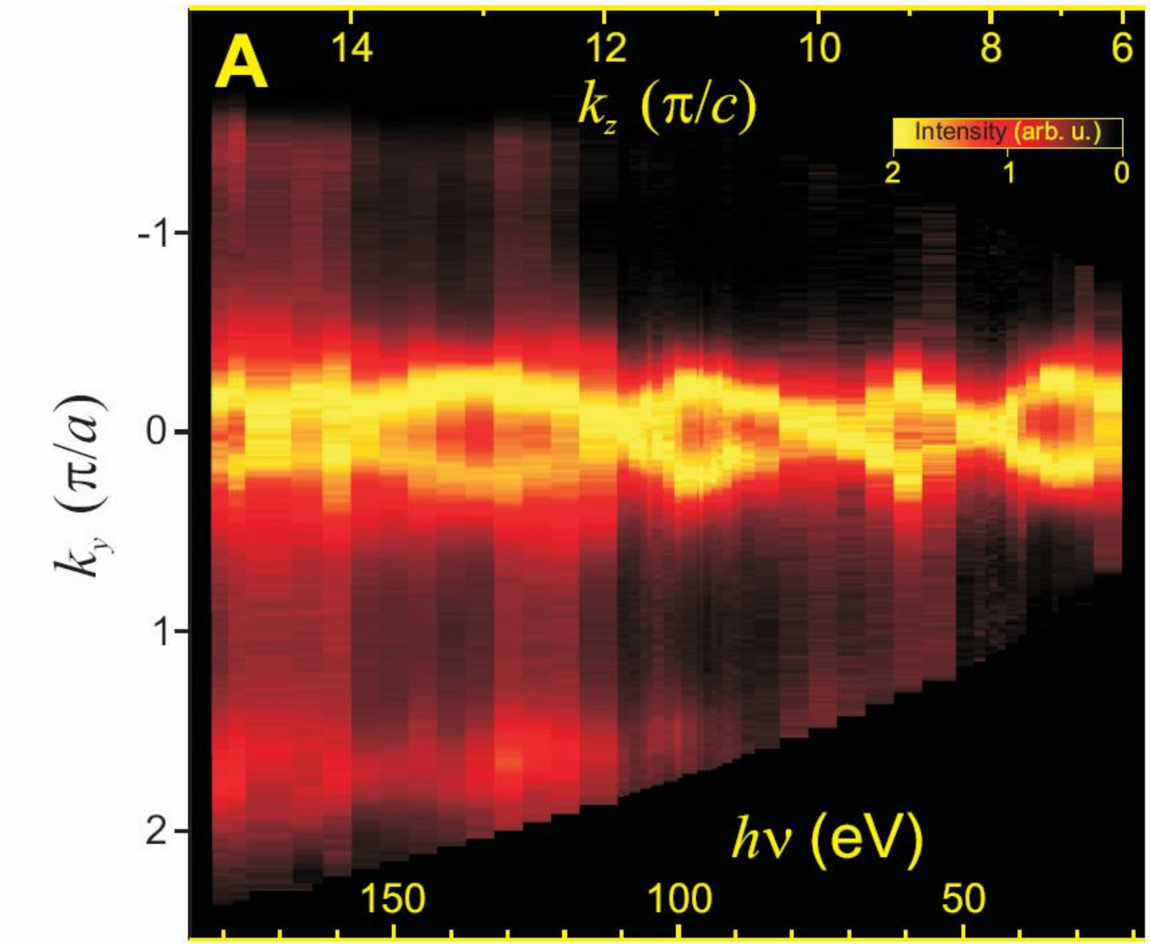

k_z-dependence of the superconducting gap in BKFA

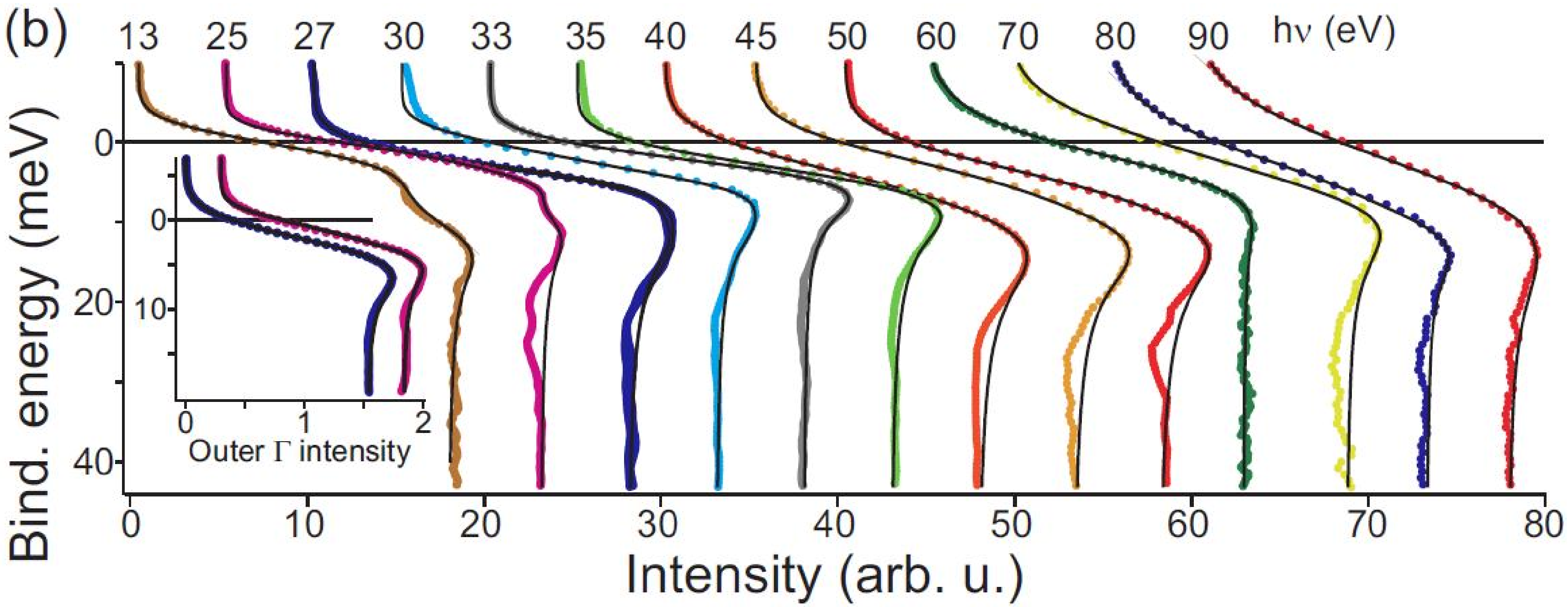

k_z-dependence of the superconducting gap in BKFA

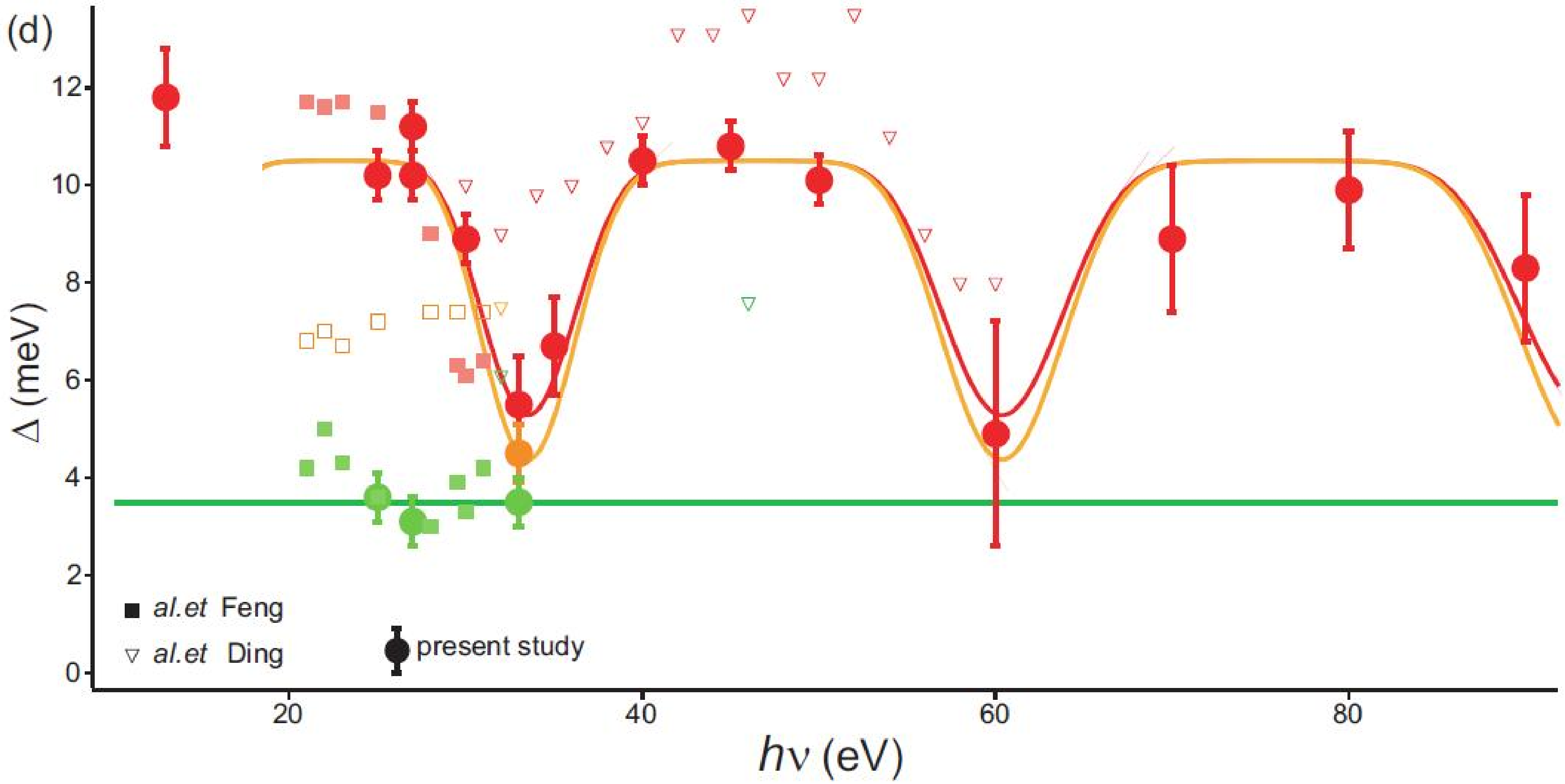

3D band structure

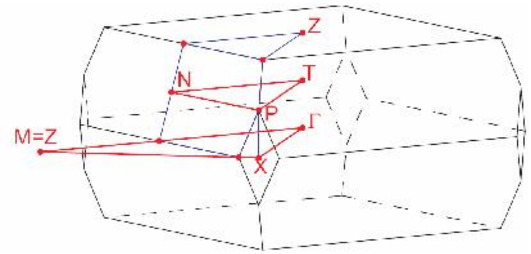

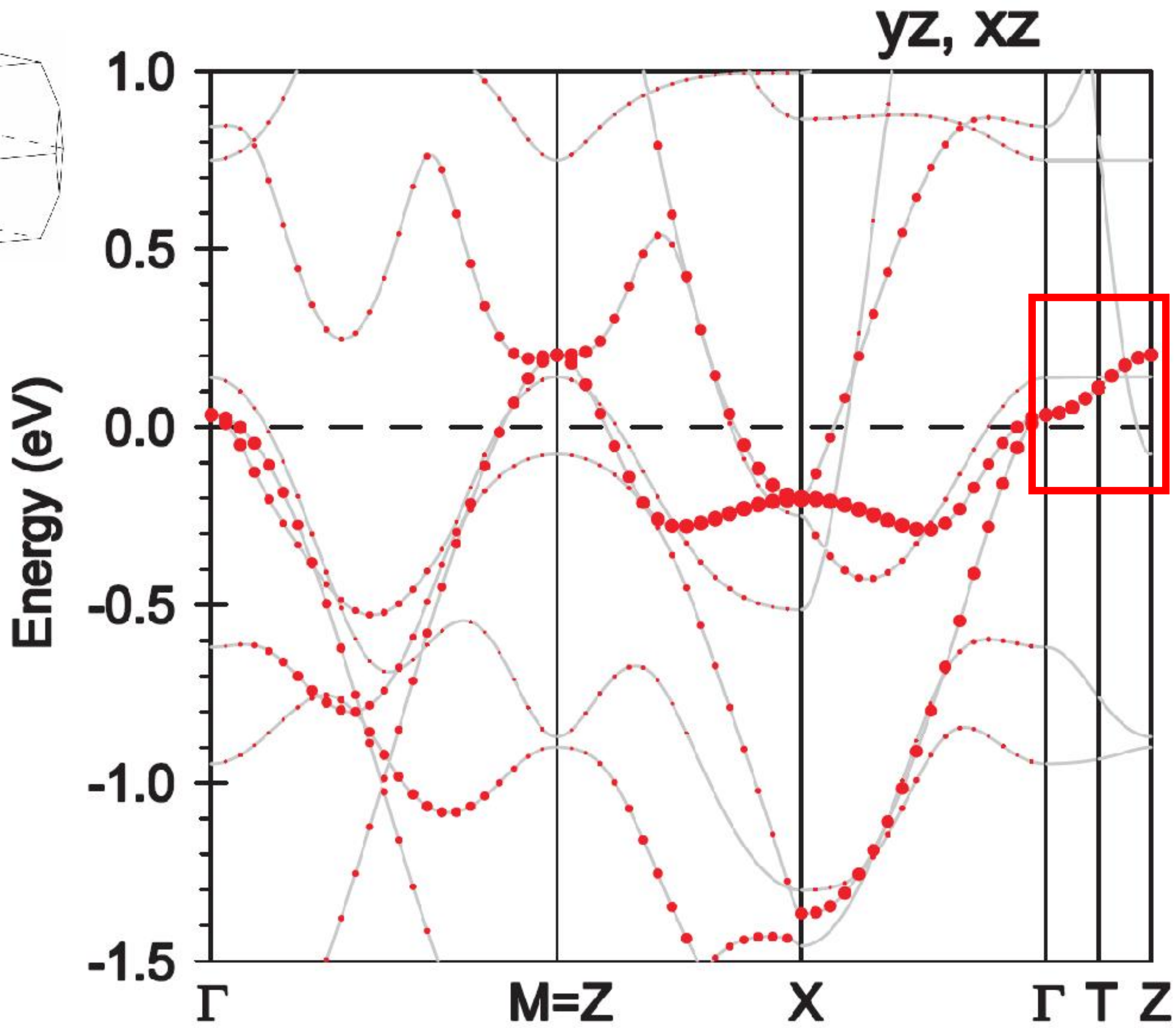

Comparison of calculated and measured band dispersions

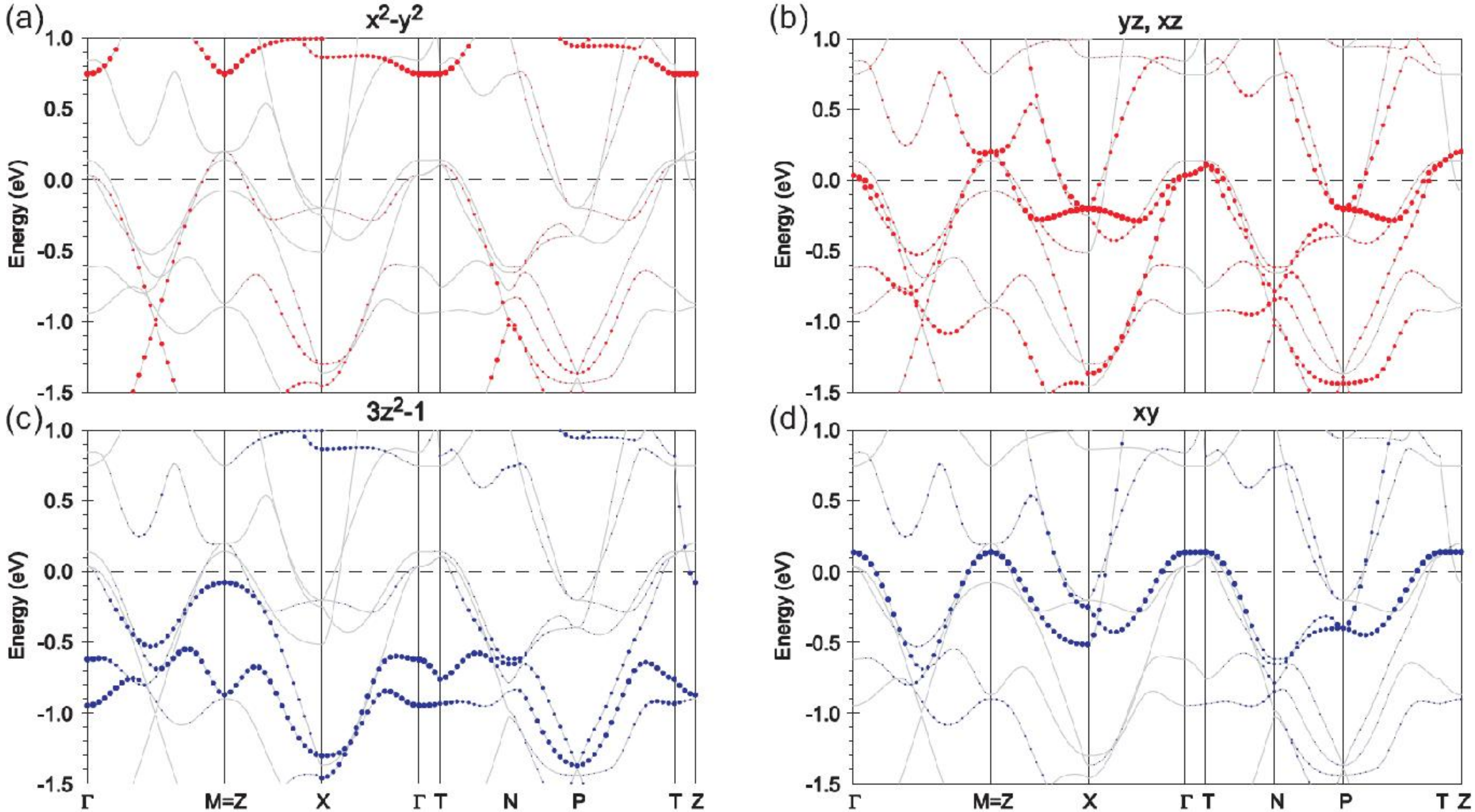

Yaresko (2011)

Comparison of calculated and measured band dispersions

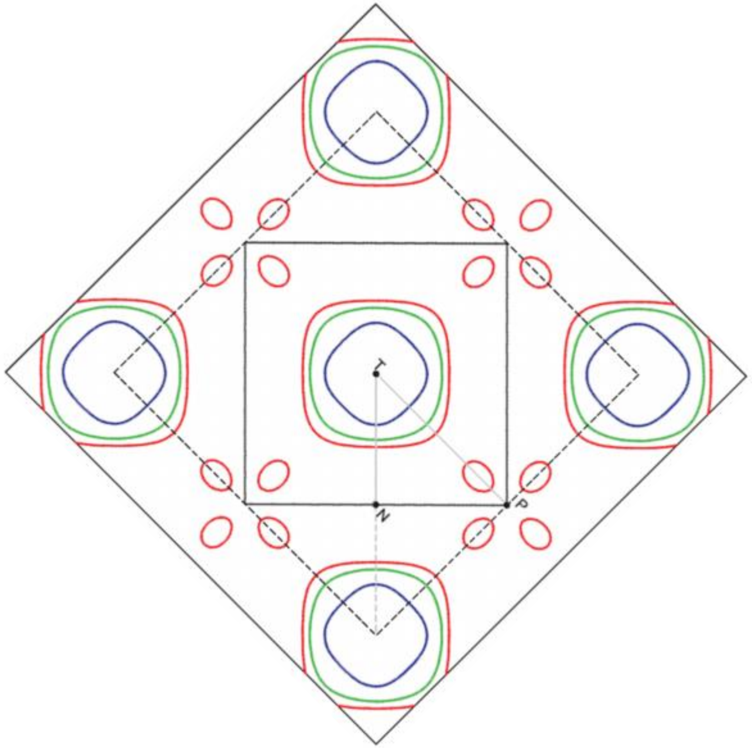

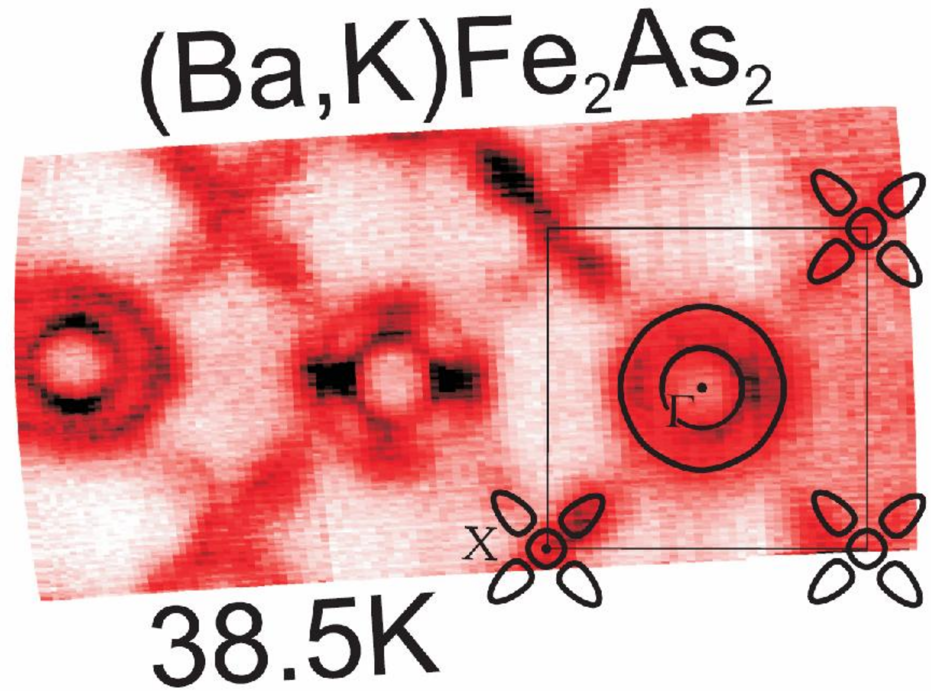

Comparison of calculated and measured band dispersions

T_c = 38K

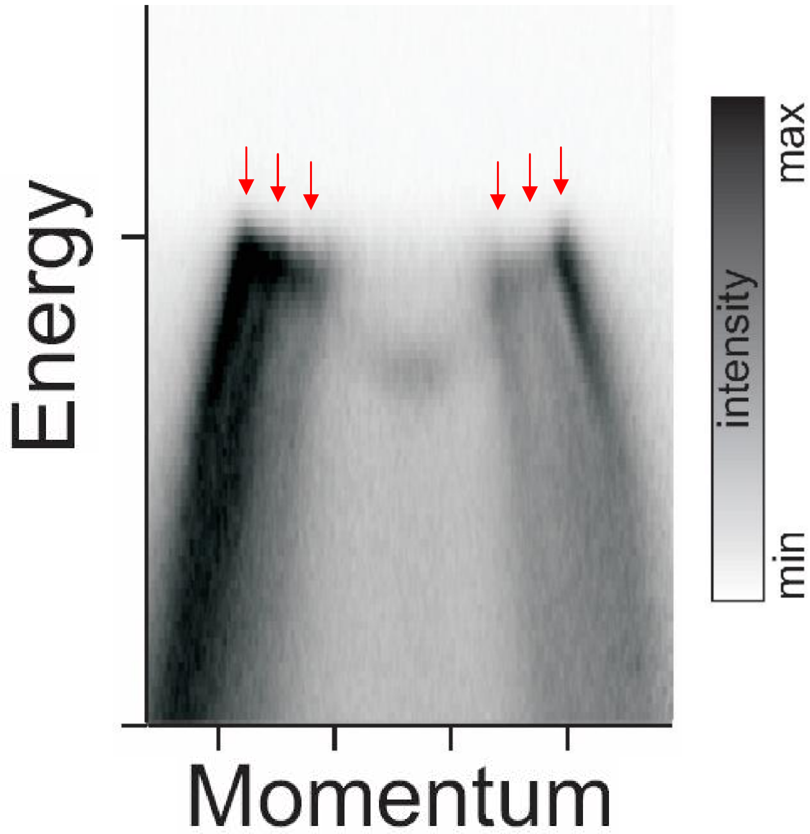

T = 1K

Hole-doped $BaFe_2As_2$

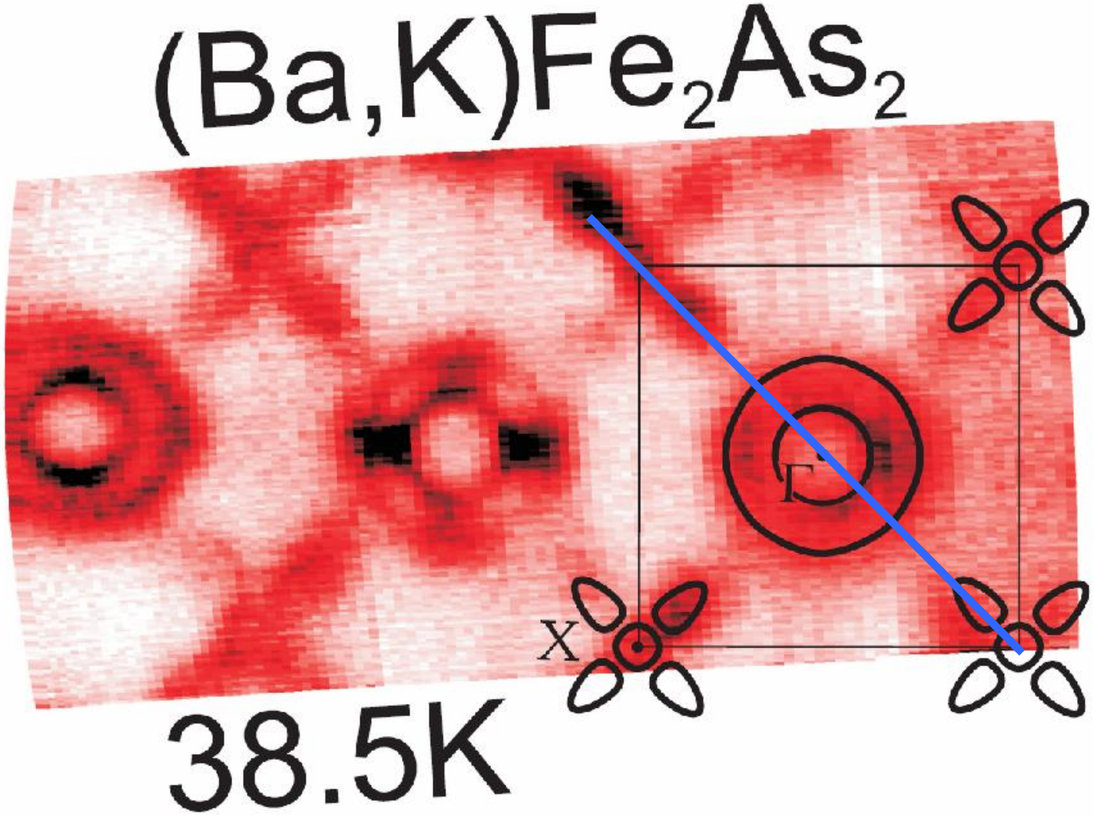

Comparison of calculated and measured band dispersions

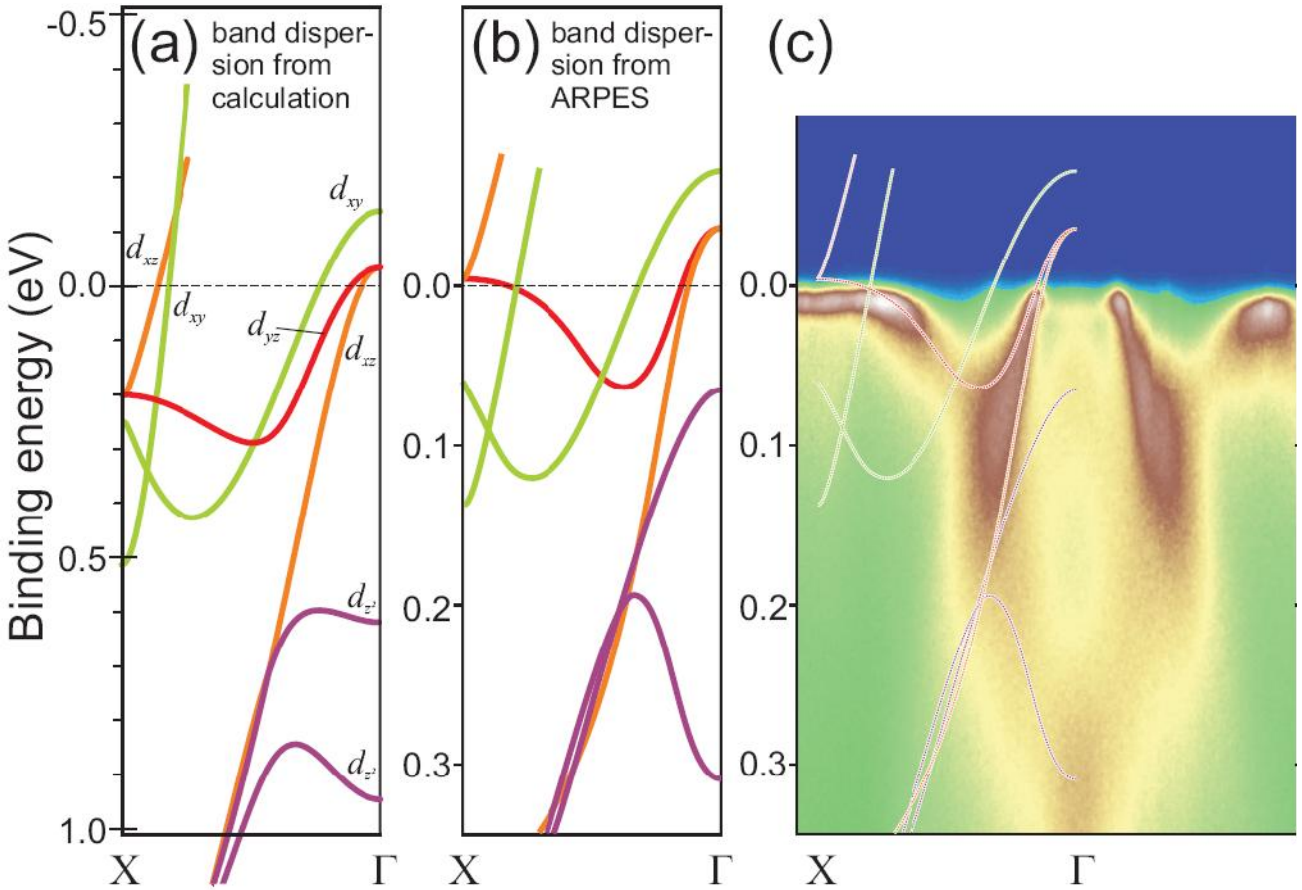

Zeroing matrix element due to symmetry reasons

$$\int u_f^*(\mathbf{r})\mathbf{A} \cdot \nabla u_i(\mathbf{r}) d^3\mathbf{r}$$

wave, propagating to detector

polarization of incoming light

initial state of electron in crystal

Zeroing matrix element due to symmetry reasons

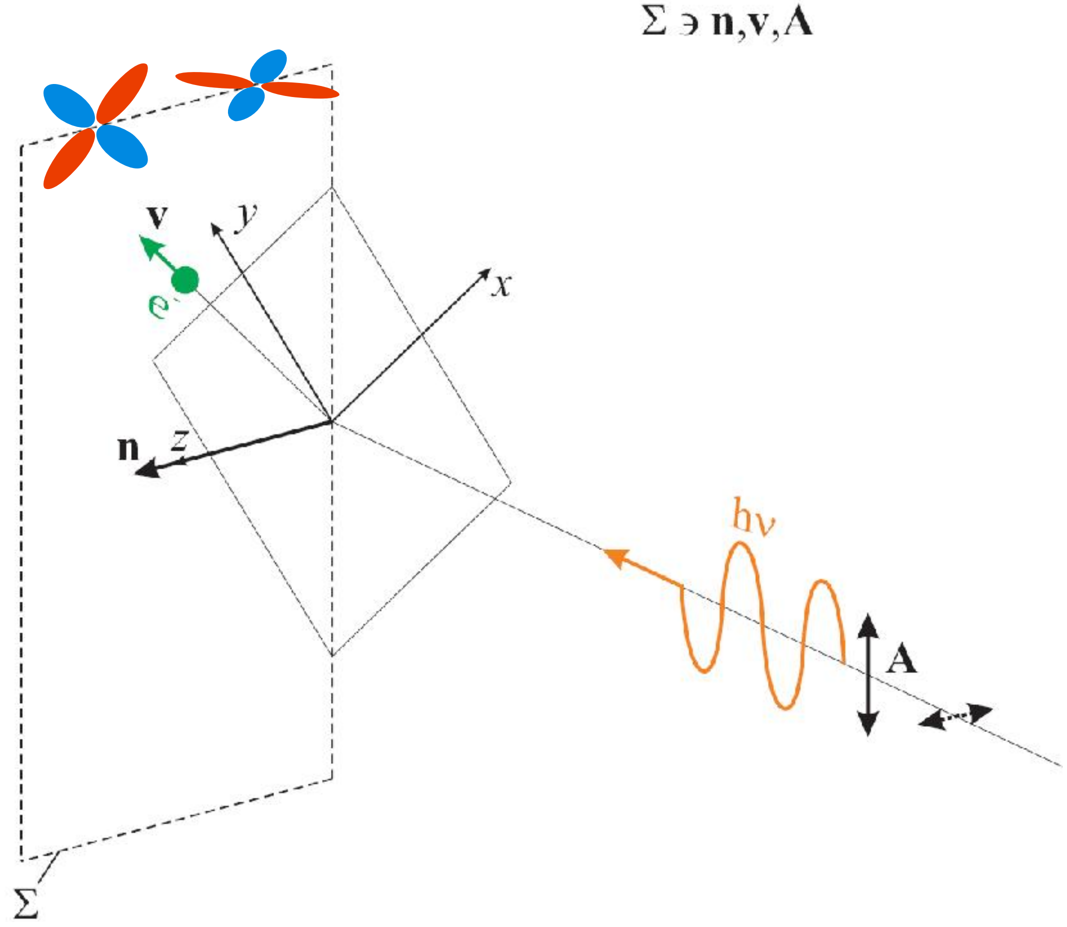

Comparison between of and measured band dispersions

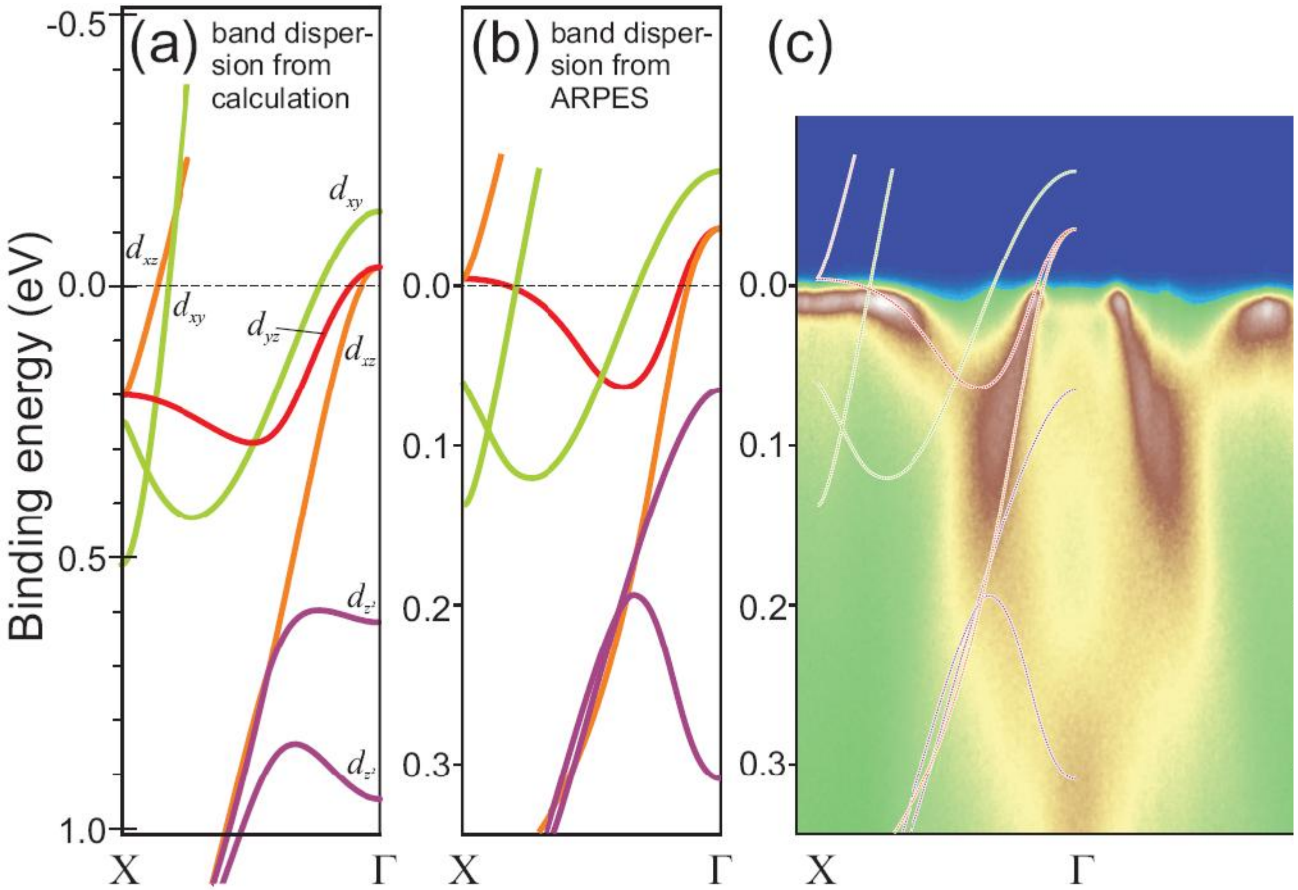

Special role of iron $3d_{xz,yz}$ orbitals in magnetism

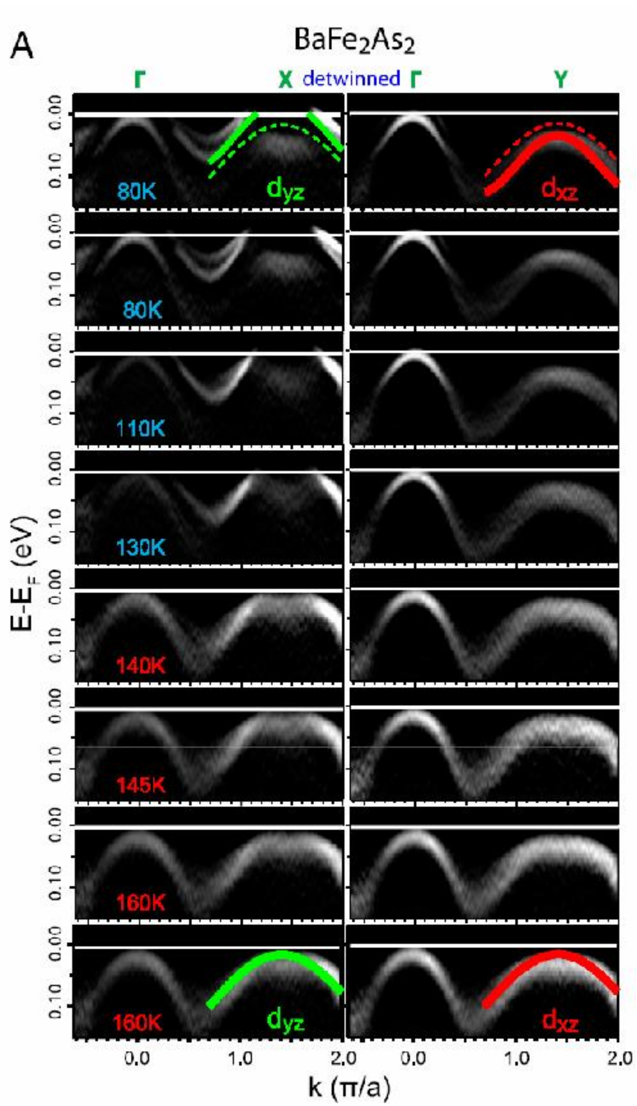

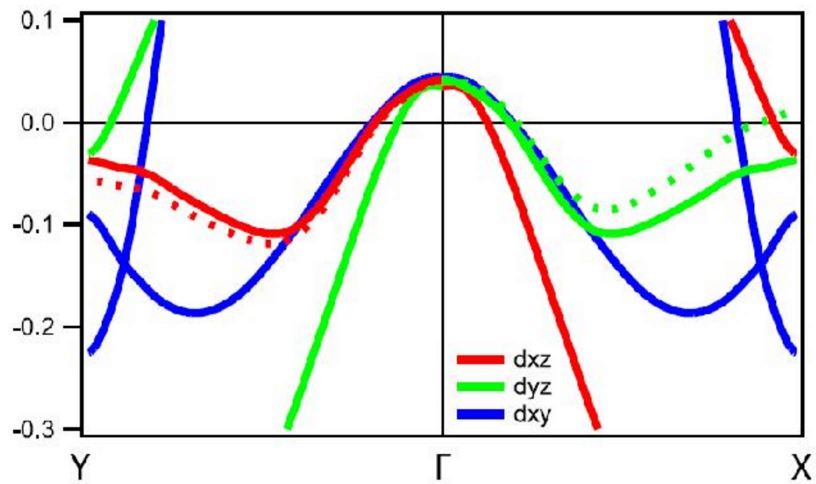

Yi *et al.*, *PNAS* (2011)

Node-like behavior in BFAP

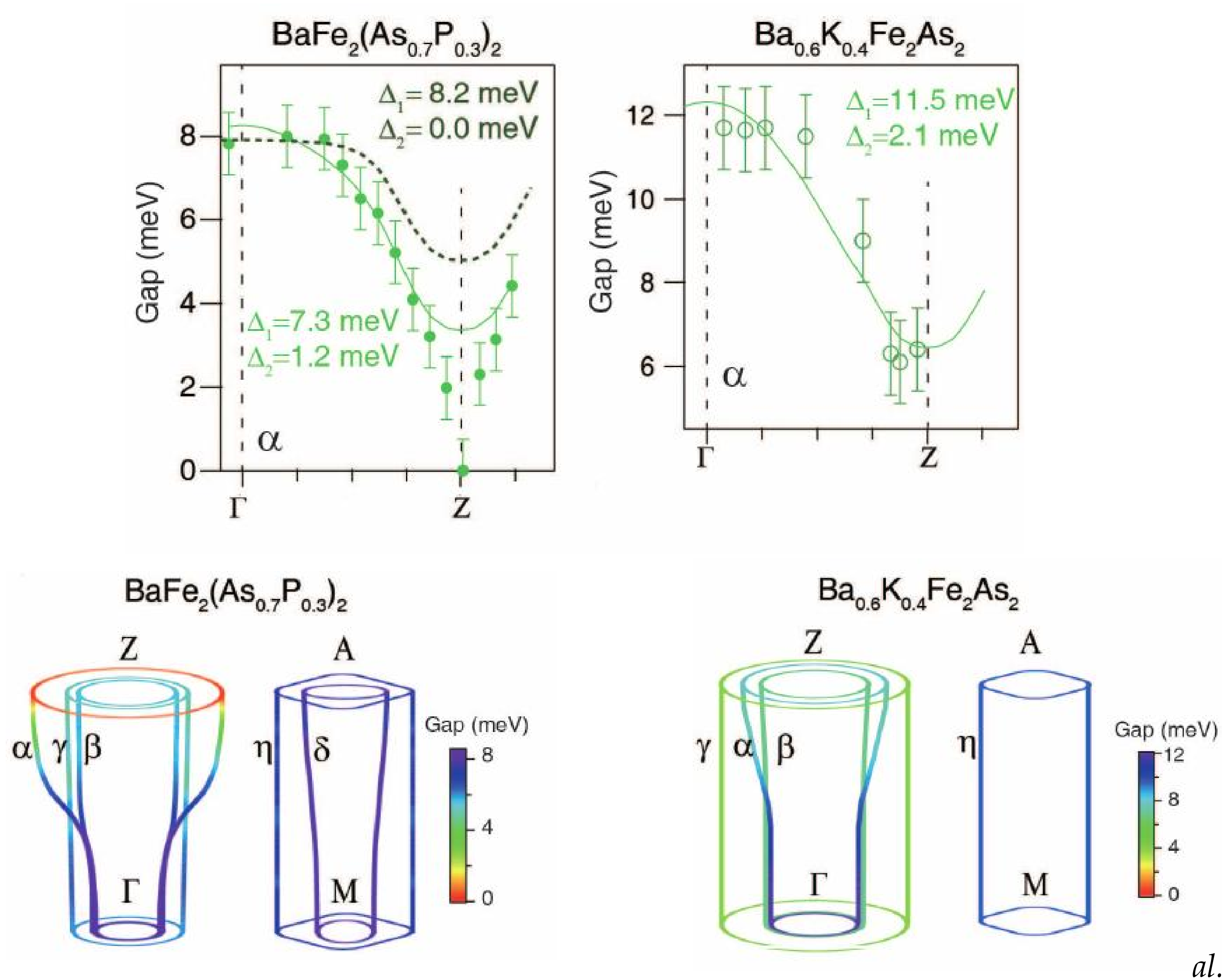

al. et Feng (2011)

$Ba_{1-x}Na_xFe_2As_2$

Fermi surface

$Ba_{1-x}K_xFe_2As_2$

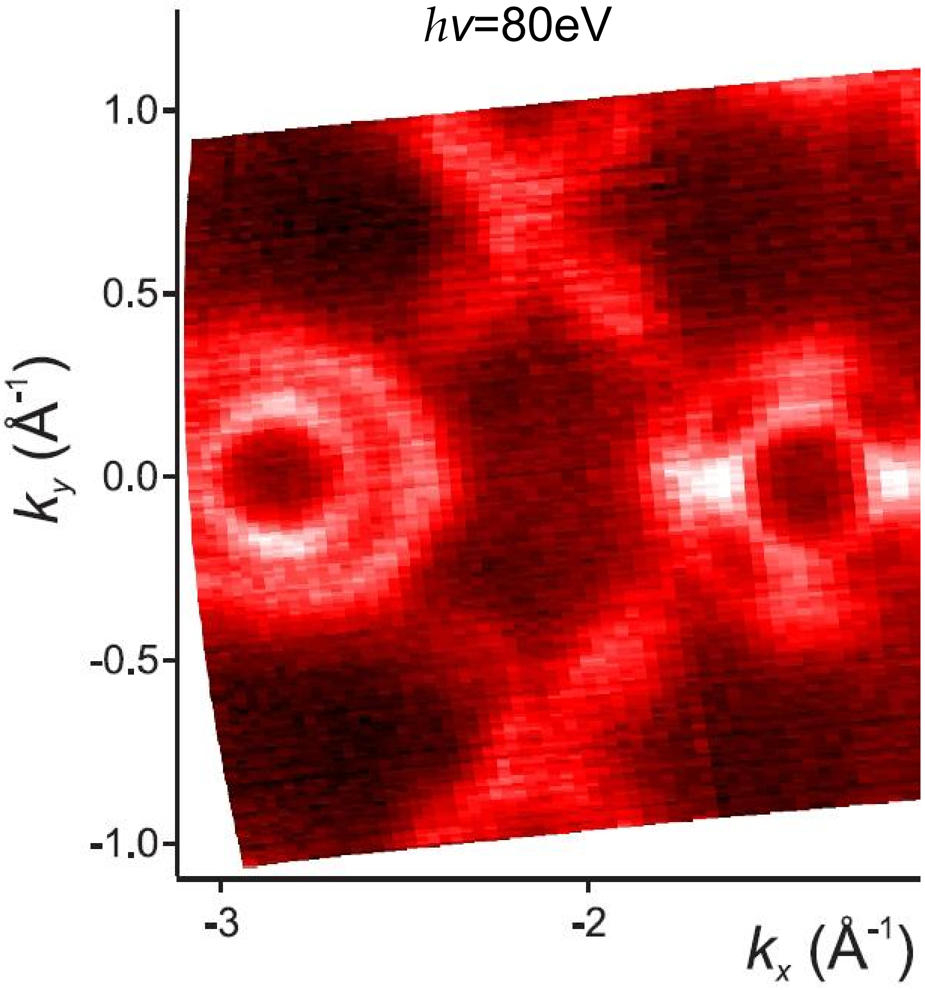

$Ba_{1-x}Na_xFe_2As_2$

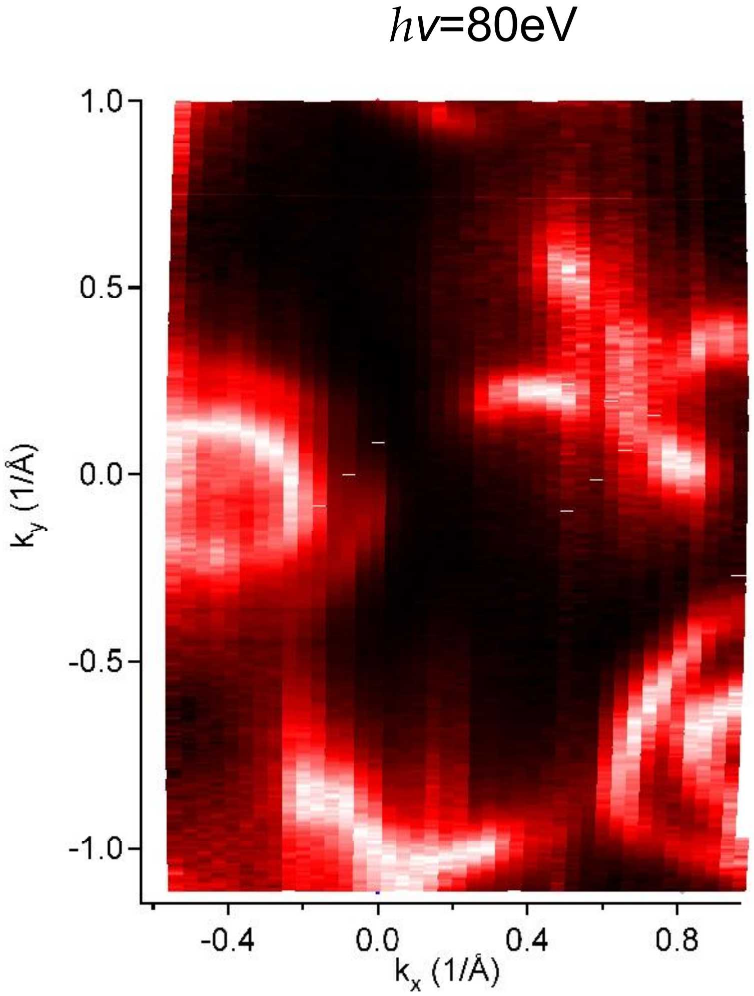

Gap on the inner Γ-barrel in $Ba_{1-x}Na_xFe_2As_2$

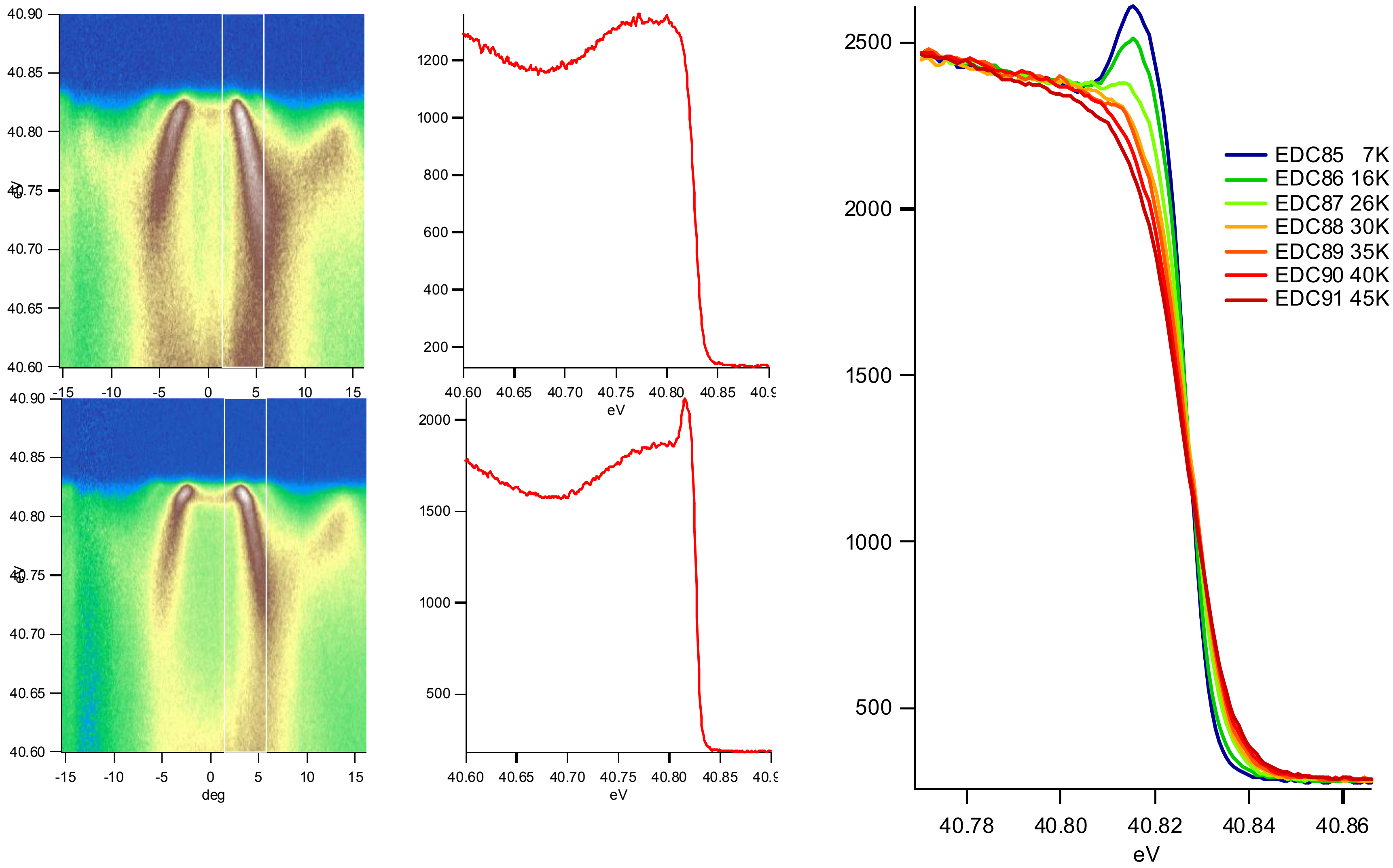

Gap on the electron-like pocket in $Ba_{1-x}Na_xFe_2As_2$

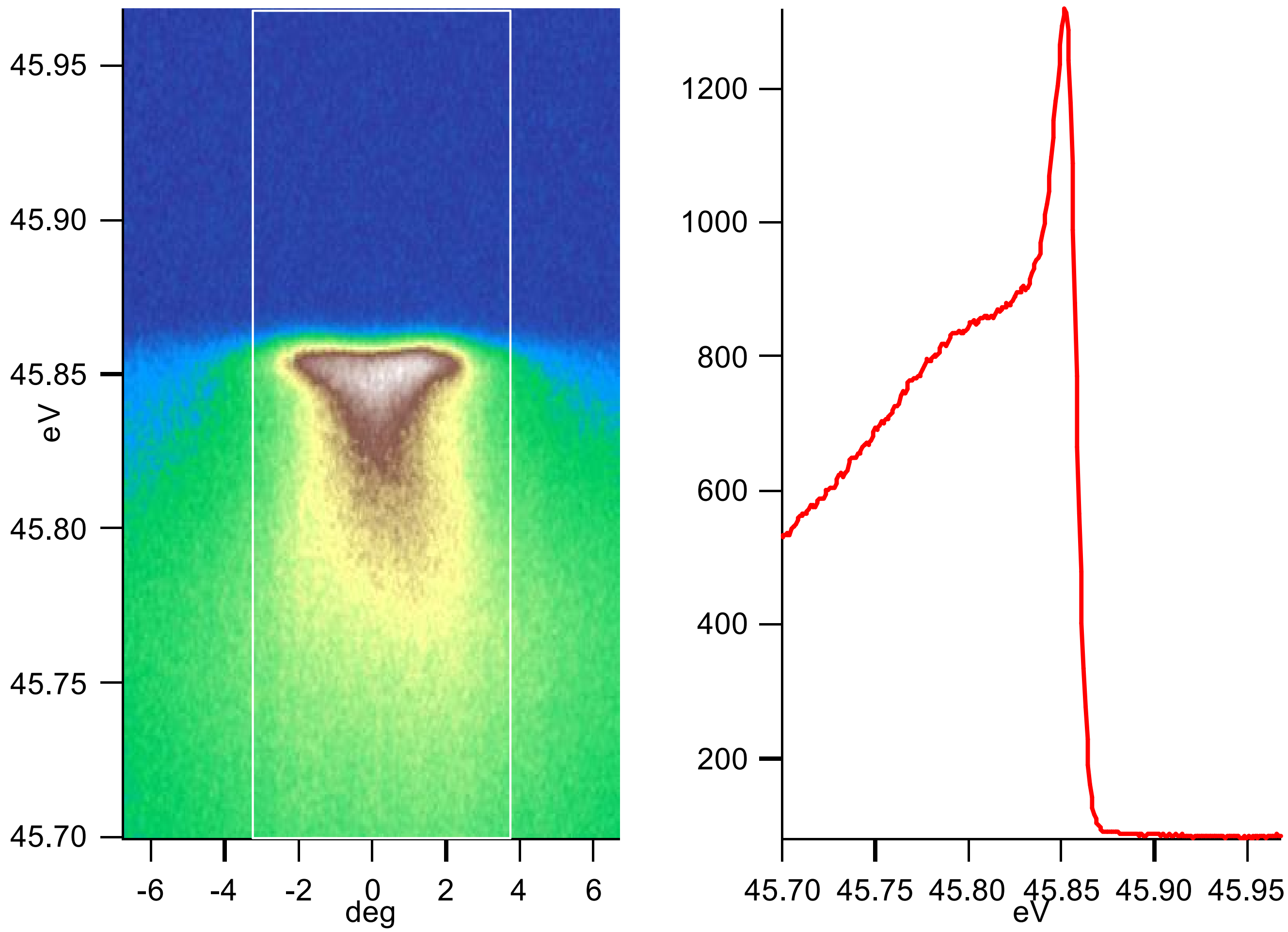

Gap on the outer Γ-barrel in $Ba_{1-x}Na_xFe_2As_2$

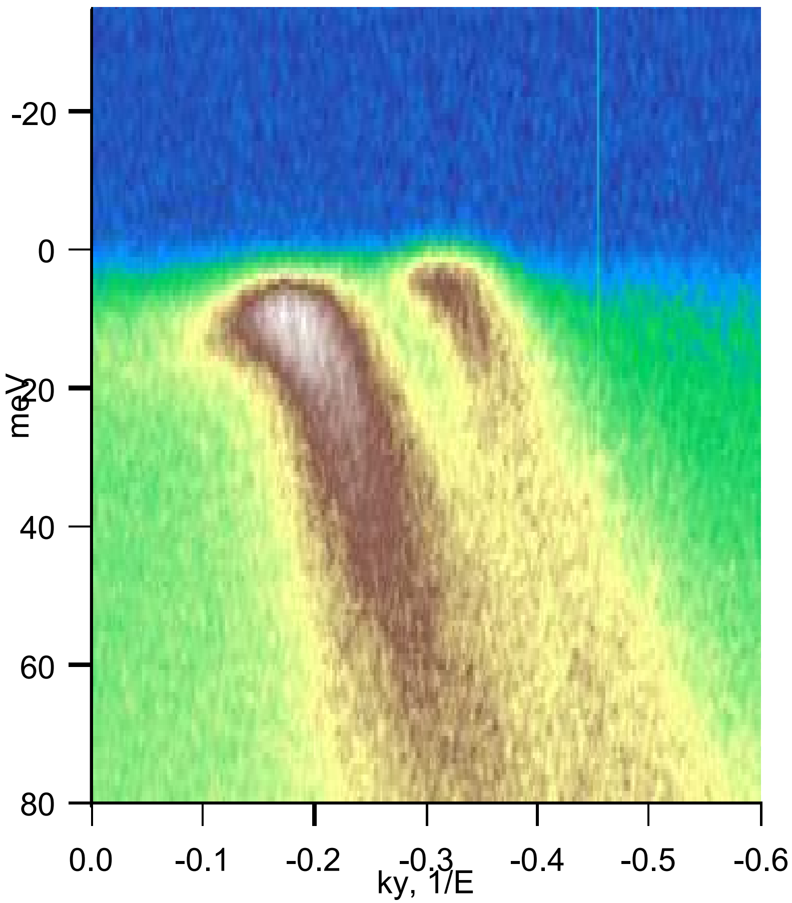

Surface sensitivity

Surface component of photoemission signal in YBCO

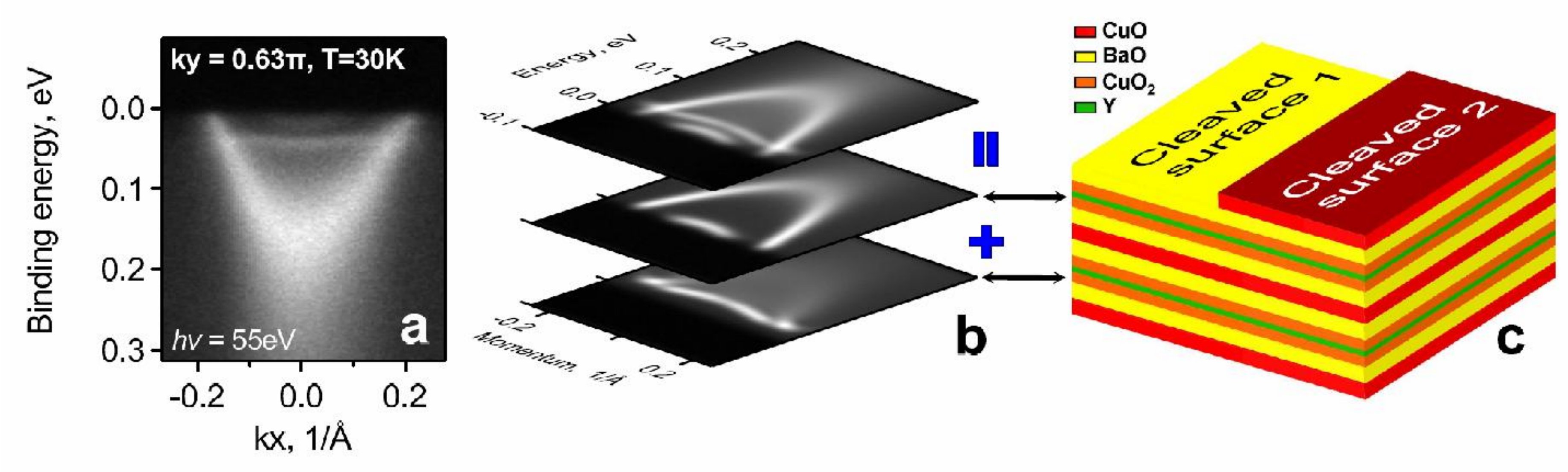

V. Zabolotnyy *et al.*, *PRB* (2006)

Surface component in BKFA

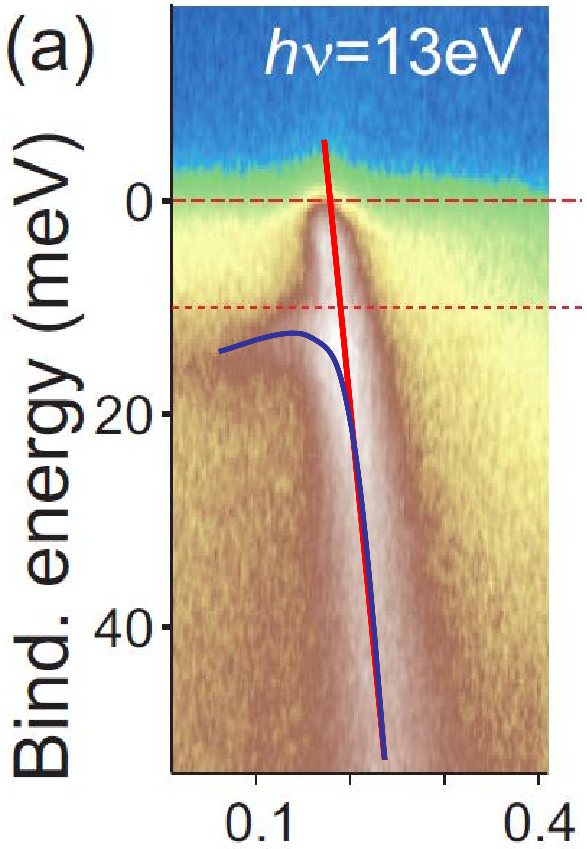

Surface component in BKFA

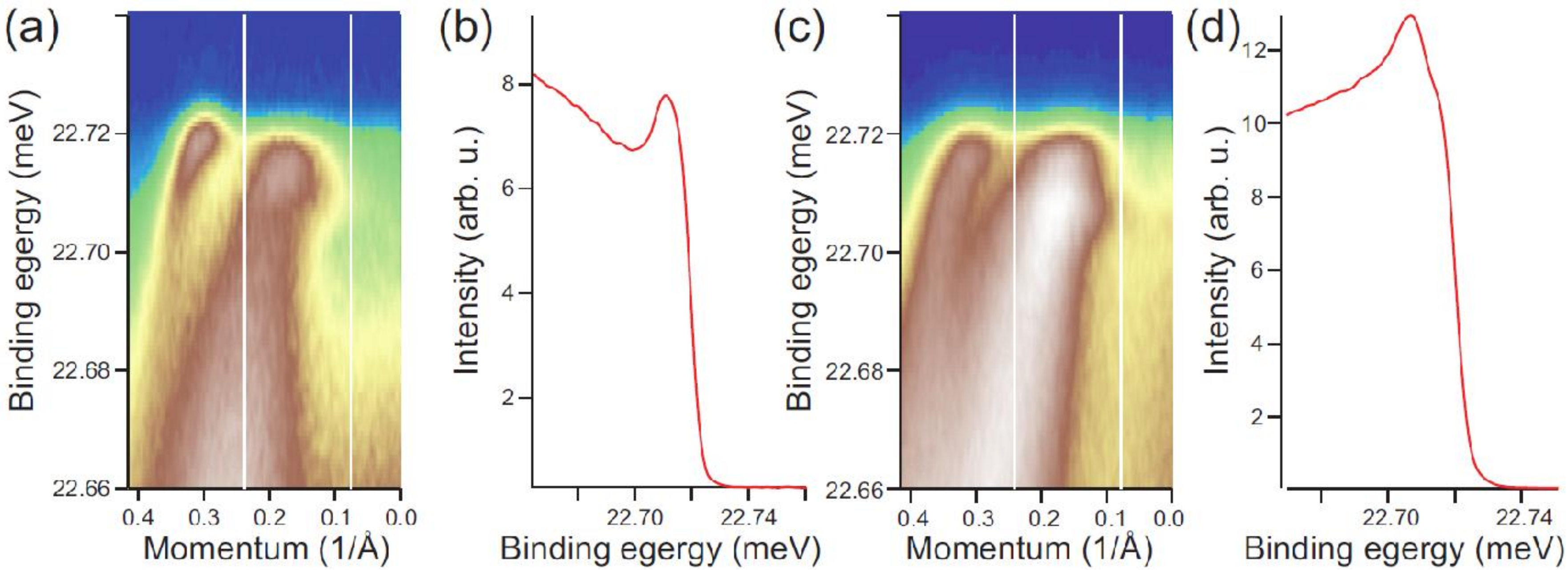

Surface component in BKFA

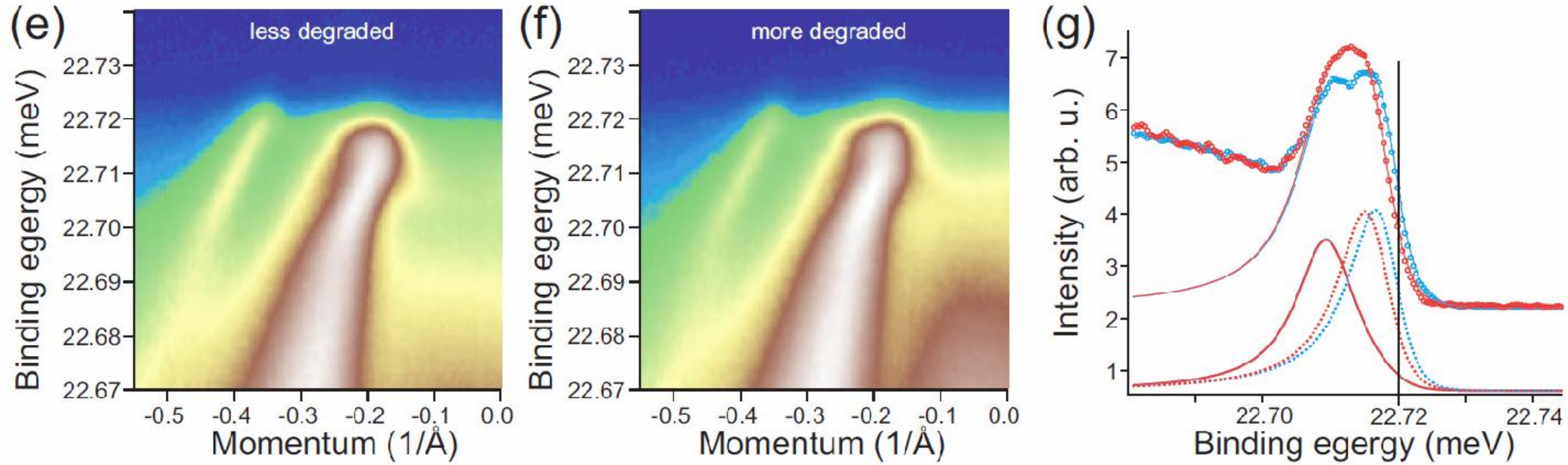

Surface component in BKFA

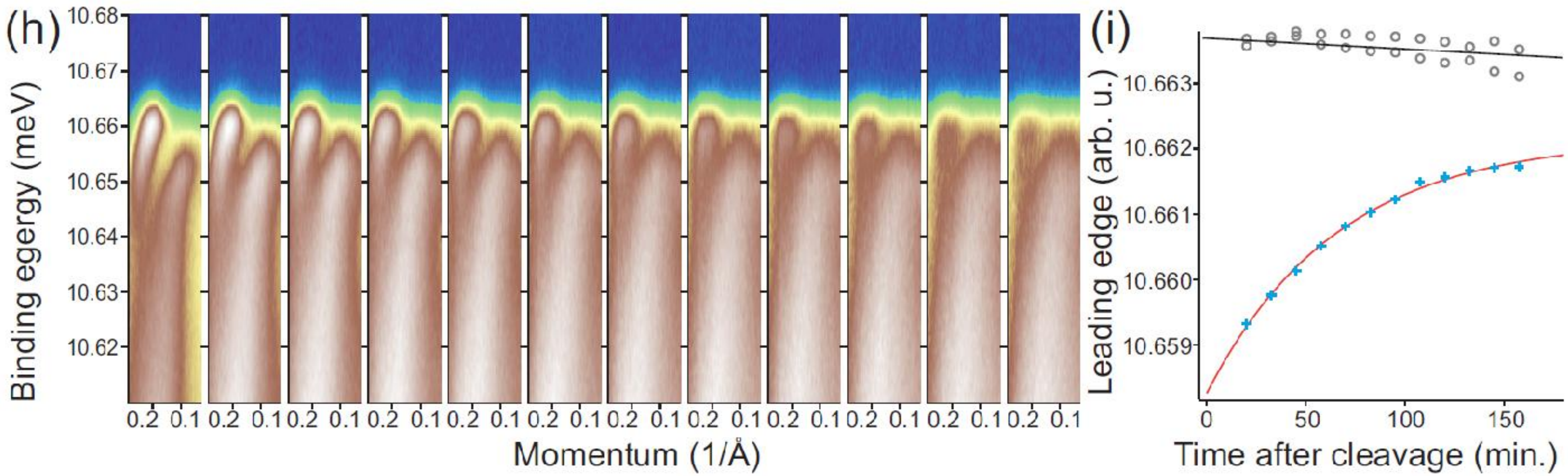

Absence of surface states in LiFeAs

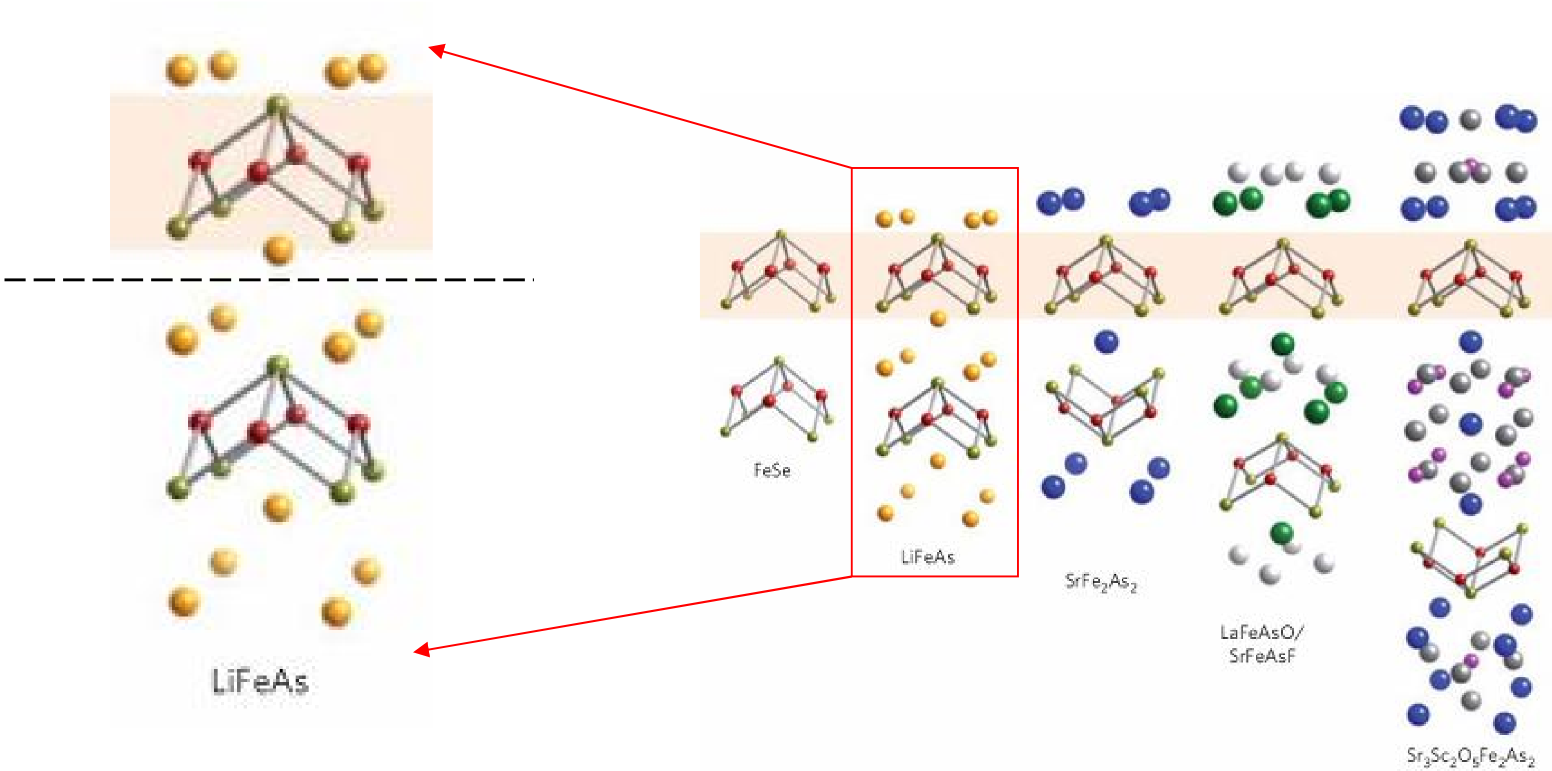

Absence of surface states in LiFeAs

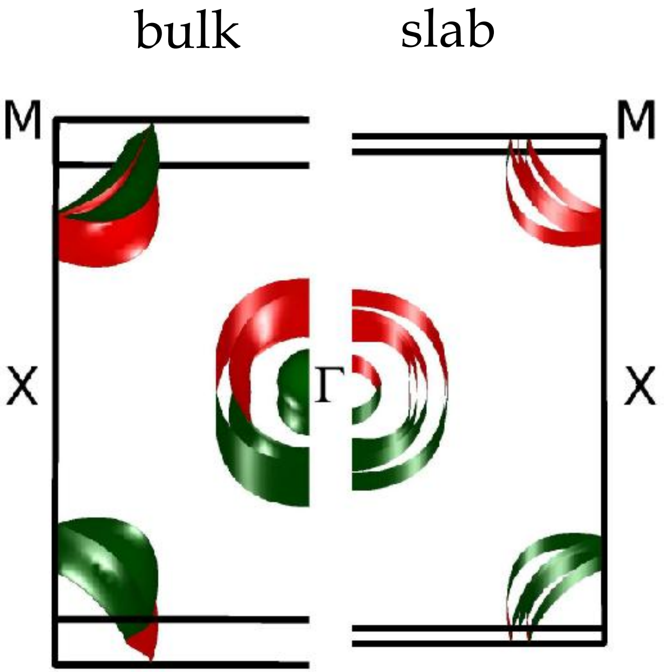

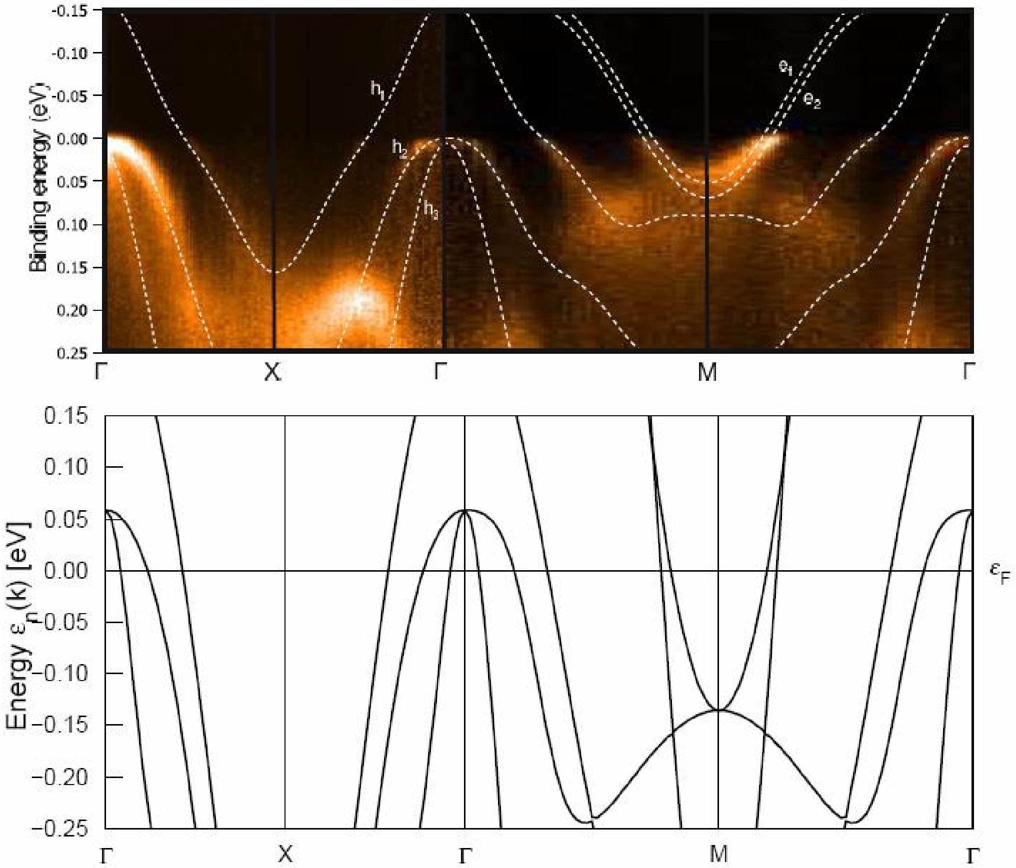

Lankau *et al.*, *PRB* (2011)

Surface sensitivity:

- no surface states at the Fermi level observed in 111 and 122 iron arsenides

- surface layer may be non-superconducting, but band dispersion doesn’t differ from the bulk

$SrPd_2Ge_2$

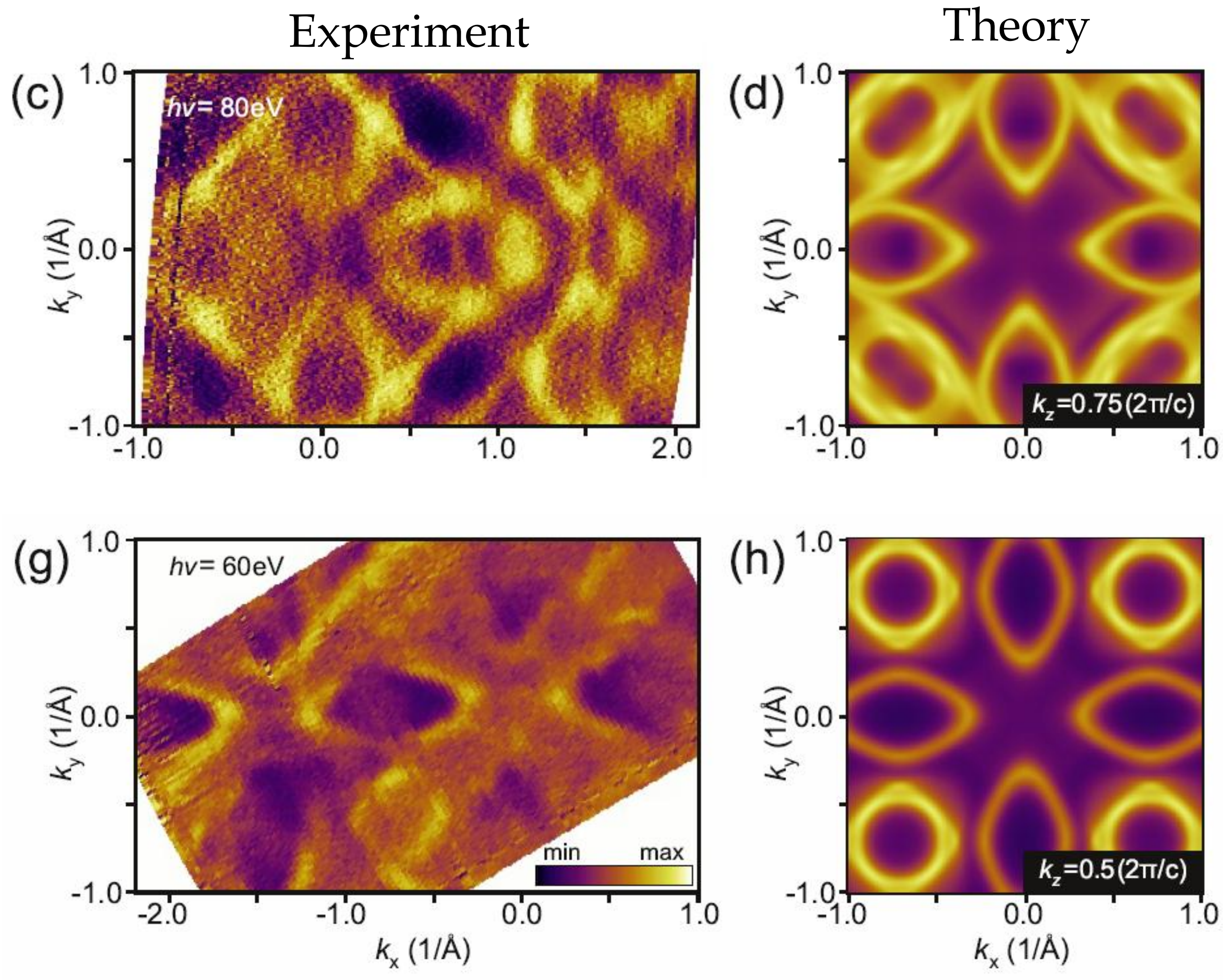

Kim *et. al.*, *PRB* (2012)

$SrPd_2Ge_2$

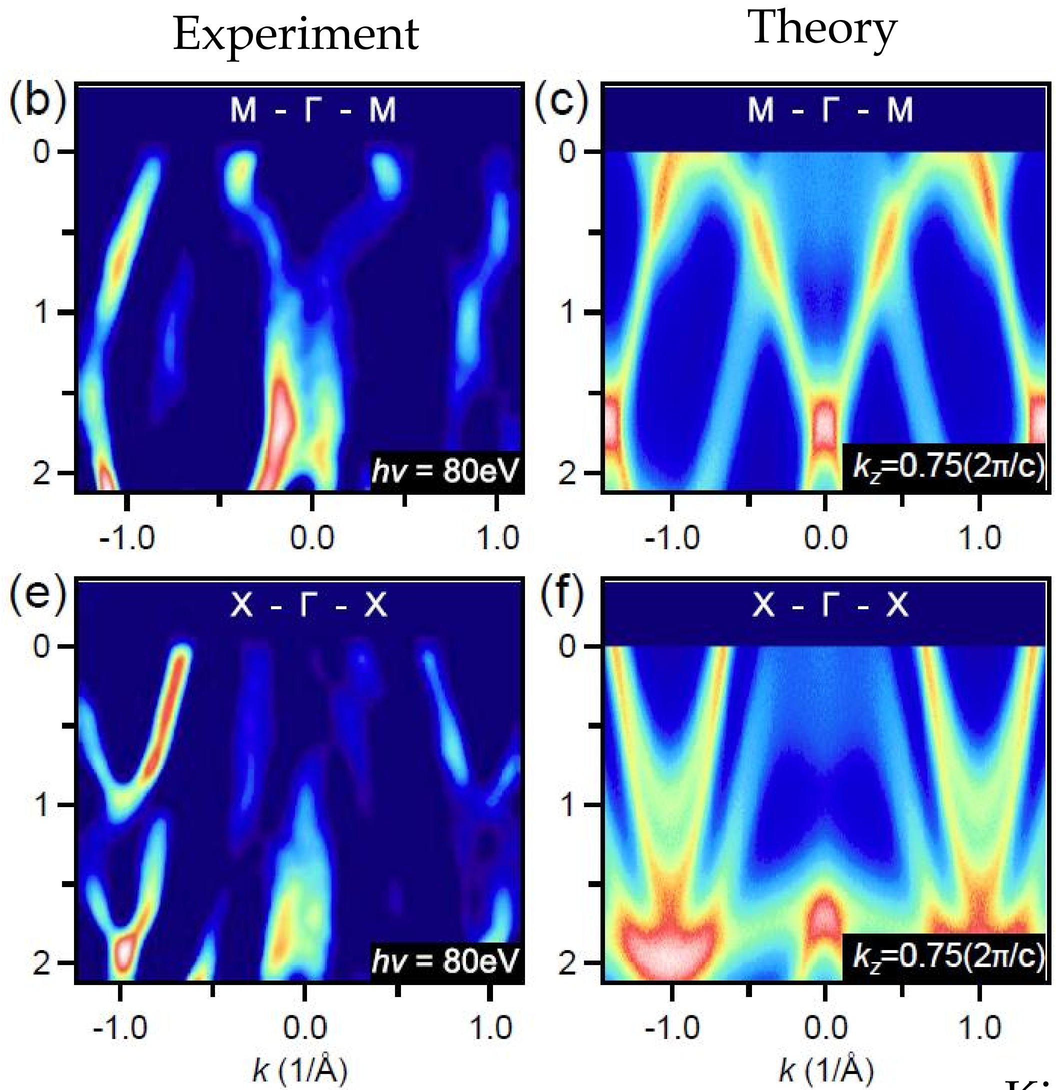

Kim *et. al.*, *PRB* (2012)

$SrPd_2Ge_2$

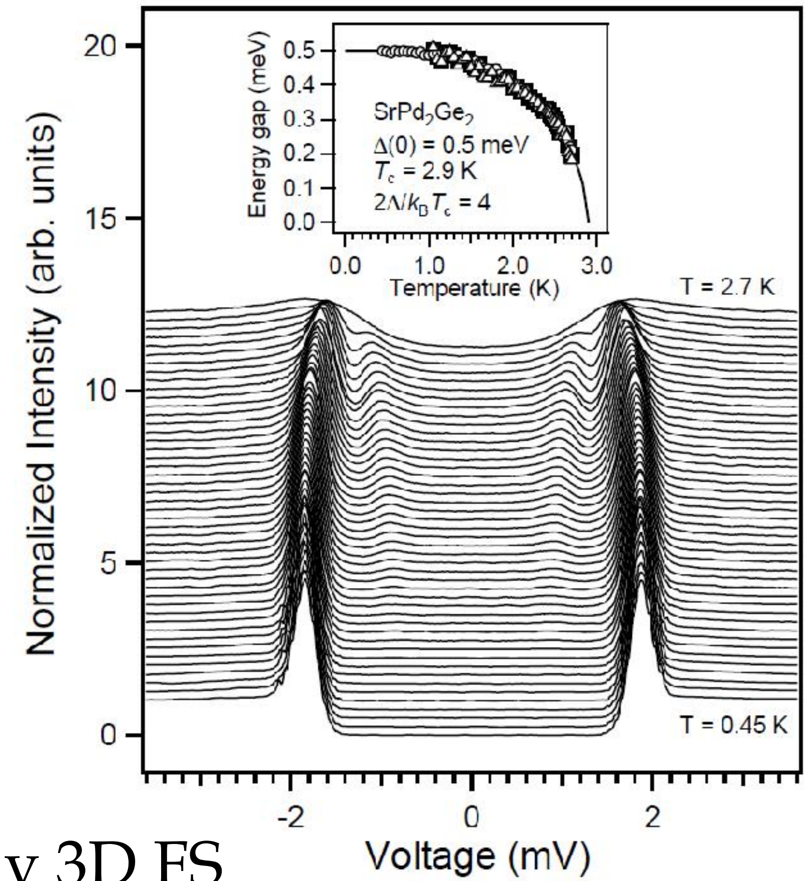

- Completely 3D FS
- No band renormalization
- Likely conventional superconductivity

Kim *et. al.*, *PRB* (2012)

Mode

DOS of strongly coupled superconductor

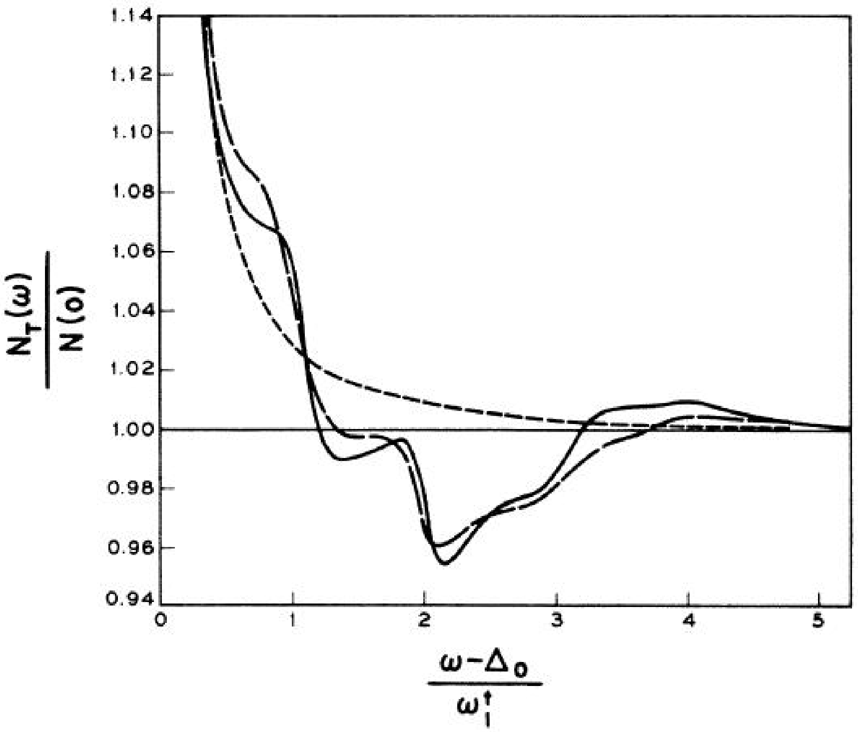

FIG. 2. The effective tunneling density of states $N_T(\omega)/N(0)$ vs $(\omega-\Delta_0)/\omega_1{}^t$ (solid) and the density of states of the simplified BCS model $\omega/(\omega^2-\Delta_0{}^2)^{1/2}$ (short dash). The ratio of the differential conductance of Pb in the superconducting to that in the normal state,

$$\frac{dI_s(\omega)/d\omega}{dI_n(\omega)/d\omega},$$

is plotted (long dash) as a function of $(\omega-\Delta_0)/\omega_1{}^t$ for $T=1.3^\circ$K. These data were obtained from the tunneling experiments reported by Rowell, Anderson, and Thomas.

Mode effects on the spectra of $Ba_{1-x}K_xFe_2As_2$ below T_c

kink_energy = 23 meV
Δ = 10 meV

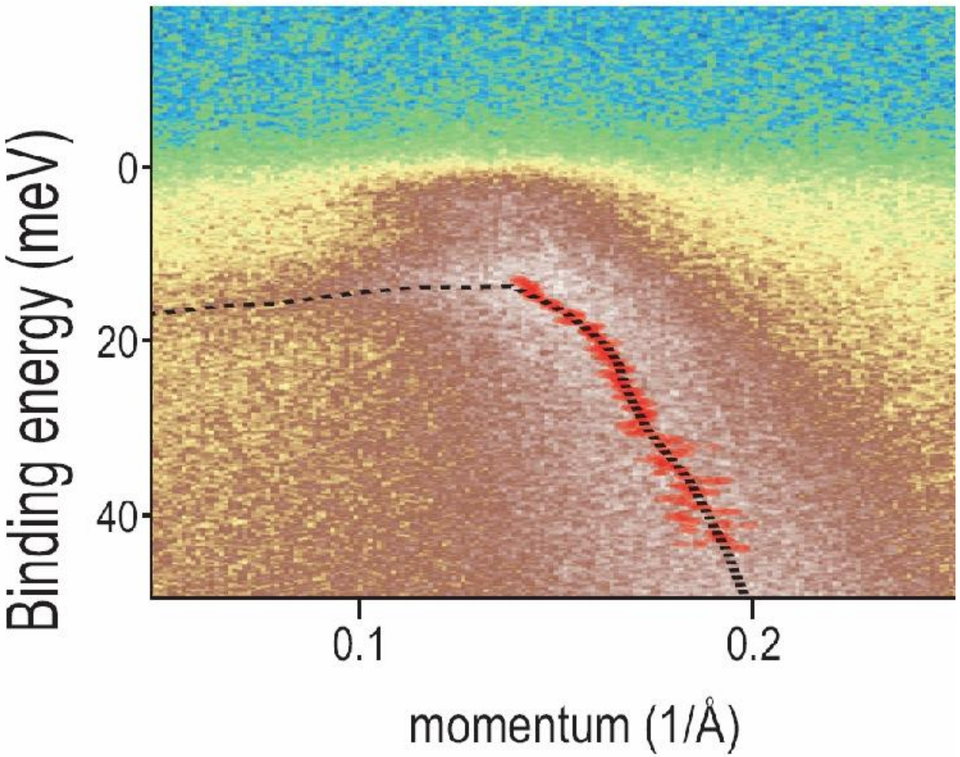

Ω_M = 13-14 meV

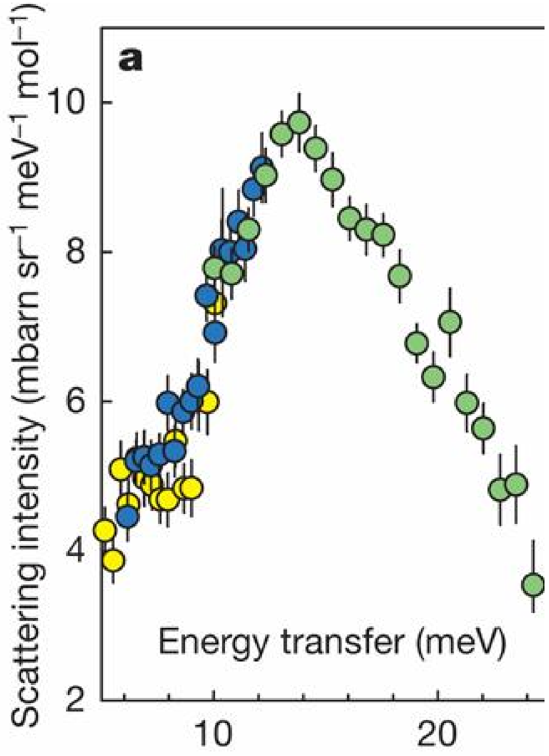

Christianson *et al.*, *Nature* (2008)

Kink in $Ba_{1-x}Na_xFe_2As_2$

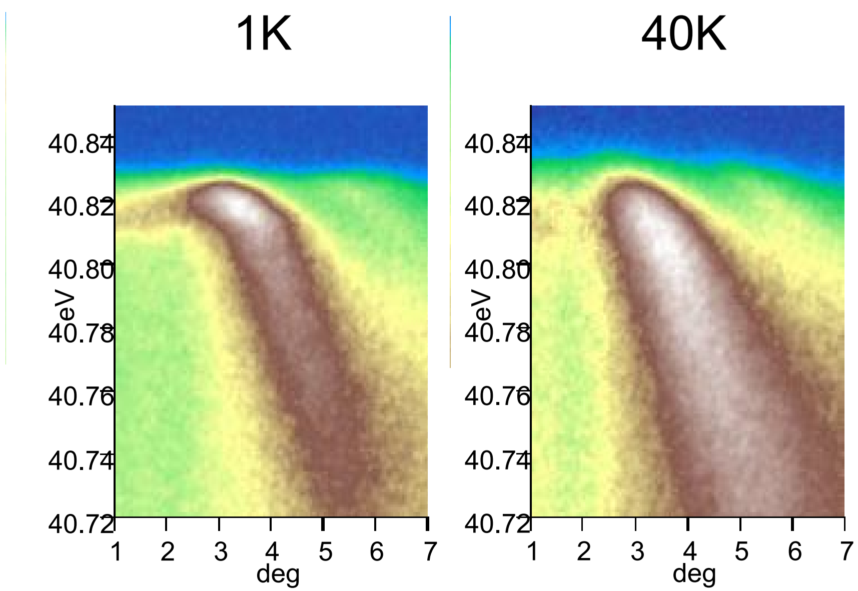

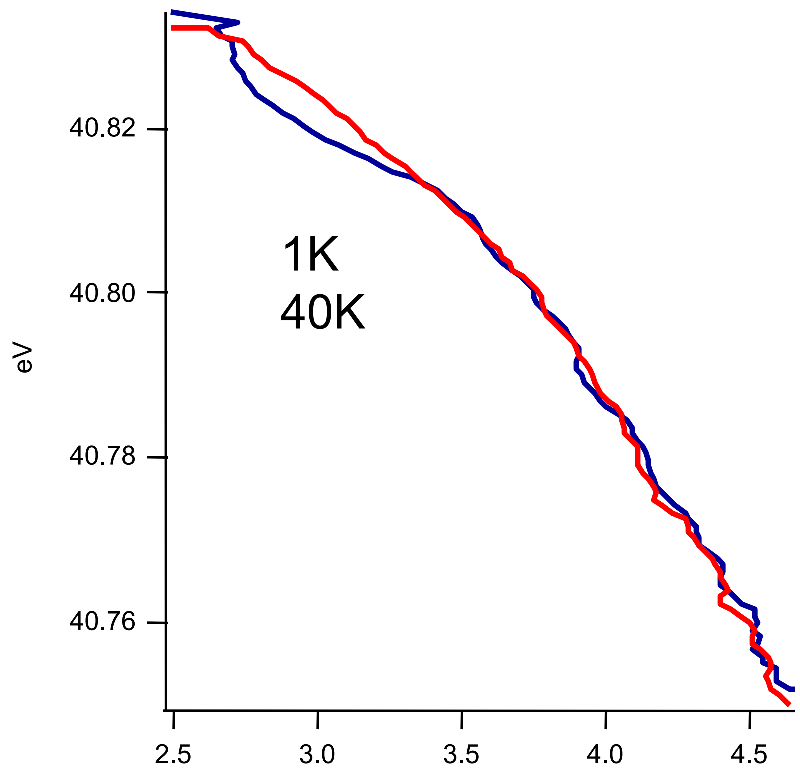

Mode effect at X-pocket in $Ba_{1-x}K_xFe_2As_2$

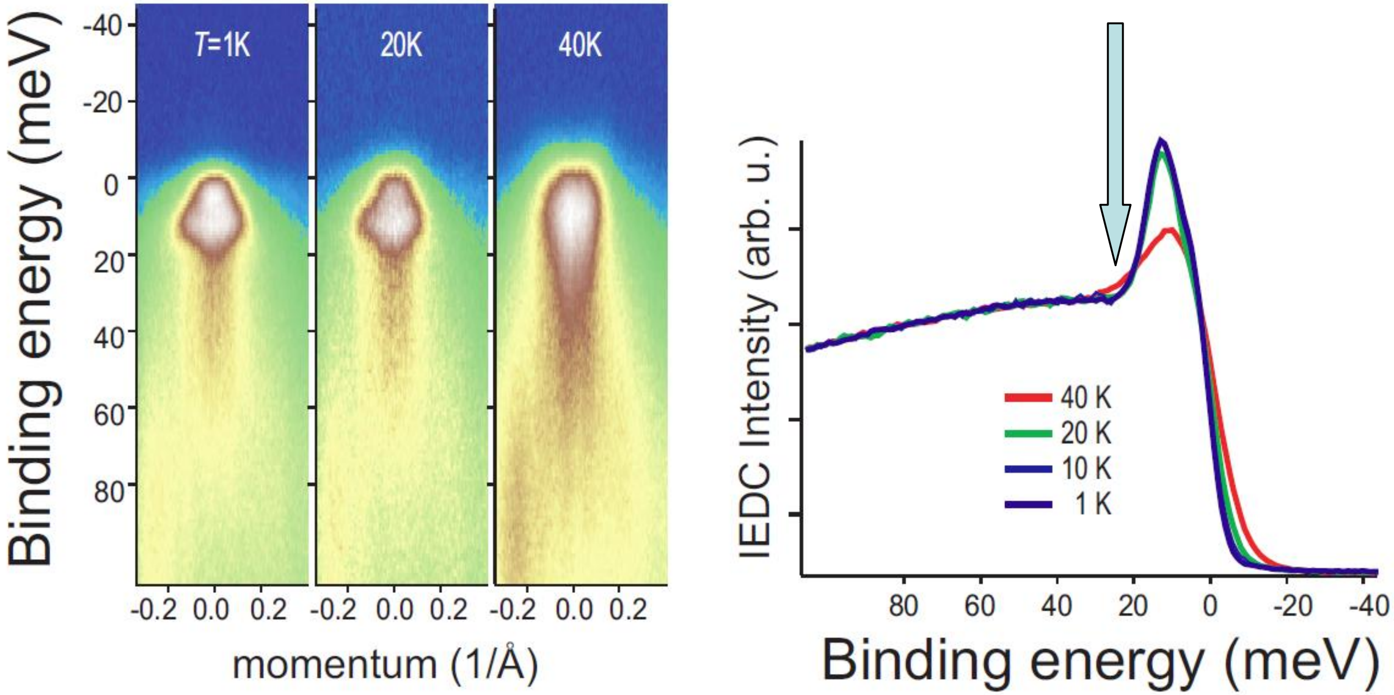

$T_c = 38K$

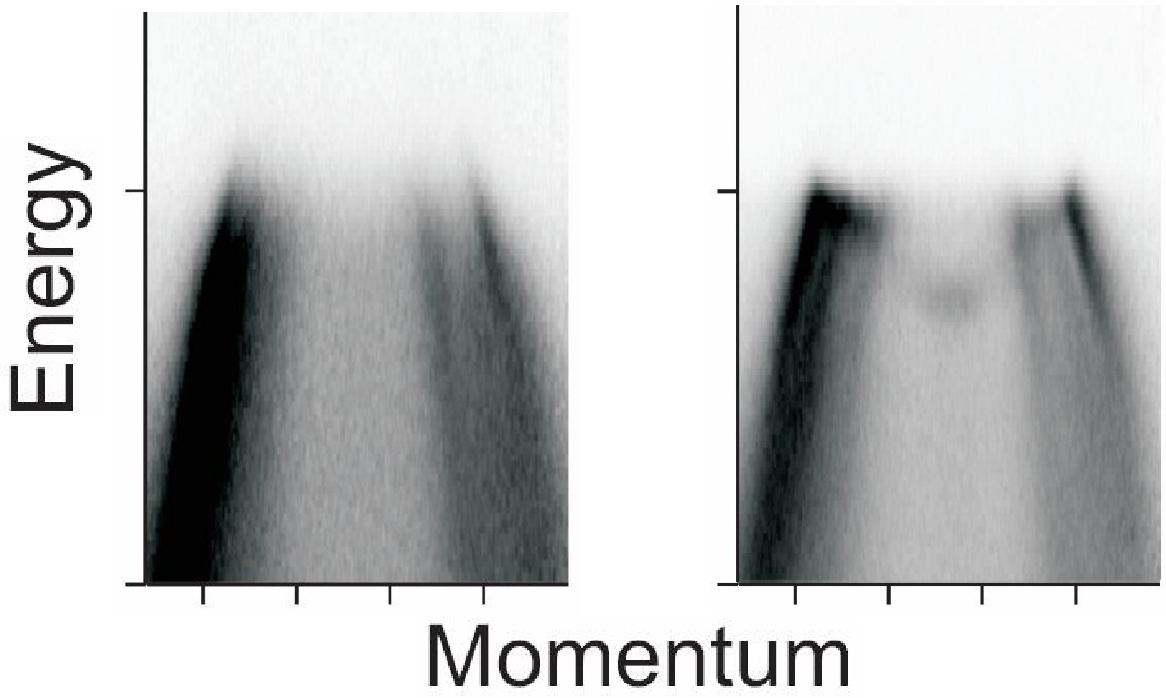

$T = 40K$ $T = 1K$

Fusion of bogoliubons

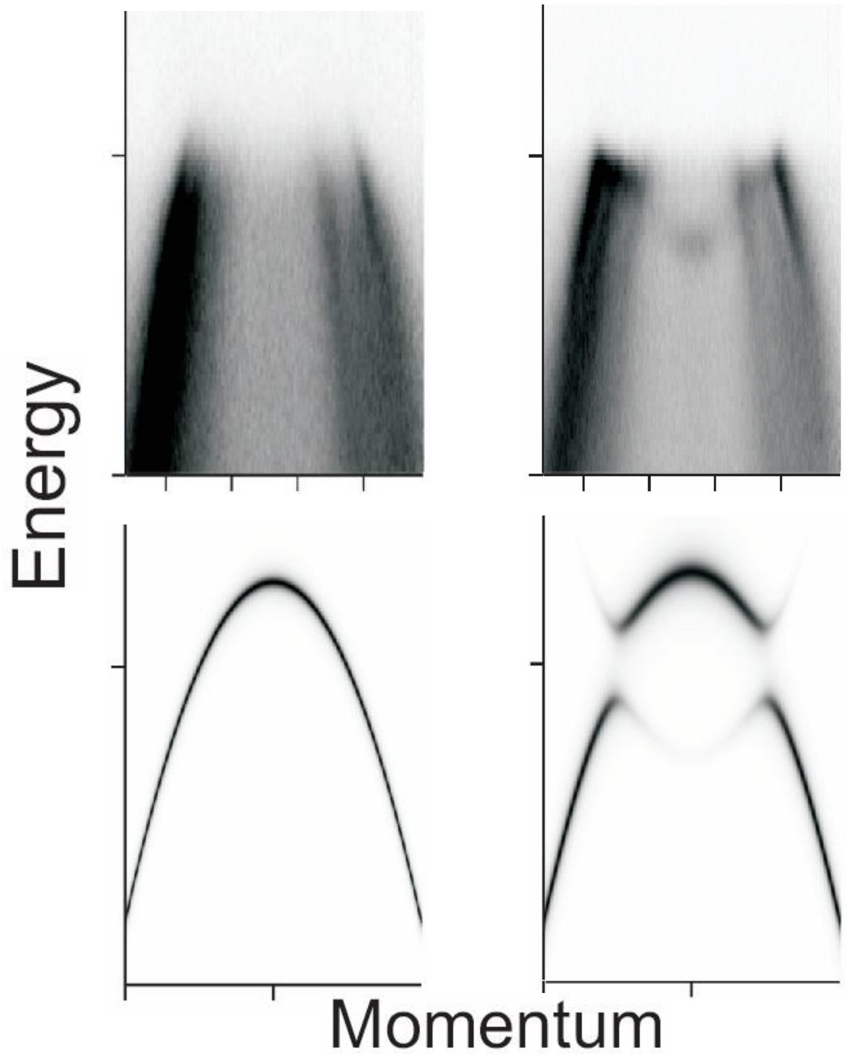

T = 40K T = 1K

Fusion of bogoliubons

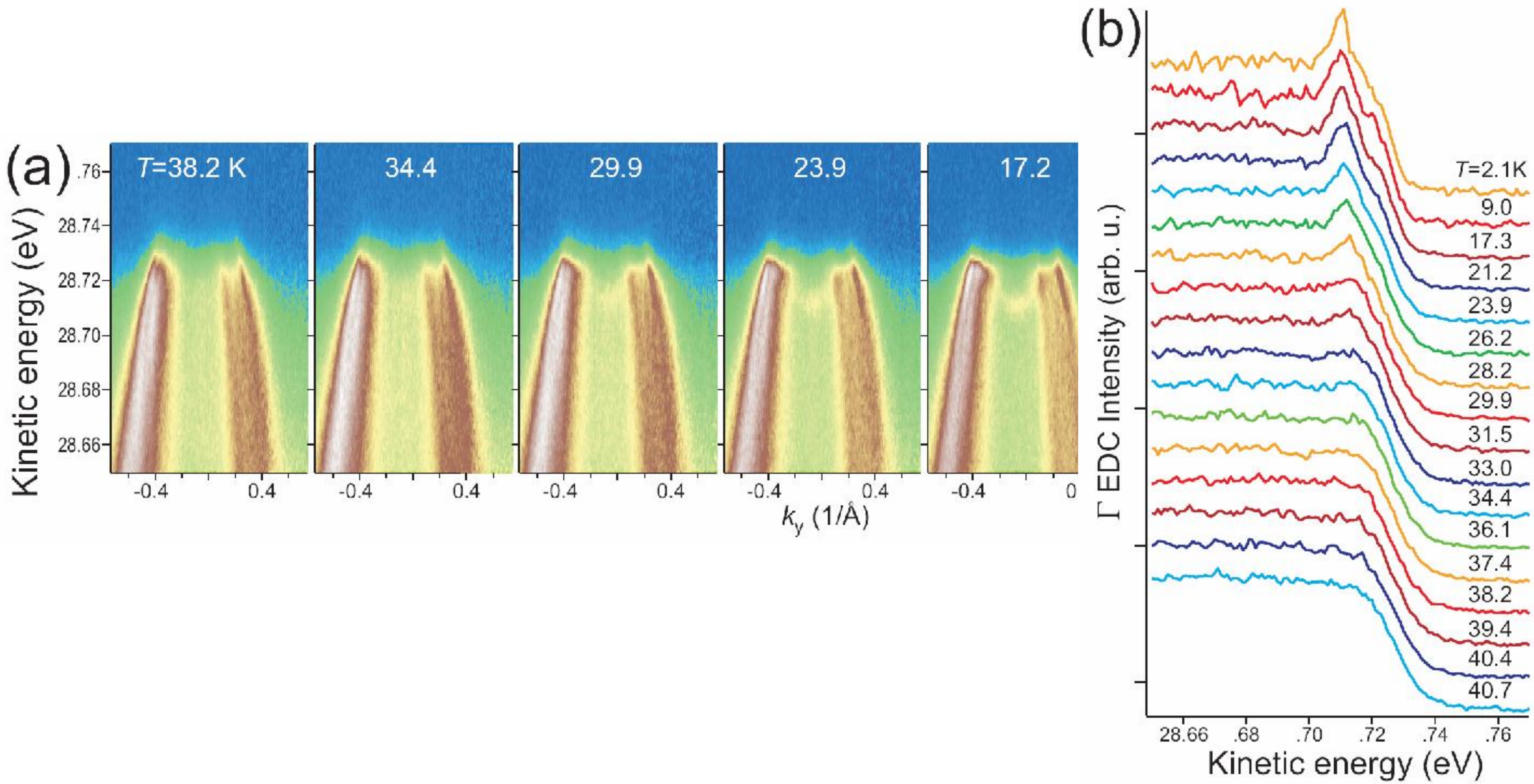

Fusion of bogoliubons

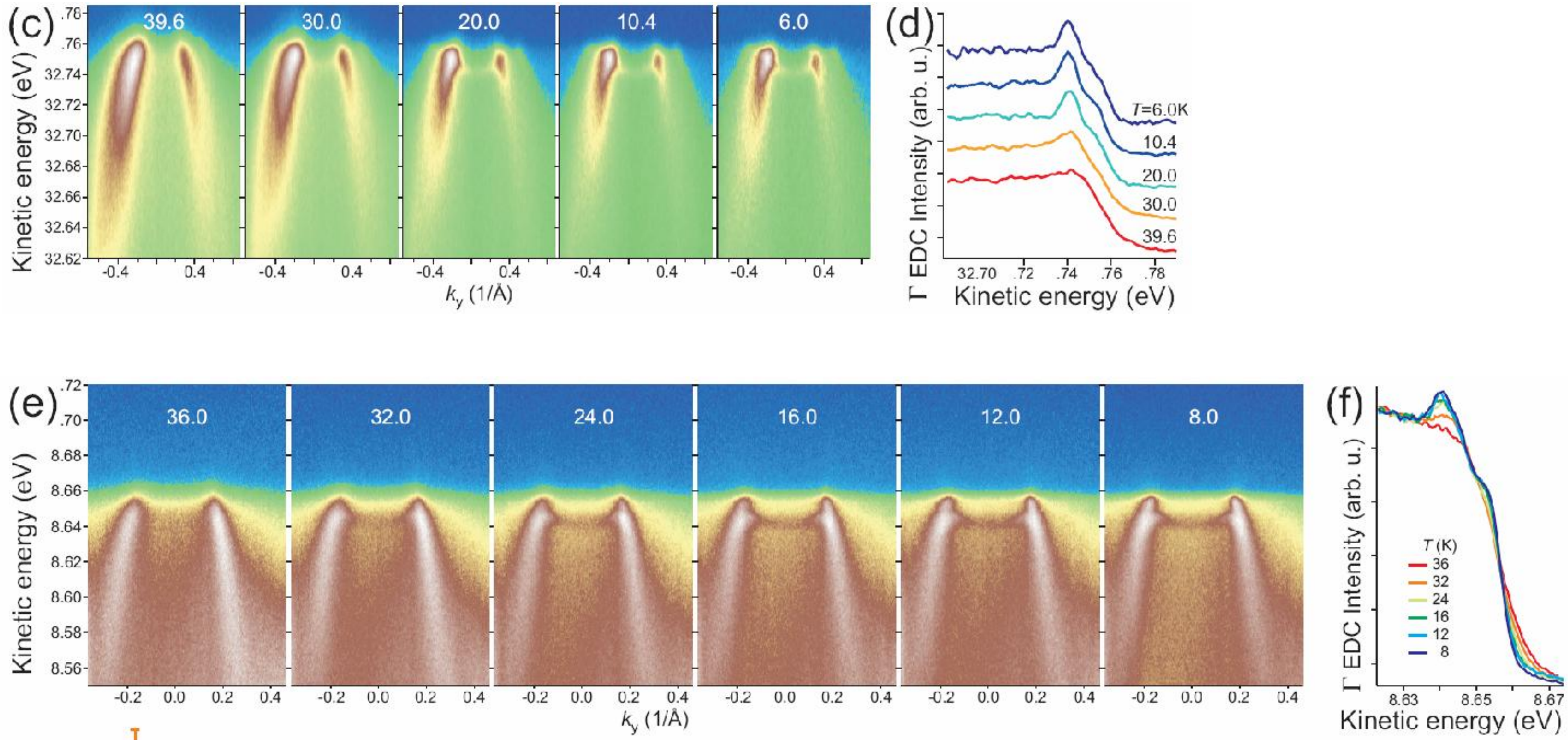

Fine structure of electronic spectrum below T_c

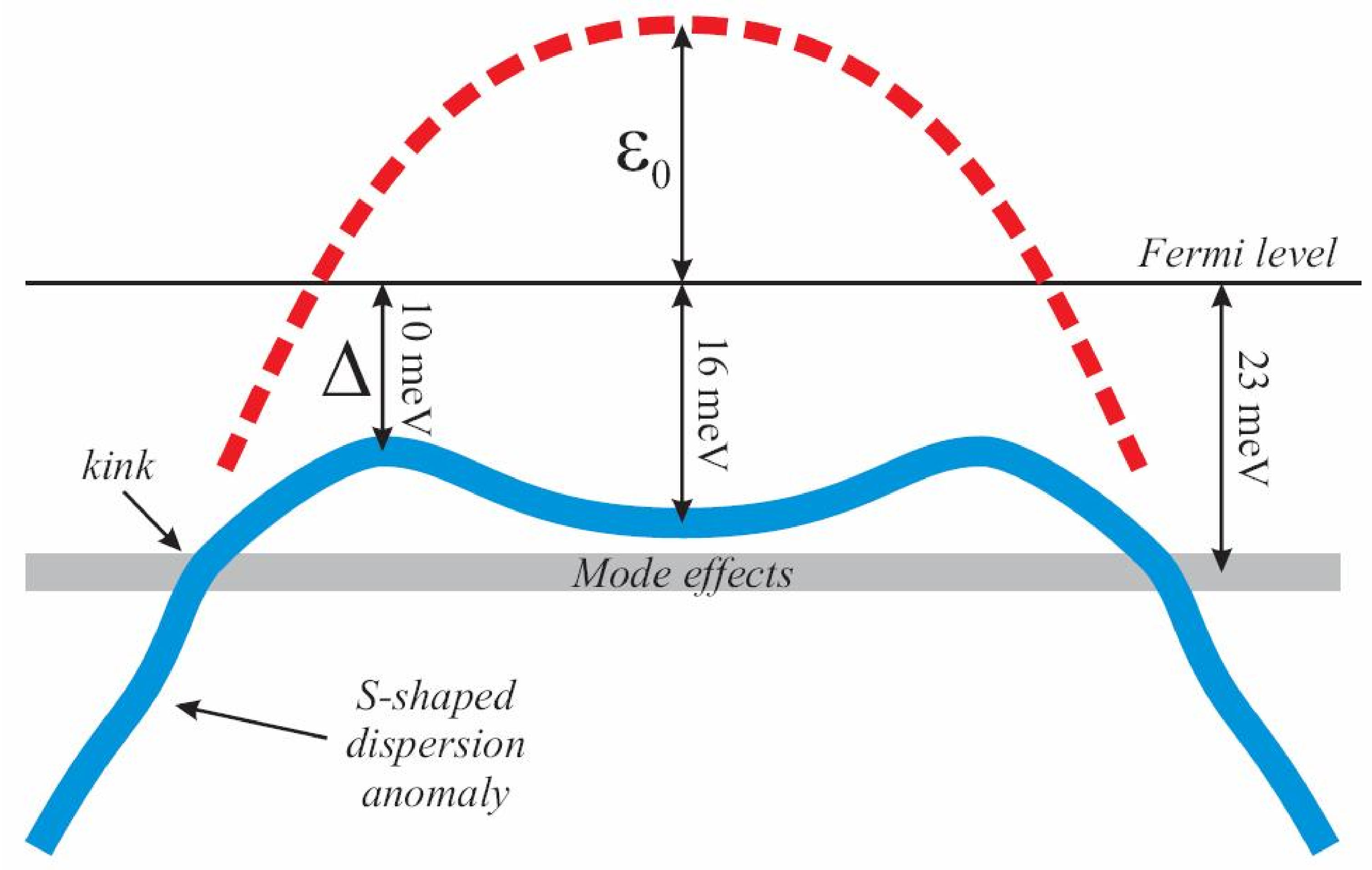

Temperature dependence: faster saturation for the larger gap

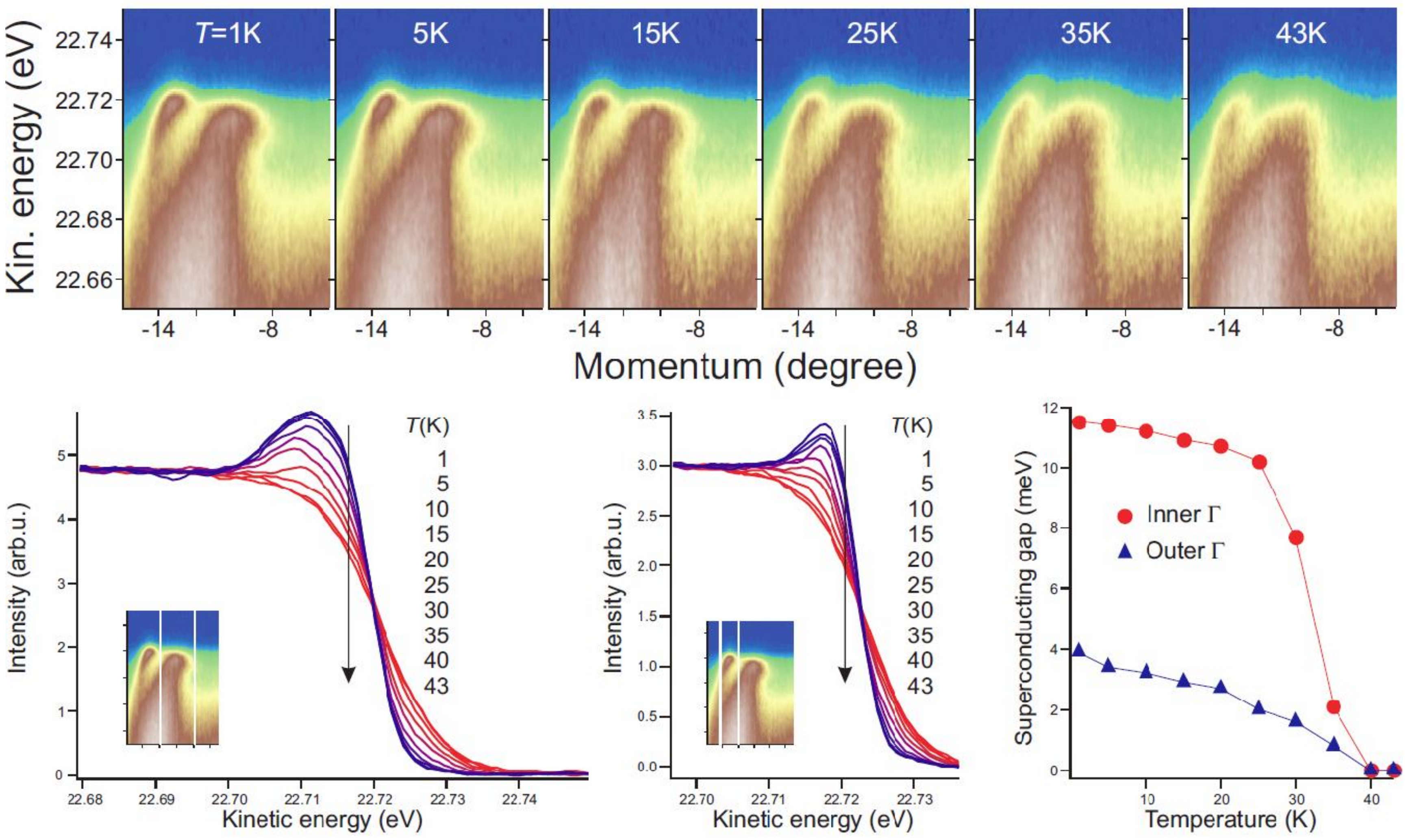

Relation between energy scales of band structure and superconductivity

$$\Delta \ll \omega_{\rm m} \ll \varepsilon_0$$

$$\Delta \sim \omega_{\rm m} \sim \varepsilon_0$$

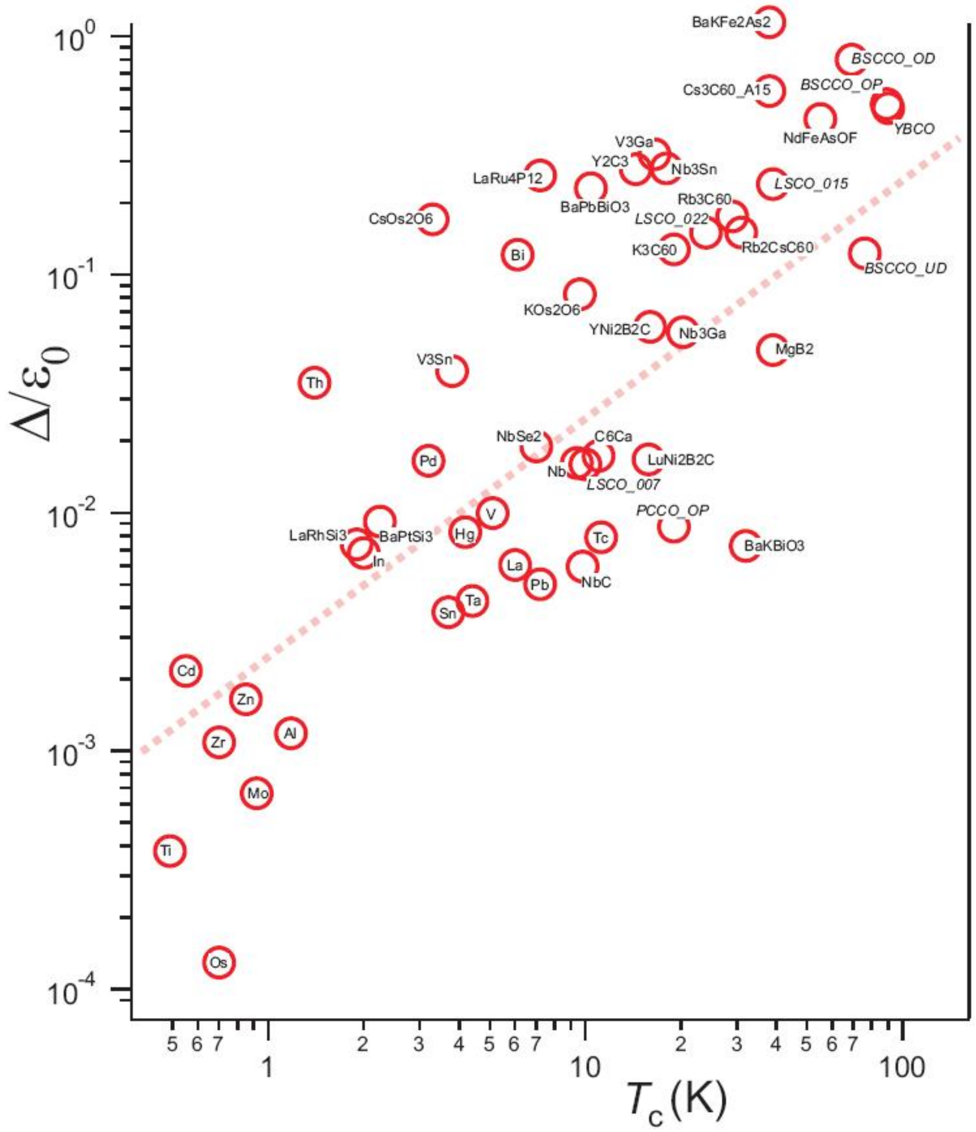

Conclusions for iron-based

- Various Fermi surface shape for different iron-based superconductors

- Large and small superconducting gaps in $Ba_{1-x}K_xFe_2As_2$ and other materials, large $2\Delta/kT_c$

- Correlation of superconducting gap magnitude with orbital composition: importance of iron $\mathbf{3}\boldsymbol{d}_{xz,yz}$

Acknowledgements

V. B. Zabolotnyy
A. A. Kordyuk
T. K. Kim
J. Maletz

S. Aswartham
I. Morozov
S. Wurmhel
G. Behr
C. Hess
R. Hübel
A. Koitzsch
M. Knupfer

B. Büchner

S. V. Borisenko

D. S. Inosov
A. N. Yaresko
A. V. Boris
G. L. Sun
D. L. Sun
V. Hinkov
C. T. Lin
B. Keimer

A. Varykhalov
E. Rienks
R. Follath

H. Q. Luo
Z. S. Wang
H. H. Wen

DFG Research Unit 538

Acknowledgements

S. V. Borisenko

A. A. Kordyuk

V. B. Zabolotnyy

R. Follath

B. Büchner

thank you for your attention

blank

slide